ISSN 0021-9673

VOL. 664 NO. 2 APRIL 1, 1994

THIS ISSUE COMPLETES VOL. 664

JOURNAL OF CHROMATOGRAPHY A

INCLUDING ELECTROPHORESIS AND OTHER SEPARATION METHODS

ELSEVIER

JOURNAL OF CHROMATOGRAPHY A

INCLUDING ELECTROPHORESIS AND OTHER SEPARATION METHODS

Scope. The *Journal of Chromatography A* publishes papers on all aspects of **chromatography, electrophoresis** and related methods. Contributions consist mainly of research papers dealing with chromatographic theory, instrumental developments and their applications. In the *Symposium volumes*, which are under separate editorship, proceedings of symposia on chromatography, electrophoresis and related methods are published. *Journal of Chromatography B: Biomedical Applications* —This journal, which is under separate editorship, deals with the following aspects: developments in and applications of chromatographic and electrophoretic techniques related to clinical diagnosis or alterations during medical treatment; screening and profiling of body fluids or tissues related to the analysis of active substances and to metabolic disorders; drug level monitoring and pharmacokinetic studies; clinical toxicology; forensic medicine; veterinary medicine; occupational medicine; results from basic medical research with direct consequences in clinical practice.

Submission of Papers. The preferred medium of submission is on disk with accompanying manuscript (see *Electronic manuscripts* in the Instructions to Authors, which can be obtained from the publisher, Elsevier Science B.V., P.O. Box 330, 1000 AH Amsterdam, Netherlands). Manuscripts (in English; *four* copies are required) should be submitted to: Editorial Office of *Journal of Chromatography A*, P.O. Box 681, 1000 AR Amsterdam, Netherlands, Telefax (+31-20) 5862 304, or to: The Editor of *Journal of Chromatography B: Biomedical Applications*, P.O. Box 681, 1000 AR Amsterdam, Netherlands. Review articles are invited or proposed in writing to the Editors who welcome suggestions for subjects. An outline of the proposed review should first be forwarded to the Editors for preliminary discussion prior to preparation. Submission of an article is understood to imply that the article is original and unpublished and is not being considered for publication elsewhere. For copyright regulations, see below.

Publication information. *Journal of Chromatography A* (ISSN 0021-9673): for 1994 Vols. 652–682 are scheduled for publication. *Journal of Chromatography B: Biomedical Applications* (ISSN 0378-4347): for 1994 Vols. 652–662 are scheduled for publication. Subscription prices for *Journal of Chromatography A*, *Journal of Chromatography B: Biomedical Applications* or a combined subscription are available upon request from the publisher. Subscriptions are accepted on a prepaid basis only and are entered on a calendar year basis. Issues are sent by surface mail except to the following countries where air delivery via SAL is ensured: Argentina, Australia, Brazil, Canada, China, Hong Kong, India, Israel, Japan, Malaysia, Mexico, New Zealand, Pakistan, Singapore, South Africa, South Korea, Taiwan, Thailand, USA. For all other countries airmail rates are available upon request. Claims for missing issues must be made within six months of our publication (mailing) date. Please address all your requests regarding orders and subscription queries to: Elsevier Science B.V., Journal Department, P.O. Box 211, 1000 AE Amsterdam, Netherlands. Tel.: (+31-20) 5803 642; Fax: (+31-20) 5803 598. Customers in the USA and Canada wishing information on this and other Elsevier journals, please contact Journal Information Center, Elsevier Science Inc., 655 Avenue of the Americas, New York, NY 10010, USA, Tel. (+1-212) 633 3750, Telefax (+1-212) 633 3764.

Abstracts/Contents Lists published in Analytical Abstracts, Biochemical Abstracts, Biological Abstracts, Chemical Abstracts, Chemical Titles, Chromatography Abstracts, Current Awareness in Biological Sciences (CABS), Current Contents/Life Sciences, Current Contents/Physical, Chemical & Earth Sciences, Deep-Sea Research/Part B: Oceanographic Literature Review, Excerpta Medica, Index Medicus, Mass Spectrometry Bulletin, PASCAL-CNRS, Referativnyi Zhurnal, Research Alert and Science Citation Index.

US Mailing Notice. *Journal of Chromatography A* (ISSN 0021-9673) is published weekly (total 52 issues) by Elsevier Science B.V., (Sara Burgerhartstraat 25, P.O. Box 211, 1000 AE Amsterdam, Netherlands). Annual subscription price in the USA US$ 4994.00 (US$ price valid in North, Central and South America only) including air speed delivery. Second class postage paid at Jamaica, NY 11431. **USA POSTMASTERS**: Send address changes to *Journal of Chromatography A*, Publications Expediting, Inc., 200 Meacham Avenue, Elmont, NY 11003. Airfreight and mailing in the USA by Publications Expediting.

See inside back cover for Publication Schedule, Information for Authors and information on Advertisements.

0021-9673/94/$07.00

Printed in the Netherlands

VOL. 664, NO. 2 JOURNAL OF CHROMATOGRAPHY A APRIL 1, 1994

CONTENTS

(Abstracts/Contents Lists published in Analytical Abstracts, Biochemical Abstracts, Biological Abstracts, Chemical Abstracts, Chemical Titles, Chromatography Abstracts, Current Awareness in Biological Sciences (CABS), Current Contents/Life Sciences, Current Contents/Physical, Chemical & Earth Sciences, Deep-Sea Research/Part B: Oceanographic Literature Review, Excerpta Medica, Index Medicus, Mass Spectrometry Bulletin, PASCAL-CNRS, Referativnyi Zhurnal, Research Alert and Science Citation Index)

REGULAR PAPERS

Column Liquid Chromatography

Gas Chromatography

(Continued overleaf)

Contents (continued)

ELSEVIER

Journal of Chromatography A, 664 (1994) 139–147

JOURNAL OF CHROMATOGRAPHY A

Influence of analyte stereochemistry and basicity on peak shape of basic compounds in high-performance liquid chromatography with reversed-phase columns, using pyridine and alkyl-substituted derivatives as probe compounds

David Victor McCalley

Department of Chemical and Physical Sciences, University of the West of England, Frenchay, Bristol BS16 1QY, UK

(First received November 26th, 1993; revised manuscript received December 22nd, 1993)

Abstract

Column efficiency, peak asymmetry and retention factor of a series of sixteen compounds comprising pyridine and some alkyl-substituted derivatives, with pK_a values ranging from 5.17 to 6.74 is reported on a RP-HPLC column previously shown to be especially suitable for the analysis of basic compounds. Compound stereochemistry in close vicinity of the basic group is found to influence peak shape strongly: however, stereochemistry at more remote positions is also of some significance. The effect of pK_a on peak shape is discussed in the light of measurements of the degree of protonation of the compounds in the methanolic mobile phase as well as water.

1. Introduction

The analysis of basic compounds by HPLC using RP columns continues to be an area of concern, and the problems inherent in such work are now well recognised [1,2]. Nevertheless, relatively little is known about the effect of compound stereochemistry and basicity on the reduction of column performance which is often experienced with these compounds. Ascah and Feibush [3] found peak asymmetry increased with increasing pK_a of the analyte, while the stereochemistry in close vicinity of the basic nitrogen atom was also thought to influence peak shape. Vervoort *et al.* [4] also found that there was a strong correlation between the pK_a of a compound and its asymmetry factor, with peak tailing increasing with increasing pK_a. The same authors postulated that the so-called "flexibility" of protonated N atoms influenced their ability to interact with underivatised silanol groups. Nevertheless, these studies have incorporated basic compounds of quite varied stereochemistry and pK_a, which can make attribution of peak shape to specific features of the compound difficult.

We have evaluated a series of RP columns for the analysis of basic compounds using a test based on that of Engelhardt *et al.* [5]. This procedure has allowed the identification of columns which give acceptable and reproducible peak shape for analysis of pyridine, even when the mobile phase does not contain buffering components [6]. In the present study we have investigated the analysis of sixteen compounds comprising pyridine and various alkyl-substituted derivatives. These compounds form a more closely related group than those used in previous

0021-9673/94/$07.00
SSDI 0021-9673(93)E0082-6

studies, with a fairly narrow range of pK_a values (5.17 to 6.74) and similar stereochemistries. The compounds include derivatives with substitution of alkyl groups of varying chain length in 2-, 3- and 4-positions relative to the basic group; furthermore some compounds have virtually identical pK_a values but different stereochemical features, enabling the influence of stereochemistry to be studied in the absence of the other variable. In this way we hoped to be able to discover more about the influence of compound nature on peak shape. A few commercial companies report test results for pyridine and substituted pyridines with their columns. A related aim of the work was to assess the relative degree of difficulty of analysis of these compounds, and to identify compounds more difficult to analyse than pyridine, which could be used to assess the performance of improved RP columns which are likely to become available in the future.

2. Experimental

The HPLC system consisted of an SP8800 pump, a Spectra 100 variable-wavelength UV detector with time constant 0.1 s and a 9-μl flow cell (all from Spectra-Physics, San Jose, CA, USA) and a valve injector equipped with a 5-μl loop (Rheodyne, Cotati, CA, USA). We did not wish to make measurements at constant retention factor (k') by varying the proportion of organic solvent in the mobile phase, since this could affect both the wetting of the stationary phase and the degree of ionisation of these analytes. However, we attempted to keep the dead volume of the system to a minimum, and used a relatively large diameter column in order to limit the influence of extra-column effects. Column efficiency values (N) were determined from peak widths at half height. Asymmetry factors (A_s) were calculated at 10% of the peak height from the ratio of the widths of the rear and front sides of the peak, using a Model 2000 data station (Trivector, Bedford, UK) in conjunction with a BASIC program. All results were the mean of at least duplicate injections of the analyte. The new column used was Inertsil ODS 5 μm, 25 × 0.46 cm I.D. (GL Sciences, Tokyo, Japan) with 14% carbon loading. All analyses were performed at 20°C. Pyridine and alkyl-substituted compounds were obtained from Sigma–Aldrich (Poole, UK). Phosphate buffer solutions (concentration 50 mM) were prepared by dissolving 6.803 g of KH_2PO_4 in 1 l of pure water, and adjusting the pH with either concentrated H_3PO_4 or 0.05 M KOH. Unless stated otherwise, the pH of the buffer was measured before addition of the organic modifier. Uracil was used as a column void volume marker for calculation of k'. UV measurements were made with a Lambda-15 spectrometer (Perkin-Elmer, Beaconsfield, UK). Dilute solutions of the compounds (concentration about 10 mg l^{-1}) were made up in phosphate solutions with preparation and subsequent adjustment of pH as above. In order to test the UV method used to investigate the protonation of the compounds in organic solvent–water mixtures (data not available in the literature), we measured the pK_a of pyridine in water (a well known value) using the same procedure. This gave a value of 5.2, in agreement with literature values [7,8].

3. Results and discussion

In a previous report [6] it was shown that the peak shape of pyridine in addition to that of other basic test substances, could be used as a measure of the suitability of RP columns for the analysis of basic compounds. The mobile phase consisted of methanol–water (55:45, v/v): under these conditions, the RP is totally wetted, and solute molecules can penetrate the bonded layer to interact freely with residual silanol groups. At higher water concentrations, the bonded ligands may fold up, and form a dense layer impenetrable to solutes [5,9]. If buffer solutions are not utilised, some variables connected with their composition can be eliminated from the test, and it also becomes simpler to perform. A problem with this approach is the possibility of irreproducible results for ionisable compounds which could arise due to the poor buffering capacity of the mobile phase. This could cause changes in the ionisation of analyte or column

surface groups. For this reason, we also performed experiments using a mobile phase buffered at pH 7.0, a value which should not result in excessive dissolution of the silica, which could occur at higher pH with prolonged use. Table 1 shows the reproducibility of the analysis of a solution of pyridine injected repeatedly into a column which we have found especially suitable for the analysis of basic compounds, using a simple methanol–water mixture as eluent. Many commercial columns give severe tailing for pyridine under these conditions, and furthermore we have found column performance data irreproducible. Using the Inertsil-ODS column however, the results in terms of peak shape and retention factor seem very reproducible. We performed these experiments with a new column which had not previously been used with buffered mobile phases: otherwise extensive washing may be necessary to remove the influence of these substances completely.

We investigated the effect of sample concentration by injection of pyridine solutions over a range 10 to 700 mg l^{-1}, corresponding to 50-ng to 3.5-μg amounts injected. Values of N, A_s, k' and peak height/area were calculated for both buffered and unbuffered mobile phases. Fig. 1 shows that trends were similar for both mobile phases: in both cases the efficiency (monitored at half peak height) remains approximately constant with increasing sample concentration whereas the peak asymmetry shows a gradual worsening. Use of the Dorsey–Foley equation, or some other alternative algorithms for calculation of column efficiency, would give greater weight to the increasing asymmetry of peaks in the calculation of N. Nevertheless, the James–Martin procedure is precise, and the asymmetry of the peaks monitored throughout our work was not excessive [10]. Both for measurement of N and A_s, the buffered mobile phase appears to give slightly better results for these basic compounds. Peak area and peak height measurements showed an excellent linear response with increasing concentration over the range 0–700 mg l^{-1}, even with the unbuffered mobile phase. For peak area (peak height) measurements, the slope of the line obtained from eight data points with methanol–water (55:45, v/v) was 7.00 (0.934), intercept 5.41 (−0.118), standard deviation of the slope 0.00851 (0.00368), standard deviation of the intercept 2.82 (1.22) standard error 5.78 (2.50), and correlation coefficient r = 0.99999 (0.99995). These results indicate the absence of concentration-dependent adsorption effects. Also, the relative standard deviation of k' measurements when varying the concentration of injected solutions over the range indicated in Fig. 1 was still less than 1%. These reproducible results may not be typical for more active columns. We concluded that providing the concentration of injected solutions is approximately the same, results would be sufficiently precise for meaningful comparisons of column performance for different compounds to be made, even if the mobile phase does not contain buffer components. We chose 100 mg l^{-1} injections for all subsequent work because column performance data were particularly reproducible at this level.

Claessens *et al.* [2] found considerably greater peak asymmetry for analysis of heptylpyridine on some columns when using acetonitrile–water

Table 1
Reproducibility of analysis of pyridine on Inertsil ODS column using unbuffered mobile phase

	k'	Peak height (integrator units)	Peak area (integrator units)	N (plates)	A_s
Mean	0.63	93.9	689	10 400	1.65
R.S.D. (%)	0.32	0.97	1.53	1.01	1.21

Mobile phase methanol–water (55:45, v/v), flow-rate 1 ml min^{-1}. UV detection at 254 nm. Column temperature 20°C. Results based on eight repeated injections of 100 mg l^{-1} solution.

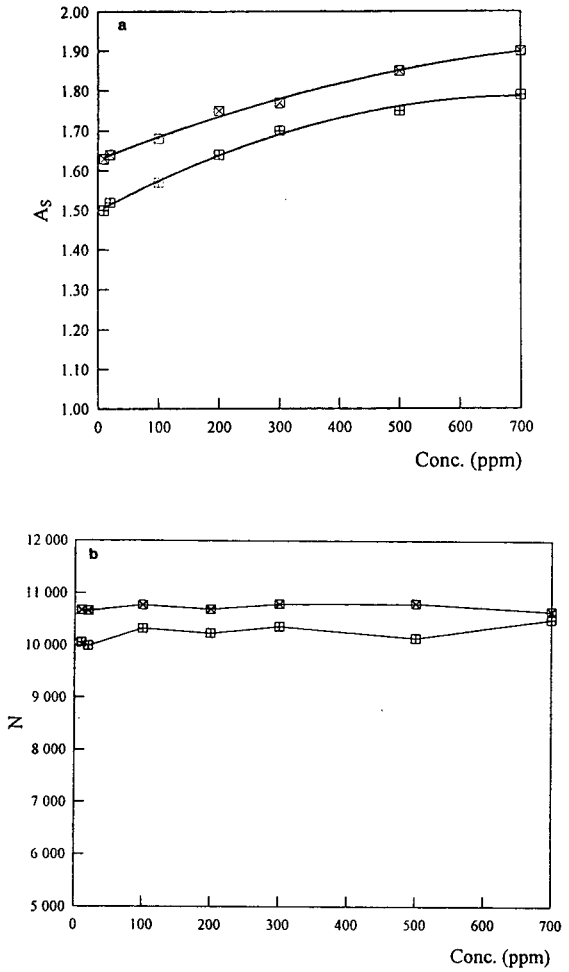

Fig. 1. (a) Plot of asymmetry factor against concentration of injected pyridine solution; mobile phase: upper curve methanol–water (55:45, v/v), lower curve methanol–phosphate buffer pH 7.0 (55:45, v/v). (b) Plot of column efficiency against concentration of injected pyridine solution; mobile phase: upper curve methanol–phosphate buffer pH 7.0 (55:45, v/v), lower curve methanol–water (55:45, v/v). Flow-rate 1 ml min^{-1}; column temperature 20°C; sample volume 5 μl; column Inertsil ODS; detector UV at 254 nm. ppm = mg l^{-1}.

mixtures rather than methanol–water mixtures. They attributed this result to the ability of methanol to hydrogen bond with silanol groups, and thus give a deactivation effect in comparison with acetonitrile. We found that substitution of an isoeluotropic acetonitrile–water mixture (approximately 45:55) for the methanol–water mixture gave an increase of only about 10% in A_s for pyridine, for injections of the same amount of analyte. The small difference we found may be due to the relative inertness of the stationary phase employed in our work. Most of the RP-columns investigated in the other study [2] were well established materials not especially suited for the analysis of basic compounds.

The seventeen compounds selected for study in Table 2 allow investigation of the effect on peak shape of a number of different features of the analyte. These include steric effects around the basic pyridine nitrogen atom, whole molecule steric effects, and ionisation effects which are related to the various indicated pK_a values of the derivatives. Values of N, A_s and k' are reported in Table 2 for each substance. All compounds gave reduced performance in comparison with benzene, a neutral substance included for comparison purposes. Duplicate injections were performed to give mean results reported for the unbuffered mobile phase; the same procedure was repeated for the buffered mobile phase. For each mobile phase, the individual results contributing to the mean value showed close agreement, which was predicted by the more detailed reproducibility study for pyridine shown in Table 1. Fig. 2 shows a representative chromatogram of six of the compounds using the methanol–water mobile phase. As with pyridine, all compounds showed slightly better performance with a mobile phase buffered at pH 7.0 rather than water in admixture with methanol, although differences were rather small. Some clear trends are visible in the results. Peak asymmetry increases and column efficiency drops along the series 2-methylpyridine ($A_s = 1.41$ in methanol–water), 3-methylpyridine ($A_s = 1.56$) and 4-methylpyridine (1.83), with a corresponding drop in N. Similar results are seen for 2-ethylpyridine ($A_s = 1.36$ in methanol–water), 3-ethylpyridine ($A_s = 1.52$) and 4-ethylpyridine ($A_s = 1.70$). The same trends are seen for these two sets of compounds when considering performance using the buffered mobile phase. Evidently, 2-substitution of the pyridine ring reduces the access of the basic nitrogen atom to column active sites, with the

Table 2
Column performance data for pyridine and alkyl-substituted pyridines

Compound	pK_a (water at 25°C)[a]	k'	N (plates)	A_s
Pyridine	5.17	0.63	10 400	1.65
		0.60	*10 600*	*1.57*
2-Methylpyridine	5.96	1.15	12 500	1.41
		1.10	*12 800*	*1.35*
3-Methylpyridine	5.68	1.34	11 700	1.56
		1.29	*12 100*	*1.47*
4-Methylpyridine	6.00	1.33	10 600	1.83
		1.27	*11 400*	*1.64*
2-Ethylpyridine	5.89	2.08	13 300	1.36
		2.03	*14 000*	*1.24*
3-Ethylpyridine	5.80	2.58	12 500	1.52
		2.51	*12 800*	*1.39*
4-Ethylpyridine	5.87	2.67	11 800	1.70
		2.68	*13 100*	*1.47*
2,3-DMP	6.57	2.30	12 000	1.43
		2.19	*12 700*	*1.26*
2,4-DMP	6.74	2.47	12 200	1.58
		2.37	*13 000*	*1.36*
2,6-DMP	6.71	2.07	12 600	1.49
		1.98	*13 500*	*1.29*
3,4-DMP	6.47	2.49	11 000	1.85
		2.39	*12 200*	*1.58*
3,5-DMP	6.09	2.86	12 500	1.57
		2.78	*13 100*	*1.46*
2-Propylpyridine	6.30	4.09	14 300	1.27
		4.02	*14 000*	*1.20*
4-Isopropylpyridine	6.02	4.93	13 100	1.53
		4.99	*13 100*	*1.38*
3-Butylpyridine	[b]	11.4	14 900	1.31
		11.7	*16 300*	*1.25*
4-*tert.*-Butylpyridine	5.99	7.94	13 600	1.47
		8.30	*13 600*	*1.34*
Benzene	–	4.99	19 200	1.12
		5.00	*19 100*	*1.13*

Results for mobile phase methanol–water (55:45, v/v) shown in normal characters; for mobile phase methanol–phosphate buffer pH 7.0 (55:45, v/v) shown in italics. All other conditions as in Table 1.
[a] All pK_a values from ref. 7 except 2,3-DMP, ref. 8.
[b] Value not available.

effect decreasing successively for 3- and 4-substitution. Peak shapes for the dimethylpyridines (DMPs) are almost entirely predictable by a summation of the position-dependent steric effects of the individual methyl groups. For example, peak asymmetry increases along the series 2,3-DMP ($A_s = 1.43$ in methanol–water), 2,4-DMP ($A_s = 1.58$) and 3,4-DMP ($A_s = 1.85$). Increasing the size of the substituent at the 2-position seems to reduce peak asymmetery: a decrease is observed for the series 2-methylpyridine ($A_s = 1.41$ in methanol–water), 2-ethylpyridine ($A_s = 1.36$) and 2-propylpyridine ($A_s = 1.27$), accompanied by an increase in N. Despite the apparent importance of stereochemistry in close proximity to the basic group however, steric effects still appear to influence results when alkyl groups are present at more remote

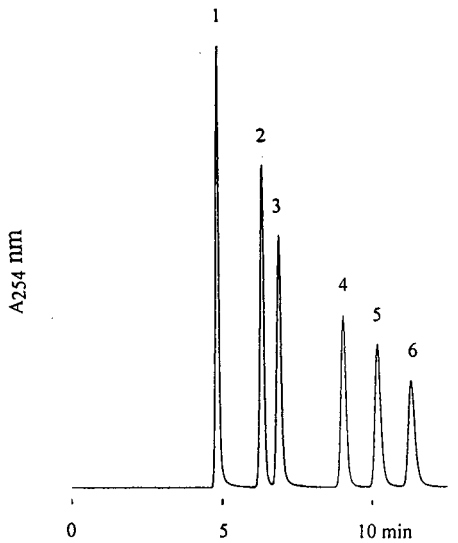

Fig. 2. Separation of pyridine and some derivatives using Inertsil ODS column. Mobile phase methanol–water (55:45, v/v). Peaks: 1 = pyridine; 2 = 2-methylpyridine; 3 = 3-methylpyridine; 4 = 2,6-DMP; 5 = 2,4-DMP; 6 = 3,5-DMP. Other conditions as in Fig. 1.

sites. Thus N increases and peak asymmetry decreases for the series 4-methylpyridine (A_s = 1.83 in methanol–water), 4-ethylpyridine (A_s = 1.70), 4-isopropylpyridine (A_s = 1.53) and 4-*tert.*-butylpyridine (1.47). It would appear for these compounds that the overall size of the molecule may also influence its ability to penetrate the bonded ligands and interact with the column surface. The relative effect of substituents in positions adjacent to, and remote from the basic centre can be judged by inspection of results for 2-methylpyridine and 4-*tert.*-butylpyridine which have virtually identical pK_a values. Thus, a methyl group in the 2-position seems to give a similar steric effect to the *tert.*-butyl group in the 4-position. In summary it appears that steric effects around the basic nitrogen atom are of major importance, while steric effects for the whole molecule have a significant but lesser effect.

Finally, the influence of pK_a of these compounds on peak shape must be considered. From the results in Table 2 it appears that using this inert ODS phase, pK_a has a lesser influence within this group of compounds than stereochemical effects, although the range of pK_a values within the group is not very large. Pyridine with the smallest pK_a in the set (5.17) gives more asymmetric peaks than 2,4-DMP with the largest (6.74). In fact only 4-methylpyridine and 3,4-DMP, which according to the above arguments should give relatively small stereochemical effects, give peaks which are substantially more asymmetric than pyridine:these results could be attributed to their significantly higher pK_a. This result is also evident from the data reported by Ascah and Feibush [3]; however, these authors worked with a much more limited set of pyridine derivatives and used an electrostatically shielded RP column, which is not directly comparable with the more conventional column used in our work. Furthermore the mobile phase used [3] contained only 2% organic modifier which would not lead to full wetting of the bonded ligands. Nevertheless, it does appear that 4-methylpyridine and 3,4-DMP can be used as more severe tests of a column for activity towards basic compounds.

In order to investigate more fully the effect of compound pK_a on peak asymmetry we monitored the variation of the degree of protonation with pH, of the compound with highest and lowest pK_a. We used a UV spectrophotometric method based on the increased absorptivity of the pyridium cations over that of the unprotonated species. Fig. 3 shows the absorbance spectra of 2,4-DMP in methanol–buffer solutions, at pH 1.6 and 9.0 (55:45, v/v). In a

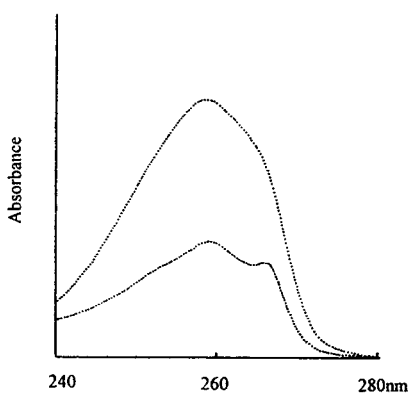

Fig. 3. Absorbance spectra of same concentrations 2,4-DMP in methanol–phosphate buffer pH 1.6 (55:45, v/v) (upper curve) and methanol–phosphate buffer pH 9.0 (55:45, v/v) (lower curve).

standard procedure, the absorbance of the compound is measured at a wavelength where the largest difference in absorptivity of the species occurs [11]; we chose 255 nm for pyridine and 259 nm for 2,4-DMP. Fig. 4a and c show plots of absorbance at the selected wavelength *versus* pH of the buffer for both compounds studied. It can be seen that even 2,4-DMP appears to be unprotonated in methanol–phosphate buffer pH 7.0 (55:45, v/v), which is unexpected by casual consideration of its pK_a in water. There has been much debate about the measurement of pH in mobile phases containing significant proportions of organic solvents [12], although such measurements are not necessary to establish the above result. (Fig. 4a and c). Nevertheless, measurement of pH prior to addition of the organic solvent could not reveal any resultant effect on pH, or possible contamination by acids or bases. Therefore, we also measured the pH of the solutions after addition of the methanol. Bates *et al.* [13] noted that pH values obtained with glass electrodes standardised with aqueous buffers in alcohol–water mixtures, are subject to no simple interpretation. However, it was shown that for methanol–water mixtures over the range 8:92 to 68:32, the liquid junction potential of the electrode was sufficiently constant with pH to estab-

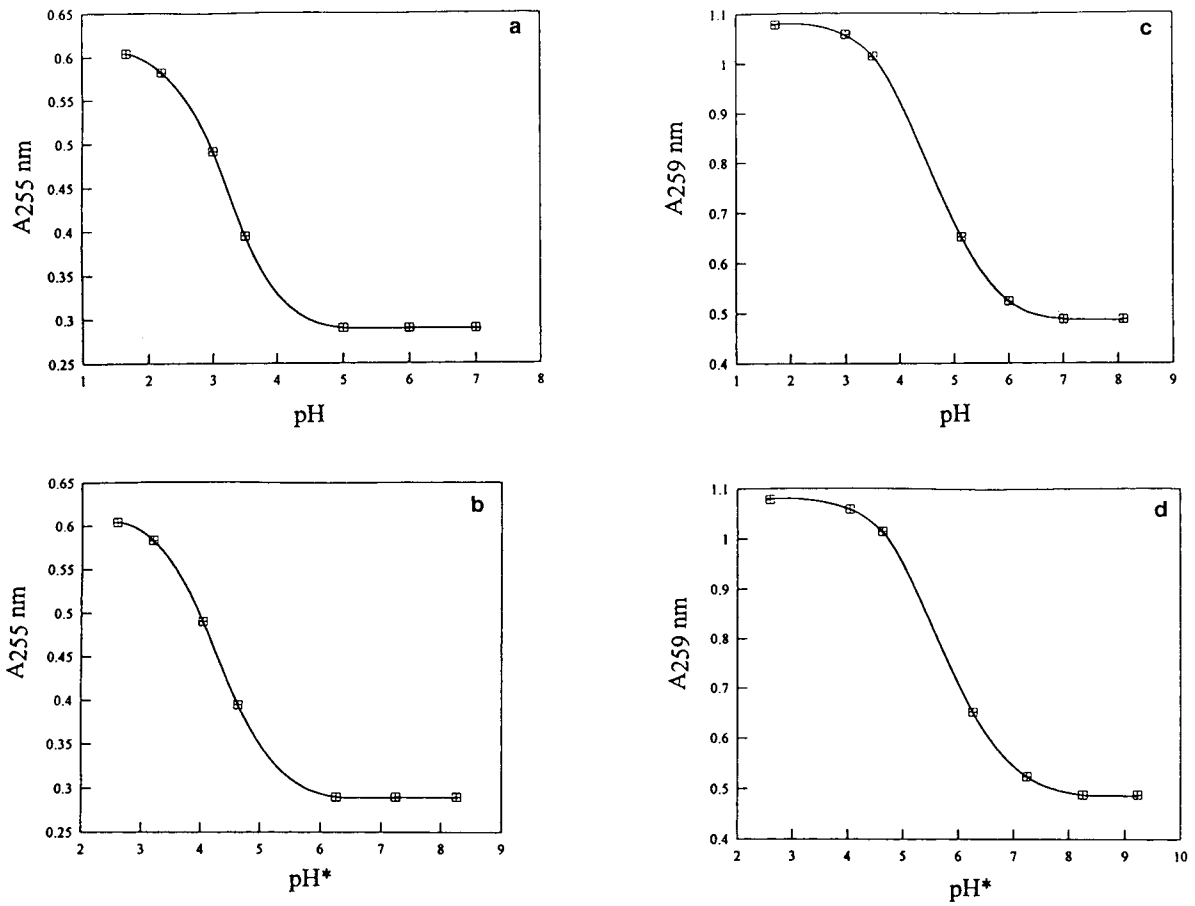

Fig. 4. Plot of UV absorbance against pH. (a) Pyridine in methanol–phosphate buffer (55:45, v/v); pH measured *before* organic solvent addition. (b) Pyridine (same concentration) in methanol–phosphate buffer (55:45, v/v); pH* measured *after* organic solvent addition. (c) 2,4-DMP in methanol–phosphate buffer (55:45, v/v); pH measured *before* organic solvent addition. (d) 2,4-DMP (same concentration) in methanol–phosphate buffer (55:45 v/v); pH* measured *after* organic solvent addition.

lish an operational scale of pH* measurements, where pH* = (observed pH − δ) and δ is a correction term [13]. Fig 4b and d shows absorbance for the compounds plotted against pH*. The previous results are confirmed in that pH* of the methanol–phosphate buffer pH 7.0 (55:45, v/v) was approximately 8.25, indicating 2,4-DMP was virtually unprotonated in this system. The approximate pK_a values for pyridine and 2,4-DMP in methanol–water (55:45, v/v) were calculated as 4.3 and 5.8, respectively. The depression of the pK_a of bases in alcohol–water mixtures compared with the values in aqueous solution is well known [11]. More accurate calculation of these values would require measurements in buffer solutions over a much narrower pH range around the pK_a values. Nevertheless, our results for the diminution of pK_a for these compounds in this solvent are broadly comparable with those found by Bacarella *et al.* [14] for aniline, N-methylaniline and N,N-dimethylaniline in methanol–water mixtures of similar concentration.

The lesser influence of the pK_a of the compounds within the pyridine group on chromatographic peak shape could be attributed to the probability that they are all largely unprotonated under the conditions of study, since it is likely that the protonation of all these compounds in methanol–water follows a similar pattern. Larger effects of pK_a within a group might occur when some compounds are partially protonated, some fully protonated, and some not protonated, at the prevailing pH of the mobile phase. Thus, these compounds seem to give rise to asymmetric peaks when present as the neutral compounds, probably by hydrogen bonding with silanol groups. Nevertheless, the possible contribution of ion-exchange interactions between a basic analyte (B) and dissociated silanol groups on the column surface cannot be ruled out. Such interactions are governed by two equilibria:

solute ionisation: $B + H^+ \rightleftharpoons BH^+$

ion exchange: $BH^+ + K^+SiO^- \rightleftharpoons K^+ + BH^+SiO^-$

Depending on the values of pK_a (in the mobile phase) and of the ion-exchange constant, it is possible to obtain substantial retention of BH^+ in this way, even if there is relatively little ionisation in the mobile phase. Thus, ionic effects may still contribute significantly to peak asymmetry for 2,4-DMP even at pH 7, in view of the much stronger ion-exchange attraction between protonated bases and silanols. Furthermore, on more active ODS phases, compounds with high pK_a could show greater peak asymmetry, due to increased influence of ion exchange. Ion-exchange effects probably account for the differences in performance results for buffered compared with unbuffered mobile phases shown in Table 2. Finally, the existence of interactions with impurities in the silica such as metals cannot be ignored even though these compounds could not possibly undergo the very strong interactions experienced by analytes with chelating properties [15].

4. Conclusions

Measurements of column performance for pyridine and alkyl-substituted derivatives were performed reproducibly using a stationary phase especially suitable for the analysis of basic compounds. In comparative studies, the concentration of injected solutions should be kept reasonably constant, since peak asymmetry shows a gradual increase with the amount of compound injected. Steric factors have an important influence on peak shape. Alkyl groups in close proximity to the basic site have the most pronounced effect, apparently hindering interactions with the column surface. Nevertheless, steric effects are still demonstrable at more remote sites. On the inert ODS phase studied here, the effect of pK_a was less important. Furthermore, for this set of compounds, UV measurements showed that the analytes were largely unprotonated under the conditions of the study. A scale of the degree of difficulty of analysis of these compounds was established: only 4-methylpyridine and 3,4-DMP appear to be significantly more severe tests of column activity towards basic compounds than pyridine itself.

5. Acknowledgements

The author thanks M. Norman, University of the West of England, for assistance with the preparation of the figures in this work and GL Sciences for the generous gift of HPLC columns.

6. References

[1] J.W Dolan, *LC·GC Int.*, 6 (1993) 142.
[2] H.A. Claessens, E.A. Vermeer and C.A. Cramers, *LC·GC Int.*, 6 (1993) 692.
[3] T.L. Ascah and B. Feibush, *J. Chromatogr.*, 506 (1990) 357.
[4] R.J. Vervoort, F.A. Maris and H. Hindriks, *J. Chromatogr.*, 623 (1992) 207.
[5] H. Engelhardt, H. Loew and W. Goetzinger, *J. Chromatogr.*, 544 (1991) 371.
[6] D.V. McCalley, *J. Chromatogr.*, 636 (1993) 213.
[7] J.A. Dean (Editor), *Lange's Handbook of Chemistry*, McGraw-Hill, New York, 13th ed., 1985.
[8] R.C. Weast (Editor), *CRC Handbook of Chemistry and Physics*, CRC Press, Boca Raton, FL, 1st student ed., 1988.
[9] T. Welsch, H. Frank and Gy. Vigh, *J. Chromatogr.*, 506 (1990) 97.
[10] W.W. Yau, S.M. Rementer, J.M. Boyajian, J.J. DeStefano, J.F. Graff, K.B. Lim and J.J. Kirkland, *J. Chromatogr.*, 630 (1993) 69.
[11] A. Albert and E.P. Serjeant, *Determination of Ionisation Constants*, Chapman & Hall, London, 3rd ed., 1984.
[12] B.A. Bidlingmeyer, *J. Chromatogr. Sci.*, 31 (1993) 347.
[13] R.G. Bates, M. Paabo and R.A. Robinson, *J. Phys. Chem.*, 67 (1963) 1833.
[14] A.L. Bacarella, E. Grunwald, H.P. Marshall and E.L. Purlee, *J. Org. Chem.*, 20 (1955) 747.
[15] K. Kimata, N. Tanaka and T. Araki, *J. Chromatogr.*, 594 (1992) 87.

ELSEVIER

Journal of Chromatography A, 664 (1994) 149–158

JOURNAL OF CHROMATOGRAPHY A

Characterization of some silica-based reversed-phase liquid chromatographic columns based on linear solvation energy relationships

Jung Hag Park*, Je Joon Chae, Tae Hwa Nah, Myung Duk Jang

Department of Chemistry, Yeungnam University, Kyongsan 712-749, South Korea

(First received August 24th, 1993; revised manuscript received November 4th, 1993)

Abstract

The characterization of six silica-based reversed-phase liquid chromatographic columns was attempted by calculating characteristic interaction constants for the stationary phases based on linear solvation energy relationships. Four interaction properties of the stationary phase, m (the cavity formation/dispersive interaction strength), s (dipolarity/polarizability), b (hydrogen bond donating acidity) and a (hydrogen bond accepting basicity), are readily determined by multiple regression analyses of logarithmic capacity factors (k') for a set of test solutes measured on it in an aqueous mobile phase of a given organic content *versus* the solute properties represented by the Van der Waals molar volume, Kamlet–Taft dipolarity/polarizability, π^*, hydrogen bond accepting basicity, β, and hydrogen bond donating acidity, α. The magnitudes of the four constants vary with the type of bonded ligand and with brand in the case of stationary phases having the same ligand, while they generally decrease in the order $m > b > a > s$, regardless of the type of the organic modifier in the mobile phase for all six columns. Although the four interaction strength constants are not as general as the widely used Rohrschneider and McReynolds constants for GLC stationary phases, it is believed that they will be useful in choosing the best column for a given separation among a number of nominally equivalent columns and columns with different bonded functionality.

1. Introduction

Practising chromatographers have noted the significant differences in retention characteristics between nominally equivalent reversed-phase liquid chromatographic (RPLC) columns such as C_{18} [1] and cyano-bonded materials [2]. This variability is to be expected, as retention in RPLC is determined by both solvophobic and chemical interactions between solute molecules and reactive sites of the stationary phase, which involve not only interactions between solute molecules and the organic bonded phase (solvophobic) [3] but also hydrogen bonding interactions with unreacted silanol groups and complexation with trace metals on the silica surface [4]. The relative contribution of these two types of interactions depends on the characteristics of the stationary phase, which include the nature of the base silica particles such as the specific surface area, pore size and volume, the nature of the bonded organic ligand and the bonding process. Chemical interactions are often re-

* Corresponding author.

0021-9673/94/$07.00
SSDI 0021-9673(93)E0016-N

garded as undesirable as these types of interactions, in particular silanophilic interactions, are responsible for the excessive peak tailing and long retention times observed for basic solutes. The presence of these types of interactions also leads to poorer control of the column packing, resulting in column-to-column irreproducibility [3,4]. As the diversity in retention properties of various stationary phases due to this variability has caused many difficulties for chromatographers in selecting the best column for a given separation, a knowledge of the nature and relative contributions of possible interactions between the solute and stationary phase to RPLC retention is of great value in that it can be utilized to help chromatographers in the task of selecting the best column and to optimize the selectivity for a given separation.

As direct measurement of interaction properties of bulk material is difficult and often less sensitive than chromatographic measurements, classification of columns has most often been attempted by measuring their retentivity and selectivity for a particular class of compounds. A good summary of chromatographic methods can be found in a book by Unger [5]. Snyder and co-workers characterized, on the basis of gradient elution theory, a number of columns having different bonded functional groups such as C_{18}, C_8, phenyl, C_1 and cyano groups according to their solvophobic retention [3,6]. They combined the phase-volume ratio and the polarity of the stationary phase into a column-strength parameter and determined the retention strength of the columns to be in the order $C_{18} > C_8 >$ phenyl $> C_1 >$ cyano. They also concluded that the contribution of the polarity of the column to the retention strength is small compared with the contribution of the phase-volume ratio. Differences in the solvophobic strength of these columns have been successfully utilized in RPLC method development [7] and in optimizing separations of complex mixtures such as phenylthiohydantoin-amino acid derivatives [8].

Recently, Ying and Dorsey [9] reported a method for characterizing the retentivities of a number of commercial ODS, a phenylpropyl and a cyanopropyl columns for RPLC which utilizes a value of ln k'_w, the retention of a compound with water as eluent and the slope of the plot of ln k' *vs.* $E_T(30)$, a measure of solvent polarity. They used 26 solutes of widely varying size and chemical properties. Their study was, however, centred only on the determination of the retentivity of the column. Information on the retentivity of a column will be useful in the characterization of a column. In addition to these solvophobic strength or retentivity data, if information on interaction characteristics of the column, analogous to the Rohrschneider and McReynolds constants for GLC stationary phases [10], is available, the task of choosing the best column and optimizing for a given separation will be much easier.

In this paper, we describe a simple method for characterizing the stationary phase in RPLC in terms of the type and relative strength of the solute–stationary phase interactions by multiple regression analysis of retention data for a set of test compounds based on linear solvation energy relationships (LSERs) [11,12] using the Van der Waals molar volumes and the Kamlet–Taft solvatochromic parameters for the test solutes, π^* (dipolarity/polarizability), β (hydrogen bonding acceptor basicity) and α (hydrogen bonding donor acidity). As will be shown, this approach provides characteristic interaction constants for RPLC stationary phases, which are similar to Rohrschneider and McReynolds constants for GLC stationary phases. The use of column selectivity based on these interaction constants might be useful in method development in RPLC.

2. Theory

Kamlet, Taft and co-workers applied the LSER approach to about 600 processes [12], including a large number of systems of immediate relevance to chromatography, such as Rohrschneider's gas–liquid partition coefficients [13], retention of McReynolds solutes on polymeric silicone oil gas chromatographic phases [14], retention in NPLC [15] and RPLC [16–19], log k'_w in RPLC [20] and surface polarity of

carbon fibres for use in gas–solid chromatography [21]. According to the LSER formalism, when applied to phase-transfer processes, a general solute or solvent property (SP) can be correlated via the use of three types of terms as follows [11,12]:

$$SP = SP_0 + \text{cavity term} + \text{dipolar term} + \text{hydrogen bonding term(s)} \quad (1)$$

where SP_0 denotes the value of SP when all the three terms in the equation are zero. The cavity term is usually taken as the product of the solute Van der Waals molar volume (V_I) and the square of the Hildebrand solubility parameter (δ) of the solvent. The dipolar term is the product of the solute π^* and the solvent π^*. The π^* parameter measures a combination of dipolarity/polarizability of a compound. The hydrogen bonding (HB) terms are written as a cross-product of the solute α and the solvent β (type B HB) and the product of the solute β and the solvent α (type A HB). The parameters α and β measure HB donor acidity and HB acceptor basicity of the compound, respectively. In chromatographic retention, SP in Eq. 1 denotes a logarithmic capacity factor and the relevant LSER is given by

$$\log k' = \log k'_0 + M(\delta_s^2 - \delta_m^2)V_{I,2}/100 + S(\pi^*_s - \pi^*_m)\pi^*_2 + B(\alpha_s - \alpha_m)\beta_2 + A(\beta_s - \beta_m)\alpha_2 \quad (2)$$

where the subscript 2 designates a solute property, the subscripts s and m denote the stationary and mobile phases, respectively, and the coefficients M, S, B and A are the fitting parameters.

When a system with a fixed pair of mobile and stationary phases is considered, Eq. 2 is reduced to

$$\log k' = \log k'_0 + mV_{I,2}/100 + s\pi^*_2 + b\beta_2 + a\alpha_2 \quad (3)$$

The $\log k'_0$ term includes the volume phase ratio and dipolar interactions between the solute and the chromatographic phases when π^*_2 is zero. The coefficients m, s, b and a are obtained by multiple linear regression of $\log k'$ *vs.* the solute parameters. The sign and magnitude of the coefficients measure the direction and relative strength of different types of solute–stationary (and mobile) phase interactions affecting retention for a given pair of mobile–stationary phase conditions. When capacity factors for a set of solutes measured on a number of different stationary phase columns using a mobile phase of the same composition are examined, the mobile phase parameters in Eq. 2 (δ^2_m, π^*_m, α_m and β_m) are fixed. Then any variations in the coefficients m, s, b and a with different columns are due to variations in the properties (δ^2_s, π^*_2, α_s and β_s) of the stationary phases. Modification of the stationary phase by the mobile phase components varies with the type of bonded functional group and bonding density in a given mobile phase. However, when the mobile phase is constant for all the columns studied, what we measure is the actual bonded phase environment which really controls retention. Different magnitudes of these coefficients for different columns are indicative of the differences in the extent of contributions to retention from various types of interactions of the stationary phase with the solute. The values of the coefficients m, s, b and a can therefore be regarded as measures of the relative strength of corresponding interaction properties of the column in a mobile phase of given composition. Eq. 2 does not contain an explicit term for dispersive interactions between the solute and the chromatographic phases. It has been shown that the $M(\delta_s^2 - \delta_m^2)V_{I,2}/100$ term is in fact a combination of cavity formation and dispersive interaction [15]. Different values of the coefficient m for different columns should indicate the relative magnitude of the Hildebrand solubility parameter and dispersive interaction strength of various stationary phases. Similarly, the coefficient s is indicative of the relative magnitude of dipolarity, and the coefficients b and a are indicative of the relative strength of HB donating and HB accepting capability of various stationary phases, respectively.

This approach has been found useful for the characterization of the chromatographic prop-

Table 1
Properties of the selected compounds (from ref. 23)

No.	Compound	$V_1/100$	π^*	β	α
1	Acetophenone	0.690	0.90	0.49	0.03
2	Propiophenone	0.788	0.88	0.49	0
3	Butyrophenone	0.886	0.86	0.49	0
4	Naphthalene	0.753	0.70	0.15	0
5	2-Phenylethanol	0.732	0.97	0.55	0.33
6	Benzyl alcohol	0.634	0.99	0.52	0.35
7	Phenol	0.536	0.72	0.33	0.61
8	1-Naphthol	0.798	0.82	0.33	0.61
9	*p*-Chlorophenol	0.626	0.72	0.23	0.69
10	*p*-Cresol	0.634	0.68	0.34	0.58
11	Chlorobenzene	0.581	0.71	0.07	0
12	Bromobenzene	0.624	0.79	0.06	0
13	Nitrobenzene	0.631	1.01	0.30	0
14	Benzene	0.491	0.59	0.10	0
15	Toluene	0.592	0.55	0.11	0
16	Ethylbenzene	0.687	0.53	0.12	0
17	Pyridine	0.470	0.87	0.44	0
18	Aniline	0.562	0.73	0.50	0.16
19	4-Methylpyridine	0.570	0.84	0.47	0
20	*p*-Bromoaniline	0.695	0.79	0.40	0.20
21	*p*-Toluidine	0.660	0.69	0.52	0.13
22	Phenetole	0.727	0.69	0.30	0
23	Benzaldehyde	0.606	0.92	0.44	0
24	Ethyl benzoate	0.736	0.76	0.39	0

erties of some stationary phases for use in NPLC (silica and alumina) [15] and RPLC (octadecyl-bonded silica and octadecyl-bonded alumina) [22]. Once these interaction constants, which are analogous to Rohrschneider and McReynolds constants for GLC stationary phases, have been determined for a wide variety of columns, the task of choosing the best column and optimizing for a given separation will be much easier. We were careful to choose 24 compounds of widely varying chemical properties to ensure that the results will be broadly applicable to everyday separation problems. Values of the Van der Waals molar volume and Kamlet–Taft solvatochromic parameters for the solutes are given in Table 1.

3. Experimental

Retention measurements were made with an HPLC system composed of a Shimadzu LC-9A pump, a Rheodyne Model 7125 injector equipped with 20-μl sample loop, a Hitachi L-4200 UV–Vis detector set at 254 nm and a Hewlett-Packard 3396 Series II integrator. Columns investigated were Nucleosil C_8 (250 × 4.6 mm I.D., 10 μm) (Alltech, Deerfield, IL, USA), Hypersil CPS-1 (150 × 4.6 mm I.D., 5 μm) (Alltech), Ultrasphere CN (150 × 4.6 mm I.D., 5 μm) (Beckman Instruments, Fullerton, CA, USA), Supelcosil LC-DP (phenyl) (250 × 4.6 mm I.D.) (Supelco, Bellefonte, PA, USA) and μBondapak C_{18} and μBondapak CN (300 × 3.9 × 300 I.D., 10 μm) (Waters–Milipore, Milford, MA, USA). Some of the properties of these columns, as supplied by the manufacturers, are given in Table 2. The column was placed in a water-jacket and the temperature was controlled at 30 ± 0.1°C. The eluents used were methanol–pH 7 buffer or acetonitrile–pH 7 buffer in different proportions. The eluent flow-rate was 1 ml min^{-1}. An aliquot of 10% aqueous sodium

Table 2
Properties of the columns as supplied by the manufacturers

Column No.	Stationary phase	Ligand	Surface area (m^2 g^{-1})	Carbon loading (%)[a]	Bonding density[b] (μmol m^{-2})	End-capped
I	μBondapak C_{18}	C_{18}	330	10 (0.030)	1.43	Yes
II	Nucleosil C_8	C_8	350	8 (0.023)	2.15	–
III	Supelcosil LC-DP	Diphenylmethyl	170	–	–	–
IV	Ultrasphere CN	Cyanopropyl	200	4.4 (0.022)	3.31	Yes
V	Hypersil CPS-1	Cyanopropyl	170	3.5 (0.020)	3.06	No
VI	μBondapak CN	Cyanopropyl	330	6.0 (0.018)	2.82	Yes

[a] Values in parentheses are %C m^{-2}.
[b] Bonding densities in μmol m^{-2} were calculated using an equation by Berendsen and De Galan [24].

nitrate was injected to determine the column void volume. The capacity factors were calculated from the mean retention times of triplicate injections. The relative standard deviation for three replicate retention time measurements was usually less than 1.5% for all solutes. In order to check the stability of the column, we injected toluene before and after a day's measurements and found that the retention times of toluene were reproducible to within 1% for the day. This check was done every day and we observed that the retention times of toluene agreed to within 2% before and after the whole series of experiments.

All the solutes were of analytical-reagent grade from Aldrich (Milwaukee, WI, USA) and used as received. Methanol and acetonitrile were of HPLC grade and from Ajax (Auburn, Australia).

4. Results and discussion

In order to see how to arrive at the best LSER describing retention on various stationary phases, let us examine the capacity factors for the 24 test solutes on a μBondapak C_{18} column in methanol–water (20:80) as an example.

$$\log k' = -0.57(\pm 0.24) + 3.35(\pm 0.27)V_I/100 - 0.003(\pm 0.270)\pi^* - 1.70(\pm 0.23)\beta - 0.47(\pm 0.12)\alpha \quad n = 24,\ r = 0.961,\ \text{S.D.} = 0.131 \quad (4)$$

The coefficient s for the π^* parameter is statistically zero, indicating that dipolar interactions do not affect the retention. The π^* parameter was therefore excluded in the following regression. The resulting triple regression equation is given by

$$\log k' = -0.57(\pm 0.17) + 3.35(\pm 0.26)V_I/100 - 1.70(\pm 0.23)\beta - 0.47(\pm 0.12)\alpha \quad n = 24,\ r = 0.961,\ \text{S.D.} = 0.128 \quad (5)$$

In further regressions for log k' on various columns, other statistically insignificant parameter(s), if there are any, were excluded in a similar manner. Results of multiple linear regressions of log k' on the six columns in aqueous methanol and acetonitrile mixtures *vs.* the solute properties are given in Tables 3 and 4. The correla-

Table 3
Calculated coefficients in regressions of log k' on the six columns in aqueous methanol *vs.* solute parameters

Column[a]	Organic modifier (%, v/v)	Log k'_0	m	s	b	a	r
I	20	−0.57	3.35	NS[b]	−1.70	−0.47	0.961
	40	−0.47	2.51	NS	−1.68	−0.37	0.980
II	20	−0.33	3.16	NS	−1.38	−0.63	0.934
	40	−0.25	2.19	NS	−1.32	−0.48	0.956
III	20	−0.58	3.10	NS	−1.17	−0.47	0.927
	40	−0.53	2.28	NS	−1.18	−0.33	0.978
IV	20	−0.56	2.50	NS	−1.33	NS	0.940
	40	−0.44	1.70	NS	−1.15	NS	0.965
V	20	−0.55	2.15	NS	−1.18	NS	0.930
	40	−0.57	1.53	NS	−1.15	NS	0.971
VI	20	−0.61	2.09	NS	−1.11	−0.12	0.926
	40	−0.45	1.31	NS	−0.90	−0.08	0.927

[a] Column designations as in Table 2.
[b] NS = not significant.

Table 4
Calculated coefficients in regressions of log k' on the six columns in aqueous acetonitrile *vs.* solute parameters

Column[a]	Organic modifier (%, v/v)	Log k'_0	m	s	b	a	r
I	20	−0.34	3.03	−0.22	−1.93	−0.41	0.994
	40	−0.06	1.65	−0.35	−1.14	−0.36	0.992
II	20	−0.11	2.78	−0.10	−1.80	−0.47	0.981
	40	−0.13	1.41	−0.17	−1.07	−0.43	0.984
III	20	−0.32	2.98	−0.14	−1.81	−0.29	0.992
	40	−0.17	1.74	−0.18	−1.26	−0.30	0.990
IV	20	−0.32	2.32	NS[b]	−1.64	−0.10	0.980
	40	−0.18	1.39	NS	−1.19	−0.15	0.977
V	20	−0.40	2.22	NS	−1.60	NS	0.979
	40	−0.24	1.27	NS	−1.09	−0.13	0.979
VI	20	−0.45	1.95	NS	−1.28	−0.11	0.978
	40	−0.20	1.11	NS	−0.92	−0.13	0.983

[a] Column designations as in Table 2.
[b] NS = Not significant.

tion coefficients are mostly close to unity, indicating that the retention behaviour of the solutes on the RPLC columns is well represented by the LSER model.

In order to gain an understanding of the factors responsible for the differences in retention properties of various RPLC columns, let us examine the sign and magnitude of the coefficients in Tables 3 and 4. It is seen that m and b are much larger than a and s. The coefficients s for all six columns with aqueous methanol and for three cyano-bonded columns with aqueous acetonitrile are statistically zero, and are very small for non-polar alkyl- and phenyl-bonded phases with aqueous acetonitrile, indicating that the solute dipolarity plays only a very minor role in determining retention and selectivity and in turn the column dipolarity is not a significant factor in characterizing the column. Other workers have made similar observations on the relative unimportance of the column polarity in RPLC [16,17]. In further discussions we therefore consider only the coefficients m, b and a in detail.

It is seen from the signs of the coefficients that increasing solute size (V_I) causes an increase in retention, *i.e.*, free energy concepts favour solute transfer from the more cohesive mobile phase to the less cohesive stationary phase. The magnitude of the coefficient m decreases with increasing content of organic modifier on a given column. If δ^2 of the stationary phase does not change with changes in the mobile phase composition, m should be proportional to δ^2 of the mobile phase. As water is more cohesive (δ = 23.4 $cal^{1/2}$ $cm^{-3/2}$) than methanol (14.3 $cal^{1/2}$ $cm^{-3/2}$), acetonitrile (11.75 $cal^{1/2}$ $cm^{-3/2}$) and free-form analogues of the stationary phases (δ = 8.02 $cal^{1/2}$ $cm^{-3/2}$ for *n*-hexadecane, 7.54 $cal^{1/2}$ $cm^{-3/2}$ for *n*-octane, 8.64 $cal^{1/2}$ $cm^{-3/2}$ for *n*-propylbenzene and 10.17 $cal^{1/2}$ $cm^{-3/2}$ for butyronitrile), the cavity-forming process in the solvent becomes decreasingly endoergic with decreasing water content.

As the coefficient m indicates a combination of cohesiveness and dispersive interaction strength of the bonded moiety, it is expected to increase with increasing solubility parameter and the amount of the ligand per unit area of the stationary phase surface in a mobile phase of a

given composition. The magnitude of m for an ODS column is greater [$\delta = 8.02$ cal$^{1/2}$ cm$^{-3/2}$, %C m$^{-2} = 0.03$; *e.g.*, $m = 2.51$ in methanol–water (40:60)] than that for an octyl column [$\delta = 7.54$ cal$^{1/2}$ cm$^{-3/2}$, %C m$^{-2} = 0.023$; *e.g.*, $m = 2.19$ in methanol–water (40:60)].

It is interesting to compare the coefficient m with the solvophobic column strength J of Snyder and co-workers [3,6]. They used a set of 22 solutes of widely differing chemical properties but compounds such as acids and bases that were likely to exhibit chemical selectivity were generally excluded. They combined the phase-volume ratio and the polarity of the stationary phase into J. As they excluded the solutes that can undergo HB interactions with the stationary phase, the polarity contribution to J is from solute–stationary phase dipole–dipole and dipole–induced dipole interactions. It has been shown above and from observations by other workers [16,17] that these types of interactions are unimportant in RPLC retention processes. In view of the negligible contribution from the dipolar interaction strength of the stationary phase, the column strength measured by J is mainly solvophobic in nature and is expected to vary in a parallel direction with the coefficient m, which represents, in essence, the non-polar solvophobic interaction strength of the given column. The coefficient m for an ODS column is greater than that for an octyl column and this is in agreement with observations made on Zorbax columns by Snyder and co-workers [3,6] and Ying and Dorsey [9]. Snyder and co-workers [3,6] also noted that retention in RPLC increases with increase in the amount and surface area of bonded phases. The stationary phase volumes decrease in the order $C_{18} > C_8$, but the bonded-phase surface area (and bonding density) tends to increase from C_{18} to C_8. Their J value is a combination of stationary phase volume and stationary phase surface area when the polarity of the stationary phase is unimportant. In view of this, it seems likely that the %C m^{-2} of the stationary phase, rather than bonding density in μmol m^2, better represents the combination of volume and surface area of the bonded ligand. The carbon percentage per unit surface area of our ODS column, which has a greater m value, is greater than that of the octyl column. They also observed that a more polar, cyanopropyl-bonded phase has a smaller J value than C_{18} and C_8 columns. The coefficients m for all cyano columns studied are smaller than those of ODS and octyl columns. For different brands of the cyano-bonded phase columns, the value of m increases with increasing %C m^{-2} (Table 2) in both methanol- and acetonitrile-modified mobile phases.

It is well known that the stationary phase is preferentially solvated by the organic component in the mobile phase and the extent of this solvation is different for different modifiers [25–28]. Different values of the coefficients m for the same column are thus observed in methanol- and acetonitrile-modified eluents.

Opposing this effect, increases in HB donor acidity (α) and HB acceptor basicity (β) lead to lower log k' values because the solutes have greater affinities for the more strongly hydrogen bonding aqueous mobile phase. Values of HB donor acidity and HB acceptor basicity for aqueous organic mobile phases are generally greater (10–90 vol.-% methanol, $\alpha = 1.17$–1.02 [29], $\beta = 0.25$–0.60 [30]) than free-form analogues of the stationary phases (alkanes, $\alpha = 0$, $\beta = 0$; butyronitrile, $\alpha = 0$, $\beta = 0.31$ [31]). The magnitude of the coefficient b is greater than that of the coefficient a. This indicates that type A HB interactions between the solute and the mobile phase predominate over type B HB interactions. Comparison of the magnitude of each coefficient indicates that the most important factor influencing RPLC retention for the solutes studied is the endoergic cavity formation term. The HB terms are less important and contributions to retention from the type A and type B HB vary with the type of bonded functional group and with brand for the cyano-bonded phases. The negative sign of both the coefficients b and a also indicates that both type A and type B HB interactions occur mainly between the solute and the mobile phase. If HB interactions of the solute with the bonded moiety of the stationary phases were greater than those with the mobile phase, the retention must have been

increased with increasing solute α and β values.

The magnitudes of the coefficients b and a vary with the type of bonding moiety of the column and with brand for stationary phases with the same ligand. If interactions between the solute and the mobile phase dominate retention, what is causing the magnitude of those coefficients (*i.e.*, retention properties) for different brands of cyano-bonded column to vary? As discussed above, the coefficient b, for example, is a cross-product of a constant (B) and the difference in properties of the stationary phase and the mobile phase. It is well known that end-crapping cannot block the surface silanol groups completely. If there is any variability in the concentration of surface silanol groups on the initial silica, which might affect the HB properties of the stationary phase (α_s and β_s), this will cause these ostensibly equivalent columns to show different HB interaction strengths toward the solute, hence yielding different values of coefficients b and a for different brands.

Comparison of the magnitude of the coefficients b (the HB donating acidity) for non-polar alkyl- and phenyl-bonded phases with those for polar cyano-bonded phases indicates that in general b is smaller for polar cyano-bonded phases than for non-polar phases. It seems that polar cyano-bonded phases are better solvated owing to stronger dipolar and HB interactions of cyano groups with the mobile phase components than non-polar alkyl- and phenyl-bonded phases, so residual silanol groups on alkyl- and phenyl-bonded phases are more exposed to solutes and the HB interactions between the solutes and the stationary phase become more significant. This is in agreement with the observation that retention and excessive peak tailing for basic solutes due to strong HB interactions are less prominent on cyano-bonded phase columns [2]. In both methanol- and acetonitrile-modified mixtures the magnitude of b for the stationary phases becomes smaller with increasing amount of organic modifier. This is because the stationary phase is more solvated at higher organic content mobile phases, hence residual silanol groups on the stationary phase might be less exposed to solutes and the HB interaction between the solutes and the stationary phase becomes less significant.

Similar trends in variation of the coefficient a (HB accepting basicity) for columns with the type of bonded ligand and brand in the case of stationary phases having the same ligand are also observed. However, as can be seen from the much smaller magnitudes of a relative to those of b, the HB basicity of the stationary phase is of minor importance in characterizing the column. Similar observations of unimportance of the $a\alpha$ terms have also been made by other workers [16,17].

It might be better to present the coefficients for every column as the characteristic column constants after multiplying by 100 for the sake of convenience of presentation. This will also make the values of the column constants have an order similar to widely used Rohrschneider and McReynolds constants for GLC phases. As we already know well in which direction a given type of interaction between the solute and the stationary phase affects retention, we may also remove the sign for the coefficients. The characteristic interaction constants for the six stationary phases observed in mobile phases containing 40% of organic modifier are given in Table 5. The log k'_0 values are also included as this term includes the volume phase ratio and dipolar interactions between the solute and the stationary phases when π^* is zero and might be useful in characterizing other characteristics of the stationary phase than characterized by the interaction constants. This term is necessary if one wants to predict log k' for a solute with a given combination of the mobile and stationary phase.

By examining the interaction constants for the six columns in Table 5 we can infer the following practically significant results. The much greater magnitudes of the coefficient m and b in both methanol- and acetonitrile-modified mobile phases indicates that the more important interaction characteristics of the column are cavity/dispersion and type A hydrogen bonding, and solute dipolarity and HB acidity are not effectively differentiated in RPLC. In both mobile phases, the coefficients m for ODS-, octyl- and phenyl-bonded phases columns are greater than those for cyano-bonded phases. This indicates that the first three stationary phases have greater discriminating capabilities in the separation of

Table 5
Characteristic interaction constants for the six columns

Mobile phase	Column[a]	Log k'_0	m	b	a	s
Methanol–water (40:60)	I	47	251	168	37	NS[b]
	II	25	219	132	48	NS
	III	53	228	118	33	NS
	IV	44	170	115	NS	NS
	V	57	153	115	NS	NS
	VI	45	131	90	8	NS
Acetonitrile–water (40:60)	I	6	165	114	36	35
	II	23	141	107	43	17
	III	17	174	126	30	18
	IV	18	139	119	15	NS
	V	24	127	109	13	NS
	VI	20	111	92	13	NS

[a] Column designations as in Table 2.
[b] NS = Not significant.

compounds that differ in their size but have similar HB donor and acceptor strengths. In practice, the retention of a solute in RPLC on a given column is controlled simultaneously by all types of interactions. We believe, however, that it is safe to say that if the two solutes have a significant difference in size then the ODS column will produce the greatest chromatographic selectivity. With methanol–water (40:60) as mobile phase, the solute HB basicity is best discriminated by the ODS column. Although minor, the better discrimination of the HB acidity of solutes can be achieved by the three non-polar columns than cyano-bonded columns. The interaction constants for the six columns are, in general, greater in a methanol- than an acetonitrile-modified mobile phase, indicating that differentiation of more subtle differences in the solute properties may be achieved by using a methanol-modified mobile phase.

In conclusion, for RPLC columns the variabilities in the retention properties of apparently equivalent columns have caused many difficulties for practising chromatographers in that choosing the best column for a given separation is most often a trial-and-error process. However, these variabilities can now be a very useful feature in choosing the best column for a given separation. Further, these interaction constant can be readily calculated by simply regressing retention data for a set of solutes *vs.* the solute parameters based on the LSER. Although the four interaction strength constants (m, s, b and a) are, of course, not as general as Rohrschneider and McReynolds constants, we believe they would give helpful information for choosing the best column for a given separation among a number of nominally equivalent columns and columns with different bonded functionalities. In order to ensure that these measures of column strengths are broadly applicable to everyday separation problems, interaction constants for a greater number of RPLC columns with more diverse bonding ligands from various manufacturers than used in this study need to be determined. Work for utilizing these interaction constants in selecting and optimizing separations of practical samples is in progress.

5. Acknowledgements

This work was supported in part by the Non-Directed Research Fund, Korea Research Foundation (1992), and in part by the Korea Science and Engineering Foundation.

6. References

[1] M.F. Delaney, A.N. Papas and M.J. Walters, *J. Chromatogr.*, 410 (1987) 31.
[2] R.M. Smith and S.L. Miller, *J. Chromatogr.*, 464 (1989) 297.
[3] P.E. Antle, A.P. Goldberg and L.R. Snyder, *J. Chromatogr.*, 321 (1985) 1.
[4] H. Engelhardt, H. Low and W. Gotzinger, *J. Chromatogr.*, 544 (1991) 371.
[5] K. Unger (Editor), *Packings and Stationary Phases in Chromatographic Techniques*, Marcel Dekker, New York, 1990.
[6] P.E. Antle and L.R. Snyder, *LC*, 2 (1984) 840.
[7] J.J. DeStefano, J.A. Lewis and L.R. Snyder, *LC · GC*, 10 (1992) 130.
[8] J.L. Glajch, J.C. Gluckman, J.G. Charikofsky, J.M. Minor and J.J. Kirkland, *J. Chromatogr.*, 318 (1985) 23.
[9] P.T. Ying and J.G. Dorsey, *Talanta*, 38 (1991) 237.
[10] W.O. McReynolds, *J. Chromatogr. Sci.*, 8 (1970) 685.
[11] M.J. Kamlet, J.L.M. Abboud and R.W. Taft, *Prog. Phys. Org. Chem.*, 13 (1981) 591.
[12] M.J. Kamlet and R.W. Taft, *Acta Chem. Scand., Ser. B*, 39 (1985) 611.
[13] M.J. Kamlet, R.W. Taft, P.W. Carr and M.H. Abraham, *J. Chem. Soc., Faraday Trans. 1*, 78 (1982) 1689.
[14] J.E. Brady, D. Bjorkman, C.D. Herter and P.W. Carr, *Anal. Chem.*, 56 (1984) 278.
[15] J.H. Park and P.W. Carr, *J. Chromatogr.*, 465 (1989) 123.
[16] P.C. Sadek, P.W. Carr, R.M. Doherty, M.J. Kamlet, R.W. Taft and M.H. Abraham, *Anal. Chem.*, 57 (1985) 2971.
[17] P.W. Carr, R.M. Doherty, M.J. Kamlet, R.W. Taft, W. Melander and Cs. Horváth, *Anal. Chem.*, 58 (1986) 2674.
[18] J.H. Park, P.W. Carr, M.H. Abraham, R.W. Taft, R.M. Doherty and M.J. Kamlet, *Chromatographia*, 25 (1988) 373.
[19] J.H. Park, M.D. Jang and S.T. Kim, *Bull. Korean Chem. Soc.*, 11 (1990) 297.
[20] M.-M. Hsieh and J.G. Dorsey, *J. Chromatogr.*, 631 (1993) 63.
[21] J.H. Park, Y.K. Lee and J.B. Donnet, *Chromatographia*, 33 (1992) 154.
[22] J.H. Park, *Bull. Korean Chem. Soc.*, 11 (1990) 568.
[23] M.J. Kamlet, R.M. Doherty, M.H. Abraham, P.W. Carr, R.F. Doherety and R.W. Taft, *J. Phys. Chem.*, 91 (1987) 1996.
[24] G.E. Berendsen and L. de Galan, *J. Chromatogr.*, 1 (1978) 561.
[25] R.M. McCormick and B.L. Karger, *Anal. Chem.*, 52 (1980) 2249.
[26] R.M. McCormick and B.L. Karger, *J. Chromatogr.*, 199 (1980) 259.
[27] C.R. Yonker, T.A. Zwier and M.F. Burke, *J. Chromatogr.*, 241 (1982) 257.
[28] C.R. Yonker, T.A. Zwier and M.F. Burke, *J. Chromatogr.*, 241 (1982) 269.
[29] J.H. Park, M.D. Jang, D.S. Kim and P.W. Carr, *J. Chromatogr.*, 513 (1990) 107.
[30] T.M. Krygowski, P.K. Wrona and U. Zielkowska, *Tetrahedron*, 41 (1985) 4519.
[31] M.J. Kamlet, J.L.M. Abboud, M.H. Abraham and R.W. Taft, *J. Org. Chem.*, 49 (1983) 2877.

ELSEVIER

Journal of Chromatography A, 664 (1994) 159–167

JOURNAL OF CHROMATOGRAPHY A

Structural features affecting chiral discrimination of terpene derivatives on a carbamated amylose stationary phase

Saleh Abu-Lafi[a], Marina Sterin[a], Shulamit Levin*[,a], Raphael Mechoulam[b]

[a]*Pharmaceutical Chemistry Department, School of Pharmacy, P.O. Box 12065, Hebrew University of Jerusalem, Jerusalem 91120, Israel*

[b]*Department of Natural Products, School of Pharmacy, P.O. Box 12065, Hebrew University of Jerusalem, Jerusalem 91120, Israel*

(First received November 1st, 1993; revised manuscript received December 9th, 1993)

Abstract

The chiral discrimination of enantiomeric derivatives of α-pinene was studied using amylose tris(3,5-dimethylphenylcarbamate) as a chromatographic stationary phase. The effect of structural features of these enantiomeric pairs on their chromatographic resolution was systematically studied to understand further the correlation between these features and chiral discrimination by the carbamated amylose. Structural analysis by molecular mechanics indicated that the conformation of the α-pinene skeleton was preserved with substitution in all its derivatives. However, in spite of the rigidity of the molecular backbone of these molecules, their resolution capabilities were different. Apparently, the site of the hydrogen-bonding substituents affected chiral discrimination by the stationary phase rather than conformational changes. Separation was achieved in spite of the fact that none of the members in the series had an aromatic moiety, and therefore π–π interactions with the stationary phase were insignificant. Hence it was concluded that the most important interaction of the terpene derivatives with the carbamated amylose was hydrogen bonding.

1. Introduction

Terpenes are well known natural products in plant leaves, flowers and fruits [1]. One of the most widespread bicyclic monoterpenes is α-pinene, whose (+)- and (−)-enantiomers are both found in nature. It is used industrially as a solvent (turpentine) and as starting material in the manufacture of α-terpinol and camphor [1]. The alcoholic derivative, *cis*-verbenol is found in the oleo-resin of the East African tree *Boswellia carterii*, and its corresponding ketone, verbenone, is a major constituent of Spanish verbena oil [1]. The (−)- and (+)-verbenone (via verbenol) were the starting materials for the first synthesis of the (−)- and (+)-enantiomers of Δ^1-tetrahydrocannabinol (Δ^1-THC). The (−)-enantiomer is the major psychoactive constituent of *Cannabis sativa* and its preparations (marijuana, hashish, etc.) [2].

The enantiomeric purity of the terpenic derivatives dictates the degree of purity of the final product of the chiral synthesis of cannabinoids. Therefore, it is essential to ensure that optically pure terpenoids are used in the syntheses. An example is the synthetic (3*S*,4*S*)-1,1-dimethylheptyl-Δ^6-THC (HU-211), which is potentially an antiemetic agent [3] and acts as a

* Corresponding author.

0021-9673/94/$07.00
SSDI 0021-9673(93)E0022-M

functional N-methyl-D-aspartate (NMDA) receptor blocker [4] without producing psychotropic effects. It also has been found that HU-211 has cerebroprotective effects after head trauma in rats [5]. The corresponding (3*R*, 4*R*)-enantiomer (HU-210) is one of the most potent psychotropic cannabinoids known [6]. The total synthetic route of these two enantiomers, using commercial (+)- and (−)-α-pinene as a starting material, involves 4-oxomyrtenyl pivalate and its corresponding alcohol as intermediates [7] (see Fig. 1). The minimum requirement for optical purity of HU-211 (and its precursors) should be greater than 99.8 enantiomeric excess (e.e.), in order to prevent psychotropic effects.

Stereoselective analysis of enantiomeric drugs using liquid chromatography has been the focus of intensive research in recent years [8]. Separations of enantiomers and diastereomers of terpenes and their alcohols by liquid chromatography, using cyclodextrin inclusion complexes in the mobile or in the stationary phase, have been reported [9,10]. The inclusion capability of cyclodextrin is frequently compared with that of amylose, which can also form inclusion complexes, although more flexible ones [11]. Therefore, the resolution of enantiomeric terpenes has been attempted on an amylose-based stationary phase as well. A successful preliminary resolution of two derivatives of α-pinene was reported in a previous paper [12]. A comparative study of their chromatographic behaviour was made to shed more light on the mechanism of chiral discrimination in the amylose stationary phase. The understanding of chiral discrimination by the stationary phase is essential in order to use a more rational approach in the optimization of the separation.

Polysaccharides such as amylose consist of linked D-(+)-glucose units with α(1→4)-glycosidic linkages that form a helical structure. Derivatives of amylose, particularly carbamates, have exhibited a relatively high degree of chiral discrimination [13]. It has been proposed that the mechanism of chiral discrimination by amylose involves stereoselective inclusion of enantiomers based on hydrogen bonding and dipole–dipole interactions with the CO and NH portions, in addition to π–π interactions with the phenylcarbamate [13,14]. Most of the studies of chiral discrimination by the carbamated polysaccharides have involved solutes with aromatic fragments [15]. We demonstrate in this work that the efficient resolution of non-aromatic mole-

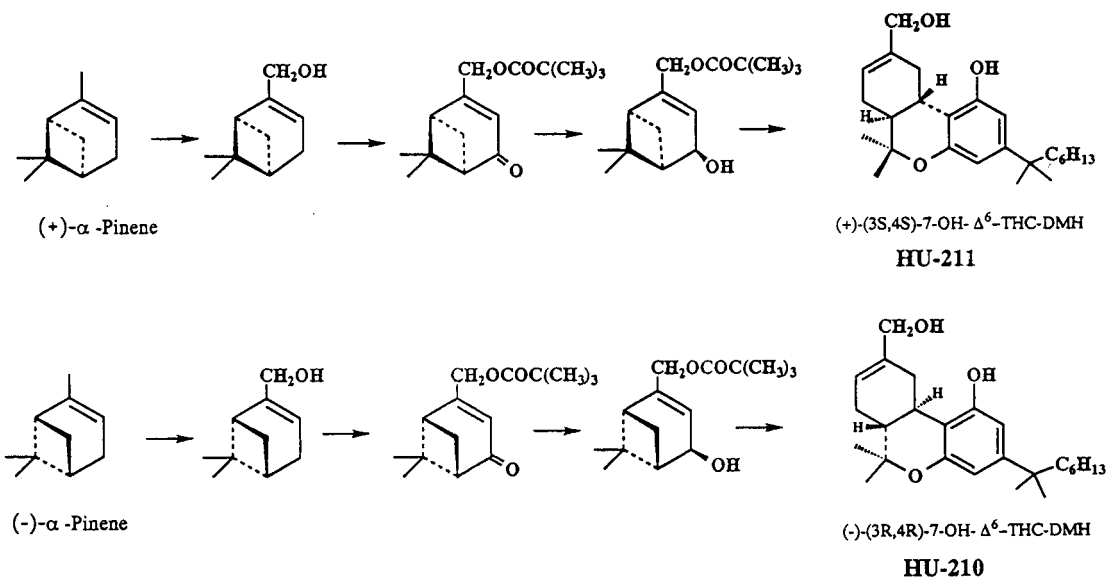

Fig. 1. Total step-synthesis of HU-210 and HU-211.

cules, such as terpenoids, can also be obtained using a carbamated polysaccharide stationary phase. Such a resolution indicates that in some instances the contribution of $\pi-\pi$ interactions to chiral discrimination might not be as significant as perceived generally. Another example of the resolution of aliphatic enantiomers by a substituted polysaccharide stationary phase, benzoylcellulose, was reported by Francotte and Wolf [16].

In addition to the chromatographic studies, conformations of the terpenic enantiomers were analysed by molecular mechanics to confirm that the rigid skeleton of α-pinene is preserved throughout the entire series.

2. Experimental

2.1. Instrumentation and materials

The HPLC analysis was performed using an HP1050 instrument (Hewlett-Packard, Palo Alto, CA, USA) equipped with a diode-array UV detector, an HPCHEM data station, and a ThinkJet printer. A Rheodyne (Cotati, CA, USA) injection valve was used, equipped with a 20-μl loop. A ChiralPak AD chiral column (250 mm × 4.6 mm I.D.; 10 μm film thickness (Daicel Chemical Industries, Tokyo, Japan) was used.

HPLC-grade solvents (ethanol or 2-propanol) were purchased from Lab-Scan (Dublin, Ireland) and α-pinene and myrtenol from Aldrich (Milwaukee, WI, USA). The other terpenic pairs were prepared as described previously [7].

2.2. Procedure of analysis

A flow-rate of 1 ml/min at room temperature was used in all the experiments. Each run was monitored at two wavelengths simultaneously, 254 and 240 nm. At the end of a session the column was washed with ethanol–hexane (20:80). When regeneration was needed, the column was washed with pure ethanol. When not in use, the column was stored in 2-propanol–hexane (5:95).

2.3. Computational method

Construction and treatment of the terpene structures were performed with the InsightII/Discover 2.0.0 software package from BIOSYM Technologies (San Diego, CA, USA). All calculations were carried out on a Silicon Graphics 4D/310VGX workstation. The following molecular mechanics (MM) potential energy function was used:

$$E_{\text{Tot.}} = E_s + E_q + E_f + E_{\text{VWD}} + E_{\text{elec}} \quad (1)$$

where E_s is the stretching energy, E_q is the bending energy, E_f is the dihedral (torsion) energy, E_{VWD} is the Van der Waals energy and E_{elec} is the electrostatic energy. The force field used in the calculations was CVFF (consistent valence force field). All parameters defining the geometry of the molecule were modified by small increments until the overall structural energy reached a local minimum. First, 1000 iterations were made in the steepest descent algorithm, then it was transferred to the conjugate gradient minimizer until the convergence criterion had been achieved.

3. Results and discussion

Nine pairs of bicyclic monoterpenes that belong to the α-pinene series were studied. The structural skeleton of the α-pinene moiety according to the terpenic numbering system is shown in Fig. 2. The structures of the nine bicyclic monoterpenes are presented in Fig. 3. A

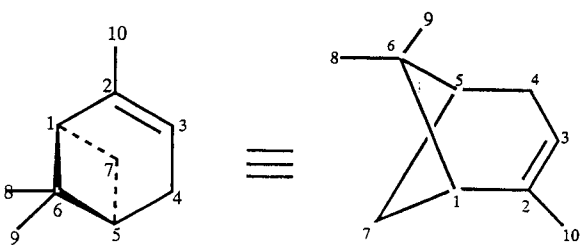

(+)-α -Pinene

Fig. 2. Structure of α-pinene according to the terpenic numbering system.

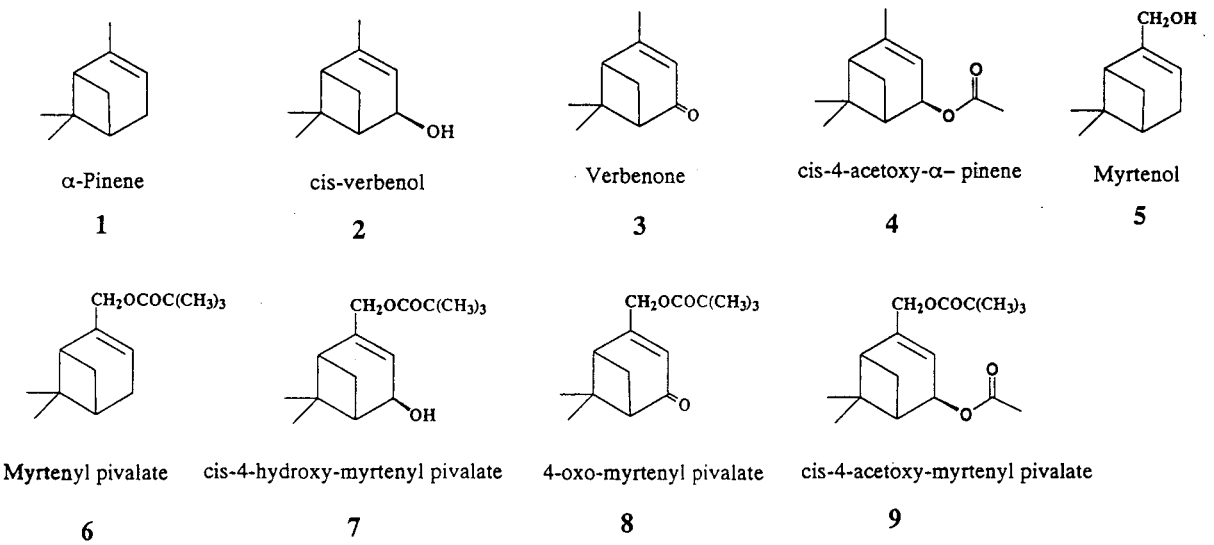

Fig. 3. Structures of the nine enantiomeric bicyclic monoterpenes used.

major question in this study was what structural features are essential to the chiral discrimination of these solutes by the amylose tris(3,5-dimethylphenylcarbamate). Conformational analysis by molecular mechanics was performed parallel to the chromatographic studies to answer this question.

3.1. Structural analysis

Systematic and comparative studies of the structural features of solutes that give rise to chiral discrimination can be greatly advanced by using molecular modelling of the enantiomers. The feature common to the monoterpenes in this study is the α-pinene skeleton, and therefore the first step was to simulate the most stable conformation of α-pinene. The structure obtained was used as a starting point for the construction of the other terpenes. All the energy-minimized structures of the substituted pinenes were superimposed on α-pinene, which was used as a reference structure, to examine whether there was a change in the conformation of the skeleton as a result of substitution. A quantitative criterion of the deviation between two different structures or their portions, when superimposed on each other, is given by the RMS values. These values are the least-squares fit between the two sets of *xyz* coordinates (Å units) of the two superimposed structures, and are calculated as follows:

$$\mathrm{RMS} = \sqrt{\sum_{i=1}^{N} \frac{(x-x_0)^2 + (y-y_0)^2 + (z-z_0)^2}{N}} \quad (2)$$

where N is the number of atoms compared. Each structure in the terpenoid series was superimposed on the α-pinene skeleton, and the RMS deviations of the common ten heavy atoms were calculated. The results are given in Table 1. The very small RMS values (≤ 0.023) that were obtained for all the terpenes indicated that the conformation of the α-pinene skeleton was preserved. Therefore, differences in the chromatographic behaviour of the terpenic pairs can be correlated with the type and position of their substituents rather than with conformational changes.

3.2. Chromatographic analysis

Chiral discrimination by amylose tris(3,5-dimethylphenylcarbamate) was studied from the chromatographic behaviour of the nine pairs,

Table 1
Values of the root mean square (RMS) of the differences in *xyz* coordinates of the ten heavy atoms common to all the structures compared with (+)-α-pinene

No.	Solute	RMS (Å)
1	(+)-α-Pinene	000
2	(+)-*cis*-Verbenol	0.021
3	(+)-Verbenone	0.017
4	(+)-*cis*-4-Acetoxy-α-pinene	0.010
5	(+)-Myrtenol	0.017
6	(+)-Myrtenyl pivalate	0.020
7	(+)-*cis*-4-Hydroxymyrtenyl pivalate	0.022
8	(+)-4-Oxomyrtenyl pivalate	0.023
9	(+)-*cis*-4-Acetoxymyrtenyl pivalate	0.021

using ethanol or 2-propanol as the mobile phase additives to hexane. The parameters studied were the retention factor, k', selectivity factor, α, resolution, R_s, and elution order. Tables 2 and 3 summarize these results using 1–10% of ethanol and 1–10% of 2-propanol in hexane, respectively. The results show the following general behaviour: the alcoholic and ketonic derivatives (pairs 2, 3, 7 and 8) could be easily separated, whereas compounds without these groups, α-pinene (pair 1), myrtenyl pivalate (pair 6) and *cis*-4-acetoxy-α-pinene (pair 4), were not separated at all. Myrtenol (pair 5) was partially separated and so was 4-acetoxymyrtenyl pivalate (pair 9), but the latter also exhibited an inversion of the elution order from +, − to −, +.

Structural features required for chiral discrimination

Role of hydroxyl and carbonyl groups. On the basis of previous studies on amylose-based stationary phases [12–14], it is reasonable to assume that hydrogen bonding and dipole–dipole interactions between the solutes and the carbamate moieties are responsible for the chiral fit of the separated terpenes. Therefore, it was not surprising that the presence of hydroxyl or ketone groups permitted the resolution of the enantiomeric pairs 2, 3 and 7, 8, whereas α-pinene (pair 1) was not separated at all. The alcoholic derivatives were better resolved than the ketonic derivatives, as can be seen in Figs. 4 and 5. The difference between the ketones and the alcohols can be attributed to inductive effects of the methyl groups on the phenyl carbamate. As a result, the hydrogen bonding between the hydroxylic solute and CO is probably stronger than that between the ketonic solute with NH of the carbamate in the stationary phase. Although the enantiomeric terpenes had no aromatic portions, separation took place, *i.e.*, the contribution of $\pi-\pi$ interactions in the chiral discrimination process was insignificant. This observation highlights the domination of hydrogen bonding in the mechanism of chiral recognition.

Substitution of position 4 vs. position 10. The presence of hydroxyl group did not necessarily ensure separation. It was the combination of hydrogen bonding at the appropriate position that allowed their chiral discrimination. A comparison between the derivative with a hydroxyl group in the 4-position, *cis*-verbenol (pair 2), and that with a hydroxyl group in the 10-position, myrtenol (pair 5), reveals that the two solutes behaved differently. Myrtenol was only partially separated, whereas *cis*-verbenol was easily separated in both solvents. This difference indicates that the hydroxyl group in position 4 had an anchoring function in the chiral fit into the stationary phase. Further, esterification of position 10 did not affect the resolution, as shown by myrtenyl pivalate (pair 6), which was not resolved. On the other hand, the combination of pivalate ester in the 10-position and hydroxyl in the 4-position (*cis*-4-hydroxymyrtenyl pivalate, pair 7) yielded a high selectivity factor, relative to the other enantiomeric pairs of terpenes. This enantiomeric pair was resolved under all conditions studied here, even with a relatively high percentage of the alcoholic modifiers (10%) in the mobile phase, as shown in Fig. 4.

Blocking the hydroxyl group by acetylation. The hydroxyl group in the 4-position of *cis*-verbenol (pair 2) and in *cis*-4-hydroxymyrtenyl pivalate (pair 7) was blocked with an acetyl ester group.

Table 2
Chromatographic parameters of the nine pairs of bicyclic monoterpenes in Fig. 3 using various ethanol concentrations (1–10%, v/v) in the mobile phase

Terpenic pair No.	1%				2%				4%				6%				8%				10%			
	k'_+ [a]	k'_- [a]	α [b]	R_s [c]	k'_+	k'_-	α	R_s	k'_+	k'_-	α	R_s	k'_+	k'_-	α	R_s	k'_+	k'_-	α	R_s	k'_+	k'_-	α	R_s
1	Eluted as void peak																							
2	2.26	2.55	1.12	1.19	1.65	1.84	1.12	1.09	0.88	0.99	1.13	0.95	0.78	0.85	1.09	0.94	0.63	0.68	1.08	0.75	0.53	0.57	1.07	0.66
3	2.82	3.01	1.07	0.88	2.03	2.17	1.07	0.91	1.16	1.23	1.06	0.52	1.02	1.06	1.04	0.43	0.87	0.89	1.02	0.22	0.75	0.77	1.02	0.26
4	0.42	0.42	1.00	0.00	0.30	0.31	1.00	0.00																
5	2.46	2.61	1.06	0.61	1.61	1.71	1.06	0.72	0.84	0.90	1.06	0.41												
6	Eluted as void peak																							
7	3.79	6.84	1.81	4.56	2.42	4.38	1.81	8.28	1.15	1.97	1.72	5.69	0.78	1.30	1.66	4.77	0.58	0.96	1.63	3.13	0.48	0.76	1.58	3.24
8	2.93	4.25	1.45	5.07	2.07	2.85	1.37	4.04	1.15	1.51	1.31	2.78	1.10	1.27	1.17	2.11	0.91	1.05	1.15	2.97	0.8	0.89	1.12	1.80
9	1.64	1.44	1.14	0.5	0.32	0.27	1.18	0.35																

[a] $k' = (t_R - t_0)/t_0$, where t_R is the retention time and t_0 is the void time.
[b] $\alpha = k'_-/k'_+$, whenever the (+)-isomer eluted first.
[c] $R_s = 2[t_{R(-)} - t_{R(+)}]/[w_{(-)} + w_{(+)}]$, where w is the peak width at the base.

Table 3
Chromatographic parameters of the nine pairs of bicyclic monoterpenes in Fig. 3 using various 2-propanol concentrations (1–10%, v/v) in the mobile phase

Terpenic pair No.	1%				2%				4%				6%				8%				10%			
	k'_+ [a]	k'_- [a]	α [b]	R_s [c]	k'_+	k'_-	α	R_s	k'_+	k'_-	α	R_s	k'_+	k'_-	α	R_s	k'_+	k'_-	α	R_s	k'_+	k'_-	α	R_s
1	Eluted as void peak																							
2	3.22	3.37	1.05	0.65	2.19	2.32	1.06	0.70	1.18	1.26	1.07	0.67												
3	3.43	3.86	1.13	1.59	2.07	2.22	1.07	0.80	1.23	1.36	1.05	0.48	0.84	0.87	1.03	0.21	0.73	0.75	1.03	0.17	0.64	0.66	1.03	0.16
4	0.99	0.97	1.02	0.08	0.63	0.62	1.00	0.03																
5					2.45	2.53	1.03	0.42	1.4	1.45	1.04	0.40	0.95	0.96	1.00	0.00								
6	Eluted as void peak																							
7	6.91	9.69	1.40	4.11	4.00	5.43	1.36	4.26	1.73	2.28	1.32	1.38	1.09	1.43	1.30	2.75	0.78	1.00	1.28	1.89	0.61	0.79	1.29	1.62
8	4.05	5.04	1.24	2.9	2.56	2.84	1.1	1.31	1.5	1.62	1.08	0.98	1.08	1.12	1.04	0.57	0.88	0.91	1.04	0.59	0.75	0.75	1.00	0.00
9	0.84	0.63	1.34	0.85	0.62	0.51	1.21	0.78																

[a–c] See Table 2.

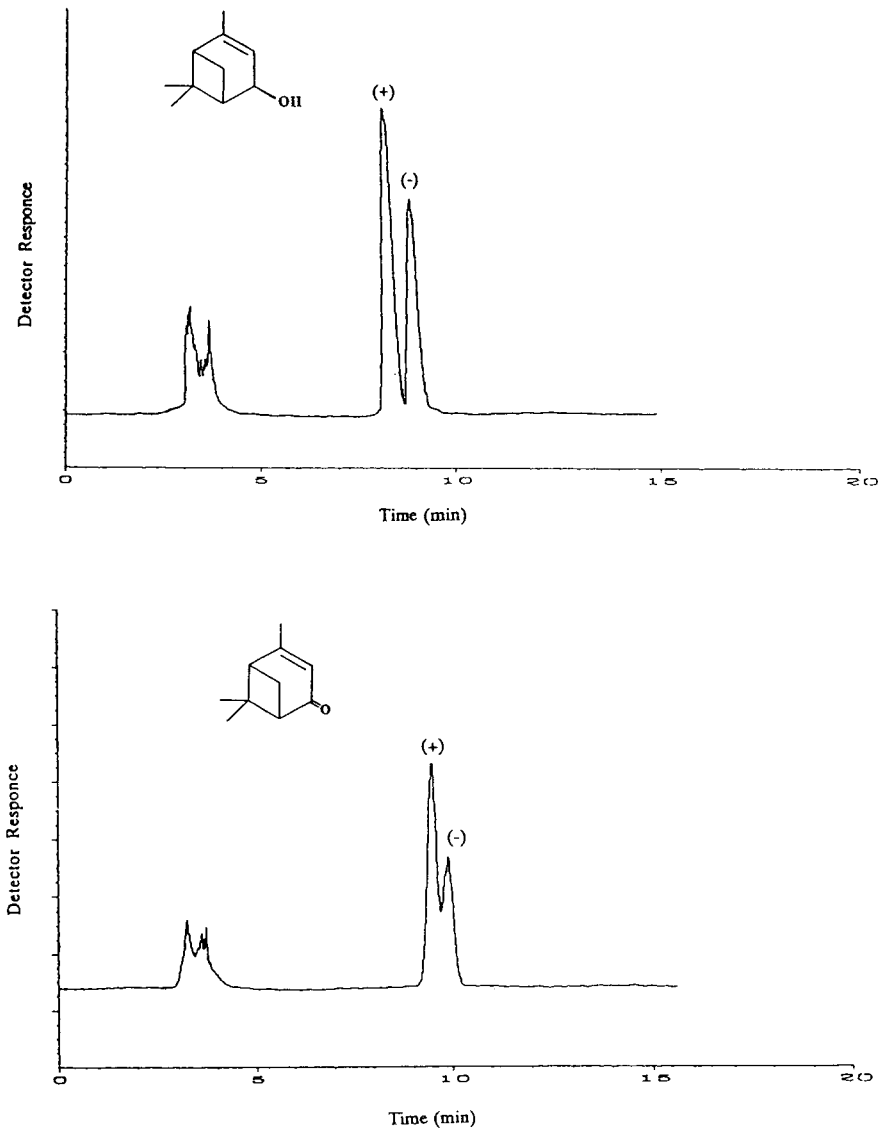

Fig. 4. Chromatograms showing the separation of the (−)- and (+)-enantiomers of *cis*-verbenol (pair 2) and verbenone (pair 3). Mobile phase, hexane–ethanol (98:2, v/v); wavelength of detection, 240 nm.

As a hydrogen-bonding group in the 4-position is essential for chiral discrimination, blocking this sensitive position with an acetoxy group was expected to diminish the resolution. Indeed, the separation of *cis*-4-acetoxy-α-pinene (pair 4) was lost. On the other hand, *cis*-4-acetoxymyrtenyl pivalate (pair 9) behaved unexpectedly. An unusual reversal of elution order of the (+)- and (−)-enantiomers was observed using 1 and 2% 2-propanol in the mobile phase with partial resolution. This change indicates a possible change in the recognition process by the station-

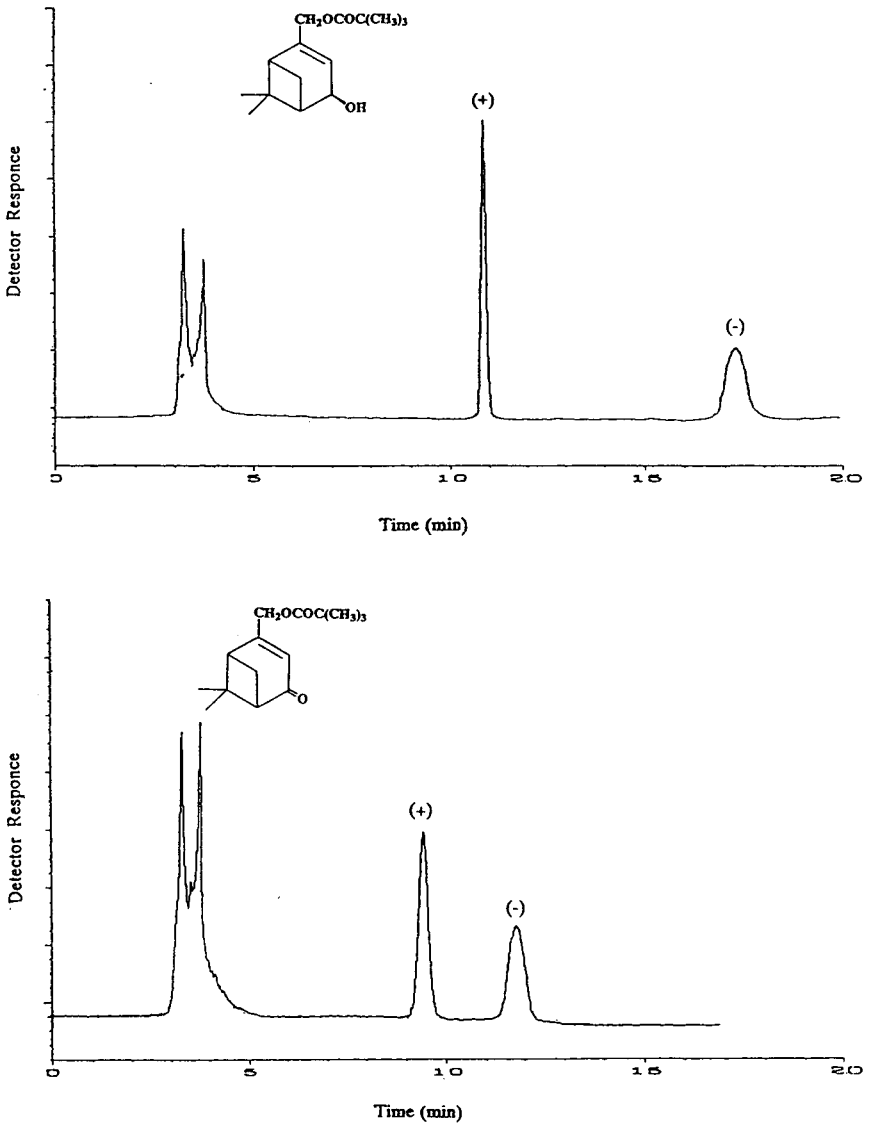

Fig. 5. Chromatograms showing the separation of the (−)- and (+)-enantiomers of *cis*-4-hydroxymyrtenyl pivalate (pair 7) and 4-oxomyrtenyl pivalate (pair 8). Conditions as in Fig. 4.

ary phase. A similar observation was reported by Wainer *et al.* [14] using an aryl-substituted alcohol in a cellulose tribenzoate.

Effects of solvent additives

Generally, normal-phase behaviour was observed for all the solutes in this study. Shorter retention times were obtained with ethanol as the modifier, and the retention decreased with the increase in the percentage of modifier in the mobile phase. The chromatographic parameters obtained using 1–10% of the two modifiers are given in Tables 2 and 3.

Solvent effects were observed in two instances. First, with 4-hydroxymyrtenyl pivalate (pair 7) and 4-oxomyrtenyl pivalate (pair 8), the selec-

tivity and resolution were better using ethanol as the mobile phase modifier. Second, 4-acetoxymyrtenyl pivalate (pair 9) was separated only in 2-propanol, displaying a reversal of elution order. It has already been reported in some instances that the two alcoholic modifiers were not always interchangeable [12,14]. It is also known that the degree of helicity of the amylose and its conformation may be solvent dependent [11]. In some instances, therefore, modification of the mobile phase composition may change the mechanism of chiral recognition and cause a reversal of elution order, especially when the hydroxyl functionality is lost.

4. Conclusions

This systematic comparative study of a series of α-pinene derivatives indicated that substitution of the 4-position on the α-pinene skeleton with hydrogen-bonding functional groups (OH and CO) facilitated chiral discrimination by the carbamated amylose. Molecular modelling of all the solutes under study indicated that substitution did not significantly change the most stable conformation of the α-pinene skeleton, hence the position of the functional groups rather than their effect on the overall conformation was more important. The role of hydrogen bonding as the major interaction was highlighted by the fact that the carbamated stationary phase was capable of resolving the enantiomers although they had no aromatic moiety.

5. Acknowledgements

This work was financed by the Israel Ministry of Health, grant No. 2293, and by the US National Institute on Drug Abuse. We thank Dr. Aviva Breuer for her guidance and assistance in preparing the terpenic enantiomers, and Galia Tawil for technical help.

6. References

[1] W. Templeton, *An Introduction to the Chemistry of Terpenoids and Steroids*, Butterworths, London, 1969.
[2] R. Mechoulam, P. Braun and Y. Gaoni, *J. Am. Chem. Soc.*, 89 (1967) 4552–4554.
[3] J.J. Feigenbaum, S.A. Richmond, Y. Weissman and R. Mechoulam, *Eur. J. Pharmacol.*, 169 (1989) 159–165.
[4] J.J. Feigenbaum, F. Bergmann, S.A. Richmond, R. Mechoulam, V. Nadler, Y. Kloog and M. Sokolovsky, *Proc. Natl. Acad. Sci. USA*, 86 (1989) 9584–9587.
[5] E. Shohami, M. Novikiv and R. Mechoulam, *J. Neurotrauma*, 10 (1993) 109–119.
[6] R. Mechoulam, W.A. Devane and R. Glaser, in L. Murphy and A. Bartke (Editors), *Marijuana/Cannabinoids: Neurobiology and Neurophysiology*, CRC Press, Boca Raton, FL, 1992, pp. 1–33.
[7] R. Mechoulam, N. Lander, A. Breuer and J. Zahalka, *Tetrahedron: Asymmetry*, 1 (1990) 315–318.
[8] S. Levin and S. Abu-Lafi, *Adv. Chromatogr.*, 33 (1993) 233–266.
[9] A. Italia, M. Schiavi and P. Ventura, *J. Chromatogr.*, 503 (1990) 266–271.
[10] J. Zukowski, *J. High Resolut. Chromatogr.*, 14 (1991) 361–362.
[11] Y. Hui and W. Zou, in H.-J. Schneider and H. Durr (Editors), *Frontiers in Supramolecular Organic Chemistry and Photochemistry*, VCH, Weinheim, 1991, pp. 203–221.
[12] S. Levin, S. Abu-Lafi, J. Zahalka and R. Mechoulam, *J. Chromatogr. A*, 654 (1993) 53–64.
[13] Y. Okamoto and Y. Kaida, *J. High Resolut. Chromatogr.*, 13 (1990) 709–712.
[14] I.W. Wainer, R.M. Stiffin and T. Shibata, *J. Chromatogr.*, 411 (1987) 139–145.
[15] *Application Guide for Chiral Column Selection*, Daicel Chemical Industries, Tokyo.
[16] E. Francotte and R.M. Wolf, *Chirality*, 3 (1991) 43–55.

ELSEVIER

Journal of Chromatography A, 664 (1994) 169–176

JOURNAL OF CHROMATOGRAPHY A

High-performance liquid chromatography of diamine enantiomers as Schiff bases on a chiral stationary phase ☆

A.L.L. Duchateau*, J.J. Guns, R.G.R. Kubben, A.F.P. van Tilburg

DSM Research, Department FC, P.O. Box 18, 6160 MD Geleen, Netherlands

(First received July 12th, 1993; revised manuscript received December 14th, 1993)

Abstract

A high-performance liquid chromatographic method for the enantiomeric analysis of chiral 1,2-diamines is described. By derivatization with benzaldehyde, aliphatic and aromatic 1,2-diamines were converted into Schiff base derivatives. Separation of the enantiomeric derivatives was performed on a commercially available cellulose tris(3,5-dimethylphenylcarbamate) chiral stationary phase. To investigate the effect of the reagent structure on enantioseparation, a series of twenty ring-substituted benzaldehydes were reacted with an aliphatic and an aromatic diamine. The influence of the type of substituent of the benzaldehyde reagent on the enantioselectivity obtained for Schiff base derivatives is discussed.

1. Introduction

Enantiopure diamines are important intermediates for the production of several pharmaceuticals [1]. One of the routes to obtain these compounds is by reduction of enantiopure amino acid amides with lithium aluminium hydride in tetrahydrofuran [2]. In conjunction with this synthesis, analytical methods are required for the control of the enantiopurity of the reaction products. Preliminary experiments in our laboratory showed that by means of high-performance liquid chromatography (HPLC) on a crown ether chiral stationary phase and ligand-exchange chromatography, using N,N-dipropyl-L-alanine as chiral selector, no enantioseparation could be achieved for series of aliphatic 1,2-diamines. Recently, an HPLC method was described for the enantioseparation of chiral 1,2-diamines [3]. However, the Ni(II) chelates that are used as chiral selectors in the mobile phase are not commercially available.

In this paper, we describe an HPLC method for the enantioseparation of a series of chiral 1,2-diamines as their Schiff bases on a cellulose tris(3,5-dimethylphenylcarbamate) chiral stationary phase (OD-CSP). For Schiff base formation, benzaldehyde was used as a reagent. Further, a series of twenty-ring-substituted benzaldehydes were reacted with an aliphatic and an aromatic diamine in order to investigate the effect of ring substitution on the enantioselectivity of the diamines.

* Corresponding author.

☆ Parts of this paper were presented at the *4th International Symposium on Chiral Discrimination, Montreal, September 19–22, 1993.*

0021-9673/94/$07.00
SSDI 0021-9673(93)E0061-X

2. Experimental

2.1. Materials

(±)- and (*R*)-1,2-diamino-3-methylbutane, (±)- and (*R*)-1,2-diamino-4-methylpentane, (±)-1,2-diamino-3,3-dimethylbutane, (±)- and (*S*)-1,2-diamino-2-phenylethane and (±)-1,2-diamino-2,3-dimethylbutane were prepared according to ref. 2.

(±)-1,2-Diaminopropane, benzaldehyde, 2-methylbenzaldehyde, 3-methylbenzaldehyde, 4-methylbenzaldehyde, 1-naphthaldehyde, 2-naphthaldehyde, 2-methoxybenzaldehyde, 3-methoxybenzaldehyde, 4-methoxybenzaldehyde, 4-ethoxybenzaldehyde, 4-butoxybenzaldehyde, 3,4-dimethoxybenzaldehyde, 3,4,5-trimethoxybenzaldehyde, 3-methoxy-4-ethoxybenzaldehyde, 3-phenoxybenzaldehyde, 4-cyanobenzaldehyde, 2-chlorobenzaldehyde, 3-chlorobenzaldehyde, 4-chlorobenzaldehyde and 3,4-dichlorobenzaldehyde were obtained from Janssen (Beerse, Belgium) and 4-ethylbenzaldehyde from Aldrich (Milwaukee, WI, USA). HPLC-grade methanol, 2-propanol and *n*-hexane were purchased from Merck (Darmstadt, Germany). All other chemicals were of analytical-reagent grade.

2.2. Instrumentation

The chromatographic system consisted of a Gilson (Villiers-le-Bel, France) Model 302 pump and a Spark (Emmen, Netherlands) Marathon autosampler for injection. The injection loop had a 20-μl capacity. The column used was a Daicel Chiralcel OD (250 × 4.6 mm I.D., 10 μm) from J.T. Baker (Deventer, Netherlands). The flow-rate was 1.0 ml/min and the column was operated at ambient temperature. The column effluent was monitored with a Linear Instruments (Reno, NV, USA) Model 204 absorbance detector set at 245 nm. UV spectra of Schiff base derivatives were recorded with a Hewlett-Packard (Palo Alto, CA, USA) Model 1040A diode-array detector. ^{13}C NMR analysis of Schiff base derivatives was performed with a Bruker (Karlsruhe, Germany) AM 400 instrument. Spectra were recorded at 100 MHz. For LC–mass spectrometry (MS), a Finnigan MAT (San José, CA, USA) TSQ-70 triple quadrupole mass spectrometer equipped with a thermospray interface (Finnigan MAT) was used. The chromatographic conditions for LC–MS analysis were identical with those for HPLC–UV analysis. MS analysis was performed using chemical ionization with gaseous ammonia [4].

2.3. Derivatization

About 5 mg of the diamine were dissolved in 1 ml of methanol and the solution was adjusted to pH 12 with 1 *M* sodium hydroxide solution. Benzaldehyde (0.25 mmol) was added, after standing for 20 min at 40°C in a thermostated mixing bath methylamine (8 mmol) was added and the reaction mixture was allowed to stand for another 20 min at 40°C. A 50-μl volume of the reaction mixture was diluted with *n*-hexane (1 ml) and an aliquot of this solution was injected into the HPLC system.

For ring-substituted benzaldehydes, the same derivatization procedure was applied.

3. Results and discussion

3.1. Schiff base derivatization

The products of the reaction of diamines with benzaldehyde were studied by means of ^{13}C NMR spectrometry and LC–MS. The NMR data showed that Schiff base formation occurred at both amino groups of the diamines. No *syn–anti* isomers could be observed by means of NMR. A reaction scheme for Schiff base formation of chiral diamines with benzaldehyde is given in Eq. 1.

To validate the enantioseparation obtained by HPLC–UV analysis, Schiff base derivatives of racemic diamines were analysed by means of LC–MS. For the racemic diamines studied, the mass chromatograms showed both enantiomers whose mass spectra were in accordance with the Schiff base structure shown in Eq. 1.

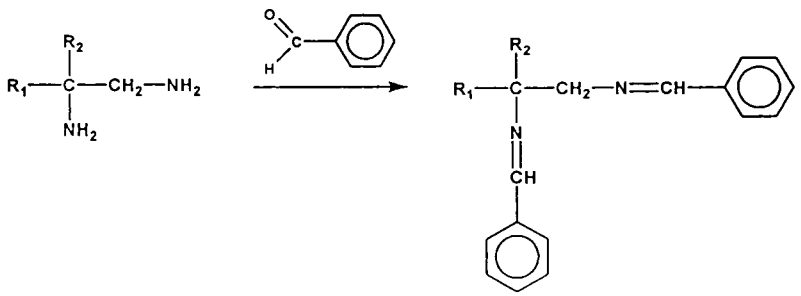

(1)

UV spectra were recorded for the Schiff bases of the aliphatic diamines studied. From these spectra, an absorbance maximum of 245 nm was selected for detection of the derivatives.

The rates of derivative formation of diamines with benzaldehyde were studied as a function of the reaction time at 40°C. As an example, the formation of the Schiff base of 1,2-diamino-3,3-dimethylbutane is given in Fig. 1.

Complete derivatization of the diamines studied was accomplished within 2 h at 40°C. A good compromise between yield and derivatization times was found by choosing 20 min as the reaction time, which resulted in a Schiff base yield of 75 ± 5% for the compounds studied.

Methylamine was added to the reaction mixture to convert the excess aldehyde into the corresponding Schiff base. Whereas in several instances the benzaldehydes studied interfered with the chromatographic separation of diamine enantiomers, the Schiff bases of the aldehydes with methylamine eluted with a larger k' than the diamine derivatives. For further optimization of a particular separation, the use of other alkylamines may be considered.

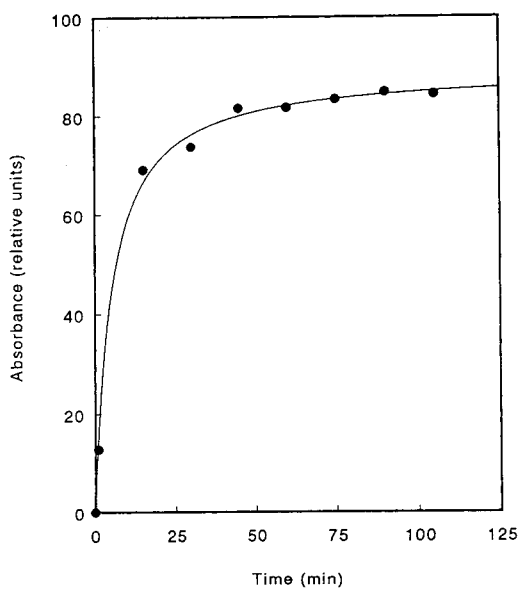

Fig. 1. Absorbance response of the Schiff base derivatization of 1,2-diamino-3,3-dimethylbutane with benzaldehyde as a function of reaction time at 40°C. The molar excess of benzaldehyde was tenfold relative to the amine studied.

3.2. Enantioselective analysis

Using benzaldehyde as a reagent, the enantioselectivity of a series of 1,2-diamines as their Schiff bases was examined on an OD-CSP. The chromatographic data for the diamines studied are given in Table 1.

It can be seen that the type of substituent (R_1, R_2) on the chiral carbon has a marked effect on the enantioselectivity and resolution. The highest α values were obtained for the diamines with R_1 = H and R_2 = Me or iPr. With respect to the structural isomers studied, *i.e.*, R_1, R_2 = (H, iBu), (H, tBu) and (Me, iPr), it appears that (H, tBu) substitution gives the best selectivity. In comparison with the aliphatic substituents, the phenyl-substituted diamine shows a lower α value. Typical chromatograms of the Schiff base derivatives are shown in Fig. 2.

On the basis of the availability of one of the enantiopure forms, the elution order of the enantiomers of 1,2-diamino-3-methylbutane, 1,2-diamino-4-methylpentane and 1,2-diamino-2-

Table 1
Capacity factors (k'), selectivities (α) and resolution (R_s) of Schiff bases derived from benzaldehyde and chiral diamines with the structure shown

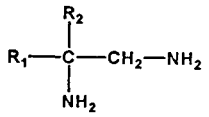

R_1	R_2	k'^a	α	R_s
H	Me	2.04	5.75	18.21
H	iPr	0.87	6.43	21.55
H	iBu	1.27	2.19	9.62
H	tBu	0.49	5.44	15.62
H	Ph	1.24	1.49	4.76
Me	iPr	0.61	2.56	9.20

Mobile phase: *n*-hexane–2-propanol (90:10). For other conditions, see Experimental.
[a] Capacity factor of the first-eluted enantiomer.

phenylethane was determined. In all instances the *R*-form eluted before the *S*-form.

To investigate the effect of ring-substituted benzaldehydes on the chromatographic behaviour of the corresponding Schiff base derivatives of 1,2-diamines, a series of twenty ring-substituted benzaldehydes were reacted with 1,2-diamino-2-phenylethane (DAPE) and 1,2-diamino-4-methylpentane (DAMP). The results are presented in Table 2.

For the enantioseparation of both DAPE and DAMP enantiomers, sixteen out of the twenty ring-substituted benzaldehydes gave successful results. In general, the enantioselectivities obtained for the DAMP derivatives were higher than those for DAPE derivatives. Only three reagents gave higher α values for DAPE than for DAMP. With DAPE, the highest enantioselectivity was obtained for 3-phenoxybenzaldehyde ($\alpha = 3.27$). 3-Methylbenzaldehyde gave the highest α value (2.69) for DAMP. Large differences were found for the structural isomers of the benzaldehydes studied. For the methyl-substituted benzaldehydes, substitution at the 3- or 4-position resulted in higher enantioselectivities than for the 2-substituted analogue. The same phenomenon was observed with the structural isomers of chloro-, methoxy- and naphthyl-substituted benzaldehydes. With respect to the k'

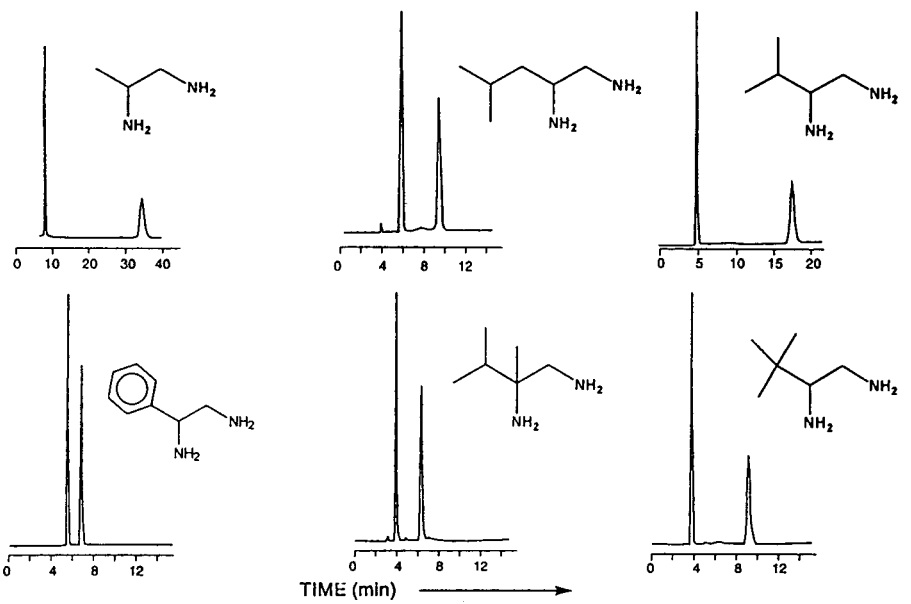

Fig. 2. Separation of the enantiomers of 1,2-diamines after derivatization with benzaldehyde. Mobile phase: *n*-hexane–2-propanol (90:10). Except for 1,2-diaminopropane [t_R (benzaldehyde) = 5 min], the excess benzaldehyde was reacted with methylamine [t_R (Schiff base) = 24 min]. For other conditions, see Experimental.

Table 2
Capacity factors (k'), selectivities (α) and resolution (R_s) of 1,2-diamino-2-phenylethane and 1,2-diamino-4-methylpentane enantiomers after derivatization with several ring-substituted benzaldehydes

Reagent	Compound						
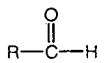	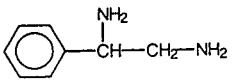				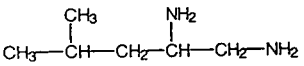		
R	k'^a	α	R_s	pK_a^b	k'^a	α	R_s
	1.53	1.55	4.80	6.00 5.79	1.86	2.31	10.60
	0.84	1.28	2.21	6.28 6.07	0.63	1.83	5.03
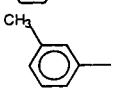	1.54	1.62	5.67	6.12 5.91	1.69	2.69	11.50
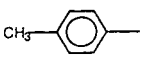	1.49	1.57	4.57	6.28 6.07	1.54	2.24	10.70
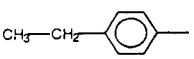	1.69	1.15	1.40	6.30 6.09	1.92	1.43	4.20
	2.83	1.16	1.79	6.00 5.79	1.88	1.13	1.47
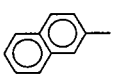	4.16	2.66	11.70	6.00 5.79	3.43	2.68	12.00
	0.98	1.00	0	6.56 6.35	0.97	1.00	0
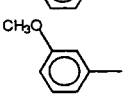	4.18	1.55	5.48	5.78 5.57	5.31	2.34	11.20
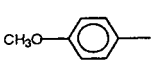	6.10	1.38	4.49	6.56 6.38	7.02	1.72	7.15
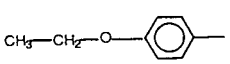	2.95	1.42	3.86	6.48 6.27	3.02	2.07	8.20
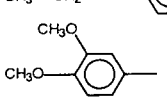	1.65	1.00	0	6.34 6.16	1.65	1.00	0
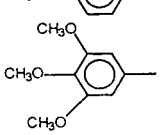	1.54	1.00	0	6.12 5.94	1.55	1.00	0

(Continued on p. 174)

Table 2 *(continued)*

Reagent	Compound						
	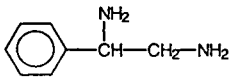				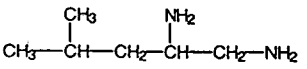		
R	k'^a	α	R_s	$pK_a{}^b$	k'^a	α	R_s
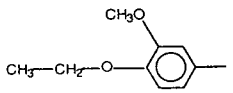	1.19	1.00	0	6.26 6.05	1.21	1.00	0
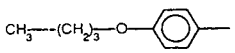	2.07	1.49	4.27	6.64 6.43	2.01	2.66	10.20
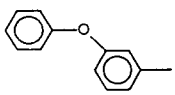	8.55	3.27	13.10	5.50 5.29	3.44	1.78	6.86
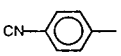	12.50	1.06	0.84	4.60 4.39	4.30	1.06	1.57
	0.76	1.10	0.68	5.52 5.31	0.49	1.18	1.05
	1.30	1.13	1.32	5.26 5.05	0.86	1.47	3.77
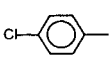	1.08	1.18	1.60	5.52 5.31	0.57	1.27	1.76
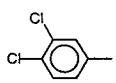	1.50	1.28	2.75	4.78 4.57	0.67	1.14	1.04

Mobile phase: *n*-hexane–2-propanol (95:5). For other conditions, see Experimental.

[a] Capacity factor of the first-eluted enantiomer.

[b] Calculated pK_a values [11] for both nitrogens of the Schiff base derivatives of 1,2-diamino-2-phenylethane. For the corresponding Schiff bases of 1,2-diamino-4-methylpentane the pK_a values were $pK_{a_{1(DAPE)}} + 0.04$ and $pK_{a_{2(DAPE)}} + 0.03$.

values, 2-substituted benzaldehydes showed lower values than the corresponding 3- or 4-analogues. These effects occurred for both DAMP and DAPE enantiomers. For 4-alkoxy-substituted benzaldehydes, an increase in enantioselectivity was observed on going from methoxy, to ethoxy and to butoxy substituents. However, the retention decreased in this series (for both DAPE and DAMP). In contrast to the mono-substituted alkoxybenzaldehydes, no chiral recognition was obtained for the di- or tri-substituted analogues.

In the following, the results obtained will be discussed in terms of chiral recognition mechanisms. In general, chiral recognition on cellulose carbamate phases is believed to occur mainly

through hydrogen bond formation between the urethane groups of the CSP and functional groups of the solutes capable of forming hydrogen bonds [5–10]. More particularly, the NH and C = O groups of the urethane moiety may act as hydrogen bond donor and acceptor, respectively, for the solutes. All the Schiff base derivatives in this study have sites for hydrogen bond acceptance, *i.e.*, the imine nitrogens. Consequently, the main hydrogen bond is expected to be formed between the imine nitrogens of the solute and the hydrogen atom on the carbamate nitrogen. In addition to the interaction via hydrogen bonds, the aromatic groups in the Schiff bases might be expected to participate in $\pi-\pi$ interactions with the CSP.

With regard to the different types of substituted benzaldehydes used, it is of interest to investigate the effect of the electron-donating and electron-withdrawing power of the substituents on the basicity of the imine nitrogens. A change in the basicity of the imine nitrogens is expected to cause a change in the capability for hydrogen bond formation of the derivatives with the CSP, which in turn might influence chiral recognition. In order to investigate possible relationships between the basicity of the Schiff bases and their retention and enantioselectivity, pK_a values were calculated using the program pKalc 2.0 [11] for the derivatives studied (Table 2).

Regression analysis was used to correlate the pK_a values of the Schiff bases with each of the following chromatographic data: k'_{DAPE}, k'_{DAMP}, k'_{DAMP}/k'_{DAPE}, α_{DAPE} and α_{DAMP}. Of these, only the relationship between pK_a and the ratio k'_{DAMP}/k'_{DAPE} was found to be statistically significant (confidence level > 99.99%). For $pK_{a_1(DAPE)}$, the relationship is shown in Fig. 3. The explained variance (r^2) was 62%. When not taking 3-methoxybenzaldehyde into account, r^2 increased to 75%. The straight line in Fig. 3 shows the result of the fit between the data. From the plot it can be seen that the retention of the DAPE derivative compared with that of the corresponding DAMP derivative increases with decreasing basicity of the derivative. This may be explained by an additional $\pi-\pi$ association of the phenyl group of DAPE with the CSP in the case of Schiff bases with low basicity.

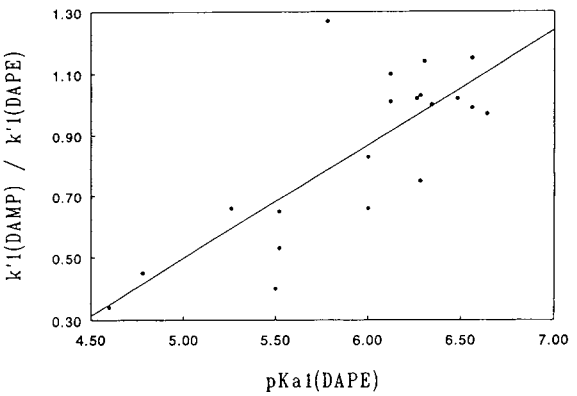

Fig. 3. Plot of $k'_{1(DAMP)}/k'_{1(DAPE)}$ *versus* $pK_{a_1(DAPE)}$.

For all the Schiff base derivatives studied, except that derived from 1,2-diamino-4-methylpentane and 4-cyanobenzaldehyde, the *R*-enantiomer eluted before the *S*-form.

4. Conclusions

Derivatization of chiral 1,2-diamines with benzaldehyde yields the corresponding Schiff base enantiomers, which can readily be resolved on a cellulose tris(3,5-dimethylphenylcarbamate) CSP. The enantioseparation of an aliphatic and an aromatic 1,2-diamine with twenty ring-substituted benzaldehydes revealed that the enantioselectivity depended greatly on the type of substituent and the position and number of substituents on the phenyl rings. For the benzaldehydes tested, substitution at the 2-position showed lower enantioselectivities than with the same substituent in the 3- or 4-position. Statistical analysis showed that there was no significant correlation between the pK_a values and α values of the Schiff base derivatives.

5. Acknowledgements

We thank Mr. G. Kwakkenbos for the LC–MS analysis and Dr. N.K. de Vries for the ^{13}C NMR measurements.

6. References

[1] H. Brunner, M. Schmidt, G. Unger and H. Schönenberger, *Eur. J. Med. Chem.*, 20 (1985) 509.
[2] J.A. Garbarino, *Ann. Chim. (Rome)*, 59 (1969) 841.
[3] G. Bazylak and B. Maslowska, *Analusis*, 20 (1992) 611.
[4] R.G.J. van Leuken and G.T.C. Kwakkenbos, *J. Chromatogr.*, 626 (1992) 81.
[5] T. Shibata, K. Mori and Y. Okamoto, in A.M. Krstulović (Editor), *Chiral Separations by HPLC*, Ellis Horwood, Chichester, 1989, Ch. 13, p. 337.
[6] A. Ichida, T. Shibata, I. Okamoto, Y. Yuki, H. Namikoshi and Y. Toga, *Chromatographia*, 19 (1984) 280.
[7] Y. Okamoto, M. Kawashima and K. Hatada, *J. Am. Chem. Soc.*, 106 (1984) 5357.
[8] Y. Kaida and Y. Okamoto, *Bull. Chem. Soc. Jpn.*, 65 (1992) 2286.
[9] Y. Okamoto, Y. Kaida, R. Aburatani and K. Hatada, in S. Ahuja (Editor), *Chiral Separations by Liquid Chromatography (ACS Symposium Series*, No. 471), American Chemical Society, Washington, DC, 1991, Ch. 5.
[10] Y. Okamoto, M. Kawashima and K. Hatada, *J. Chromatogr.*, 363 (1986) 173.
[11] *pKalc 2.0 Program*, Compudrug Chemistry, Budapest.

ELSEVIER

Journal of Chromatography A, 664 (1994) 177–182

JOURNAL OF CHROMATOGRAPHY A

Determination of mono- and di-nitro polycyclic aromatic hydrocarbons by on-line reduction and high-performance liquid chromatography with chemiluminescence detection

Hang Li, Roger Westerholm*

Department of Analytical Chemistry, Arrhenius Laboratory, Stockholm University, S-106 91 Stockholm, Sweden

(First received October 20th, 1993; revised manuscript received December 17th, 1993)

Abstract

The determination of mono- and di-nitro polycyclic aromatic hydrocarbons (PAHs) was accomplished by on-line reduction to the corresponding amino PAHs, which were then separated and detected using high-performance liquid chromatography (HPLC) and chemiluminescence detection. The on-line reduction was carried out in a methanol–water mobile phase by the use of a catalyst column packed with material originating from a grained automobile three-way catalyst. HPLC separation was completed with acetonitrile–buffer mobile phase at pH = 7.5. Bis(2,4,6-trichlorophenyl) oxalate and hydrogen peroxide was used as the reagent for chemiluminescence detection. The detection limits for some mono- and di-nitro PAHs were in the range of 1 to 10 picogram. The developed method was demonstrated on samples originating from diesel exhaust particle material extracts.

1. Introduction

Diesel and gasoline engine exhaust emissions are complex mixtures containing thousands of chemical components. Among these components, some nitrated polycyclic aromatic hydrocarbons (nitro PAHs) have been identified as mutagens and possible carcinogens [1]. Nitro PAHs have been estimated to be responsible for up to 40% of the total mutagenic activity determined in diesel particulate extracts [2]. Among the nitro-PAHs, great attention has been directed to 1-nitropyrene and 1,3-, 1,6- and 1,8-dinitropyrenes. This is because 1-nitropyrene is one of the most abundant of these compounds, and the three dinitropyrenes are found to be much more mutagenic than 1-nitropyrene [3]. The amount of dinitropyrenes present in motor vehicle exhaust samples is lower than mono-nitro-PAHs. The determination of nitro PAHs in complex sample matrices is usually carried out using analytical methods, such as gas chromatography with nitrogen–phosphorus detection (GC–NPD) or a chemiluminescence detection (GC–CD), and gas chromatography with negative-ion chemical ionisation mass spectrometry (GC–NICIMS) [4,5]. HPLC with fluorescence detection [6] and electrochemical and fluorescence detection [7] has also been developed. The peroxyoxalate chemiluminescence reaction was originally developed by Rauhut *et al.* [8] and combined with HPLC by Kobayashi and Imai [9]. It is used for the detection of fluorescent compounds such as PAHs, amino PAHs and

* Corresponding author.

0021-9673/94/$07.00
SSDI 0021-9673(93)E1302-G

nitro PAHs [10–13]. Detection limits are in the range of picomole to subfemtomole [14,15]. Two review papers, which present progress and developments in this field of research, were recently published by Robards and Worsfold [16] and Kwakman and Brinkman [17]. The peroxyoxalate chemiluminescence reaction mechanism was previously described by Sigvardson *et al.* [18]. The detector used is usually a photo multiplier tube (PMT) without a light source which gives an improved signal-to-noise ratio when compared with conventional fluorescence detection [19].

The objective of the present study is to develop a sensitive and routine analytical method by on-line reduction and combining HPLC separation and peroxyoxalate chemiluminescence detection for determining mono- and di-nitro PAHs in engine exhaust emission. The major advantages of this approach are: (1) the catalyst column shows enough reduction capacity and lifetime, (2) both mono- and di-nitro PAHs can be identified and (3) the detection limits are in the range of 1–10 picogram.

2. Experimental

2.1. Chemicals

All the organic solvents used were HPLC grade. Bis(2,4,6-trichlorophenyl) oxalate (TCPO), H_2O_2, imidazole, and nitro PAH standards (1,8-dinitropyrene, 2-nitroanthracene, 1-nitropyrene, 6-nitrochrysene, 3-nitroperylene and 1-nitroperylene) were obtained from either Aldrich Chemical Co. (Steinheim, Germany) or Sigma Chemical Co. (St. Louis, MO, USA). Water was purified by an Elgastat UHQ II unit (Elga Ltd., UK). All solvents were degassed using reduced pressure conditions and an ultrasonic bath before use.

2.2. Instrumentation

Fig. 1 illustrates the system by means of a schematic diagram. Three pump units were used in this study. The first pump (P1), a Varian Star 9010 (Varian, Walnut Creek, CA, USA), was

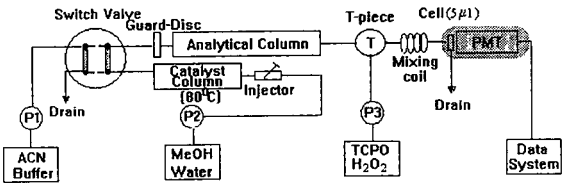

Fig. 1. Schematic diagram of the HPLC–CL system. The details are described in the text.

used for acetonitrile–buffer solution (65:35) eluent delivery, the second pump (P2), a BAS 400 (Bioanalytical Systems Inc., Lafayette, USA) was used for on-line reduction solution supply, methanol–water (65:35) as mobile phase, and the third pump (P3), Waters M45 (Waters, Milford, MA, USA), was used for reagent (TCPO–H_2O_2) delivery. A catalyst column was used for on-line reduction of nitro PAHs to corresponding amino PAHs. A heater was used for heating the catalyst column to 80°C, and a four-port switch valve was used for transferring the eluent. The analytical column was a C_{18} column (150 × 4.6 mm I.D., 3 mm particles) which was protected by a C_{18}-A Guard-Disc (1.0 × 4.6 mm I.D., 0.2 mm pore size) (Sarasep, Inc., USA). A Rheodyne Model 7125 syringe injector with a 20-μl loop was used for injection. The analytical column outlet was connected to a T-piece, which was connected to the detector flow cell by way of a 12-cm (0.25 mm I.D.) stainless-steel coil. The detector used was a Kratos FS970 fluorescence detector (Schoeffel Instruments, USA) with a 5-μl flow cell. The detector was operated with its light off and without an emission cut-off filter. Emitted light was detected using the photomultiplier tube (PMT). An ELDS 900 laboratory chromatography data system (Chromatograph Data Systems AB, Kungshög, Sweden) was used for recording and integrating the chromatograms.

2.3. On-line reduction

On-line reduction of nitro PAHs to amino PAHs was carried out using a catalyst column packed with grained three-way catalyst material, which was originally designed to reduce gasoline fuelled vehicle exhaust emissions (0.25% platinum and 0.05% rhodium, preheated to

800°C, Volvo Personvagnar AB, Sweden). The column was prepared by dry packing (40.0 × 3.0 mm I.D., 140–160 mm particle size). The catalyst was tested from ambient temperature up to 80°C with flow rates from 0.20 ml/min to 1.0 ml/min, using methanol–water (65:35) solution as the carrier stream. The catalytic column reduction dynamic range was examined from 0.012 ng to 120.0 ng 1-nitropyrene. On-line reduction was carried out by holding sample in the catalyst column for 90 s at stop-flow, the elution was then accomplished with methanol–water (65:35) at a flow rate of 0.3 ml/min for 60 s, in order to transfer the amino PAHs peak into the analytical column; during the procedure the temperature was held at 80°C. Because the methanol–water solution is not appropriate to the chemiluminescence detection system, it is necessary to change to an acetonitrile–buffer solution as mobile phase by using a switch valve, Fig. 1.

2.4. HPLC separation and chemiluminescence detection

Chromatographic separation of the amino compounds was carried out using an acetonitrile–buffer solution (65:35) at flow rate of 1.0 ml/min. The nitrated imidazole buffer (pH = 7.5, 50 m*M*) provides the necessary base catalysis for the peroxyoxalate reaction to run. Since acetonitrile was used in the chromatography separation as mobile phase and TCPO has a high solubility in ethyl acetate, the reagent solution of TCPO–H_2O_2 was prepared in acetonitrile–ethyl acetate that was mixed in the ratio of 3:1. The concentrations of TCPO and H_2O_2 were 0.25 m*M* and 25 m*M*, respectively, the flow rate was set to 0.7 ml/min. A standard mixture containing six mono- and di-nitro PAHs was examined by the system, the chromatogram is presented in Fig. 2A.

2.5. Diesel exhaust samples

Two samples were investigated in this present study: a diesel particulate material and a diesel exhaust emission particulate sample. The samples are described in detail elsewhere [20,21]. The samples were Soxhlet extracted with dichloromethane and the crude extract was fractionated on a silica column into five fractions, according to polarity. This is described in detail elsewhere [22]. The fractions containing mono-nitro PAHs, fraction III and di-nitro PAHs, fraction IV, were analysed by the system, the

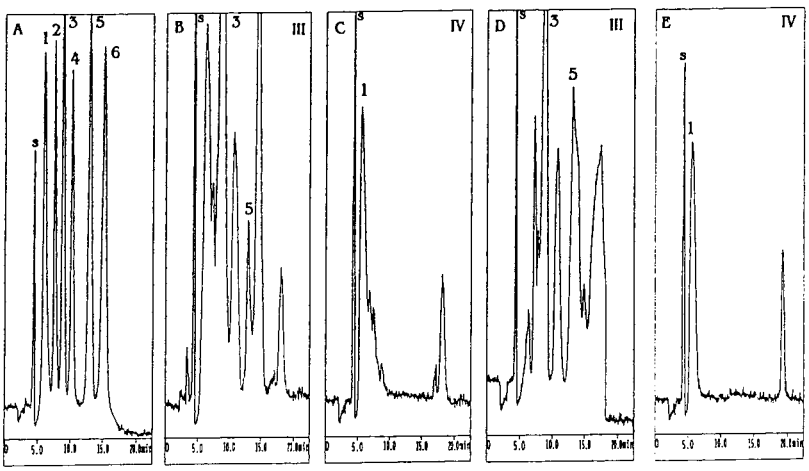

Fig. 2. (A) Chromatogram of a standard mixture. Peaks: 1 = 1,8-dinitropyrene, 2 = 2-nitroanthracene, 3 = 1-nitropyrene, 4 = 6-nitrochrysene, 5 = 3-nitroperylene and 6 = 1-nitroperylene. Detection limits are presented in Table 1. (B) and (C) Chromatograms of a diesel particulate extract from fractions containing mono-nitro PAHs and di-nitro PAHs, respectively. (D) and (E) Chromatograms of a diesel exhaust emission filter extract sample from fractions containing mono-nitro PAHs and di-nitro PAHs, respectively. Chromatographic conditions are described in the text.

chromatograms are presented in Fig. 2B, 2C, 2D and 2E, respectively.

3. Results and discussion

3.1. On-line reduction

Initial experiments with zinc powder mixed with silica as the catalyst material were performed but, due to a limited lifetime (3–5 days), the catalyst was excluded as inappropriate. Instead, a three-way catalyst column was selected and investigated in the present study. It was observed that the reduction reaction needs a certain temperature and time to reach high reduction efficiency. The catalyst was tested from ambient temperature up to 80°C with flow rates from 0.20 ml/min to 1.0 ml/min of methanol–water (65.35) as carrier stream. Initially the methanol–water ratio varied from 50:50 to 90:10, however, the best response was obtained at the ratio of 65:35. The best efficiency was obtained when the sample was held in the catalyst column for 90 s at stop-flow, then the elution was carried out with flow rate of 0.3 ml/min, the temperature was held at 80°C. Six replicate injections of 1.0 ng of 1-nitropyrene gave relative standard deviations (R.S.D.s) of less than 2.4%, showing that the reduction of nitro PAHs to amino PAHs is reproducible. The catalytic reduction dynamic range was examined from 0.012 ng to 120.0 ng 1-nitropyrene. Repeated injections ($n \geq 2$) gave a R.S.D. of less than 5%, the correlation coefficient r was 0.995 at the 95% confidence level. Because the amount of nitropyrene in the injected exhaust samples is less than 100 ng [6], the maximum capacity for the catalyst column was not determined.

In order to examine and to check the efficiency of the catalyst column, a test mixture containing known concentrations of mono- and dinitro PAHs (see Table 1, however, no 2-nitroanthracene present) and 2-aminoanthracene was analyzed. On a regular basis the test mixture was analysed with respect to retention times, absolute and relative chemiluminescence (CL) intensity in comparison to 2-aminoanthracene. The catalyst column has been employed for more than six months of daily use, and is still active. These results strongly suggest that the reduction process is catalytic. The zinc catalyst column having a finite lifetime was previously observed by Sigvardson and Birks [12] and MacCrehan *et al.* [7]. Hayakawa and co-workers [13] have reported that in determination of 1-nitropyrene and three dinitropyrenes in vehicle exhaust particulate, an off-line hydrosulphide reduction method was used. The disadvantages of this method are tedious sample treatment procedure and a considerable reduction time.

3.2. HPLC separation and chemiluminescence detection.

The peroxyoxalate-CL reaction is known to be base-catalysed so the pH has a significant influence on the chemiluminescence kinetics. Two

Table 1
Retention times, injected amounts and detection limits of a standard mixture consisting of mono- and di-nitro PAHs

Peak no. [a]	Compound	R_s [b]	Retention time (min)	Injected amount (picogram)	Detection limit [c] (picogram)
1	1,8-Dinitropyrene		6.01	75	< 3
2	2-Nitroanthracene	1.57	7.57	75	< 3
3	1-Nitropyrene	1.44	8.85	50	< 2
4	6-Nitrochrysene	1.38	10.21	250	< 10
5	3-Nitroperylene	2.32	12.94	25	< 1
6	1-Nitroperylene	1.56	15.13	25	< 1

[a] Peak numbers refer to the standard compounds which are presented in Fig. 2A.
[b] Resolution is defined as the ratio between the two peak maxima and the average base width of the two peaks.
[c] ($S/N > 3$).

buffer compounds were tested in the system, imidazole and tris(hydroxymethyl)aminomethane. Initial experiments were performed ranging from pH 5 to 8 using both buffer compounds, however, imidazole gave the highest relative CL intensity at pH 7.5. Below pH 7.5, the intensity decreased dramatically and no attempt to measure above pH 8.0 was made due to damage to the analytical column used. The imidazole buffer was selected in present system, at a concentration of 50 m*M* and the pH was adjusted to 7.5 with HNO_3. The imidazole buffer concentration was investigated in the range of 10 to 200 m*M* and the best response was obtained at 50 m*M*.

The effects of the selection of solvent on the chemiluminescence reaction have been reported by Kobayashi and Imai [9]. The stability of TCPO–H_2O_2 has been measured in methanol, acetone, dioxane, acetonitrile and ethyl acetate, as well as mixtures of them. Due to the use of acetonitrile as the mobile phase and the fact that TCPO dissolves easily in ethyl acetate, acetonitrile and ethyl acetate (3:1) were selected as the TCPO–H_2O_2 solvent. The concentrations of TCPO and H_2O_2 were optimised in the range of 0.05–1.0 *M* and in the range of 15–150 m*M*, respectively. The most favourable concentrations of TCPO and H_2O_2 are 0.25 m*M* and 25 m*M*, respectively. The reagent flow rate was optimised to be 0.7 ml/min which was introduced into the T-piece and mixed with the mobile phase. The highest CL intensity was obtained using a mixing coil length of 12 cm (0.25 mm I.D.) at present conditions.

The HPLC separation was carried out by an acetonitrile–buffer mobile phase (65:35). The flow rate was set to 1.0 ml/min, and a standard mixture was examined by this system. The chromatogram is presented in Fig. 2A. The separation took less than 20 min. The resolution (R_s) value for the least separated peaks, *i.e.* 1-nitropyrene and 6-nitrochrysene, is 1.38. Other R_s values are presented in Table 1. A good separation for the six compounds can be observed from Fig. 2A. A blank sample was investigated which was at baseline level. Detection limits are defined as the mass of analyte that provides a signal equal to three times that of the baseline. As can be seen from Table 1, the individual nitrated PAHs have different detection limits under the applied conditions; for the six standards, the detection limits range from less than 1 to less than 10 picogram. The detection limits in the present study are better than those data obtained using HPLC with fluorescence detection [6,7] and electrochemical detection [7], and as good as those data obtained by other researchers by means of HPLC with chemiluminescence detection [12,13].

3.3. Diesel exhaust samples

The chromatograms originating from the diesel particulate material extract fraction, fractions III (mono-nitro PAHs) and IV (di-nitro PAHs) are presented in Fig. 2B and 2C, respectively. The results obtained show that the concentrations of 1-nitropyrene and 3-nitroperylene are about 4.5 μg/g and 1.1 μg/g, respectively. In fraction IV the dinitropyrene content was 0.3 μg/g. The chromatograms of the diesel exhaust particulate filter extract fractions III and IV are presented in Fig. 2 D and 2 E, respectively. It can be seen that 1-nitropyrene and 3-nitroperylene can be identified in fraction III, the emission rates being 1.2 μg/km (2 μg/g particulate material) and 0.5 μg/km (0.8 μg/g particulate material), respectively. In fraction IV the emission factor is 0.18 μg/km (0.3 μg/g particulate material). The quantification was made with 1-nitroperylene as internal standard. The present results are in the same order as previously published data [23], *i.e.* 1-nitropyrene 6.5 μg/g particulate material.

4. Conclusions

The three-way catalyst has a lifetime of more than 6 months of daily use with methanol–water as the carrier stream which suggests that the reduction process is catalytic. The on-line catalyst column has a capacity for quantitative on-line reduction of mono- and di-nitro PAHs to the corresponding amino PAHs. The HPLC separation with chemiluminescence detection has a high sensitivity. The major advantages of this

approach are: (1) the catalyst column shows enough reduction capacity and lifetime, (2) both mono- and di-nitro PAHs can be quantified and (3) the detection limits are in the range of 1–10 picograms of the standard compounds injected. Compounds determined using this method are: 1,8-dinitropyrene, 2-nitroanthracene, 1-nitropyrene, 6-nitrochrysene, 3-nitroperylene and 1-nitroperylene.

5. Acknowledgements

The authors wish to thank Lennart Ekman, Volvo Personvagnar AB, Göteborg, for providing the vehicle three-way catalyst material, Lena Elfver for laboratory assistance and Anders Dyremark for fruitful discussions, and Professor Lars Blomberg and Professor Björn Josefsson for critical comments.

6. References

[1] *On the Evaluation of Carcinogenic Risks to Humans—Diesel and Gasoline Engine Exhausts and Some Nitroarenes*, International Agency for Research on Cancer (IARC) Monographs, 1989, World Health Organization (WHO), Lyon, France.

[2] D. Schuetzle and J.A. Frazier, in N. Ishinishi, A. Koizumi, R.O. McClellan and W. Stöber (Editors), *Carcinogenic and Mutagenic Effects of Diesel Engine Exhaust*, Elsevier, Amsterdam, 1986, p. 41.

[3] H. Matsushita, S. Goto, O. Endo, L. Jang-Ho and A. Kawai, in N. Ishinishi, A. Koizumi, R.O. McClellan and W. Stöber (Editors), *Carcinogenic and Mutagenic Effects of Diesel Engine Exhaust*, Elsevier, Amsterdam, 1986, p. 103.

[4] C.W. White (Editor), *Nitrated Polycyclic Aromatic Hydrocarbons*, Hüthig, Heidelberg, 1985.

[5] A. Robbat, N.P. Corso, P.J. Doherty and M.H. Wolf, *Anal. Chem.*, 58 (1986) 2078.

[6] S.B. Tejada, R.B. Zweidinger and J.E. Sigsby, *Anal. Chem.*, 58 (1986) 1827.

[7] W.A. MacCrehan, W.E. May and S.D. Yang, *Anal. Chem.*, 60 (1988) 194.

[8] M.M. Rauhut, L.J. Bollyky, B.G. Roberts, M. Loy, R.H. Whitman, A.V. Ianotta, A.M. Semsel and R.A. Clarke, *J. Am. Chem. Res.*, 2 (1967) 6515

[9] K. Kobayashi and K. Imai, *Anal. Chem.*, 52 (1980) 424.

[10] M.L. Grayeski and A.J. Weber, *Anal. Lett.*, 17 (1984) 1539.

[11] K.W. Sigvardson and J.W. Birks, *Anal. Chem.*, 55 (1983) 432.

[12] K.W. Sigvardson and J.W. Birks, *J. Chromatogr.*, 316 (1984) 507.

[13] K. Hayakawa, K. Butoh and M. Miyazaki, *Anal. Chim. Acta*, 266 (1992) 251.

[14] K. Imai and R. Weinberger, *Trends Anal. Chem.*, 4 (7) (1985) 170.

[15] K. Imal, A. Nishitani and Y. Tsukamoto, *Chromatographia*, 24 (1987) 77.

[16] K. Robards and P.J. Worsfold, *Anal. Chim. Acta*, 266 (1992) 147.

[17] P.J.M. Kwakman and U.A.Th. Brinkman, *Anal. Chim. Acta.*, 266 (1992) 175.

[18] K.W. Sigvardson, J.M. Kennish and J.W. Birks, *Anal. Chem.*, 56 (1984) 1096.

[19] R. Weinberger, C.A. Mannan, M. Cerchio and M.L. Grayeski, *J. Chromatogr.*, 288 (1984) 445.

[20] R. Westerholm and K.-E. Egebäck (Editors), *Impact of Fuel on Diesel Exhaust Emissions: A chemical and biological characterization*, Swedish Environmental Protection Agency, Report 3968, Solna, 1991.

[21] G.G.F. Mason, J.-Å. Gustafsson, R.N. Westerholm and H. Li, *Environ. Sci. Technol.*, 26 (1992) 1635.

[22] T. Alsberg, U. Stenberg, R. Westerholm, M. Strandell, U. Rannug, A. Sundvall, L. Romert, V. Bernson, B. Petterson, R. Toftgård, B. Franzen, M. Jansson, J.-Å. Gustafsson, K.-E. Egebäck and G. Tejle, *Environ. Sci. Technol.*, 19 (1985) 43.

[23] D. Schuetzle and J.M. Perez, *J. Air Pollut. Control Assoc.*, 33 (1983) 751.

ELSEVIER

Journal of Chromatography A, 664 (1994) 183–188

JOURNAL OF CHROMATOGRAPHY A

Rapid method for the isolation of the mature collagen cross-links, hydroxylysylpyridinoline and lysylpyridinoline

Y. Açil*, P.K. Müller

Institut für Medizinische Molekularbiologie, Universität zu Lübeck, Ratzeburger Allee 160, 23538 Lübeck, Germany

(First received September 28th, 1993; revised manuscript received December 24th, 1993)

Abstract

Hydroxylysylpyridinoline (HP) and lysylpyridinoline (LP) are two non-reducible cross-links of mature collagen which are formed by a sequence of post-translational modifications. HP is a derivative of three residues of hydroxylysine and is present in almost all mature tissues (*e.g.*, tendons, vessel walls, cartilage, teeth and bone). LP is a derivative of two residues of hydroxylysine and one residue of lysine and is present only in dentine and bone. Neither cross-link is found in normal human skin. HP and LP were purified from commercially available bone gelatine ("ossein hydrolysate") by preparative reversed-phase HPLC and the degree of purity was verified by amino acid determination (>98% dry mass). Hydroxylysylpyridinoline and lysylpyridinoline are promising markers in urine of collagen resorption because their levels in urine should reflect only the breakdown of collagen fibres of skeletal tissues. The two components were used as external standards and the determination of HP and LP in urine provides a good means for the specific evaluation of pathological conditions associated with increased bone resorption, *e.g.*, high turnover post-menopausal osteoporosis.

1. Introduction

Collagen is the predominant structural protein of all forms of connective tissues. The covalent intermolecular cross-links between collagen molecules in macromolecular fibrils are essential in providing connective tissue matrices with the required physico-chemical properties and biomechanical stability. Hydroxylysylpyridinoline (HP) and lysylpyridinoline (LP) are the two non-reducible intermolecular cross-links of collagen derived from post-translationally modified hydroxylysyl and lysyl residues of collagen chains [1,2].

HP is found in almost all mature tissues [2–5] whereas LP is present only in calcified tissues (bone and dentine [2,5]). During the process of collagen turnover the two cross-links are released into the blood and are subsequently excreted into the urine [6]. HP and LP are excreted in urine in two forms, one being the free form (about 40%) and the other being represented by a variety of peptide-bond components (about 60%). The total amount of both components can be measured by fluorimetry after reversed-phase high-performance liquid chromatography (HPLC) of hydrolysed urine [4,7,8].

The urinary hydroxylysyl- and lysylpyridinoline are potentially more useful than is urinary

* Corresponding author.

0021-9673/94/$07.00
SSDI 0021-9673(93)E0079-A

hydroxyproline as a marker of the catabolism of collagen fibres from skeletal tissues, because urinary hydroxyproline has a lower specificity profile as it is found in all collagen types in all connective tissues. Moreover, a large proportion of hydroxyproline is metabolized in the liver, and escapes quantitative analysis of collagen breakdown by urinary measurements [9].

One fundamental problem is the current lack of synthetic standards of HP and LP for calibration so as to allow inter- and intra-laboratory comparisons with greater confidence [1,7,10,11]. In all instances questions arise about compound stability and comparability of molar fluorescence rates between HP and LP on the one hand and a reference compound on the other. Until now, adult bovine cartilage (for HP) and powdered and decalcified adult bovine bone (for HP and LP) have been used to prepare the reference standards. In this paper, we describe an alternative procedure for the isolation and purification of HP and LP and report on their use as external calibration standards. Thus, validity of the quantitative analytical data has been greatly improved.

2. Experimental

2.1. Materials

Gelatines from bone ("ossein") and other tissues were a gift from Deutsche Gelatine-Fabriken Stoess (Eberbach/Baden, Germany). Sephadex G-10 was purchased from Pharmacia–LKB (Freiburg, Germany). Fibrous cellulose powder (CF 1) was obtained from Whatman (Maidstone, UK). A Polyprop Econo-Column (4 × 0.8 cm I.D.) was supplied by Bio-Rad (Munich, Germany). A System 6300 amino acid analyser (Beckman, Munich, Germany) was used. Acetonitrile, *n*-heptafluorobutyric acid, glacial acetic acid and *n*-butanol were obtained from Sigma (Deisenhofen, Germany) and gelatine and hydrochloric acid (32%) from Merck (Darmstadt, Germany). All chemicals were of the highest analytical grade.

2.2. Hydrolysis of bone gelatine ("ossein") and batch adsorption chromatography on CF 1 cellulose

A 25-g amount of bone gelatine was dissolved in 1250 ml of 6 *M* hydrochloric acid using a glass bottle flushed with nitrogen for 5 min and sealed with a screw-cap and a PTFE liner. The sample was hydrolysed at 110°C for 24 h. The hydrolysate was filtered through a glass filter (porous glass G2) and evaporated to dryness at 50°C and the residue was dissolved in the mobile phase [*n*-butan-1-ol–glacial acetic acid–water (4:1:1)] to a final volume of 250 ml. A 250-g amount of cellulose powder (CF 1) was washed in 1000 ml of mobile phase and stirred for 2 h. The slurry was filtered to dryness through a glass filter (G2) and suspended in 1000 ml of mobile phase. The hydrolysate and CF 1 slurry were mixed and stirred for 1 h. Subsequently, the hydrolysate–slurry mixture was loaded on to a glass filter and washed with mobile phase (3 × 2 l). The pyridinium-containing fraction was eluted with water (3 × 1 l).

2.3. Molecular sieve chromatography

Following adsorption chromatography (CF 1), the HP- and LP-containing eluate was evaporated to dryness in a rotary evaporator at 50°C and the residue was dissolved in 10 ml of 10% (v/v) acetic acid. Subsequently the solution was applied to a Sephadex G-10 (90 × 2.5 cm I.D.). Elution was performed using 10% (v/v) acetic acid at a flow-rate of 20 ml/h at room temperature. Fractions of 6 ml were assayed for pyridinoline fluorescence (excitation at 297 nm, emission at 397 nm). The enriched pyridinium-containing fractions (32–54, see Fig. 1) were collected and dried (see above).

2.4. Preparative reversed-phase HPLC for isolation of HP and LP

The HPLC system consisted of a two-pump gradient system (Gynkotek Model M 480) equipped with a Gynkotek RF 1002 fluorescence

monitor. Chromatography was performed at room temperature and the flow-rate was 4 ml/min using two solvents: (A) 0.22% (v/v) *n*-heptafluorobutyric acid (HFBA) in water and (B) 0.22% (v/v) HFBA in 80% (v/v) aqueous acetonitrile. The resin (Gynkochrom Spherisorb ODS-II C_{18}; 5 μm; 250 × 8.0 mm I.D. column) was equilibrated with solvent B–solvent A (5:95, v/v) prior to the application of the sample [70 μl in 10% (v/v) HFBA in water]. The column was washed with solvent B–solvent A (5:95, v/v) for 5 min and developed with the following gradients: (1) from 5% to 27% solvent B in 5 min and (2) from 27% to 31% solvent B in 15 min.

The eluate was monitored for HP and LP fluorescence (excitation at 279 nm, emission at 397 nm, range 1 and sensitivity low). The individual peaks of the HP- and LP-containing fractions were collected (see Fig. 2) and evaporated to dryness at 50°C and the purity was checked by amino acid determination.

2.5. Amino acid determination

Hydroxylysyl- and lysylpyridinolines and potentially contaminating amino acids were determined on a Beckman Model 6300 automated analyser using postcolumn derivatization with ninhydrin. The eluate was monitored at 570 and 440 nm.

3. Results and discussion

We determined both the concentration of total cross-link components and the proportions of both HP and LP in a variety of gelatine and connective tissue samples. It is evident that gelatine specimens contain the cross-link compounds (HP and LP) in varying amounts depending on the tissue of origin. Table 1 summarizes the results from various types of gelatines and also from adult human vertebral bone, adult bovine cortical bone, adult bovine cartilage and adult bovine tendon. Clearly, human bone powder contains the highest proportion of LP followed by "ossein hydrolysate", the latter being gelatine made of bone. For reasons of convenience (no demineralization required) and because of its commercial availability (no ethical limitations), we used "ossein" as a raw material to isolate collagen cross-link components.

Black *et al.* [4] isolated 9.6 mg of HP and 1.5 mg of LP from demineralized sheep bone (80 g dry mass) by a modification of the previously described method [12,13]. Our results correspond with theirs. By a single series of the consecutive chromatographic steps, we isolated and purified from 25 g of ossein hydrolysate 2.5 mg of HP and 0.2 mg of LP. The fluorescence characteristics in dilute solutions of pyridinoline isolated by the methods described in here were identical with those described by Fujimoto *et al.*

Table 1
Concentration (dry mass) of hydroxylysylpyridinoline (HP) and lysylpyridinoline (LP) in various gelatines and in a variety of adult tissues

Material	HP:LP molar ratio	HP:LP concentration ratio (nmol/mg dry mass)	Species/tissue
Ossein hydrolysate	22:1	242:11	Adult bovine bone
Ossein gelatine	22.4:1	228:10.2	Adult bovine bone
Middle-layer hydrolysate	33:1	46:1.4	Adult bovine
Middle-layer gelatine	49:1	54:1.1	Adult bovine
Pig rind gelatine	15:1	24:1.6	Adult swine
Gelatine from Merck	17:1	205:12	Adult bovine
Bone	7.4:1	331:44.5	Adult human spine
Bone	33:1	237:18.5	Adult bovine cortex
Cartilage		933:–	Adult bovine
Tendon		55:–	Adult bovine

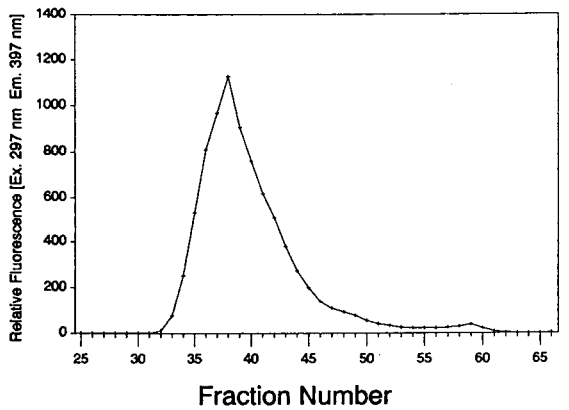

Fig. 1. Gel filtration chromatography (Sephadex G-10, 90 × 2.5 cm I.D. column) using 10% (v/v) acetic acid. The eluate was monitored by fluorescence detection with excitation at 297 nm and emission at 397 nm. Fractions of 6 ml (32—54) were collected and evaporated to dryness at 50°C.

[13]. The excitation maximum is at 297 nm and the fluorescence maximum (emission) is at 397 nm in acid. Using a two-step procedure we achieved virtually complete removal of concomitant impurities such as free amino acids. In the first step, a combination of adsorption and molecular sieve chromatography (Fig. 1) removed about 70% of all amino acids. In the second step of chromatography, two consecutive linear gradients were applied: first, a gradient from 5% to 27% solvent B in 5 min, during which time all amino acids were eluted, and second, a gradient from 27% to 31% solvent B in 15 min to elute HP (16 min) and LP (18 min) (Fig. 2). Subsequently the column was washed free with solvent B. The HP and LP preparations recovered after the series of chromatographic steps had a purity higher than 98% as judged by amino acid determination. The purity results are summarized in Table 2.

Table 2
Purification of hydroxylysylpyridinoline (HP) and lysylpyridinoline (LP) from "ossein"

Method	Purity (%)
CF 1 cellulose	25
Sephadex G-10	70
RP C_{18} preparative	98

The individual isolated peaks pooled after the HPLC each showed a single fluorescence signal and a unique ninhydrin-positive peak following

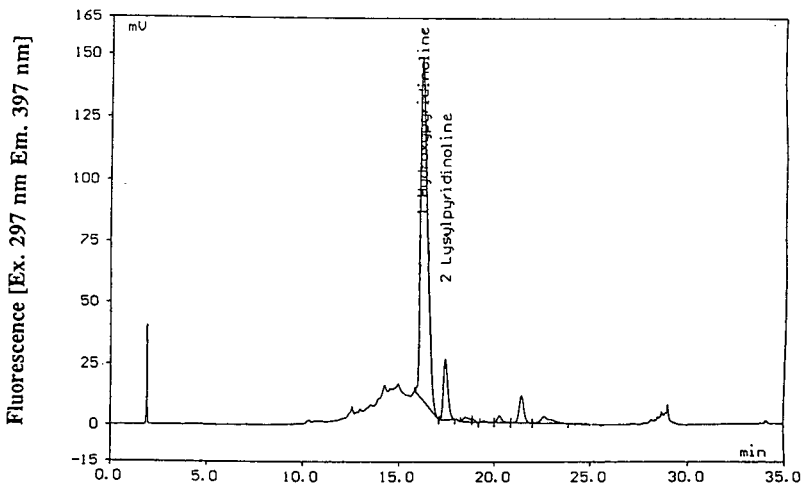

Fig. 2. HPLC of HP and LP with stepwise elution at a flow-rate of 4 ml/min at room temperature with solvent A = 0.22% (v/v) HFBA in water and solvent B = 0.22% (v/v) HFBA in 80% (v/v) aqueous acetonitrile. The pooled HP and LP were evaporated to dryness at 50°C and their degree of purity was checked by amino acid determination.

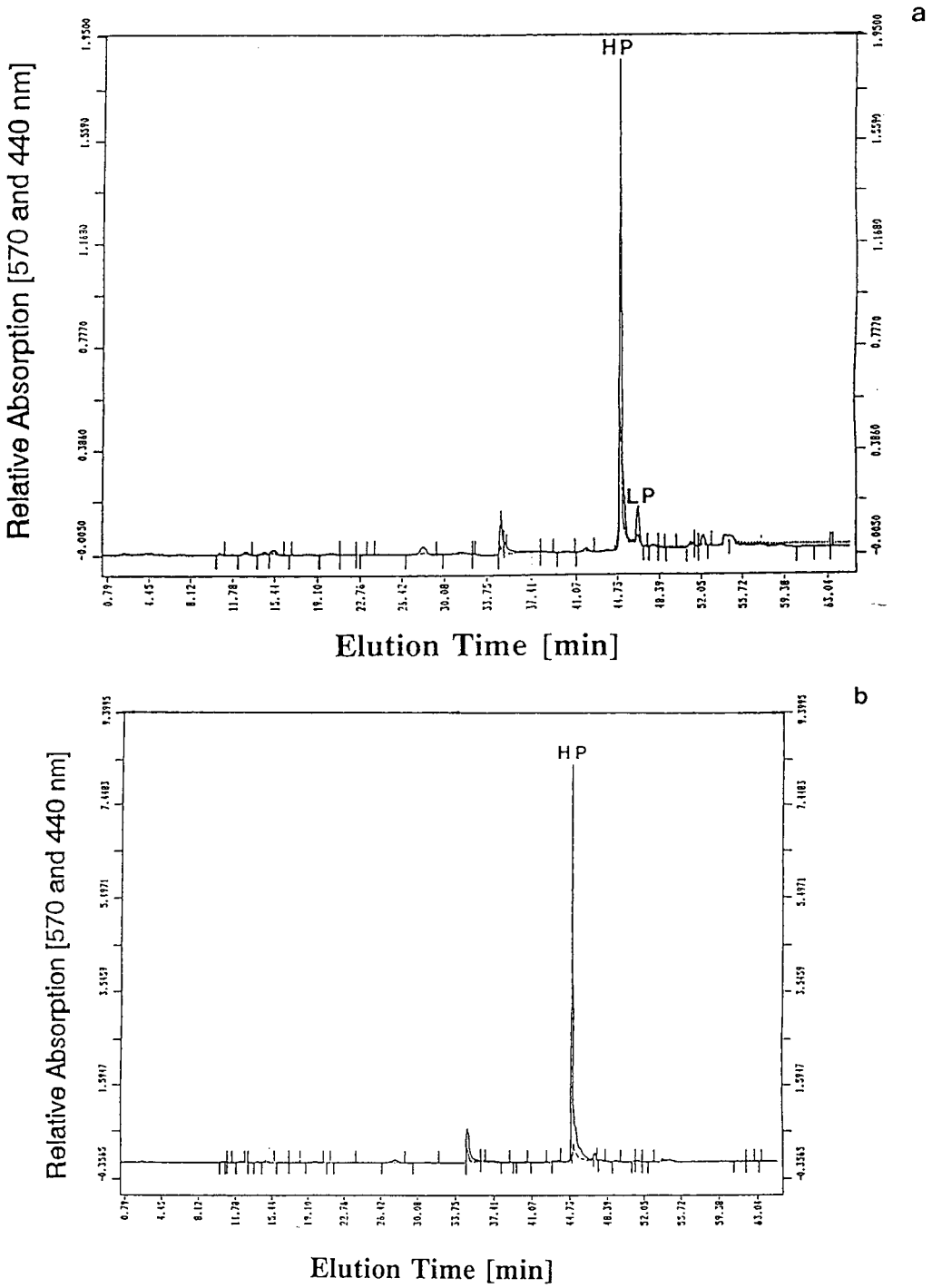

Fig. 3. Determination of purity of HP and LP standards by ion-exchange chromatography on an amino acid analyser. The HP and LP peaks were eluted at 45 and 47 min, respectively. (a) Amino acid analysis of pure HP and LP isolated from "ossein". (b) Pure HP isolated from "ossein".

ion-change chromatography on the amino acid analyser (see Fig. 3a and b).

We analysed serial dilutions of HP and LP in 0.22% (v/v) HFBA. The detector response was found to be linear up to the highest standard concentrations tested of 2250 nmol/ml HP and 1200 nmol/ml LP and gave good reproducibility throughout the assay range (see Fig. 4a and b). The ratio of HP to LP was identical when measured in aliquots of the same sample with ninhydrin on the amino acid analyser and by reversed-phase HPLC with fluorescence detection.

In conclusion, the efficient isolation of the highly purified collagen cross-links HP and LP from bone gelatine can greatly facilitate the determination of the breakdown products of tissue turnover and allows in particular the monitoring of human bone resorption rates in urine. Further, the HP-to-LP ratio is of diagnostic significance in rare connective tissue disorders, such as Ehlers–Danlos syndrome type VI.

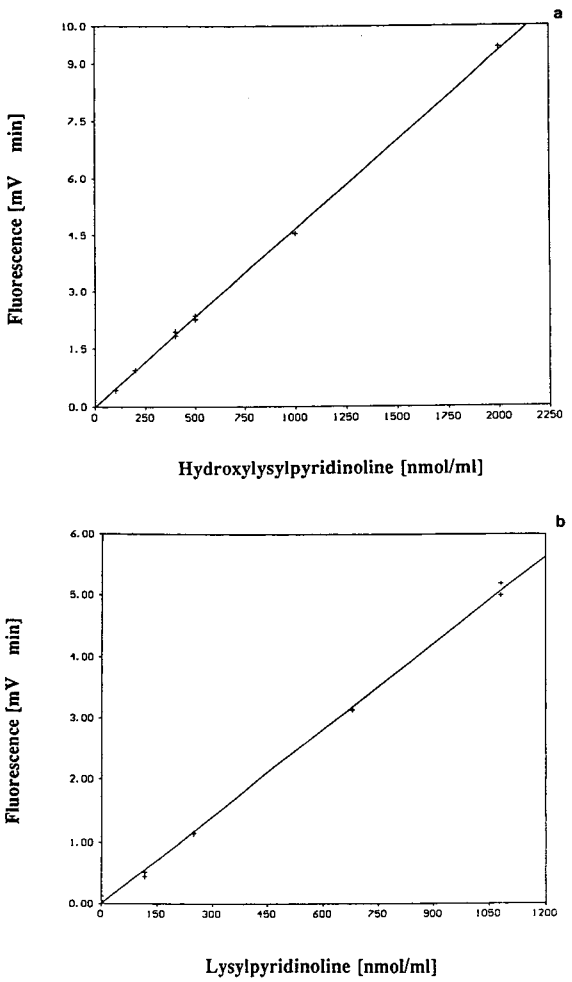

Fig. 4. Calibration graphs for (a) HP and (b) LP. Serial dilutions of the HP and LP standards were analysed by HPLC and their fluorescence intensity was measured using a Gynkotek RF 1002 spectrofluorimeter with excitation at 297 nm and emission at 397 nm. Serial dilutions of the HP and LP standards showed a linear response of integrated fluorescence between 1.0 and 2250 nmol/ml.

4. Acknowledgements

We gratefully acknowledge the excellent technical assistance of Mrs. M. Eichler, I. Fleischhauer and C. Sesselmann. This work was supported by BMFT No. 01 KM 9303.

5. References

[1] D.R. Eyre, *Methods Enzymol.*, 144 (1987) 115–139.
[2] V.R. Preedy, R.A. Sherwood, C.O. Akpoguma and D. Black, *Alcohol Alcoholism*, 26 (1991) 191–198.
[3] P.D. Delmas, E. Gineyts, A. Bertholin, P. Garnero and F. Marchand, *J. Bone Miner. Res.*, 3 (1993) 643–648.
[4] D. Black, A. Duncan and S.P. Robins, *Anal. Biochem.*, 169 (1988) 197–203.
[5] P.D. Delmas, *Bone*, 13 (1992) 17–21.
[6] Z. Gunja-Smith and R.J. Boucek, *Biochem. J.*, 197 (1981) 759–762.
[7] V.T. Kung, H.S.J. Ju, M.J. Cerelli, R.H. Hesley and S.M. Seyedin, presented at the *XXIIIrd European Symposium on Calcified Tissues, Heidelberg, April 25–29, 1993.*
[8] D.R. Eyre, *J. Clin. Endocrinol. Metab.*, 74 (1992) 470A–470C.
[9] D. Fujimoto, M. Suzuki, A. Uchiyama, S. Miyamoto and T. Inoue, *J. Biochem. (Tokyo)*, 94 (1983) 1133–1136.
[10] L.J. Beardsworth, D.R. Eyre and I.R. Dickson, *J. Bone Miner. Res.*, 5 (1990) 671–676.
[11] A. Colwell, R.G.G. Russell and R. Eastell, *Eur. J. Clin. Invest.*, 23 (1993) 341–349.
[12] S.P. Robins, *Biochem. J.*, 215 (1983) 167–173.
[13] D. Fujimoto, K. Akiba and N. Nakamura, *Biochem. Biophys. Res. Commun.*, 76 (1977) 1124–1125.

ELSEVIER

Journal of Chromatography A, 664 (1994) 189–194

JOURNAL OF CHROMATOGRAPHY A

Determination of phylloquinone in intravenous fat emulsions and soybean oil by high-performance liquid chromatography

Fathi Moussa*[,a], François Depasse[b], Véronique Lompret[b], Jean-Yves Hautem[b], Jean-Phillippe Girardet[b], Jean-Loup Fontaine[b], Pierre Aymard[c]

[a]*Faculté de Pharmacie de Tours, Service de Chimie Analytique, 2 Bis Boulevard Tonnellé, 37042 Tours Cedex, France*
[b]*Laboratoire de Biochimie et Service de Gastro-entérologie et Nutrition Pédiatriques, Hôpital Trousseau, 26 Avenue du Dr. A. Netter, 75012 Paris, France*
[c]*Faculté de Pharmacie, Service de Physiologie, Rue Jean Baptiste Clément, 92296 Chatenay-Malabry Cedex, France*

(First received June 28th, 1993; revised manuscript received November 12th, 1993)

Abstract

A method for determining vitamin K_1 (VK_1) in intravenous fat emulsions (IVFE) and soybean oil (SBO) using a single-step HPLC procedure is described. The method is linear from 9.7 to 617 ng of VK_1 per gram of IVFE and from 41 to 5234 ng of VK_1 per gram of SBO (signal-to-noise ratio = 3). The results obtained by this method with four samples of IVFE indicate the existence of a variability in VK_1 content depending on the nature of the preparation (long- or medium-chain triglycerides), the producer and the production batch. This variability of the VK_1 content, also observed with the same method in SBO, is ascribable to the raw materials used to produce the different preparations.

1. Introduction

Intravenous fat emulsions (IVFE) are used as a source of energy and essential fatty acids for adults and for children and infants on total parenteral nutrition (TPN). These emulsions contain 5–20% of soybean oil, considered to have a high vitamin K_1 or phylloquinone (VK_1) content [1–5]. Two studies have shown that, under certain conditions, the VK_1 content of IVFE is amply sufficient to cover the needs of children on TPN [6,7]. However, as doctors lack specific data on the vitamin content of these emulsions, they continue to prescribe daily injections of phylloquinone to their patients on TPN. Whereas the essential role of this vitamin in blood coagulation is well known, there is no proof of its presumed functions on calcium metabolism [8–10]. Further, a recent study [11] showed that intramuscular administration of vitamin K to newborns was statistically related to the later development of childhood cancer. In order to be able to control the VK_1 intake of patients of TPN, a simple, reliable method for determining phylloquinone in IVFE is needed. To our knowledge such a method is not available to date. It is also important, at the production level, to be able to determine this vitamin in the soybean oil used to prepare IVFE.

The method for assaying phylloquinone in soybean oil proposed by Zonta and Stancher [1] is difficult to implement on a routine basis. More

* Corresponding author.

0021-9673/94/$07.00
SSDI 0021-9673(93)E0046-W

recently, Ferland and Sadowski [2] applied the method for the determination of plasma VK_1 developed by Haroon *et al.* [12] to the study of various vegetable oils. More sensitive and specific than the former [1], this latter method nonetheless includes two chromatographic steps, the second of which is coupled to a precolumn derivatization [2].

In this paper, we propose a one-step HPLC method for the determination of VK_1 in IVFE and soybean oil. The proposed method was applied to the study of VK_1 content and conservation in four samples of IVFE and three samples of soybean oil.

2. Experimental

2.1. Samples

The study was conducted on four samples of IVFE commonly used for the various medical departments in the Trousseau hospital: two IVFE samples composed of long-chain triglycerides [(i) LCT_1 containing 20% of soybean oil and (ii) LCT_2 containing 10% of soybean oil]; two IVFE samples composed of LCT and medium-chain triglycerides [(iii) MCT_1 containing 5% of soybean oil and (iv) MCT_2 containing 10% of soybean oil]; three samples of commercial soybean oil, including two from the same producer (SBO_1, 1-l clear bottle, expiry date January 1993, and SBO_2, 5-l opaque bottle, expiry date December 1992). The third sample (SBO_3, 1-l clear bottle, expiry data February 1993) came from another producer.

2.2. Reagents

Standards of vitamin $K_{1(20)}$ and vitamin $K_{1(25)}$ [13] used as internal standards (I.S.) were purchased form Hoffmann-La Roche (Neuilly-Sur-Seine, France). Stock standard solutions of the different vitamins, 1 g l^{-1} in hexane, were stored at −20°C in the dark. These standard solutions were diluted with hexane as required and stored under the same conditions.

Hexane, acetonitrile and diisopropyl ether were of Uvasol grade from Merck (Darmstadt, Germany). Absolute ethanol was obtained from Carlo Erba (Milan, Italy) and sodium perchlorate from Merck. All chemicals were used as received.

2.3. Apparatus

The HPLC system was the same as described previously for the determination of *trans*-phylloquinonemia [13], namely a reversed phase system with a 70 mm × 4.7 mm I.D. XL 3-μm octyl cartridge (Beckman, Gagny, France) combined with fluorimetric detection after post-column coulometric reduction. We are currently using a Linear Fluor LC 304 detector (Spectra-Physics, Courtaboeuf, France).

During the tests, we also used Sep-Pak silica cartridges (Waters, St. Quentin-en-Yvelines, France) to purify the fat emulsions containing VK_1 and I.S. before injection into the chromatograph.

2.4. Method

The concentration of the standard solutions of vitamin K_1 ($SS_1 = 0.4$ mg l^{-1} for IVFE analysis and $SS_2 = 4$ mg l^{-1} for soybean oil analysis) in hexane was determined, after equilibration at room temperature, by measuring the absorbance (after suitable dilution) at 248 nm (molar absorptivitiy = 19 900 l mol^{-1} cm^{-1}). For each type of determination (IVFE or soybean oil), a calibration graph was produced by adding incremental amounts of VK_1 to a blank sample exposed to daylight to eliminate endogenous vitamin.

Preparation of blank sample

Introduce 6–7 g of IVFE or soybean oil into a 40 − ml clear glass tube, stopper the tube and place it horizontally near a window. After 48 h of exposure to daylight, the sample no longer contains any VK_1 detectable by the proposed method.

Preparation of calibration graph

Fill four 5-ml glass tubes with aliquots of standard VK_1 solution (0.10, 0.50, 1.00 and 2.00

ml of SS_1 and 0.10, 0.25, 0.50 and 1.00 ml of SS_2, depending on the circumstances) and evaporate to dryness under a stream of nitrogen. Pipette into each tube 1 g of blank sample and shake the tubes gently for 10 min in the dark. The samples thus enriched can be stored for at least 1 month in the dark.

Assay of VK_1 in IVFE and soybean oil

Pipette into a glass tube 0.10 ml of I.S. solution at the appropriate concentration (0.2 mg l^{-1} for IVFE analysis and 2 mg l^{-1} for soybean oil analysis) and evaporate under a stream of nitrogen. Pipette into the same tube about 100 mg (determine the amount accurately) of test or calibration sample and shake for 15 s. Next add 0.50 ml of 0.9% NaCl solution and 1.00 ml of ethanol. After shaking for 2 min, add 3.00 ml of hexane and agitate for 30 min at room temperature in the dark. After centrifuging at 7000 rpm for 10 min (5000 *g*), collect the supernatant in a conical tube and evaporate to dryness under a stream of nitrogen. Dissolve the dry residue (lipid extract) in 0.50 ml (5.00 ml for soybean oil analysis) of mobile phase [acetonitrile–ethanol (95:5, v/v) containing 0.005 *M* $NaClO_4$], and inject 0.05 ml into the chromatograph.

Purification of lipid extract

During the tests, we purified several lipid extracts on a Sep-Pak silica cartridge prior to injection into the chromatograph. The protocol was as follows: the lipid extract is dissolved in 1.00 ml of hexane (10.00 ml for soybean oil) and 0.10 ml is injected into a Sep-Pak cartridge prepared in advance using 10.00 ml of hexane. After passage of 10.00 ml of hexane to eliminate the less polar lipids, VK_1 and IS are eluted using 10.00 ml of hexane–diisopropyl ether (90:10, v/v). The eluent is collected in a conical tube and evaporated to dryness under a stream of nitrogen. The dry residue is carefully dissolved in 1.00 ml of hexane and the solution is evaporated to dryness under a stream of nitrogen. The final residue is dissolved in 0.05 ml of mobile phase and 0.04 ml is injected into the chromatograph.

Study of conservation

Conservation of VK_1 in IVFE (in the original packaging) was studied under three different conditions: (1) at room temperature in the dark; (2) at 4°C in the dark; and (3) at room temperature in daylight. After sampling an aliquot for an initial assay (day 0), the flask was restoppered and stored as already described. Aliquots of each sample thus stored were then taken for assaying VK_1 on days 4, 22, 40, 50 and 60.

Soybean oil conservation was studied at room temperature in the dark.

3. Results

The chromatographic profiles of an IVFE and a soybean oil sample obtained by the proposed method are shown in Fig. 1a and b, respectively. The peaks are qualitatively identical, confirming the presence of soybean oil in the IVFE samples. After 48 h of exposure to daylight, according to the operating protocol described above, we observe on the chromatogram of the soybean oil, for example, the complete resolution of the peak attributed to VK_1 (Fig. 1c).

Different criteria enabled us to identify and verify the purity of the VK_1 peak. In addition to the retention time, the disappearance caused by exposure to daylight and the effect of supplementing, the identity of the VK_1 peak and its purity were checked by analysing the hydrodynamic voltammogram and the fluorescence characteristics of the molecule [13,14].

By purifying the lipid extract on a Sep-Pak silica cartridge, we were able to eliminate the unidentified peaks of k' higher than those of the I.S. and to shorten the run time (Fig. 1d). This treatment also affords a gain in detection sensitivity of *ca.* 10%, ascribable to the elimination during purification of the interfering substances that co-eluted with the two vitamins during the HPLC step. The interferences probably occur at the level of the electroreduction of the two vitamins by competition with the active sites of the working electrode. In fact, injection into the chromatograph of *ca.* 30 samples not purified on the Sep-Pak cartridge led to gradual passivation

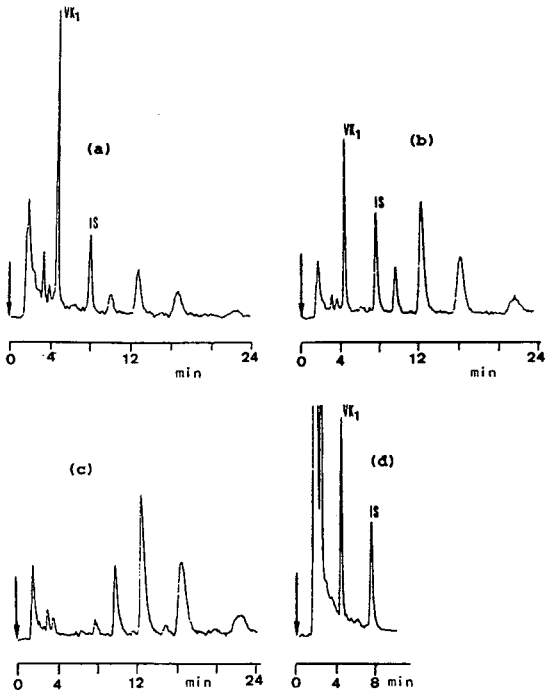

Fig. 1. Chromatograms of (a) an extract of IVFE (MCT) and of an extract of soybean oil (b) before and (c) after 48 h of exposure to daylight and (d) after Sep-Pak silica cartridge purification. Column, 70 mm × 4.6 mm I.D. XL 3-μm octyl cartridge; mobile phase, acetonitrile–ethanol (95:5, v/v), containing 0.005*M* sodium perchlorate; flow-rate, 0.80 ml min^{-1}. Electrochemical reduction followed by fluorescence detection [13]. Unmarked peaks are unidentified.

of the working electrode, which resulted in a decrease in the sensitivity of the detection system. Applying a positive potential (+0.9 V) for a few minutes regenerates the electrode surface and leads to recovery of the initial sensitivity after desorption of the material adsorbed. We therefore decided to retain the direct injection method, leaving aside the long and costly purification of the lipid fractions on Sep-Pak cartridges. Lastly, prior lipase treatment of the IVFE or soybean oil samples, as proposed by Zonta and Stancher [1], makes no noticeable difference in terms of the chromatographic profiles.

The linearity of the proposed method was studied using a range of concentrations obtained through successive dilutions with blank sample of a sample of IVFE with an initial VK_1 content of 617 ng g^{-1}. The method is linear from 9.7 to 617 ng g^{-1} of VK_1 [$y = 0.85x + 7.5$, $r = 0.998$, $n = 6$, where y is the area ratio: VK_1/I.S. and x is the sample VK_1 concentration (ng g^{-1})]. For soybean oil, the linearity was studied using a range of concentrations obtained by supplementing an oil sample, followed by successive dilutions with blank sample. The method proved linear from 41 to 5234 ng of VK_1 per gram of oil ($y = 0.77x + 3.6$, $r = 0.996$, $n = 7$).

The detection limit of the method is 2 ng of VK_1 per gram of IVFE and 5 ng per gram of soybean oil (signal-to-noise ratio = 3).

The accuracy of the method is shown in Table 1. The relative standard deviation (R.S.D.) is satisfactory for both the upper and lower values.

The recoveries of VK_1 and the I.S. were determined after supplementing a blank sample, by comparing their peak areas with those obtained after direct injection into the chromato-

Table 1
Precision of the method

Sample	Within-run ($n = 5$)		Between-run ($n = 3$)	
	Mean (ng g^{-1})	R.S.D. (%)	Mean (ng g^{-1})	R.S.D. (%)
MCT_1	46	3.5	44	7.1
MCT_2	216	–	–	–
LCT_1	617	2.0	618	4.0
LCT_2	220	–	–	–
SBO_1	1080	1.7	1020	5.2
SBO_2	3080	0.9	3130	3.2
SBO_3	1080	–	–	–

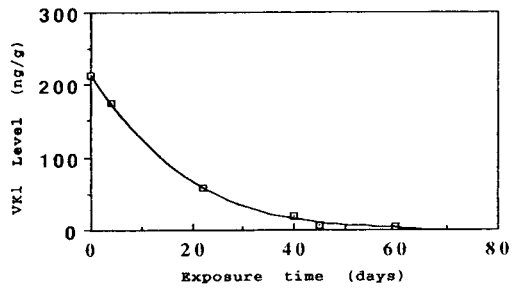

Fig. 2. Photodegradation of vitamin K_1 in a 250-ml flask of IVFE (LCT) on exposure to daylight. □ = VK_1 level (ng g^{-1}).

graph of pure solutions of the two vitamins. The recovery of VK_1 was 75–85% for IVFE ($n = 3$) and 85–91% for soybean oil ($n = 3$). Under the same conditions, the recovery of the I.S. was 65–70% for IVFE ($n = 3$) and 69–76% for soybean oil ($n = 3$).

The recovery of the method, calculated in relation to the I.S., after supplementing two samples of IVFE and two samples of soybean oil, exceeded 92% in all instances.

Fig. 2 shows the effect of daylight on the VK_1 content of a 250-ml flask of LCT. Under these conditions, there is considerable deterioration of the vitamin. However, its half-life remains relatively long (14 days). Also, the decrease in the concentration of this vitamin after 24 h of exposure remains less than 5%. Consequently, the deterioration of the vitamin during a 12–24-h infusion is negligible. Conversely, when kept in the dark, VK_1 remained stable at the two storage temperatures studied. Lastly, in the dark and at room temperature, phylloquinone remained stable for over 6 months (length of the study) in the two samples, SBO_1 and SBO_2, studied.

4. Discussion

To assay VK_1 in soybean oils, Zonta and Stancher [1] recommended, in order to eliminate interfering lipids, a 15-h enzymatic digestion step, followed by two chromatographic steps, the second by HPLC combined with UV detection. According to Lambert and De Leenheer [14], "Due to the complexity of the matrices and the problems in the detection, the quantification of endogenous vitamin $K_{1(20)}$ levels in humans, as well as the analysis of vitamin $K_{1(20)}$ in food samples, remains an analytical challenge". However, when a sample has a relatively high VK_1 content (several tens of nanograms of VK_1 per gram of sample), our results show that use of a sufficiently sensitive detection mode makes it possible to simplify sample purification. In their method, which features a low detection sensitivity, they used 15 g of sample [1]. By decreasing this amount to 0.25–1 g, Ferland and Sadowski [2] succeeded in adapting the method for the determination of phylloquinonemia developed by Haroon *et al.* [12] to the determination of VK_1 in vegetable oils. However, the latter method consists of two chromatographic steps, including chemical reduction of the VK_1 molecule to make it fluorescent. Now, in the reduced form, VK_1 is highly unstable and difficult to handle [14]. The use of a detection mode as sensitive as fluorescence for VK_1 makes it possible to work with a sample of a few milligrams, thereby considerably decreasing the amount of lipids to be treated. Under these conditions, the enzymatic digestion step becomes useless. Likewise a single HPLC step is sufficient to separate and assay VK_1 in soybean oils and *a fortiori* in IVFE containing only 10–20% oil. This is what is proposed in our method in which the final amount of oil injected into the chromatograph is *ca.* 1 mg.

The results obtained with the various IVFE samples indicate the existence of a variability stemming from the origin and nature of the sample and also from the production batch studied (Table 1). Without specifying the number of samples analysed, Goulet *et al.* [6] reported VK_1 concentrations of 208 ± 34 ng ml^{-1} for the IVFE they used in their clinical study. Although they also did not specify their assay methodology, especially as regards the amount of sample and its preparation, their findings tend to confirm the origin-related variability of the emulsions observed in our study.

As regards soybean oils, the results we obtained (Table 1) agree with those of Zonta and

Stancher (121–3330 ng g^{-1}) [1]. They are lower than those obtained by Schneider *et al.* (4500–6300 ng g^{-1}) [3], while those obtained by Ferland and Sadowski [2] are even lower (1400–2000 ng g^{-1}). Zonta and Stancher attributed [1] these differences to the industrial production method and/or to the raw materials used. Our results for both the soybean oils and the IVFE tend to confirm the raw materials assumption. According to Ferland and Sadowski [2], the differences do not stem from the raw materials, but rather from the assay method. This is surprising as they asserted in another paper [15] that climate, soil and the conditions of growth can affect the VK_1 content of greenery. The influence of such factors on the phylloquinone content of soybeans is under study.

5. Acknowledgements

We thank Dr. C. Melin for his support and Ms. C. Berrivin for translation services.

6. References

[1] F. Zonta and B. Stancher, *J. Chromatogr.*, 329 (1985) 257–263.
[2] G. Ferland and J.A. Sadowski, *J. Agric. Food Chem.*, 40 (1992) 1869–1873.
[3] D.L. Schneider, H.B. Fluckiger and J.D. Manes, *Pediatrics*, 53 (1974) 273–275.
[4] Y. Haroon, M.J. Shearer, S. Rahim, W.G. Gunn, G. McEnery and P. Barkahn, *J. Nutr.*, 112 (1982) 1105–1117.
[5] S.M. Hwang, *J. Assoc. Off. Anal. Chem.*, 68 (1985) 684–689.
[6] O. Goulet, J.J. Lefrere, M. Guillaumont, M. Leclerc, J. Lerable, D. Gozin and C. Ricour, *Clin. Nutr.*, 9 (1990) 85–87.
[7] J.P. Girardet, F. Moussa, P. Aymard and J.L. Fontaine, *Arch. Fr. Pediatr.*, 47 (1990) 395–398.
[8] J.W. Suttie, *Fed. Proc. Fed. Am. Soc. Exp. Biol.*, 39 (1980) 2730–2735.
[9] P.A. Lane and W.E. Hathaway, *J. Pediatr.*, 106 (1985) 351–359.
[10] R.V. Kries, M.J. Shearer and U. Gobel, *Eur. J. Pediatr.*, 147 (1988) 106–112
[11] J. Schaub, *Eur. J. Pediatr.*, 152 (1993) 174.
[12] Y. Haroon, D.S. Bacon and J.A. Sadowski, *Clin. Chem.*, 32 (1986) 1925–1929.
[13] F. Moussa, L. Dufour, J.R. Didry and P. Aymard, *Clin. Chem.*, 35 (1989) 874–878.
[14] W.E. Lambert and A.P. De Leenheer, in A.P. De Leenheer, W.E. Lambert and H.J. Nelis (Editors), *Modern Chromatographic Analysis of Vitamins* (*Chromatographic Science Series*, Vol. 60), Marcel Dekker, New York, 2nd ed., 1992, ch. 4.
[15] G. Ferland and J.A. Sadowski, *J. Agric. Food. Chem.*, 40 (1992) 1874–1877.

ELSEVIER

Journal of Chromatography A, 664 (1994) 195–202

JOURNAL OF CHROMATOGRAPHY A

Structure elucidation of glykenin glycosidic antibiotics from *Basidiomycetes* sp. V. High-performance liquid chromatographic separation of components of glykenin

Fumiko Nishida*,[a], Mika Nishimura[a], Ken-Ichi Harada[a], Makoto Suzuki[a], Vithaya Meevootisom[b], Timothy W. Flegel[b], Yodhathai Thebtaranonth[b], Suthum Intararuangsorn[b]

[a]*Faculty of Pharmacy, Meijo University, Tempaku, Nagoya 468, Japan*
[b]*Mahidol University, Rama VI Road, Bangkok 10400, Thailand*

(First received September 13th, 1993; revised manuscript received December 9th, 1993)

Abstract

The glycosidic antibiotics of the glykenin (GK) family produced by *Basidiomycetes* sp. were separated into nine components (GK-I–VII and DG) by normal-phase chromatography. It was found that these components differ in the number and location of the acetyl groups in the sugar moiety. Each component (GK-I–VII and DG) was further separated into three isomers (A, B and C), which possess different aglycones, by reversed-phase chromatography on an ODS column with methanol–acetonitrile as eluent. The best composition of the eluent was found to be methanol–acetonitrile–1% trifluoroacetic acid (4:3.5:2.5). The profile analysis of GK-III–VII and DG was also carried out using a modified mobile phase. The combination of normal- and reversed-phase chromatography separated all components of the GK mixture except GK-I and II. The relationship between structure and separation behaviour of GK is discussed.

1. Introduction

The glycosidic antibiotics glykenins (GKs) are produced by *Basidiomycetes* sp. and exhibit inhibitory activity against Gram-positive bacteria and infection by polio and herpes virus. The GK mixture (see Experimental) was separated into GK-I–VII and deacetylated GK (DG) by TLC on a silica gel plate (Fig. 1), the main components being GK-III and -IV.

The structures of DG and GK-III and -IV were determined in previous work [1–4] and are shown in Fig. 2. DG-A, -B and -C possess hydroxylated C_{26} fatty acids as the aglycone moieties. The positions and absolute configurations of the four hydroxy groups of the aglycone-A were determined to be 2*S*, 16*R*, 17*S* and 21*R*

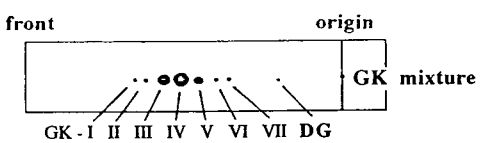

Fig. 1. Silica gel TLC of GK mixture. Solvent system, chloroform–methanol–50% acetic acid (65:20:5).

* Corresponding author.

0021-9673/94/$07.00
SSDI 0021-9673(93)E0031-O

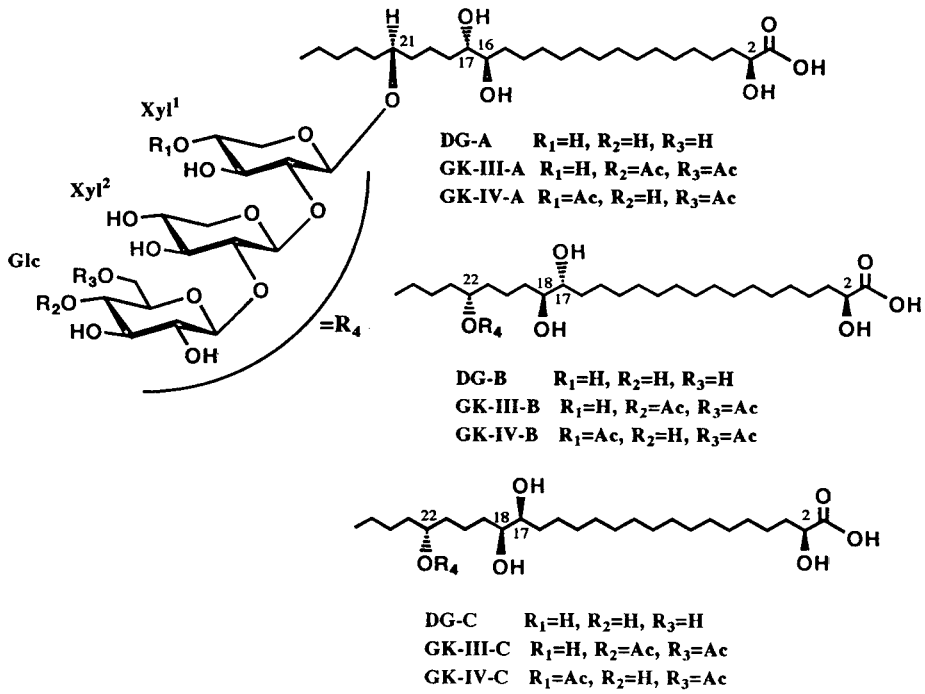

Fig. 2. Structures of DG, GK-III and GK-IV.

by a combination of degradative transformation and circular dichroism spectral measurement. Similarly, the structures of aglycone-B and -C including their stereochemistries were also determined, as shown in Fig. 2. Thus, the structural relationship between aglycone-A and -B is regioisomeric and that between the aglycone-B and -C is stereoisomeric at C-17. The basic structure of the sugar moiety is a trisaccharide composed of two xylose and one glucose residues linked through the β-1, 2-glycosidic bonds. Each of GK-III and -IV is composed of three components. GK-III-A, -B and -C have two acetyl groups in the glucose residue of DG-A, -B and -C, respectively, and GK-IV-A, -B and -C also have two acetyl groups in the glucose and xylose-1 residues of DG-A, -B and -C, respectively, but these structures were elucidated by two-dimensional NMR spectrometry without isolation of the individual components because of the difficulty of isolation.

Although DG-A, -B and -C were converted into their phenacyl esters, which were successfully purified by the preparative HPLC with UV detection, the same procedure could not be applied to the separation of GK-III and -IV, as described later. The minor components other than GK-III and -IV also have not been separated into their corresponding three components so far, mainly because GK-III and -IV are composed of mixtures of the three components of acetylated DG-A, -B and -C whose structures are closely related to each other, as mentioned above, and in addition these components do not possess an appropriate chromophore to be detected in HPLC and have poor solubility in most solvents. Other minor components are in almost the same situation as GK-III and -IV.

An additional unfavourable result has been obtained. We attempted HPLC analyses of GK-III and -IV after derivatization with phenacyl bromide. Each of the chromatograms of the phenacyl esters of GK-III and -IV gave three peaks at 10, 10.5 and 12 min and these retention times were identical with those of the phenacyl esters of DG-A, -B and -C, respectively (chromatograms not shown). These results indicate that the acetyl groups in GK-III and -IV were

removed in the process of the derivatization and then the resulting DG-A, -B and -C were esterified. It was difficult to obtain an appropriate derivative for HPLC because of the presence of two labile acetyl groups in GK.

Hence an HPLC analysis of intact GK components was required. To perform the separation of these components, optimization of the HPLC conditions with refractive index (RI) detection was carried out. The application of the optimum conditions to GK components resulted in a good separation of these components, and it became clear that each GK component is composed of three isomers. This paper describes the optimization of the HPLC conditions, the application of the optimum conditions to each component and the correlation of the structure of the GK species and its retention behaviour.

2. Experimental

2.1. General procedure

Analytical TLC was performed on precoated silica gel 60 plates (Merck) and RP-18WF$_{254S}$ (Merck). Column chromatographic separations were carried out using Sephadex LH-20 (Pharmacia) and silica gel 60 (Nacalai Tesque). Fast atom bombardment mass spectrometry (FAB-MS) was carried out using an HX-110 instrument (Jeol) fitted with a JMA-DA 5000 data system (Jeol). A neutral xenon beam was used as the primary beam for the ionization of samples by FAB. The acceleration voltages of the primary and secondary beams were adjusted to 6 and 8 kV, respectively. A high-performance liquid chromatograph equipped with an LC-9A pump (Shimadzu) was used with an ERC-7512 RI detector (Erma) to separate the components of GK and DG homologues.

2.2. Isolation of minor components

The fermentation broth [2] of GK was extracted three or four times with ethyl acetate and the organic layer was concentrated to give a brown oil. LH-20 column chromatography (90 × 8 cm I.D.) of the oil (4.95 g) gave 3.34 g of a GK mixture, 3 g of which were purified by repeated silica gel column chromatography using chloroform–methanol–50% acetic acid [(i) 65:15:5 and (ii) 65:20:5] to give GK-III (15 mg), GK-IV (75 mg) and a mixture of minor components (1 g). The minor components were further chromatographed on a silica gel column using chloroform–methanol–50% acetic acid [(i) 65:5:5, (ii) 65:10:5, (iii) 65:15:5 and (iv) 65:20:5] and were separated into GK-I (5.2 mg), -I′ (3.1 mg), -II (2.2 mg), -V (7.8 mg), -VI (3.5 mg) and -VII (7.4 mg) and DG (10.3 mg).

2.3. HPLC analysis

HPLC analyses of GK components were performed using a column of Inertsil ODS-2 (5 μm) (250 × 4.6 mm I.D.) (GL Science) at a flow-rate of 0.3 ml/min. Methanol–acetonitrile–1% trifluoroacetic acid (TFA) (4:3.5:2.5) was used as the mobile phase for analyses of GK-III–VII and DG and methanol–acetonitrile–1% TFA (3.5:3.5:3) for the profile analysis of the GK mixture.

3. Results and discussion

3.1. Isolation and molecular masses of each component of GK

GK mixture was separated into GK-I–VII and DG on a normal-phase TLC plate developed with chloroform–methanol–50% acetic acid (65:20:5) as shown in Fig. 1. It was found in a previous study [3,4] that the molecular masses of DG and GK-III and -IV are 886, 970 and 970, respectively, and the difference in molecular mass between DG and GK-III and between DG and GK-IV corresponds to two acetyl groups in the sugar moieties of GK-III and -IV. Similarly, other components are considered to have acetyl groups. The components, GK-I, -I′, -II, -V, -VI and -VII were isolated by repeated silica gel chromatography using chloroform–methanol–50% acetic acid solvent systems [(i) 65:5:5, (ii) 65:10:5, (iii) 65:15:5 and (iv) 65:20:5]. The

Table 1
Molecular masses of GK components

GK	Molecular mass	GK	Molecular mass
I	1012	V	970
I′	1012	VI	928
II	1012	VII	928
III	970	DG	886
IV	970		

molecular masses of these minor components were measured by FAB-MS in the negative-ion mode and are given in Table 1. These results indicated that GK-VI and -VII have one acetyl group, GK-III–V have two acetyl groups and GK-I and -II have three acetyl groups. Additionally, the informative fragment ions including sugar moieties in the FAB mass spectra suggested that one acetyl group of GK-VII is on the glucose residue, one acetyl group of GK-VI is on the xylose-1 residue and two acetyl groups of GK-V are on the glucose residue. Thus, GK-I–VII differ in the number and location of the acetyl groups in the sugar moiety. As DG and GK-III and -IV have individually three aglycones, -A, -B and -C, each of other components would include three isomers based on the difference in the aglycone. Although the separation of a GK mixture was attempted by normal-phase TLC with various solvent systems, no solvent system gave a good resolution. In addition, each of the GK-I–VII and DG isolated were not separated into the three corresponding isomers by silica gel chromatography. Hence a much better separation of GK components was highly desirable.

Prior to HPLC analysis of intact the GK components with RI detection, the resolution of GK-III and -IV isomers was investigated by reversed-phase TLC using of various mobile phases. The mobile phase initially tested, methanol–water (9:1), caused serious tailing of the spots. Addition of acetic acid to the aqueous portion of the mobile phase decreased the tailing in normal-phase TLC. Additionally, replacement of acetic acid with 1% TFA improved the tailing problem. However, as use of methanol–1% TFA and acetonitrile–1% TFA did not always give good results, addition of the organic solvents ethanol, 2-propanol, acetone, acetonitrile, chloroform and tetrahydrofuran to the methanol–1% TFA mobile phase was carefully examined. The addition of acetonitrile improved the resolution of the three stereoisomers of GK-III and -IV. Although the optimized solvent system, methanol–acetonitrile–1% TFA (5:3:2), could not completely separate three stereoisomers, two isomers were clearly resolved. Based on the TLC studies mentioned above, analyses of GK components by HPLC was investigated using methanol–acetonitrile–1% TFA.

3.2. Optimization of HPLC conditions for separation of stereoisomers of GK-III and -IV

Initially, the solvent system optimized in TLC, methanol–acetonitrile–1% TFA (5:3:2), was directly applied to the HPLC of GK-III and -IV on an ODS column. Whereas this mobile phase eluted these compounds too fast, a change of composition to 4:3:3 increased the elution time to 1 h. On the basis of this result, optimization of the mobile phase was performed with respect to the following factors: (1) proportion of organic solvents and aqueous solvent; (2) concentration of the acid in the aqueous acid solvent; and (3) combination of organic solvents, methanol and acetonitrile. As it was difficult to separate the first and second peaks among the three peaks of GK-III and -IV as shown in Fig. 3, the separation was mainly evaluated by the resolution factor (R_s) between the first and second peaks.

The initial investigation for the optimization of the mobile phase involved setting an appropriate combination of organic and aqueous solvents. As the retention time (t_R) was considerably affected by the aqueous portion, the proportion of the organic solvents, methanol and acetonitrile, was fixed at 4:3.5 considering the previous result, and the proportion of the aqueous portion containing 1% TFA was varied from *ca.* 1 to 4 as shown in Table 2. When the aqueous proportion was 1, GK-III and -IV showed the capacity factors (k') of 0.45 and 0.43, respectively, and both R_s values were zero, showing that they are eluted too fast. With a proportion of 2.5, both components showed the proper k' values and gave R_s

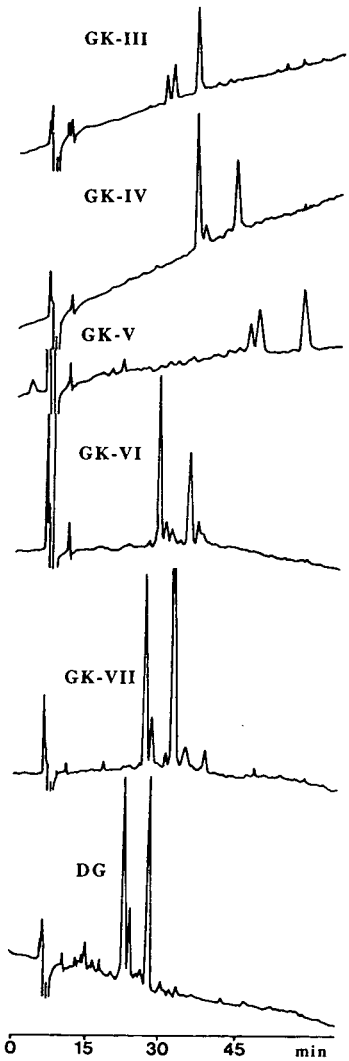

Fig. 3. Separation of the GK-III–VII and DG isomers. Column, Inertsil ODS-2 (5 μm) (250 × 4.6 mm I.D.); mobile phase, methanol–acetonitrile–1% TFA (4:3.5:2.5); flow-rate, 0.3 ml/min.

of 1.11 and 1.11, indicating almost satisfactory resolution. However, a further increase in the proportion gave too long t_R and both R_s values could not be measured owing to drift of the baseline. These results showed that the optimum proportion of the organic and aqueous portions is 7.5:2.5.

Next, to examine the influence of pH in the aqueous portion of methanol–acetonitrile–aqueous TFA (4:3.5:2.5) on resolution, the concentration of TFA was varied between 0.01% and 2% (Table 3). Although the R_s values of GK-III and IV were small at TFA concentrations below 0.1% (pH 2), they increased considerably above 0.5% TFA (pH 1) and no further improvement was observed above 1% TFA. Hence the optimum TFA concentration was *ca.* 1%.

Additionally, the proportion of methanol and acetonitrile was investigated and was carefully changed from 0:7.5 to 7.5:0 as shown in Table 4. The mobile phases without methanol did not separate the stereoisomers at all and an increase in the proportion of methanol improved the resolution. However, the solvent systems containing only methanol as the organic component did not always give satisfactory separation. As the k' of GK-III and -IV increased with increasing proportion of methanol, the optimum proportion of methanol–acetonitrile was determined to be 4:3.5 on the basis of the retention times.

3.3. HPLC analysis of each GK component using the established optimum conditions

As mentioned earlier, the GK mixture was separated into eight or nine components by normal-phase chromatography and GK-III and -IV were considered to be individually composed

Table 2
Influence of proportion of organic and aqueous solvents on three parameters, t_R, R_s and k', of GK-III and -IV

MeOH:CH_3CN:1% TFA	GK-III			GK-IV		
	t_R (min)	R_s	k'	t_R (min)	R_s	k'
4:3.5:1	12.5	0	0.45	12.3	0	0.43
4:3.5:2.5	30	1.11	2.57	35	1.11	3.17
4:3.5:4	142	–	14.8	156	–	16.3

Table 3
Influence of concentration of aqueous acid solvent on three parameters, t_R, R_s and k', of GK-III and -IV

MeOH:CH_3CN:TFA	TFA		GK-III			GK-IV		
	Concentration (%)	pH	t_R (min)	R_s	k'	t_R (min)	R_s	k'
4:3.5:2.5	0.01	4	34	0	3.05	39.1	0	3.65
4:3.5:2.5	0.05	3	32.3	0.59	2.85	38.5	0	3.58
4:3.5:2.5	0.10	2	32.3	0.65	2.85	37.3	0.8	3.44
4:3.5:2.5	0.50	1	32	0.99	2.81	38	1.09	3.52
4:3.5:2.5	1	1	30	1.11	2.57	35	1.11	3.17
4:3.5:2.5	1.50	1	31.6	1.05	2.76	37.5	1.07	3.46
4:3.5:2.5	2	1	32.4	1.06	2.86	38.8	1.1	3.96

Table 4
Influence of combination of organic solvents, methanol and acetonitrile, on three parameters, t_R, R_s and k', of GK-III and -IV

MeOH:CH_3CN:1% TFA	GK-III			GK-IV		
	t_R (min)	R_s	k'	t_R (min)	R_s	k'
0:7.5:2.5	9.4	0	0.21	11.1	0	0.42
1.5:6:2.5	15.5	0.48	0.94	15	0	0.88
3:4.5:2.5	24	0.9	1.86	27.6	0.78	2.29
3.75:3.75:2.5	30.1	1.06	2.54	36	1.07	3.24
4:3.5:2.5	30	1.11	2.57	35	1.11	3.17
4.5:3:2.5	34.7	1.02	3.08	41	1.09	3.82
6:1.5:2.5	45.4	1.23	4.34	57	1.13	5.71
7.5:0:2.5	54	0.93	5	65	1	6.22

of three stereo- and regioisomers based on the difference in the aglycone-A, -B and -C. Actually, both components could be separated into the three isomers in the course of the optimization of separation. Components other than GK-III and -IV were also analysed using the above optimum mobile phase, and GK-V–VII and DG also gave individually the three isomers in the chromatograms as shown in Fig. 3. There was a characteristic feature in each chromatogram that the first and second peaks were very close but the third peak was well separated from them. These results showed that the application of the optimum mobile phase can separate the three isomers in each component of the GK mixture. Fig. 4b shows the peak positions of isolated DG-A, -B and -C, and Fig. 4a shows the separation of these isomers in component DG obtained by silica gel chromatography. The elution

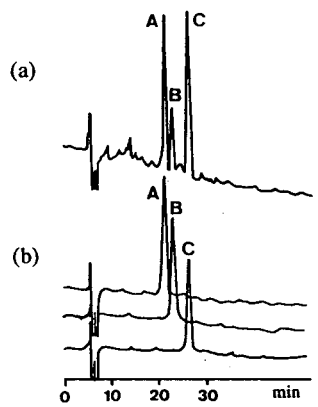

Fig. 4. (a) Separation of DG-A, -B and -C in the DG component obtained by silica gel chromatography. (b) Peak positions of the DG-A, -B and -C isomers isolated by preparative HPLC. Column, Inertsil ODS-2 (5 μm) (250 × 4.6 mm I.D.); mobile phase, methanol–acetonitrile–1% TFA (4:3.5:2.5); flow-rate, 0.3 ml/min.

order of these isomers was A, B and C. Based on the elution behaviour, it was expected that the elution order of the three individual peaks of GK-III–VII isomers would be the same.

Next, a profile analysis of the GK mixture was attempted, which might eliminate silica gel chromatography from the whole analysis procedure. When a modified mobile phase, methanol–acetonitrile–1% TFA (3.5:3.5:3) was used, the GK mixture was separated into fourteen peaks within 120 min, as shown in Fig. 5. Each peak was identified by co-injecting each isolated isomer. This results showed that GK-III–VII and DG were separated by the modified mobile phase, although a few isomers overlapped each other. As GK-I and II were not eluted within 120 min, a more hydrophobic mobile phase was required for the elution of these components.

3.4. Relationship between structure and separation behaviour of glykenin

We separated GK components by two types of chromatography, silica gel (normal phase) and ODS silica gel (reversed phase), and their combination allowed us to separate all GK species except the GK-I and -II isomers. As expected, the GK mixture was separated into nine components (GK-I–VII and DG) by normal-phase chromatography according to their polarity. The normal-phase partition mode differentiated not only the number of acetyl groups but also their positions. The difference in attachment position was further elucidated by the reversed-phase partition mode; GK-III, -IV and -V, which are positional isomers having two acetyl groups, could be clearly separated from each other. Interestingly, GK-III and -V, with two acetyl groups in the glucose moiety, were well separated, indicating that ODS can recognize the position of acetyl groups. A plausible separation mechanism has not been proposed at this stage, because the positions of the two acetyl groups of GK-V have not been yet determined. As reversed-phase chromatography also discriminated the stereochemistry of the glycol system in the aglycone, each component (GK-III–VII and DG) could be further separated into the corresponding stereo- and regioisomers. That is, the three isomers-A, -B and -C of each component are always eluted in this order, indicating that the stereochemistry of the glycol system is closely connected with the elution behaviour. Although a preferred conformation of the glycol system could not be determined by ^{1}H NMR, the *threo* isomers always interact more strongly with ODS than the *erythro* isomers.

As mentioned above, it was difficult to sepa-

GK	Peak Number		
	A	B	C
GK-III	6	7	9
GK-IV	9	10	11
GK-V	12	13	14
GK-VI	5	6	8
GK-VII	3	4	7
DG	1	2	3

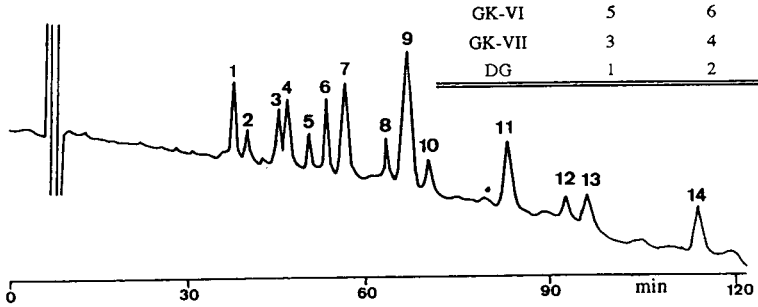

Fig. 5. Elution profile of the isomers of components GK-I–VII and DG. Column, Inertsil ODS-2 (5 μm) (250 × 4.6 mm I.D.); mobile phase, methanol–acetonitrile–1% TFA (3.5:3.5:3); flow-rate, 0.3 ml/min; sample, GK mixture (extraction mixture of fermentation broth).

rate all components by HPLC under any isocratic conditions. A combination HPLC with gradient elution and mass spectrometry would be more effective for the profile analysis of the GK mixture, because each species is expected to be discriminated not only by retention time but also by mass chromatography.

4. Conclusion

Although the GK mixture could be separated into nine components (GK-I-VII and DG) by normal-phase chromatography, each component had to be further separated into three isomers by reversed-phase chromatography. For this purpose, the separation of intact GK components was carried out with RI detection, because these components possess labile acetyl groups in the sugar moieties and hence were difficult to derivatize. The separation of each component was investigated using methanol–acetonitrile–1% TFA (4:3.5:2.5) as the optimum mobile phase. Each of GK-III–VII and DG was separated into three isomers under these conditions, and the profile analysis of the GK mixture (GK-III–VII and DG) was also tried using a modified mobile phase, methanol–acetonitrile–1% TFA (3.5:3.5:3). Nine components were separated according to their polarity in the normal-phase mode and the reversed-phase mode further separated the positional isomers due to the acetyl group in the sugar moiety and the stereochemistry of the aglycone (A, B and C). As a result a combination of both separation modes allowed us to separate all species except the GK-I and II isomers. The positions of the acetyl group in the sugar moiety determined by the profile analysis using HPLC with gradient elution combined with MS will be reported elsewhere.

5. References

[1] F. Nishida, Y. Mori, S. Isobe, T. Furuse, M. Suzuki, V. Meevootisom, T.W. Flegel and Y. Thebtaranonth, *Tetrahedron Lett.*, 29 (1988) 5287.

[2] F. Nishida, Y. Mori, N. Rokkaku, S. Isobe, T. Furuse, M. Suzuki, V. Meevootisom, T.W. Flegel, Y. Thebtaranonth and S. Intararuangsorn, *Chem. Pharm. Bull.*, 38 (1990) 2381.

[3] F. Nishida, Y. Mori, C. Sonobe, M. Suzuki, V. Meevootisom, T.W. Flegel, Y. Thebtaranonth and S. Intararuangsorn, *J. Antibiot.*, 44 (1991) 541.

[4] F. Nishida, Y. Mori, M. Suzuki, V. Meevootisom, T.W. Flegel, Y. Thebtaranonth and S. Intararuangsorn, *Chem. Pharm. Bull.*, 39 (1991) 3044.

ELSEVIER

Journal of Chromatography A, 664 (1994) 203–211

JOURNAL OF CHROMATOGRAPHY A

Separation of some enantiomers and diastereomers of propranolol derivatives by high-performance liquid chromatography

C. Facklam*, A. Modler

Max-Planck-Gesellschaft, Arbeitsgruppe "Asymmetrische Katalyse" an der Universität Rostock (in the "Institut für Organische Katalyseforschung an der Universität Rostock eV), Buchbinderstrasse 5–6, 18055 Rostock, Germany

(First received September 8th, 1993; revised manuscript received December 17th, 1993)

Abstract

The separation of some propranolol analogues **I** into their enantiomers and diastereomers respectively, by HPLC succeeded with cellulose tris(3,5-dimethylphenylcarbamate) as a chiral stationary phase and hexane–alcohol and aqueous $NaClO_4$–acetonitrile as mobile phases. Retention times and α values depend on the substituents R^1 and R^2. With non-aromatic substituents R^1 or R^2 the *R*-enantiomers are eluted first whereas with aromatic substituents the *S*-enantiomers, surprisingly, have shorter retention times.

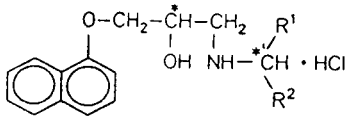

I

enantiomers: $R^1 = R^2$
diastereomers: $R^1 \neq R^2$

1. Introduction

Owing to their cardiovascular properties, β-blockers play an important role in the treatment of heart diseases. As the chirality of drugs is generally an important issue from pharmacological, toxicological and regulatory points of view, the development of methods in order to determine their optical purity is important. Enantiomeric separations of propranolol derivatives by liquid chromatography may be performed after derivatization with optically pure reagents [1,2]. A different approach, however, is the chromatographic separation of enantiomers by means of chiral stationary phases (CSPs). Lee *et al.* [3] separated the enantiomers of β-blockers using various CSPs, *e.g.*, cellulose tris(3,5-dimethylphenylcarbamate) CSP with hexane–alcohol eluents. Cellulose tris(3,5-dimethylphenylcarbamate) CSP is also suitable for reversed-phase chromatography [4]. CSPs of the α_1-acid glycoprotein type have also been utilized [5,6]. Very efficient enantiomeric resolutions of β-blockers with short retention times have been achieved by means of supercritical fluid chromatography (SFC) [7,8]. Capillary electrophoresis is also useful [9,10]. Compounds of type **I** having

* Corresponding author.

0021-9673/94/$07.00
SSDI 0021-9673(93)E0054-X

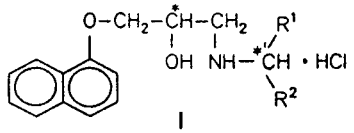

I

a second chiral centre ($R^1 \neq R^2$) have been investigated by Krause *et al.* [11]. We were interested in separating compounds of type **I** into their various stereoisomers by HPLC using Chiralcel OD-H and Chiralcel OD-R in order to analyse the products of such a synthesis.

2. Experimental

Chromatography was performed with a Model 1090 Series II liquid chromatograph equipped with a diode-array detector (Hewlett-Packard) and a Chiralyser (IBZ Messtechnik, Hannover, Germany). Separations were carried out on a Chiralcel OD-H analytical column (250 × 4.6 mm I.D.); except for resolutions at different temperatures (see Fig. 1), (150 × 4.6 mm I.D.) and a Chiralcel OD-R analytical column (250 × 4.6 mm I.D.) (Baker Chemikalien, Gross Gerau, Germany). The detection wavelengths were set at 230 and 270 nm. Chromatograms were measured at 27°C.

Acetonitrile, hexane and 2-propanol of HPLC grade were purchased from Ferak (Berlin, Germany), ethanol from Laborchemie Apolda (Apolda, Germany) and sodium perchlorate from Merck (Darmstadt, Germany). The compounds were dissolved in hexane–2-propanol at a concentration of 1 mg/ml.

Table 1
Enantiomeric separation on Chiralcel OD-H

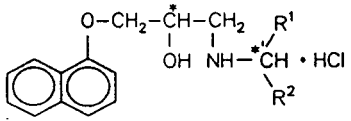

Compound	R^1	R^2	k'_1	k'_2	α	Eluent[a]
1	H	H	2.00	5.15	1.36	1[b]
2	CH_3	CH_3	1.30	1.94	1.49	2[b]
3	C_2H_5	C_2H_5	0.52	1.32	2.54	4[b]
4	C_6H_5	C_6H_5	2.17	2.46	1.13	3[c]

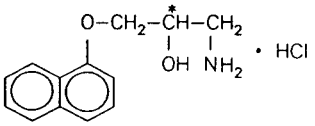

Compound	R^1	k'_1	k'_2	α	Eluent
5		0.92	1.43	1.55	3[b]
6		1.05	1.39	1.32	3[b]

[a] Eluents: 1 = *n*-hexane–ethanol–2-propanol (90:2:10); 2 = *n*-hexane–ethanol–2-propanol (90:10:10); 3 = *n*-hexane–ethanol–2-propanol (90:20:10); 4 = *n*-hexane–ethanol–2-propanol (90:30:10, v/v/v).
[b] Flow-rate = 1.5 ml/min.
[c] Flow-rate = 0.5 ml/min.

3. Results and discussion

Enantiomeric separation of propranolol analogues **1–6** (see Table 1) was performed using hexane–alcohol mobile phases. In some instances small amounts of unidentified by-products were resolved from the main products with hexane–ethanol–2-propanol eluents, but not with hexane–2-propanol eluents. Table 1 gives the k' and α values and chromatographic conditions. The retention times were dependent on the steric requirements of substituents R^1 and R^2. Depending on the size of R^1 and R^2 the alcohol content of the eluent had to be varied in order to keep the retention times low. Chiralcel OD-H shows excellent enantioselectivity for samples of **1–3** and also for **5** and **6**. Although the α value of **4** ($R^1 = R^2 = C_6H_5$) turned out to be smaller, baseline resolution of the enantiomers of **4** was achieved with eluent 3 and a flow-rate of 0.5 ml/min, but not with eluent 4 and a flow-rate of 1.5 ml/min (see Table 1). Overall, the effectiveness of separation appears to be largely dependent on the nature (aliphatic *vs.* aromatic) and size of the substituents R^1 and R^2. Although the chiral cavities of the CSP are distinguished by a high affinity for aromatic groups [12], which is in agreement with our result that compound **4** is more retained than compounds with aliphatic substituents R, the chiral recognition mechanism of the CSP–substrate interaction does not necessarily give rise to a better separation of the aromatically substituted enantiomers.

With non-aromatic substituents R^1 or R^2 the *R*-enantiomers are eluted first whereas with aromatic substituents the *S*-enantiomers [no ORD spectra of the propranolol analogues have been recorded to prove the absolute configuration, but all our substances with the *S*-configuration were prepared in the same way [11] and shown −-rotation in methanol], surprisingly, have shorter retention times. The capacity factors of the diastereomers **7** and **8** (Table 2) are sufficiently different to allow easy resolution of the four isomers of **7**; three of the four isomers of **8**, which were available to us, were likewise separated. In both instances diastereomers with the *R,R*-configuration were eluted first. Increased flow-rates and higher temperatures up to 40°C cause a decrease in retention times but do not alter the effectiveness of the separations (Fig. 1).

The enantiomeric resolution of all propranolol derivatives can be performed likewise using reversed-phase eluents with Chiralcel OD-R and

Table 2
Diastereomeric separation on Chiralcel OD-H

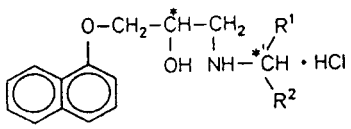

Compound	R^1	R^2	Configuration (**′)	k'	Eluent[a]
7a	CH_3	C_6H_5	*R,R′*	2.95	1
7b	CH_3	C_6H_5	*R,S′*	4.26	1
7c	CH_3	C_6H_5	*S,S′*	4.93	1
7d	CH_3	C_6H_5	*S,R′*	6.90	1
8a	CH_3	C_6H_{11}	*R,R′*	1.10	2
8b	CH_3	C_6H_{11}	*S,S′*	2.15	2
8c	CH_3	C_6H_{11}	*S,R′*	4.71	2

[a] Eluents: 1 = *n*-hexane–ethanol–2-propanol (90:3:10); 2 = *n*-hexane–ethanol–2-propanol (90:10:10 v/v/v). Flow-rate, 1.0 ml/min.

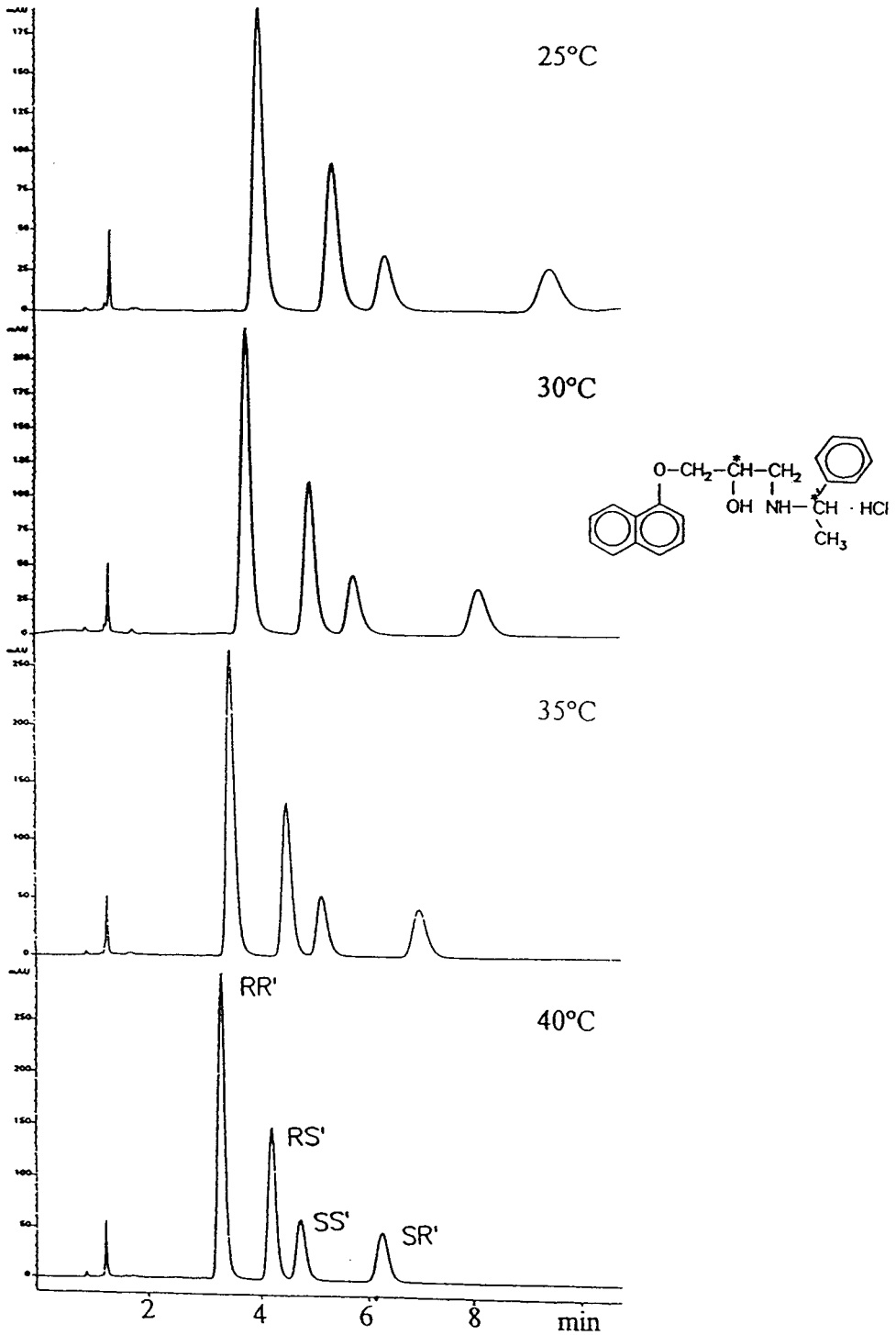

Fig. 1. Isomeric separation of **7a–d** on Chiralcel OD-H. Eluent, *n*-hexane–ethanol–2-propanol (90:3:10, v/v/v); flow-rate, 2.0 ml/min.

aqueous 1 *M* $NaClO_4$–acetonitrile and even using reversed-phase conditions again only compound **4** shows the exception from the rule that *R*-enantiomers are eluted first. Capacity and separation factors are given in Tables 3 and 4. We were able to separate the diastereomers of **7** and **8** with Chiralcel OD-R and $NaClO_4$–acetonitrile with slightly greater difficulty, the isomers of **7** being separated only after a relatively long retention time (up to 40 min) and the separation of the isomers of **8** remaining incomplete. The influence of pH and buffer was not investigated. Advances might be achieved by further optimizing the mobile phases as shown, for example, by Ishikawa and Shibata [4].

Both normal- and reversed-phase conditions were applied to separate the isomers of **9–11**.

We believe interactive forces due to stereospecific hydrogen bond formation between the CSPs and the chiral substrates to be responsible

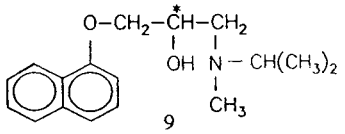

9

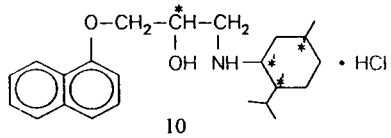

10

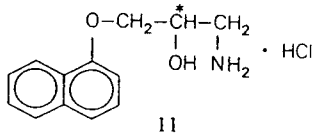

11

Table 3
Enantiomeric separation on Chiralcel OD-R

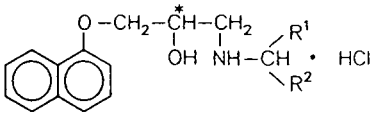

Compound	R^1	R^2	k'_1	k'_2	α	Eluent[a]
1	H	H	5.20	6.00	1.15	1[b]
2	CH_3	CH_3	9.60	13.50	1.41	1[b]
3	C_2H_5	C_2H_5	6.80	9.60	1.40	1[c]
4	C_6H_5	C_6H_5	3.35	4.18	1.24	2[c]

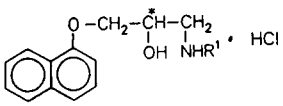

Compound	R^1	k'_1	k'_2	α	Eluent
5		1.08	1.84	1.70	3[c]

[a] Eluents: 1 = 1 *M* $NaClO_4$–acetonitrile (60:40); 2 = 1 *M* $NaClO_4$–acetonitrile (10:90); 3 = 1 *M* $NaClO_4$–acetonitrile (40:60, v/v).
[b] Flow-rate, 0.5 ml/min.
[c] Flow-rate, 1.0 ml/min.

Table 4
Diastereomeric separation on Chiralcel OD-R

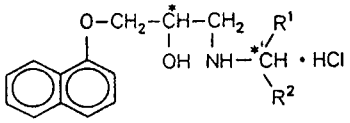

Compound	R^1	R^2	Configuration (**′)	k'	Eluent[a]
7a	CH_3	C_6H_5	*R*,*R*′	9.50	1
7b	CH_3	C_6H_5	*R*,*S*′	11.60	1
7c	CH_3	C_6H_5	*S*,*R*′	12.70	1
7d	CH_3	C_6H_5	*S*,*S*′	14.70	1
8a	CH_3	C_6H_{11}	*R*,*R*′	4.60	2[b]
8b	CH_3	C_6H_{11}	*S*,*R*′	5.80	2[b]
8c	CH_3	C_6H_{11}	*S*,*S*′	6.60	2[b]

[a] Eluents: 1 = 1 *M* $NaClO_4$–acetonitrile (60:40); 2 = 1 *M* $NaClO_4$–acetonitrile (50:50, v/v). Flow-rate, 1.0 ml/min.
[b] Temperature, 29°C.

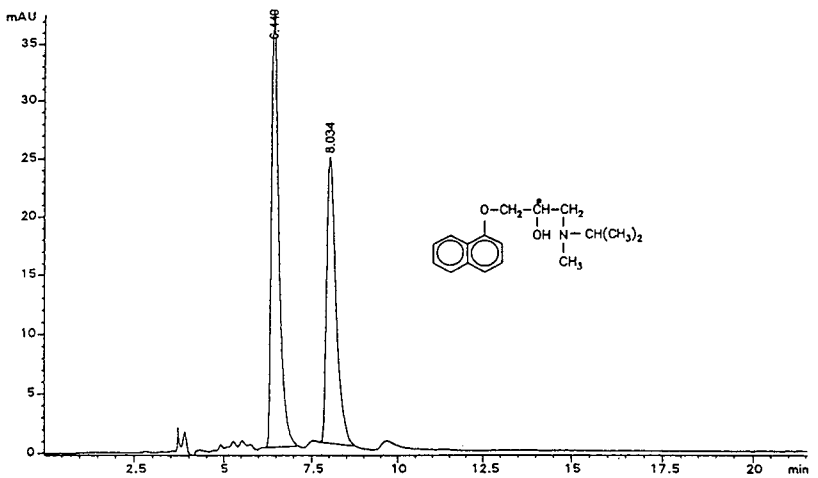

Fig. 2. Enantiomeric separation of racemate **9** on Chiralcel OD-H. Eluent, *n*-hexane–ethanol–2-propanol (90:10:10, v/v/v); flow-rate, 1.0 ml/min.

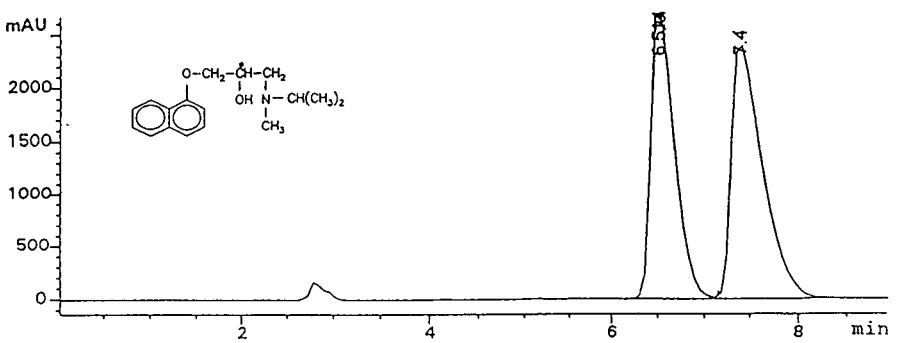

Fig. 3. Separation of racemate **9** on Chiralcel OD-R. Eluent, 1 *M* $NaClO_4$–acetonitrile (50:50, v/v); flow-rate, 1.0 ml/min.

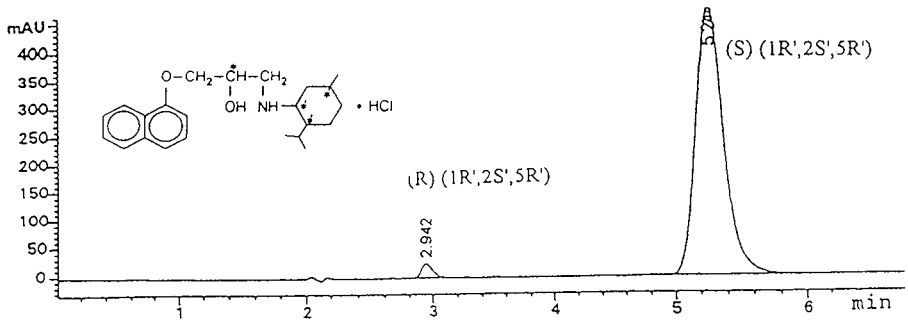

Fig. 4. Separation of **10** [excess of (*S*)(1*R*',2*S*',5*R*')-compound] on Chiralcel OD-H. Eluent, *n*-hexane–ethanol–2-propanol (90:30:10, v/v/v); flow-rate, 1.5 ml/min.

for differences in the retention times of the enantiomers [13]. Siret *et al.* [8] described the chiral separation of β-blockers on a ChyRoSine-A CSP by SFC. However, the resolution of derivatives with tertiary amino groups was shown to be ineffective. Our compound **9**, lacking an NH proton, was readily separated into its enantiomers by using Chiralcel OD (Figs. 2 and 3), which may be explained by the availability of the OH group in **9** for hydrogen-bond interactions. The influence of the NH proton on the resolution is small. Compounds **2** land **9** shows similar α values. Derivative **10**, bearing a (1*R*,2*S*,5*R*)-menthyl substituent, was also separated (Figs. 4 and 5). Compound **11** contains a primary amino group; its isomers were separated under reversed-phase conditions (Fig. 6). Hexane–alcohol eluents proved to be ineffective, but on addition of formic acid **11** was straightforwardly separated with the *R*-isomer being eluted first (Fig. 7).

4. Conclusions

Some enantiomers and diastereomers of propranolol derivatives **I** with different substituents on the nitrogen were separated by HPLC on cellulose tris(3,5-dimethylphenylcarbamate) as chiral stationary phase. Excellent chiral separations of enantiomeric propranolol analogues were obtained with $NaClO_4$–acetonitrile eluents. Baseline separation was achieved for enantiomeric and diastereomeric propranolol analogues (with amine alkyl and amine aryl substituents) using hexane–alcohol eluents. To resolve compound **11** the addition of formic acid was necessary. The presence of an amine proton is not

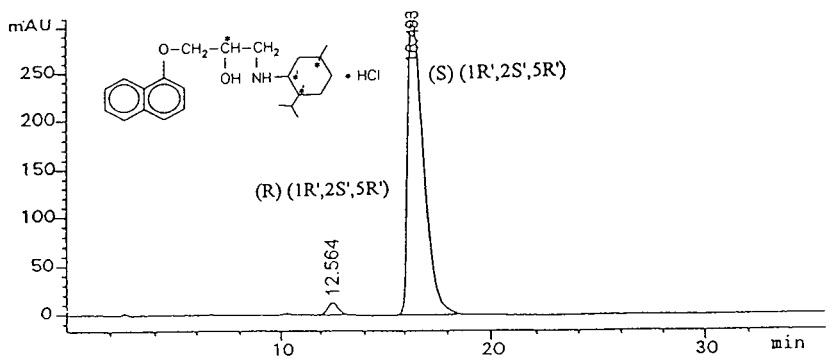

Fig. 5. Separation of **10** [excess of (*S*)(1*R*',2*S*',5*R*')-compound] on Chiralcel OD-R. Eluent, 1 *M* $NaClO_4$–acetonitrile (40:60, v/v); flow-rate, 1.0 ml/min.

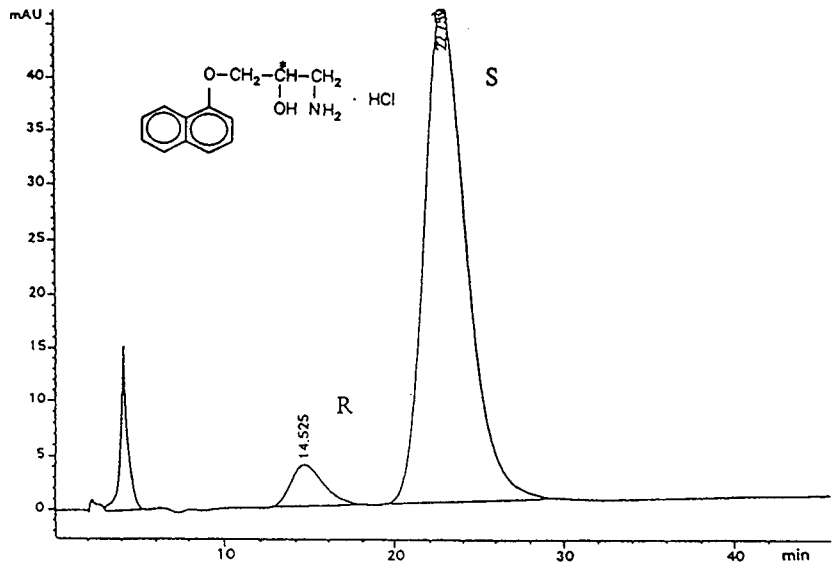

Fig. 6. Enantiomeric separation of **11** (enantiomeric excess of *S*-enantiomers) on Chiralcel OD-R. Eluent, 1 *M* $NaClO_4$–acetonitrile (70:30, v/v); flow-rate, 1.0 ml/min.

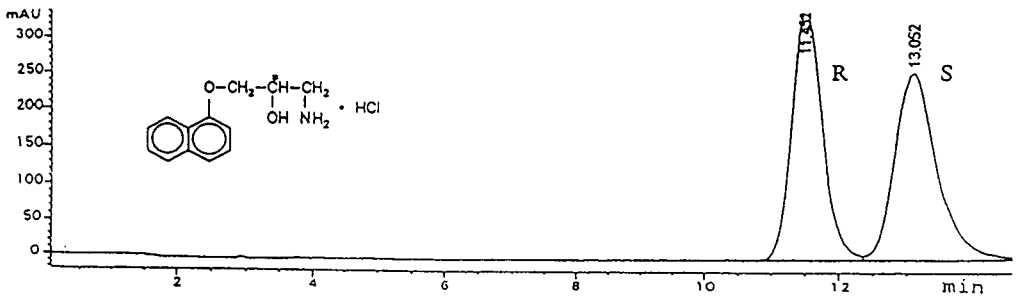

Fig. 7. Enantiomeric separation of racemate **11** on Chiralcel OD-H. Eluent, hexane–2-propanol–formic acid (80:20:1, v/v/v); flow-rate, 1.5 ml/min.

necessary to achieve chiral recognition. In this class of 1,2-amino alcohols, the *R*-enantiomers are eluted first with both normal- and reversed-phase systems if one or two amine substituents R are aliphatic. With two aromatic substituents the *S*-enantiomer has the shorter retention time.

5. Acknowledgements

We acknowledge the gift of all propranolol analogues from Professor H.-W. Krause and Mrs. U. Schmidt. We thank Mrs. H. Baudisch for the mass spectra of the compounds after the isolation of chromatographically resolved substances. Professor G. Oehme, Dr. R. Selke and Dr. H. Mennenga are thanked for helpful discussions.

6. References

[1] L. Olsen, K. Bronnum, P. Helboe, G.H. Jorgensen and S. Kryger, *J. Chromatogr.*, 636 (1993) 231.
[2] Th. Jira, Ch. Toll, Ch. Vogt and Th. Beyrich, *Pharmazie*, 46 (1991) 432.

[3] C.R. Lee, J.P. Porziemsky, M.C. Aubert and A.M. Krstulovic, *J. Chromatogr.*, 539 (1991) 55.
[4] A. Ishikawa and T. Shibata, *J. Liq. Chromatogr.*, 16 (1993) 859.
[5] C. Vandenbosch, T. Hamoir, D.L. Massart and W. Lindner, *Chromatographia*, 33 (1992) 454.
[6] J. Haginaka, Ch. Seyama, H. Yasuda and K. Takahashi, *Chromatographia*, 33 (1992) 127.
[7] A. Tambute, L. Siret, A. Begos and M. Caude, *Chirality*, 4 (1992) 36.
[8] L. Siret, N. Bargmann, A. Tambute and M. Caude, *Chirality*, 4 (1992) 252.
[9] L. Valtcheva, J. Mohammad, G. Pettersson and S. Hjerten, *J. Chromatogr.*, 638 (1993) 263.
[10] S.A.C. Wren and R.C. Rowe, *J. Chromatogr.*, 635 (1993) 113.
[11] H.W. Krause, U. Schmidt and H. Foken, *Pharmazie*, 47 (1992) 838.
[12] C.B. Ching, B.G. Lim, E.J.D. Lee and S.C. Ng, *Chirality*, 4 (1992) 174.
[13] Y. Okamoto, M. Kawashima, R. Aburatani, K. Hatada, T. Nishiyama and M. Masuda, *Chem. Lett.*, (1986) 1237.

ELSEVIER

Journal of Chromatography A, 664 (1994) 213–219

JOURNAL OF CHROMATOGRAPHY A

Determination of the alkyl esters of *p*-hydroxybenzoic acid in mayonnaise by high-performance liquid chromatography and fluorescence labelling

Giovanni Burini

Istituto di Scienza dell'Alimentazione, Facoltà di Farmacia, Università degli Studi di Perugia, S. Costanzo, 06100 Perugia, Italy

(First received August 31st, 1993; revised manuscript received December 14th, 1993)

Abstract

A reliable and sensitive high-performance liquid chromatographic method with fluorescence detection is described for the determination of methyl, ethyl and propyl *p*-hydroxybenzoates in mayonnaise with the internal standard method using *n*-butyl *p*-hydroxybenzoate as the internal standard. The parabens were extracted with acetonitrile and determined, after derivatization with 4-bromomethyl-6,7-dimethoxycoumarin, by reversed-phase liquid chromatography (C_{18} column) with fluorescence detection at $\lambda_{ex.} = 355$ nm and $\lambda_{em.} > 420$ nm using an aqueous methanolic eluent and linear gradient elution. The method was tested on a mayonnaise sample spiked with methyl, ethyl and *n*-propyl *p*-hydroxybenzoate each at different levels (100, 500 and 1000 ppm). Average recoveries ranged from 93.6 to 99.4% with R.S.D. ranging from 1.8 to 4.0%.

1. Introduction

The alkyl esters of *p*-hydroxybenzoic acid (parabens) are compounds similar to benzoic acid and are used as food additives to prevent antimicrobial food spoilage. The use of parabens is very useful as they exert antimicrobial activity at pH 7 or higher, while benzoic acid has weak antimicrobial activity at this pH. The antimicrobial activity of *p*-hydroxybenzoic acid esters increases with increasing length of the alkyl chain of the ester group, but in practice the shorter esters are commonly used because of their high solubility in water.

Many antimicrobial compounds such as sorbic acid, benzoic acid, alkyl *p*-hydroxybenzoate and sulphite are used in the food industry. Their use in foods is related to the food characteristics and to the specific laws of the different countries. In Italy the methyl, ethyl and *n*-propyl *p*-hydroxybenzoates are authorised at various concentrations in preserved fish (maximum 1000 ppm), caviar and its substitutes (maximum 1000 ppm), rennet (maximum 10 000 ppm) and mayonnaise (maximum 1000 ppm) [1].

To determine the presence of antimicrobial additives in food, samples are prepared using different procedures such as extraction with acetonitrile (MeCN) [2], extraction with a mixture of MeCN, 2-propanol, ethanol and oxalic acid [3], simple steam distillation [4,5] or the use of a Sep-Pak C_{18} cartridge [5–7] or an Extrelut column [8].

Many methods for their determination have been described. They include UV spectrophotometry [9], thin-layer chromatography (TLC)

0021-9673/94/$07.00
SSDI 0021-9673(93)E1301-F

[10] and gas chromatography (GC). The last method is carried out by directly injecting the extract obtained from the sample [11] or by injecting the trifluoroacetyl or benzoyl derivatives [12,13].

In the last 10 years, high-performance liquid chromatography (HPLC) with UV spectrophotometric detection has been used for the determination of preservatives in different foods. In particular, methods based on reversed-phase (RP) HPLC [2–4,5–8,14–17] have been more widely applied than those based on normal-phase HPLC [18]. RP-HPLC methods include ion-pair chromatography achieved using a cationic counter ion with a mobile phase that contains a pH 3.6 buffer [11], a pH 4.4 buffer [6] or an aqueous acetic acid solution at pH 4.5 [19]. Galensa and Schäfers [13], after derivatization (benzoylation), determined esters of *p*-hydroxybenzoic acid by normal- and reversed-phase HPLC.

Recently, Burini and Damiani [20] developed an HPLC method with fluorimetric detection for the determination of sorbic acid (another preservative) using 4-bromomethyl-6,7-dimethoxycoumarin as a fluorescence derivatizing reagent. This method, partially modified, has now been extended to the determination of parabens, which are characterized by a potentially reactive phenol group. 4-Bromomethyl-6,7-dimethoxycoumarin reacts with potassium salts of the alkyl esters *p*-hydroxybenzoic acid generated *in situ* with K_2CO_3 in MeCN and in the presence of 18-crown-6 to yield the corresponding fluorescent ethers as shown in Fig. 1. The derivatized compounds are separated on a reversed-phase column with gradient elution using aqueous methanol. The derivatization reaction, which converts the parabens into their corresponding fluorophores, and the chromatographic parameters were optimized; a method for the simultaneous determination of these compounds in mayonnaise was developed.

2. Experimental

2.1. Apparatus

A Varian (Palo Alto, CA, USA) Model 5000 liquid chromatograph, a sample-injection valve (Rheodyne, Cotati, CA, USA) with a 20-μl loop and a Varian Fluorichrom fluorescence detector were used. The following settings were applied: gain and lamp, LO; attenuator, ×20; excitation filters, CS 7-60/CS 7-54 ($\lambda_{ex.} = 355$ nm); emission filters, CS 3-73/CS 4-76 ($\lambda_{em.} > 420$ nm).

Separation was performed by RP-HPLC on a 5-μm Supelcosil LC-18 column (250 × 4.6 mm I.D.) (Supelco, Bellefonte, PA, USA). The system was interfaced with an HP 3394 computing integrator (Hewlett-Packard, Avondale, PA, USA), with attenuation ×0 and chart speed 0.2 cm/min.

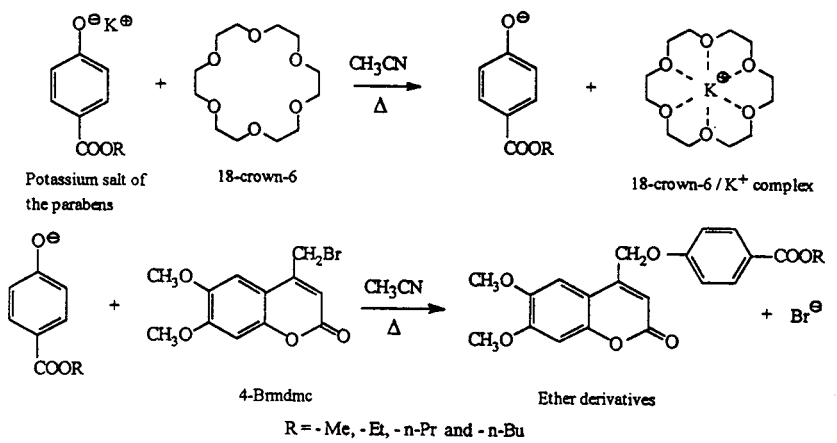

Fig. 1. Derivatization reaction for alkyl esters of *p*-hydroxybenzoic acid.

2.2. Reagents

Analytical-reagent grade methyl, ethyl, *n*-propyl and *n*-butyl *p*-hydroxybenzoate were purchased from Lancaster Synthesis (Morecambe, UK), sulphuric acid (96%) and small grains of K_2CO_3 from Carlo Erba (Milan, Italy), 4-bromomethyl-6,7-dimethoxycoumarin (4-Brmdmc) and 18-crown-6 from Sigma (St. Louis, MO, USA) and anhydrous sodium sulphate from BDH (Poole, UK). All the solvents (HPLC grade) such as acetone, water, acetonitrile and methanol were purchased from BDH.

Sulphuric acid of concentration 5 *M* was prepared by adding 14 ml of concentrated sulphuric acid to 30 ml of distilled water in a 50-ml volumetric flask. After cooling the flask, the solution was diluted to volume with distilled water.

Acetone solutions of 4-Brmdmc (1.05 mg/ml) and 18-crown-6 (1.26 mg/ml) were prepared. When refrigerated, these solution were stable for several weeks.

2.3. Preparation of standard solutions

A stock standard solution (1000 μg/ml) was prepared by dissolving 50.5 mg each of methyl, ethyl and *n*-propyl *p*-hydroxybenzoate in MeCN in a 50-ml volumetric flask. The internal standard (I.S.) solution was prepared by dissolving 51 mg of *n*-butyl *p*-hydroxybenzoate in 50 ml of MeCN. These two solutions were diluted with MeCN to obtain solutions containing 6.25 mg/ml of parabens. Aliquots of 1, 2, 3, 4, 5 and 6 ml of the solution containing methyl, ethyl and *n*-propyl *p*-hydroxybenzoate were mixed with 2 ml of the internal standard solution in separate 25-ml volumetric flasks. The solutions were then diluted to volume with MeCN. These working standard solutions, containing 0.25–1.5 μg/ml of the individual *p*-hydroxybenzoates and 0.5 μg/ml of the internal standard, were then derivatized and used to construct the calibration graph by HPLC analysis. The working standard solutions were stable for several weeks.

A solution containing 1 μg/ml of each paraben was prepared for an optimization study of the derivatization reaction.

2.4. Derivatization procedure

A 100-μl volume of the 18-crown-6 and 100 μl of the 4-Brmdmc acetone solutions were placed in a 10-ml test-tube equipped with a screw-cap and the acetone was evaporated in a gentle stream of nitrogen. Potassium carbonate (50 mg) and 0.5 ml of each working standard solution were added to the residue. The tube was then tightly closed and placed in a water-bath at 80°C for 2 min. After cooling to room temperature, 20 μl of the reaction mixture were injected into the liquid chromatograph.

Calibration graphs were obtained by plotting the peak-area ratios of methyl, ethyl and *n*-propyl *p*-hydroxybenzoate to that of the internal standard *versus* the concentration of the individual *p*-hydroxybenzoate. Fig. 2 shows a chromatogram for the derivatized standard solution containing 0.5 μg/ml of each preservative and 0.5 μg/ml of the internal standard.

2.5. Chromatographic conditions

The chromatographic conditions used were as follows: solvent A, water; solvent B, methanol; gradient elution programme, starting composition 45% of A and 55% of B, linear gradient from 55 to 100% of B in 35 min (1.29%/min), isocratic flow of 100% B for 10 min, return of the system to 55% B in 5 min; flow-rate, 1 ml/min; column pressure, initial value 105 bar, final value 46 bar; column, Supelcosil LC-18 (5 μm) (250 × 4.6 mm I.D.); fluorimetric detection.

2.6. Sample preparation

A 2-g amount of anhydrous sodium sulphate, 0.5 ml of the internal standard (1000 μg/ml), 6.5 ml of MeCN and 50 μl of 5 *M* sulphuric acid were added, in that order, to 0.5 g of sample weighed in a 10-ml test-tube equipped with

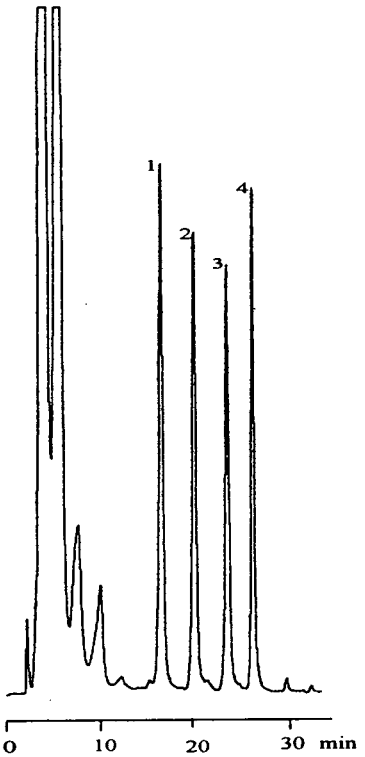

Fig. 2. Standard chromatogram of (1) methyl, (2) ethyl, (3) *n*-propyl and (4) *n*-butyl *p*-hydroxybenzoate (10 ng each).

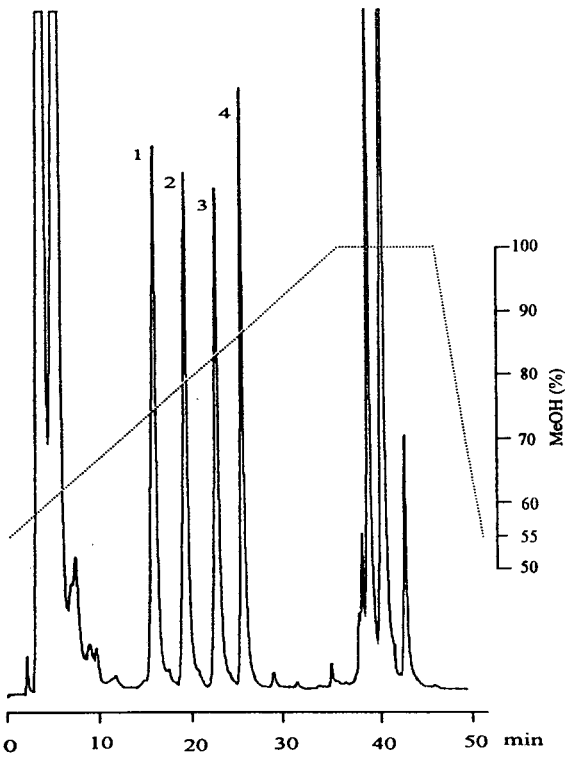

Fig. 3. Typical chromatogram of mayonnaise containing 100 μg/ml of (1) methyl, (2) ethyl, (3) *n*-propyl and (4) *n*-butyl (I.S.) paraben. Dilution factor of the extract sample = 1:2 (see Section 2.6). The linear gradient from 55 to 100% (v/v) methanol is indicated by the broken line.

screw-cap. The test-tube was closed, shaken for 20 s and centrifuged for 3 min at *ca.* 700 *g*. The supernatant was decanted into a 50-ml volumetric flask and the extraction was repeated once. Even if the solution was turbid at this stage, it was diluted to volume with MeCN (clear solution). Before derivatization and HPLC analysis this solution was diluted 1:20 with MeCN.

2.7. Determination by RP-HPLC

A 0.5-ml volume of the solution of the extract sample was derivatized as described for the working standard solutions (see section 2.4), using 200 μl of the 18-crown-6 and 200 μl of the 4-Brmdmc acetone solutions. A 20-μl volume of each solution was then injected in duplicate into the LC apparatus. The peak-area ratios of methyl, ethyl and *n*-propyl *p*-hydroxybenzoate to that of the internal standard were integrated on the calibration graphs for quantification of each paraben. The concentration of each paraben in the sample was calculated as follows:

$$\text{ppm } (\mu g/g) = \frac{c \cdot 50 \cdot 20}{m}$$

where c = concentration (μg/ml) of paraben obtained from the calibration graph, 50 = volume of the extract (ml), 20 = dilution factor of extract and m = mass of extracted sample (g). Fig. 3 shows a typical chromatogram for a sample of mayonnaise.

3. Results and discussion

The influence of temperature, time and 4-Brmdmc and 18-crown-6 concentrations on the derivatization reaction were examined; each experiment was performed as described in Section 2.4, changing one variable at a time and in each instance using a standard solution of 1 μg/ml of each paraben. Conditions of *ca.* 80°C, 2 min and a molar ratio of 30 and 40 for [4-Brmdmc]/[parabens] and [18-crown-6]/[parabens], respectively, were required for plateau formation for all the parabens. These were therefore adopted as the optimum derivatization conditions. An example of the results obtained in the optimization studies is shown in Fig. 4.

Parabens are compounds more reactive than carboxylic acids, *i.e.*, only 2 min at 80°C are required for complete derivatization.

n-Butyl *p*-hydroxybenzoate was used as the internal standard as it is similar to the sample components and further it is not allowed as an antimicrobial food additive in Italy. The internal standard (I.S.) procedure has greatest potential for precise quantitative results because the standard, which is included with each sample, eliminates the possible causes of error during extraction and derivatization of parabens. Further, changes in chromatographic conditions affect both the standard and component peaks equally.

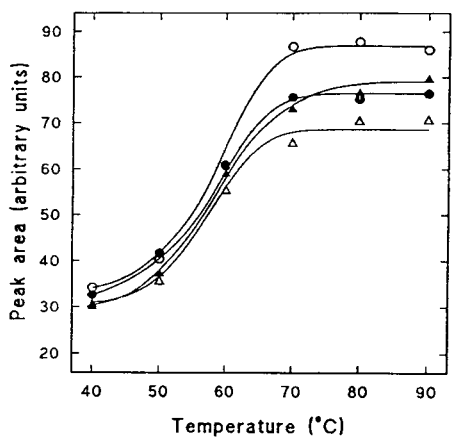

Fig. 4. Effect of temperature on the peak area for the derivatization reaction of the parabens. ○ = Methyl; ● = ethyl; △ = *n*-propyl; ▲ = *n*-butyl.

Acetonitrile was chosen as the extraction solvent of the parabens because, in addition to allowing good solubilization of the compounds of interest, it allows for their immediate derivatization without further clean-up treatment.

Calibration graphs were obtained from a plot of the peak-area ratios of methyl, ethyl and *n*-propyl *p*-hydroxybenzoate to that of the internal standard against the concentration of these preservatives. The graphs, in the concentration range 0.25–1.5 μg/ml, gave good linearity and passed through the origin. The limit of detection was 5 ng for a 20-μl injection.

For testing the method, a mayonnaise sample was selected because of the amount and frequency with which it is used with respect to preserved fish and caviar and its substitutes. The request of consumers for products without chemical additives has stimulated the food industry to put products on the market without preservatives. In fact, most of the mayonnaise on the market has no chemical additives. Because the mayonnaise samples obtained from the local stores contained no parabens, a sample spiked with known amounts of parabens was used to test the method. Parabens are most active against moulds and yeasts; the inhibitory concentrations of methyl, ethyl and *n*-propyl *p*-hydroxybenzoate range from *ca.* 80 to 1000 ppm. Based on this range of inhibitory activity and as the maximum amount of parabens authorized by Italian law is 1000 ppm, concentrations of 100, 500 and 1000 ppm were selected.

Large amounts of 4-Brmdmc and of 18-crown-6 in the derivatization of the sample solution (see Section 2.7) were verified by the presence, in the mayonnaise, of compounds that give rise other fluorophores (see peaks with high retention times in Fig. 3). The sample without addition of the parabens showed a small peak at the retention time of methyl paraben, which can yield an error of about 1% at the ppm level.

The precision of the method was assessed by submitting each sample to five runs; in addition,

Table 1
Recoveries of methyl, ethyl and *n*-propyl parabens from a mayonnaise sample

Amount added (ppm)				Amount found (ppm)				Recovery (%)		
Methyl	Ethyl	*n*-Propyl		Methyl	Ethyl	*n*-Propyl		Methyl	Ethyl	*n*-Propyl
100	100	100	Average	95.7	99.1	99.4	Average	95.7	99.1	99.4
			S.D.	1.8	3.0	3.3	S.D.	1.8	3.0	3.3
			R.S.D. (%)	1.8	3.0	3.4	R.S.D. (%)	1.8	3.0	3.4
500	500	500	Average	468.0	471.8	474.3	Average	93.6	94.4	94.9
			S.D.	17.7	13.8	12.0	S.D.	3.5	2.8	2.4
			R.S.D. (%)	3.8	2.9	2.5	R.S.D. (%)	3.8	2.9	2.5
1000[a]	1000[a]	1000[a]	Average	973.6	983.9	976.2	Average	97.4	98.4	97.6
			S.D.	32.0	39.8	35.4	S.D.	3.2	4.0	3.5
			R.S.D. (%)	3.3	4.0	3.6	R.S.D. (%)	3.3	4.0	3.6

Five replicate analyses.
[a] The maximum concentration allowed in mayonnaise in Italy.

the percentage recovery of methyl, ethyl and *n*-propyl parabens was verified by adding different amounts of each paraben to the mayonnaise sample (Table 1). The R.S.D. values in each instance (≤4%) show the good reproducibility of the method.

The validity of the procedure is demonstrated by the recovery of parabens from samples spiked with known amounts of methyl, ethyl and *n*-propyl *p*-hydroxybenzoate (Table 1).

Benzoic acid under the conditions adopted can be partly derivatized and, if present in the sample, interfere in the determination of methyl *p*-hydroxybenzoate. The identity of each of the compounds could be specified by using the peak-area ratio at two pairs of excitation or emission wavelengths. The peak-area ratio, at two wavelength pairs, for each compound should differ at least by 5%.

Even though the derivatization step is time consuming, the HPLC determination of esters of *p*-hydroxybenzoic acid in mayonnaise as the 4-Brmdmc derivatives is of interest because fluorimetric detection is both very specific and sensitive. Further, it can be used as an alternative to the earlier HPLC–UV determinations that are complex because they require extraction and further clean-up procedures and/or eluents made with buffer solutions. In time, the salts could cause deposits in the pumps and in the capillary tubes, adversely affecting the efficiency of the chromatograph, a characteristic rarely taken into account.

4. References

[1] C. Correra and A. Neri, *Codice Commentato degli Additivi e dei Coloranti Alimentari – Legislazione e Decreti – Testi Aggiornati ed Integrati*, Edizioni Scienza e Diritto, Milan, 1988, Parte II, Scheda 3.
[2] G.A. Perfetti, C.R. Warner and T. Fazio, *J. Assoc. Off. Anal. Chem.*, 64 (1981) 844.
[3] C. Gertz and K. Hermann, *Dtsch. Lebensm.-Rundsch.*, 79 (1983) 331.
[4] D. Ehlers and S. Littmann, *Dtsch. Lebensm.-Rundsch.*, 80 (1984) 44.
[5] H. Terada and Y. Sakabe, *J. Chromatogr.*, 346 (1985) 333.
[6] A. Matsunage, A. Yamamoto and M. Makino, *Eisei Kagaku*, 31 (1985) 269.
[7] K. Kobayashi, S. Tsuji, Y. Tonogai and Y. Ito, *Nippon Shokuhin Kogyo Gakkaishi*, 33 (1986) 514.
[8] Y. Ueda, K. Tamase, K. Yamada, M. Sasaki and K. Tanikawa, *Nara-ken Eisei Kenkyusho Nenpo*, 15 (1980) 86.
[9] Y. Yamamoto, M. Yamashita, Y. Hirose and K. Miyoshi, *Shokuhin Eisei Kenkyu*, 32 (1982) 1077.
[10] R. Duden, A. Fricker, R. Calverley, K.H. Park and V.M. Rios, *Z. Lebensm.-Unters.-Forsch.*, 151 (1973) 23.
[11] T. Takarai, K. Nakamura, T. Hidaka, T. Kirigaya, M. Kamijo, Y. Suzuki and T. Kawamura, *Eisei Kagaku*, 30 (1984) 322.

[12] M. Ishikawa, M. Yamamoto, T. Watanabe, T. Masui, H. Narita and S. Kimura, *Shizuoka-ken Eisei Kenkyusho Hokoku*, 22 (1979) 89.
[13] R. Galensa and F.I. Schäfers, *Z. Lebensm.-Unters.-Forsch.*, 173 (1981) 279.
[14] A. Collinge and A. Noirfalise, *Anal. Chim. Acta*, 132 (1981) 201.
[15] G. Modi, R. Biffoli and P.G. Fiorentino, *Boll. Chim. Unione Ital. Lab. Prov., Parte Sci.*, 34 (1983) 307.
[16] H. Nakaguma, K. Tajima and T. Konishi, *Eisei Kagaku*, 31 (1985) 32.
[17] H. Shiroma and Z. Oshiro, *Okinawa-ken Kogai Eisei Kenkyushoho*, 20 (1986) 73.
[18] K. Aitzetmueller and E. Arzberger, *Z. Lebensm.-Unters.-Forsch.*, 178 (1984) 279.
[19] Y. Ikai, H. Oka, N. Kawamura and M. Yamada, *J. Chromatogr.*, 457 (1988) 333.
[20] G. Burini and P. Damiani, *J. Chromatogr.*, 543 (1991) 69.

ELSEVIER

Journal of Chromatography A, 664 (1994) 221–228

JOURNAL OF CHROMATOGRAPHY A

Separations of high-molecular-mass polystyrenes on different pore size and particle size reversed-phase columns in dichloromethane–acetonitrile

Ross Andrew Shalliker[a], Peter Edwin Kavanagh*[,a], Ian Maxwell Russell[b]

[a]*School of Biological and Chemical Sciences, Deakin University, Waurn Ponds, Victoria 3217, Australia*
[b]*CSIRO Division of Wool Technology, Belmont, Victoria 3216, Australia*

(First received September 1st, 1993; revised manuscript received December 15th, 1993)

Abstract

The effect of pore size and particle size of the silica support on the retention and resolution of high-molecular-mass polystyrenes was investigated in reversed-phase gradient elution high-performance liquid chromatography using a dichloromethane–acetonitrile mobile phase. An increase in pore size was found to increase retention slightly. A decrease in particle size was found to increase retention of all molecular masses. Both pore size and particle size had effects on resolution between polystyrenes of different molecular masses. Unretained polystyrene eluted at the solvent front for some of the conditions used but, this effect decreased with an increase in pore size and a decrease in particle size. A possible explanation for the greater effect on retention of particle size compared with pore size, is that the polystyrene molecules in a gradient elution experiment do not have access to the same number of pores as they do in an isocratic or size-exclusion experiment. It is proposed that this is due to a lag in the mobile phase composition in the pores compared with interstitial composition in the gradient experiment.

1. Introduction

Even though the analysis of polymers by reversed-phase chromatographic methods has received considerable attention in the last decade, very few molecular mass separations have been published. The first molecular mass separations using reversed-phase methods were published by Armstrong and Bui [1], who separated polystyrenes from molecular mass 2700 to 10^7 in a dichloromethane–methanol solvent system using octadecyl columns. Further separations were reported by the same workers where oligomers (from $n = 1$ to $n = 20$) and high-molecular-mass polystyrenes were separated using a single gradient [2]. Recent studies by Shalliker *et al.* [3] have shown that high-quality molecular mass separations of polystyrenes to a molecular mass of 10^6 are achievable using a variety of low-cost commercial octadecyl reversed-phase columns and a dichloromethane–acetonitrile gradient solvent system. These separations have been used to determine the polydispersity of commercial polystyrenes [4] and the method compared very favourably to conventional size-exclusion chromatography.

The behaviour of polystyrene in reversed-phase chromatography has been examined by a number of other workers in a variety of solvent systems and there appears to be little consensus

* Corresponding author.

0021-9673/94/$07.00
SSDI 0021-9673(93)E0048-Y

on the mechanisms or the role of pore size. Larmann *et al.* [5] studied the behaviour of polystyrenes in a tetrahydrofuran–water solvent system for molecular masses up to 50 000. They concluded that retention followed normal chromatographic adsorption behaviour and that pore size had little effect because polymer chains could snake into excluded pores. Glöckner and Borth [6,7] studied the behaviour of polystyrene in solvent systems consisting of tetrahydrofuran–methanol and tetrahydrofuran with a number of alkanes. Glöckner [8] explained that the retention followed a precipitation redissolution mechanism. Quarry *et al.* [9] examined the retention mechanism of M_r 50 000 polystyrene in tetrahydrofuran–water and concluded that normal chromatographic behaviour, rather than precipitation–redissolution occurred, provided sample size was less than 200 μg. Northrop *et al.* [10] examined retention on a C_4 stationary phase using dichloromethane–methanol and tetrahydrofuran–acetonitrile solvent systems. They suggested that the pore size was important for the retention of the polystyrenes and showed that retention of the high-molecular-mass polystyrenes was reduced when excluded from the pores. They concluded that polystyrene retention behaviour depended on both the mobile phase and the exclusion properties of the column. Also, Lochmüller and McGranaghan [11], using a dichloromethane–acetonitrile solvent system reported a similar reduction in the expected retention of excluded polystyrenes. Studies by Shalliker *et al.* [12] in a dichloromethane–methanol solvent system and C_{18} columns of various pore sizes found that when the polystyrenes had access to the pores, elution occurred by adsorption or partitioning processes as elution occurred after the polymer solubility composition. However, when the polymers were excluded from the pores, the elution was complicated by polymer–solvent and polymer–polymer interactions that caused the polymer to elute prior to the polymer solubility composition or even before the solvent front. It is clear that the mobile phase is important for the elution of high-molecular-mass polystyrenes without unusual chromatographic effects. The best solvent systems reported to date appear to be dichloromethane–acetonitrile [3,4,11] and tetrahydrofuran–acetonitrile [10].

The development of small-diameter particles and improved methods for uniform column packing have lead to a great increase in the efficiency of the separations of small molecules. Columns packed with particles down to 2 μm in diameter have been used in protein separations [13]. The use of large diameter particles for all but preparative chromatography has generally become obsolete. Recently however large-diameter 20-μm non-porous particles have been employed for the rapid separation of protein mixtures [14]. These particles offered several advantages. They were easier to pack using the dry pack method. They operated at lower pressures and they were also less prone to clogging by strongly adsorbed species. Similar advantages are available with large particle size pellicular supports.

This paper reports the effect of pore size and particle size of the silica support on the reversed-phase retention behaviour of polystyrenes up to a molecular mass of 929 000 in the dichloromethane–acetonitrile solvent system. The effect of pore size is investigated by observing the retention on C_{18} reversed-phase supports with 10 μm particle size and three different pore sizes. For comparison, columns with a porous 6 μm particle size silica and a 35 μm particle size pellicular support were also used.

2. Experimental

All chromatographic experiments were performed using two M6000A pumps, a 660 solvent programmer and a U6K injector (Waters Associates, Milford, MA, USA). A Linear UVIS 200 variable-wavelength absorbance detector set at 262 nm was used (Linear Instruments, NV, USA). Data acquisition and analysis were done with a previously used [3] laboratory-built system and a 386 personal computer.

HPLC-grade acetonitrile and dichloromethane were used as mobile phases (Mallinckrodt Australia). The monodisperse polystyrene standards used were molecular masses 17 500, 50 000,

110 000, 410 000, 929 000 (Polyscience, Warrington, PA, USA) and 200 000 (Waters). A Zorbax ODS 150 mm packed column (DuPont, Wilmington, DE, USA) was purchased. Spherisorb 10 μm ODS (Phase Separation, Clwyd, UK) was purchased as a C_{18} packing. Perisorb A, LiChrospher SI500 and LiChrospher SI1000 (E. Merck, Darmstadt, Germany) were silylated. The reversed-phase packing materials were packed into identical column blanks of dimensions 150 mm × 4.6 mm I.D. The silylation method and packing methods are described elsewhere [15]. The details of all columns used are presented in Table 1. In this table, the surface areas were obtained from manufacturer's data. The carbon loading was obtained by drying the silylated silica in a vacuum oven at 50°C for 24 h, weighing, heating at 600°C for 24 h and reweighing. This method gave good agreement with elemental carbon and hydrogen analysis [15]. Surface ligand densities were estimated using the method of Berendsen and De Galan [16]. These surface ligand densities are all within 30% of the average. Size-exclusion calibration curves for each column were obtained by eluting the polystyrene standards in pure dichloromethane. The sample size was 10 μg and the flow-rate 0.5 ml/min. These curves are shown in Fig. 1.

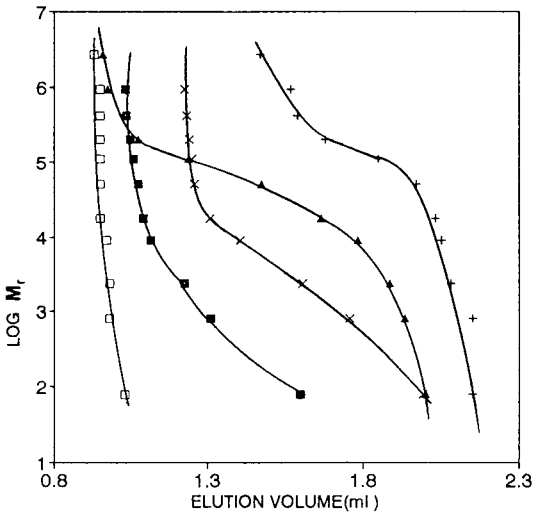

Fig. 1. Size-exclusion curves. Sample size, 10 μg; flow-rate, 0.5 ml min^{-1}; mobile phase, dichloromethane. Symbols: □ = 7-nm pore size, 6-μm particle size column; × = 8-nm pore size, 10-μm particle size column; ▲ = 50-nm pore size, 10-μm particle size column; + = 100-nm pore size, 10-μm particle size column; □ = pellicular, 30–40-μm particle size column.

Gradient elution separations were obtained by injecting polystyrenes dissolved in pure dichloromethane. Sample size was 10 μg. Sample volume was 10 μl. The gradient started at 0.48 volume fraction of dichloromethane in acetonitrile and changed to a 0.64 volume fraction dichloromethane in acetonitrile over a 6 h period at a flow-rate of 1.0 ml/min. The gradient was stopped after elution of the last peak. For the pellicular column, the initial volume fraction of dichloromethane was 0.46. Curve 3 on the Waters 660 programmer defined the gradient profile at the column outlet. This profile is represented [18] by the equation

$$\varphi_e = \varphi_i + (\varphi_f - \varphi_i)\left(\frac{V_e - V_d}{V}\right)^k \quad (1)$$

Table 1
Column data

Silica	Pore size (nm)	Particle size (μm)	Surface area (m^2/g)	Carbon (%)	Ligand density (μmol m^{-2})	Reduced plate height[a]
Zorbax	7	6	350	14.5	2.7	2.08
Spherisorb	8	10	220	8.0	1.8	3.70
LiChrospher	50	10	60	4.6	3.8	0.34
LiChrospher	100	10	30	1.8	2.9	10.0
Perisorb	Pellicular	30–40	14	0.9	2.9	20.4

[a] Measured from phentole using conditions of Bristow and Knox [17].

where φ_e = volume fraction of dichloromethane at any elution volume; φ_i = initial volume fraction of dichloromethane; φ_f = final volume fraction of dichloromethane; V_e = elution volume; V = total volume of the gradient; V_d = delay volume; k = constant determined experimentally to be 0.31 compared with the literature value of 0.33 [18]. The experimental value was found by recording the gradient profile of dichloromethane spiked with benzene and fitting the curve to Eq. 1. Except for delay time at the detector, the gradient profile was the same with a column present as without. This gradient profile was used as it was found to give good resolution over the molecular mass range studied [3]. Linear gradients were found to give worse separation at higher molecular masses.

The value of the polymer solubility composition for each molecular mass, φ_s, was obtained by titrating the polymer dissolved in dichloromethane at 200 mg/l with acetonitrile at 25.0°C. The first appearance of a turbid suspension was used as φ_s. φ_s was expected to be concentration dependent and Glöckner [6] has shown that, for polystyrene in tetrahydrofuran–methanol, the amount of non-solvent required for precipitation increases as the polystyrene concentration decreases. The concentration of polystyrene was as low as practicable to approximate chromatographic conditions but the values of $\varphi_e - \varphi_s$ quoted in results are likely to be lower than the values expected under actual chromatographic conditions.

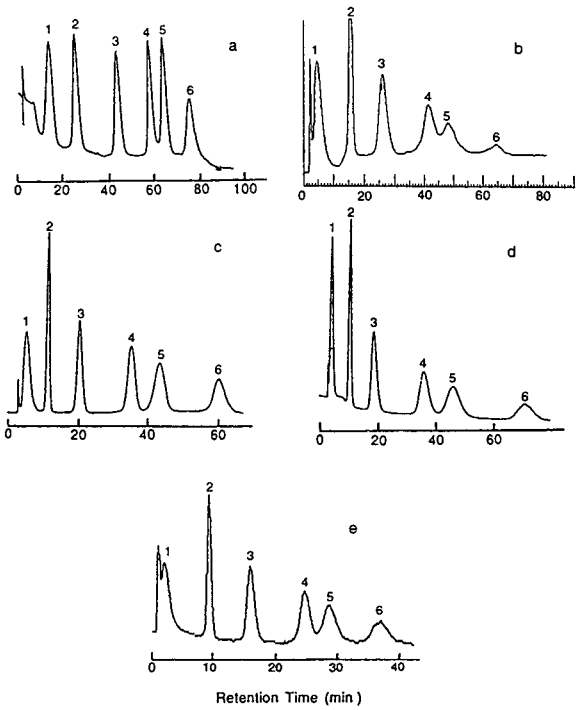

Fig. 2. Polystyrene separations. Sample size, 10 μg; injection solvent, dichloromethane; flow-rate, 1.0 ml min^{-1}; initial mobile phase, 0.48 volume fraction dichloromethane; final mobile phase, 0.64 volume fraction dichloromethane; gradient time, 6 h. (a) 7 nm pore size, 6 μm particle size column; (b) 8 nm pore size, 10 μm particle size column; (c) 50 nm pore size, 10 μm particle size column; (d) 100 nm pore size, 10 μm particle size column; (e) pellicular, 30–40 μm particle size column. Peaks: 1 = M_r 17 500 polystyrene; 2 = M_r 50 000 polystyrene; 3 = M_r 110 000 polystyrene; 4 = M_r 200 000 polystyrene; 5 = M_r 410 000 polystyrene; 6 = M_r 929 000 polystyrene.

3. Results and discussion

Fig. 2 shows the separations that were obtained on each of the columns. The high quality separations are similar to the separations obtained with commercial columns for the dichloromethane-acetonitrile solvent system [3]. No peaks eluted before the solvent front or before the polymer solubility composition φ_s, as reported for the dichloromethane–methanol solvent system [12]. However some columns did show elution at the solvent front. The important parameters describing these separations are considered to be as follows: (1) φ_e, the elution volume fraction of dichloromethane; (2) $\varphi_e - \varphi_s$, the difference between the elution volume fraction of dichloromethane and the polymer solubility volume fraction of dichloromethane (if, as in this study, this parameter is greater than zero then the polystyrenes must be eluting according to polymer stationary phase adsorption or partitioning interactions rather than a precipitation–redissolution mechanism; higher values of

$\varphi_e - \varphi_s$ indicate stronger interaction with the stationary phase); (3) R, the resolution between adjacent members of the polystyrene molecular mass series and (4) F, the area fraction of a polystyrene of given molecular mass eluting at the solvent front.

These parameters, for each column and polystyrene are shown in Table 2. The results show that gradient retention, whether determined by φ_e or $\varphi_e - \varphi_s$, increases as particle size of the silica support decreases for all molecular masses independent of pore size. Except for the M_r 17 500 polystyrene, an increase in pore size has a small but positive effect on retention.

Table 2
Polystyrene elution compositions, resolutions and fractions eluted at the solvent front

Column		M_r	φ_e [a]	$\varphi_e - \varphi_s$ [a]	R [a]	F [a]
Pore size (nm)	Particle size (μm)					
7	6	17 500	0.528	0.243	–	0
		50 000	0.543	0.148	2.23	0
		110 000	0.558	0.093	4.10	0
		200 000	0.567	0.082	3.38	0
		410 000	0.570	0.060	1.28	0
		929 000	0.575	0.035	2.14	0
8	10	17 500	0.480	0.195	–	0
		50 000	0.514	0.118	2.57	0
		110 000	0.537	0.072	2.50	0
		200 000	0.553	0.068	2.60	0
		410 000	0.558	0.048	0.71	0
		929 000	0.567	0.027	1.53	0.05
50	10	17 500	0.480	0.195	–	0
		50 000	0.519	0.124	2.50	0
		110 000	0.538	0.073	3.38	0
		200 000	0.554	0.069	4.09	0
		410 000	0.560	0.050	1.67	0
		929 000	0.570	0.030	2.74	0.02
100	10	17 500	0.480	0.195	–	0
		50 000	0.519	0.124	3.45	0
		110 000	0.535	0.088	3.27	0
		200 000	0.554	0.070	3.49	0
		410 000	0.560	0.050	1.38	0
		929 000	0.574	0.034	2.60	0
Pellicular	35	17 500	0.460	0.175	–	0.07
		50 000	0.499	0.101	3.45	0.03
		110 000	0.515	0.053	3.50	0.2
		200 000	0.529	0.047	3.00	0.2
		410 000	0.533	0.027	1.03	0.2
		929 000	0.541	0.005	2.15	0.4

Injection solvent, dichloromethane; sample size, 10 μg; initial composition, 0.46 volume fraction dichloromethane; final composition, 0.64 volume fraction dichloromethane; gradient time, 6 h, flow-rate, 1.0 ml min^{-1}.
[a] See text.

These results are surprising and this can be seen by considering the chromatographic behaviour of the M_r 50 000 polystyrene. Fig. 1 gives the size-exclusion data obtained by injecting the polystyrenes into pure dichloromethane mobile phase on each of the columns used for the reversed-phase experiments. From Fig. 1, it can be seen that the M_r 50 000 polystyrene is virtually excluded from the pores of the 7- and 8-nm pore size silicas but has access to about half the pores on the 50-nm and nearly all the pores on the 100-nm pore size silicas when eluted in pure dichloromethane. It is well known that the hydrodynamic volume of a polymer decreases on changing from a good solvent to a poor solvent. From viscosity measurements [15] it can be estimated that there is a decrease in the hydrodynamic radius of about 12% for M_r 50 000 polystyrene on changing from pure dichloromethane to 60% dichloromethane in acetonitrile. Hence similar pore volumes are accessible in the gradient elution experiment. By assuming (see Fig. 1), that the M_r 50 000 polystyrene has access to only the external surface area of the 8-nm silica but nearly all the surface area (external plus internal) of the 100-nm silica, it can be estimated that the increase in accessible surface area on changing from the 8-nm silica to the 100-nm silica is about 40 times. Yet $\varphi_e - \varphi_s$ only increases 1.05 times from the situation where the M_r 50 000 polystyrene is totally excluded on the 8-nm column to the situation where it has access to all the pores on the 100-nm column. Additionally, on changing from 10- to 6-μm particles, with similar pore size (7 to 8 nm), there is an increase in external surface area of about 1.5 times. There is a corresponding increase in $\varphi_e - \varphi_s$ of about 1.25. This increase in $\varphi_e - \varphi_s$ is essentially constant for all molecular masses used in this study as all only have access to the external surface on these small pore size particles. It appears that even when the polystyrene molecules have access to the pores, according to size-exclusion data, they have difficulty interacting with the internal pore surfaces in gradient elution. They only interact easily with the external surface of the particle, even though only a small portion of the C_{18} chains are on the external surface.

A possible reason for this is due to the gradient change in mobile phase composition. As the fraction of good solvent increases and moves down the column, the mobile phase composition in the pores will lag marginally behind the interstitial mobile phase composition. Although minor mobile phase composition variations are unimportant for small molecules this is not so for large molecules. High-molecular-mass polystyrenes have a large value of S, the slope of log k *versus* mobile phase composition [5,11,15,19]. Hence they are likely to interact with stationary phase at the pore entrance until the mobile phase composition in the pore increases in good solvent. Also, there will be a distribution coefficient for polystyrene between the pore composition and the higher interstitial composition which will decrease the chance of entry into the pores. These effects are not present in isocratic or size-exclusion experiments. The polystyrenes in a gradient elution experiment therefore may not have access to as many pores as they do in a size exclusion experiment. A number of other workers [5,12,19] have studied the effect of pore size in the gradient elution of polystyrenes. Larmann *et al.* [5] found decreased retention with increase in pore size and hence decrease in surface area for molecular masses up to 50 000. When molecular masses are increased to over 100 000, then the larger pore size packings show increased retention [12,19] even though a variety of mobile phases were used. This agrees with the results found here. There is no other work with which to compare our results which indicate that a decrease in particle size has a greater effect on retention than an increase in pore size.

Resolution between adjacent polystyrenes in the series used does not vary in a systematic way with silica size and pore size. The resolution between the M_r 17 500 and 50 000 polystyrenes is complicated by the fact that the M_r 17 500 polystyrene elutes during the isocratic portion of the run, before the gradient reaches the top of the column, on nearly all except the 6-μm particle diameter and the 100-nm pore size silicas. The two highest-molecular-mass polystyrenes show the highest resolution on the 100-nm pore size column. A plot of log resolution per 1000 molecular mass units *versus* log molecu-

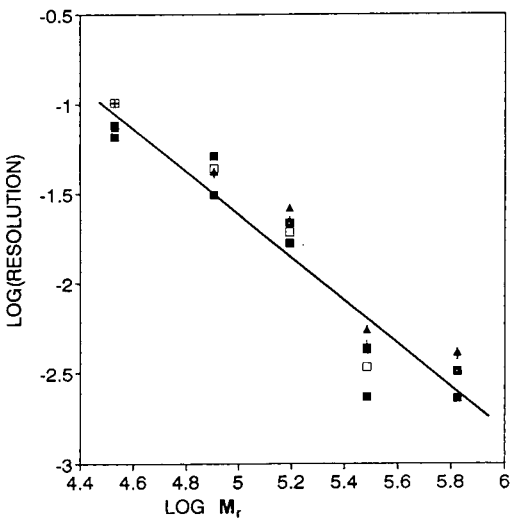

Fig. 3. Log resolution against log molecular mass. Symbols: ■ = 7-nm pore size, 6-μm particle size column; × = 8-nm pore size, 10-μm particle size column; ▲ = 50-nm pore size, 10-μm particle size column; + = 100-nm pore size, 10-μm particle size column; □ = pellicular, 30–40-μm particle size column.

lar mass (Fig. 3) shows a rapid fall in resolution with increase in molecular mass. There is little difference in resolution between columns, irrespective of pore size or particle size.

Some columns show unretained polystyrene eluting at the solvent front. This is an obvious disadvantage if molecular mass distributions are to be measured by reversed phase. The elution was most apparent on the pellicular column and injections of individual narrow disperse polystyrenes on this column showed that all tested molecular masses contributed to this peak. On the 8-nm and 50-nm pore size, 10-μm particle size columns, only the M_r 929 000 polystyrene showed elution at the solvent front. There was no indication of unretained polystyrene on the 100-nm pore size, 10-μm particle size column or the 6-μm particle size column. Re-examination of previous separations with the dichloromethane–acetonitrile solvent system and some commercial columns [3] indicates the same behaviour with the 10-μm columns, but again, a 5-μm column showed negligible solvent front peak. The fraction of unretained polystyrene, at constant injection mass, seems to be a function of available surface area and molecular mass.

The effect of injection mass on fraction of unretained polystyrene was not investigated. The injection mass was constant for all columns at 10 μg. We have previously shown that sample size up to 150 μg does not affect the chromatogram in a dichloromethane–acetonitrile solvent system [3]. This is unlike the dichloromethane–methanol system [12]. Previous workers [11,15] have shown that injection of polystyrenes dissolved in a mixture of the two solvents, rather than pure good solvent may overcome this problem. However, using a mixture of two solvents is complicated when a range of, possibly unknown, molecular masses is present because of different solubilities. Another method of eliminating elution at the solvent front is the recommendation by Lochmüller and McGranaghan [11] that a post-injection, pre-column mixer be used. This method adds considerable void volume to the system. The choice of a 5-μm particle size silica support seems a better solution.

4. Acknowledgement

One of the authors (R.A.S.) wishes to acknowledge the assistance of a Deakin University Post Graduate Award.

5. References

[1] D.W. Armstrong and K.H. Bui, *Anal. Chem.*, 54 (1982) 706.
[2] K.H. Bui and D.W. Armstrong, *J. Liq. Chromatogr.*, 7 (1984) 29.
[3] R.A. Shalliker, P.E. Kavanagh and I.M. Russell, *J. Chromatogr.*, 558 (1991) 440.
[4] R.A. Shalliker, P.E. Kavanagh, I.M. Russell and D.G. Hawthorne, *Chromatographia*, 33 (1992) 427.
[5] J.P. Larmann, J.J. DeStephano, A.P. Goldberg, R.W. Stout, L.R. Snyder and M.A. Stadalius, *J. Chromatogr.*, 255 (1983) 163.
[6] G. Glöckner, *Chromatographia*, 25 (1988) 854.
[7] G. Glöckner and H.G. Borth, *J. Chromatogr.*, 499 (1990) 645.
[8] G. Glöckner, *Pure Appl. Chem.*, 55 (1983) 1553.
[9] M.A. Quarry, M.A. Stadalius, T.M. Mourey and L.R. Snyder, *J. Chromatogr.*, 358 (1986) 1.

[10] D.M. Northrop, D.E. Matire and R.P.W. Scott, *Anal. Chem.*, 64 (1992) 16.
[11] C.H. Lochmüller and M.B. McGranaghan, *Anal. Chem.*, 61 (1989) 2449.
[12] R.A. Shalliker, P.E. Kavanagh and I.M. Russell, *J. Chromatogr.*, 543 (1991) 157.
[13] N. Nimura, H. Itoh, T. Kinoshita, N. Nagae and M. Nomura, *J. Chromatogr.*, 585 (1991) 207.
[14] S.P. Fulton, N.B. Afeyan, N.F. Gordon and F.E. Regnier, *J. Chromatogr.*, 547 (1991) 452.
[15] R.A. Shalliker, *Ph.D. Thesis*, Deakin University, Waurn Pounds, 1992.
[16] G.E. Berendsen and L. de Galan, *J. Chromatogr.*, 196 (1980) 21.
[17] P.A. Bristow and J.H. Knox, *Chromatographia*, 10 (6) (1977) 279.
[18] P. Jandera and J. Churáček, *Gradient Elution in Column Liquid Chromatography —Theory and Practice*, Elsevier, Amsterdam, New York, 1985, p. 229.
[19] A. Alhedai, R.E. Boehm and D.E. Martire, *Chromatographia*, 29 (1990) 313.

ELSEVIER

Journal of Chromatography A, 664 (1994) 229–251

JOURNAL OF CHROMATOGRAPHY A

Influence of temperature on the mechanism by which compounds are retained in gas–liquid chromatography

Salwa K. Poole, Theophilus O. Kollie, Colin F. Poole*

Department of Chemistry, Wayne State University, Detroit, MI 48202, USA

(Received August 16th, 1993)

Abstract

The influence of temperature on the retention mechanism and solvation interactions of 46 varied solutes in 10 representative stationary phases of different polarity within the temperature range of 60 to 140°C is discussed. Gas–liquid partition is shown to the dominant retention mechanism for most solutes with inrterfacial adsorption of increasing importance at low phase loadings, low temperatures and for solutes of different polarity to that of the stationary phase. Guidelines are presented for predicting those conditions for which interfacial adsorption is likely to be a significant retention mechanism.

A cavity model is used to characterize the solvation process in terms of the free energy contributions to solvation from the cavity–dispersion interactions and the sum of the remaining polar interactions. As a function of temperature it is shown that the contribution from polar interactions are only weakly temperature dependent over the temperature range studied while the cavity–dispersion interactions term shows a much more significant variation becoming less favorable for solute transfer at higher temperatures. In all cases, the contribution of the cavity–dispersion interactions term is favorable for solute transfer from the gas phase to the liquid phase.

Principal component analysis is used to identify the factors contributing to the solvation process and their individual temperature dependence. In the case of the cavity–dispersion interactions term one factor accounts for more than 99.7% of the total variance. Three factors are identified as contributing to the polar interactions term. The first principle component accounts for more than 95% of the total variance at all temperatures and by correlation with other independent scales of dipolarity/polarizability is identified as representing the contribution from orientation and induction interactions. The two remaining principal components are shown to represent hydrogen-bond formation and charge-transfer complexation involving systems with π-electrons. The temperature dependence of the principal components provides insights into the general role of polar intermolecular interactions on the solvation process and their temperature variation.

1. Introduction

Temperature is a fundamental parameter that affects both resolution and the separation time in gas–liquid chromatography [1–3]. Its optimization in both isothermal and temperature-programmed separations has been discussed extensively in the contemporary literature and will not be elaborated on here. The topic of this paper is the influence of temperature on the retention mechanism in gas–liquid chromatography and on the contribution of specific intermolecular interactions participating in the retention process. These are topics that need to be addressed

* Corresponding author.

0021-9673/94/$07.00
SSDI 0021-9673(93)E0070-B

before the applicability of the cavity model of the solvation process in gas–liquid chromatography can be assessed as a general approach to the prediction of retention and the selection of the optimum stationary phase and temperature for a given separation [4,5].

Retention in gas–liquid chromatography can be a complex process involving partitioning with the liquid stationary phase and interfacial adsorption at the support surface and/or the liquid surface [6–9]. This can be expressed as

$$V_N^* = V_L K_L + A_{GL} K_{GL} + A_{LS} K_{GLS} \quad (1)$$

where V_N^* is the net retention volume per gram of column packing, V_L the volume of liquid stationary phase per gram of column packing, K_L the gas–liquid partition coefficient, A_{GL} the gas–liquid interfacial area per gram of packing, K_{GL} the adsorption coefficient at the gas–liquid interface, A_{LS} the liquid–solid interfacial area per gram of packing and K_{GLS} the coefficient for adsorption at the liquid–solid interface. Eq. 1 was originally proposed by Martin [10] and within the constraints discussed below has been validated as an accurate representation of the retention process in gas–liquid chromatography by Purnell and co-workers [11,12], Riedo and Kováts [13], Liao and Martire [14], Nikolov [15], Karger and Liao [16], Castells and co-workers [17,18], Berezkin [9] and Poole and co-workers [4,6,7,19–22]; the general applications of Eq. 1 are reviewed in refs. 1, 4, 6–9 and 23. In deriving Eq. 1 it is assumed that the individual retention mechanisms are independent and additive, the solute concentration is in a region where the infinite dilution and zero surface coverage approximations apply, and the contributions to retention from the structured liquid-phase layer in close contact with the support surface can be neglected (generally the case at high phase loadings). The experimental data reported in this paper were obtained under conditions where the above constraints can safely be assumed to apply [24]; otherwise it would be necessary to use an alternative model to describe the retention process in terms of the same general contributions identified in Eq. 1 [3,11]. Division of both sides of Eq. 1 by V_L allows the gas–liquid partition coefficient to be evaluated independently of the other contributions to retention by extrapolating the experimental data to obtain the intercept on the V_N^*/V_L axis corresponding to an infinite stationary liquid phase volume. In virtually all cases investigated for which the general conditions used to derive Eq. 1 are applicable it has proven possible to obtain accurate values for the gas–liquid partition coefficient by a linear extrapolation, at least for intermediate temperatures around 100°C. This indicates that when adsorption contributes to the retention mechanism the dominant contribution for non-polar liquids is adsorption at the support–liquid interface and for polar liquids adsorption at the gas–liquid interface. In theory it should be possible to determine the coefficients for adsorption in Eq. 1 from a knowledge of the surface area terms A_{LS} and A_{GL}; in practice this is difficult to do because of a lack of a straightforward and reliable experimental method for determining surface areas as a function of the stationary liquid phase loading [10,13,16,25]. Insights into the importance of adsorption as a retention mechanism, however, may be obtained by comparing the observed experimental retention with the value calculated assuming that the only contribution to retention was from gas–liquid partitioning [21,26]. A lack of knowledge of the adsorption contribution to retention in gas-liquid chromatography is the primary problem in predicting retention since the solvation models that are available are applicable to gas–liquid partition chromatography and there is no easy way to extend them to situations in which a mixed retention mechanism occurs without knowing the particulars of the relationship between the surface area of the liquid and of the support as a function of the bulk liquid stationary phase volume. This is currently impractical and therefore the contributions of adsorption to retention establishes one limit to the usefulness of solvation models for the prediction of retention.

In this paper we will provide a general assessment of the importance of interfacial adsorption as a retention mechanism in gas–liquid chromatography to identify those conditions and com-

pound types for which interfacial adsorption is unimportant. This discussion will include temperature, since it impacts on the relative importance of adsorption and partitioning mechanisms for defined solutes. Previous studies have indicated that for those compounds which are retained by a mixed retention mechanism the relative contribution from gas–liquid partitioning increases with temperature when data are compared at 120 and 80°C [4]. To our knowledge there are no true studies describing how the relative contribution of partitioning and adsorption change over a wide temperature range employing a large group of solutes of varied character on a significant number of stationary liquid phases selected to encompass a wide capacity range for selective solvent intermolecular interactions.

There are numerous models that have been proposed to characterize retention in gas–liquid chromatography as a function of solvent and solute properties, reviewed in refs. 1, 6, 19, 20 and 27]. The most recent and generally useful approaches are the solvation parameter model developed by Abraham and co-workers [28–31] and Carr and co-workers [32–34] and the free energy solvation model developed by Poole and co-workers [4,35–37]. These models are derived from the cavity model of solvation, in which the process of solute transfer from the gas phase to solution in the stationary phase is considered to occur in three stages: (1) the creation of a cavity in the solvent of a suitable size to accommodate the solute, (2) reorganization of the solvent molecules around the cavity and (3) introduction of the solute into the cavity where it is able to interact with the surrounding solvent molecules. The Gibbs free energy change for the transfer process is simply the sum of the free energy changes for each step. There is no exact method to calculate the individual contributions to the total free energy change for the solvation process, as just defined, and it is necessary to resort to empirical approaches to estimate the changes involved using experimentally accessible parameters. The approach of Abraham and co-workers (and essentially also that of Carr and co-workers with some differences in the explanatory variables) results in the following general equation relating the gas–liquid partition coefficient, K_L, to the characteristic parameters for the solvation process

$$\log K_L = c + rR_2 + s\pi_2^H + a\alpha_2^H + b\beta_2^H + l \log L^{16} \quad (2)$$

where c is a constant, R_2 the solute excess molar refraction, π_2^H the effective solute dipolarity/polarizability, α_2^H the effective hydrogen-bond acidity, β_2^H the effective hydrogen-bond basicity, and L^{16} the gas–liquid partition coefficient on n-hexadecane at 25°C. The explanatory variables (R_2, π_2^H, α_2^H, β_2^H and $\log L^{16}$) are solvation parameters derived from equilibrium measurements. Values of the solvation parameters for in excess of 1000 compounds are currently available and in many cases unknown values can be estimated using simple combining rules [38]. The solvent parameters r, s, a, b and l are unambiguously defined: the r constant refers to the ability of the phase to interact with solute π- and n-electron pairs; the s constant to the ability of the phase to take part in dipole–dipole and dipole–induced dipole interactions; the a constant is a measure of the hydrogen-bond basicity of the phase; the b constant is a measure of the hydrogen-bond acidity of the phase; and the l constant incorporates contributions from solvent cavity formation and dispersion interactions, and more specifically indicates how well the phase will separate members in a homologous series. The phase constants can be determined for any solvent by multiple linear regression analysis of measured values of K_L for solutes with known values of their explanatory variables. Once the phase constants are defined, the retention of any solute for which explanatory variables are known or can be estimated with sufficient accuracy can then be estimated from Eq. 2. The validity of this approach has been demonstrated in a number of papers by Abraham and co-workers referenced above. Nearly all this work refers to a single temperature or temperatures which are close together. The explanatory variables used in the regression analysis are determined at room temperature. Any change in solute–solvent in-

teractions as a function of temperature is clearly a function of the properties of both the solute and the solvent. There is no means to separate these different contributions in multiple linear regression models and it has proved necessary to adopt the convention that any change in the characteristic phase constants with temperature are due to changes in solvent properties alone. This is not too significant for the comparison of different solvents at a fixed temperature but it precludes the phase constants being used as absolute solvent properties. It is also unclear if they can be used to quantitatively represent changes in solvent properties as a function of temperature, although a recent study has demonstrated that the individual phase constants show smooth changes as a function of temperature and can generally be fitted to a second order polynomial function (except for the constant c) [39].

The model proposed by Poole and co-workers should be more tractable to studying the influence of temperature on solvation properties. In its most useful form for this investigation it can be written as

$$\Delta G_S^{SOLN}(X) = \Delta G_S^{SOLN}(HC)^V + \Delta G_{SQ}^P(X) + \Delta G_S^{INT}(X) \quad (3)$$

where $\Delta G_S^{SOLN}(X)$ is the partial molal Gibbs free energy of solution for the transfer of solute X from the gas phase to the stationary phase S, $\Delta G_S^{SOLN}(HC)^V$ is the partial Gibbs free energy of solution for an n-alkane with an identical Van der Waals volume to solute X in the stationary phase S, $\Delta G_{SQ}^P(X)$ is the partial Gibbs free energy of interaction for the polar contribution of solute X in a non-polar reference solvent squalane, SQ, and $\Delta G_S^{INT}(X)$ is the partial Gibbs free energy of interaction for the polar contribution of solute X to solvation in solvent S. Experimentally, the Van der Waals volume of solute X is calculated along with the coefficients describing the linear fit for log K_L against the Van der Waals volume of the homologous series of n-alkanes on the non-polar reference phase squalane and the stationary phase S, together with the gas–liquid partition coefficient for solute X on squalane and stationary phase S. All the terms in Eq. 3 can then be evaluated. The contribution from cavity formation and solute–solvent dispersion interactions is represented by the sum of the first two terms on the right-hand side of Eq. 3. These two contributions cannot be evaluated separately. The $\Delta G_S^{INT}(X)$ parameter represents the sum of the polar interactions, such as orientation and hydrogen-bond formation, which must be further deconvoluted by principle component analysis for a representative collection of solutes to identity the capacity of the solvent S for specific polar intermolecular interactions.

Although the models proposed by Abraham and co-workers and Poole and co-workers were developed independently and use different approaches to evaluate the contribution of cavity formation and solute–solvent interactions to the solvation process, both models in fact yield similar results for the cavity–dispersion contribution and the contribution of polar interactions to the solution of a large number of varied solutes in a wide variety of liquid stationary phases [4,26,39,40]. There is, perhaps, a small numerical numerical difference in the magnitude of the cavity–dispersion contribution to solvation predicted by both models but this does not affect the agreement in general trends in solvation properties that have been characterized by both models. The availability of two complementary approaches for exploring the solvation processes in gas–liquid chromatography provides additional flexibility with the final choice of the model employed resting on the type of available experimental data. For studies involving the affect of temperature on the solvational process Poole's model is preferred since it involves no unambiguous assumptions as to the nature of the temperature dependence of solute–solvent interactions.

2. Experimental

The names, abbreviations, compositions and temperature ranges studied for the stationary phases used in this study are summarized in Table 1. Squalane, QF-1, CW-20M, DEGS, TCEP and Chromosorb W AW (177–250 μm)

Table 1
Stationary phases and the temperature range studied

Abbreviation	Chemical description	Temperature range (°C)
SQ	Squalane	60–120
OV-105	Poly(cyanopropylmethyldimethylsiloxane)	60–120
OV-17	Poly(methylphenylsiloxane)	80–140
QF-1	Poly(trifluoropropylmethylsiloxane)	60–120
OV-225	Poly(cyanopropylmethylphenylmethylsiloxane)	80–140
CW-20M	Poly(ethylene glycol)	80–140
THPED	N,N,N′,N′-Tetrakis(2-hydroxypropyl)ethylenediamine	60–120
TCEP	1,2,3-Tris(2-cyanoethoxypropane)	80–140
DEGS	Poly(diethylene glycol succinate)	80–140
QPTS	Tetra-*n*-butylammonium 4-toluenesulfonate	80–140

were obtained from Anspec (Ann Arbor, MI, USA); OV-105, OV-17, OV-225 from Ohio Specialty Chemicals (Marietta, OH, USA); and THPED and QPTS from Aldrich (Milwaukee, WI, USA). All solvents were of OmniSolv grade from EM Science (Gibbstown, NJ, USA). The test solutes in Table 2 were obtained from several sources and were of the highest purity generally available. The homologous series of *n*-alkanes with carbon numbers from 7 to 16 were obtained from Aldrich.

Columns containing form about 8 to 20% (w/

Table 2
Solutes and their Van der Waals volumes selected to evaluate polar interactions in the temperature range 60–140°C

Solute	Van der Waals volume (V_A)	Solute	Van der Waals volume (V_A)
Benzene	50.46	1-Nitropentane	69.61
Toluene	70.34	1-Nitrohexane	80.27
Ethylbenzene	71.00	Nitrocyclohexane	72.81
Butylbenzene	92.72	Chlorobenzene	59.50
Oct-2-yne	81.84	Bromobenzene	64.68
Dodec-1-yne	122.79	Iodobenzene	68.29
Butan-2-one	48.21	Benzaldehyde	60.64
Pentan-2-one	58.36	Acetophenone	70.34
Hexan-2-one	68.59	Methylphenyl ether	64.86
Heptan-2-one	78.47	Benzonitrile	61.30
Octan-2-one	88.95	Nitrobenzene	61.61
Nonan-2-one	98.94	Aniline	57.03
Decan-2-one	109.12	N-Methylaniline	67.15
Undecan-2-one	119.27	N,N-Dimethylaniline	78.29
Dodecan-2-one	129.42	Pyridine	47.75
Methyl hexanoate	93.40	2,4,6-Trimethylpyridine	77.44
Methyl hepatanate	103.40	Dioxane	52.99
Methyl octanate	114.00	1,1,2,2-Tetrachloroethane	65.28
Butan-1-ol	53.42	Nonanal	99.85
Pentan-1-ol	63.54	N,N-Dimethylacetamide	55.46
Hexan-1-ol	73.79	*o*-Dichlorobenzene	68.41
Heptan-1-ol	83.47		
Octan-1-ol	94.79		
2-Methyl-1-pentanol	73.59		
1-Nitropropane	49.32		

w) of liquid phase were prepared using the rotary evaporator technique [1]. After coating the damp packings were dried in a fluidized-bed dryer and packed into glass columns 2 m × 2 mm I.D. with the aid of vacuum suction and gentle vibration. Gas chromatographic measurements were made using a Varian 3700 gas chromatograph (Walnut Creek, CA, USA) fitted with a flame ionization detector.

The experimental protocol used to determine gas–liquid partition coefficients is described in detail elsewhere [24,41]. A minimum of four phase loadings was used in the extrapolation method to define the gas–liquid partition coefficients and in the study of the influence of phase loading on the contribution of interfacial adsorption to the general retention mechanism as a function of temperature. Phase loadings were determined by exhaustive Soxhlet extraction. A modified Lipkin bicapillary pycnometer was used to determine solvent densities as a function of temperature [24,42]. A mercury manometer was used to measure the column inlet pressure and a US National Institute of Standards and Technology (NIST)-certified thermometer (±0.2°C) to measure ambient and column temperatures. The uncertainty in K_L values is typically 3–5% R.S.D. for K_L values between 10 and 100 and 2–3% R.S.D. for values >100.

The experimental specific retention volume, $V_g^0(\text{ex})$, which includes contributions from all retention mechanisms, was determined using Eq. 4

$$V_g^0(\text{ex}) = \frac{273.2 V_N}{w_L T_c} \tag{4}$$

where V_N is the net retention volume, w_L the weight of liquid phase in the column and T_c the column temperature. The specific retention volume for gas–liquid partitioning only, $V_g^0(\text{part})$, was determined using Eq. 5

$$V_g^0(\text{part}) = \frac{273.2 K_L}{T_c \rho_c} \tag{5}$$

where ρ_c is the liquid phase density at the column temperature. The contribution of interfacial adsorption to the retention mechanism was evaluated by difference defining the contribution of interfacial adsorption to the specific retention volume, $V_g^0(\text{ads})$, as

$$V_g^0(\text{ads}) = V_g^0(\text{exp}) - V_g^0(\text{part}) \tag{6}$$

which for convenience can be expressed as a percentage as $100V_g^0(\text{ads})/V_g^0(\text{exp})$.

The free energy terms in the model of Poole and co-workers can be calculated in a number of ways. The following equations are useful when using a spread sheet program to perform the computations. The partial molal Gibbs free energy of solution for solute (X) on any phase S is given by

$$\Delta G_m^0(\text{X}) = -2.303\, RT_c \log \frac{1000 K_L(\text{X})}{RT_c \rho_c} \tag{7}$$

where R is the molar gas constant. $\Delta G_m^0(\text{X})$ is equivalent to $\Delta G_S^{\text{SOLN}}(\text{X})$ in Eq. 3 when the molal standard state is adopted for the calculation. The cavity–dispersion term for the molal standard state is given by

$$\begin{aligned}\Delta G_S^{\text{SOLN}}(\text{HC})^{\text{V}} + \Delta G_{SQ}^{\text{P}}(\text{X}) &= -2.303 RT_c \log(1000[K_L^{\text{NV}}(\text{X})]_S \\ &\quad \cdot [K_L(\text{X})]_{SQ})/RT_c \rho_c [K_L^{\text{NV}}(\text{X})]_{SQ}\end{aligned} \tag{8}$$

where $K_L^{\text{NV}}(\text{X})$ is the gas–liquid partition coefficient for an *n*-alkane with an identical Van der Waals volume to solute (X) and is derived from the linear correlation between log K_L^{NV} and the Van der Waals volume for the *n*-alkanes on any phase at a specified temperature

$$\log K_L^{\text{NV}}(\text{X}) = m_s V_A + b_s \tag{9}$$

where m_s and b_s are the coefficients obtained by linear regression on the stationary phase S. The method used to calculate the Van der Waals volumes is discussed below; appropriate values for the test solutes are summarized in Table 2. The polar interaction term in Eq. 3 is given by

$$\begin{aligned}\Delta G_S^{\text{INT}}(\text{X}) = -2.303 RT_c \log([K_L(\text{X})]_S \\ \cdot [K_L^{\text{NV}}(\text{X})]_{SQ})/([K_L(\text{X})]_{SQ} \cdot [K_L^{\text{NV}}(\text{X})]_S)\end{aligned} \tag{10}$$

There were some instances were it was impossible to generate accurate data for the gas–

liquid partition coefficients and alternative methods were used for their estimation to enable the data set to be evaluated as homogeneously as possible for chemometric analysis. Squalane was too volatile at 141.2°C to determine reliable values for the gas–liquid partition coefficients of any solutes. These values were needed to make use of the data that could be obtained on the polar phases at 141.2°C. In this instance estimated values were obtained by fitting the experimental data obtained over the temperature range 60–120°C to a second order polynomial for log $K_L(X)$ against $1000/T_c$. This equation was then used to estimate the value of $K_L(X)$ at 141.2°C. These data are summarized in Table 3. The correlation for the fit is very good, $r^2 = 1.000$, but it cannot be assumed that these estimated values are as reliable as the experimental values obtained at a lower temperature since it is impossible to define exactly the physical relationship describing the data set. The plot of log $K_L(X)$ against $1000/T_c$ shows genuine curvature over the temperature range used to collect the experimental data and a linear extrapolation is therefore inappropriate. A small number of gas–liquid partition coefficients were difficult to determine because of excessive retention on the stationary phases and these were estimated using the model of Abraham and coworkers, Eq. 2, and the appropriate characteristic phase constants and explanatory variables are summarized in ref. 39. These data are summarized in Table 4. It is estimated that the typical error in these values is about 0.01 to 0.04 log units.

The Van der Waals volumes for the test solutes in Table 2 were calculated with the molecular modeling program MacroModel 2.0 (Department of Chemistry, University of New York, New York, NY, USA) executed on a VAX 11/750 computer (Digital Equipment, Merrimack, NH, USA). The polynomial fit for log K_L against

Table 3
Estimated log $K_L(X)$ values for squalane at 141.2°C

Solute	Log $K_L(X)$	Solute	Log $K_L(X)$
n-Heptane	1.548	Hexan-1-ol	1.811
n-Octane	1.829	Heptan-1-ol	2.092
n-Nonane	2.111	Octan-1-ol	2.391
n-Decane	2.382	2-Methyl-2-pentanol	1.488
n-Undecane	2.672	1-Nitropropane	1.406
n-Dodecane	2.954	1-Nitropentane	1.967
n-Tridecane	3.236	1-Nitrohexane	2.273
n-Tetradecane	3.519	Nitrocyclohexane	2.537
n-Pentadecane	3.800	Chlorobenzene	1.918
n-Hexadecane	4.080	Bromobenzene	2.156
Benzene	1.446	Iodobenzene	2.455
Toluene	1.717	Benzaldehyde	2.130
Ethylbenzene	1.971	Acetophenone	2.406
n-Butylbenzene	2.541	Methylphenyl ether	2.097
Oct-2-yne	1.959	Benzonitrile	2.112
Dodec-1-yne	2.863	Nitrobenzene	2.444
Butan-2-one	1.089	Aniline	2.121
Pentan-2-one	1.332	N-Methylaniline	2.456
Hexan-2-one	1.618	N,N-Dimethylaniline	2.605
Heptan-2-one	1.898	Pyridine	1.555
Octan-2-one	2.170	2,4,6-Trimethylpyridine	2.215
Methyl hexanoate	1.950	Dioxane	1.368
Methyl heptanoate	2.222	1,1,2,2-Tetrachloroethane	2.129
Methyl octanoate	2.489	Nonanal	2.485
Butan-1-ol	1.106	N,N-Dimethylacetamide	1.912
Pentan-1-ol	1.532	*o*-Dichlorobenzene	2.420

Table 4
Gas–liquid partition coefficients estimated using Eq. 2

Stationary phase	Temperature (°C)	Solute	Log $K_L(X)$
SQ	61.2	Nitrobenzene	3.756
		N,N-Dimethylaniline	3.886
		Nonanal	3.9864
		Octan-1-ol	3.7755
		Acetophenone	3.7133
		Nitrocyclohexane	3.9715
		Methyl octanoate	3.9670
QF-1	61.2	1-Nitrohexane	4.0311
		Nitrocyclohexane	3.3731
		N,N-Dimethylacetamide	4.0745
THPED	61.2	Hexan-1-ol	4.1527
		Heptan-1-ol	4.5180
		Octan-1-ol	4.8929
		1-Nitrohexane	3.9767
		N,N-Dimethylacetamide	4.1285
		N-Methylaniline	4.0482
OV-105	61.2	Nitrocyclohexane	3.9834
QPTS	81.2	Nitrobenzene	4.1310
		Aniline	4.5453
		N-Methylaniline	4.2147
TCEP	81.2	N,N-Dimethylacetamide	3.9397
QPTS	101.2	Aniline	3.9806

$1000/T_c$ was performed on a Macintosh IIsi computer (Apple Computer, Cupertino, CA, USA) using Cricket Graph V1.3 (Cricket Software, Malvern, PA USA). Multiple linear regression analysis was performed on an Epson Apex 200 computer (Epson America, Torrance, CA, USA) using the program SPSS/PC + V3.1 (SPSS, Chicago, IL, USA). For multivariate analysis Pirouette V1.1 (Infometrix, Seattle, WA, USA) was used on the Epson Apex 200 computer. The experimental data was used without scaling for principal component analysis.

3. Results and discussion

Numerous studies have considered the gross effect of temperature on the retention properties of individual compounds and it is widely accepted that temperature is an important variable in the optimization of any separation. Where information is lacking is in the influence temperature has on the fundamental retention mechanism itself, whether individual compounds are retained by absorption and/or interfacial adsorption and the relative importance of temperature in regulating this process. Intuitively it is expected that absorption would be favored by higher temperatures and that adsorption behavior would be favored by lower temperatures, and thus temperature has to be considered as a critical variable is establishing the contributing factors to the gross retention mechanism. This becomes of additional importance because we now have good models that can predict absorption behavior of compounds and thus have the potential to simulate chromatographic separations on many stationary phases as a logical direction to approach an organized scheme for computer-aided methods development in gas–

liquid chromatography. These models, of course, will be limited in their general applications for systems that involve significant contributions to the retention mechanism from interfacial adsorption since this mechanism is not considered in their formulation. Thus we need a general picture of the importance of interfacial adsorption as a retention mechanism in gas–liquid chromatography with temperature as a variable since any useful simulation approach to separations by gas–liquid chromatography would incorporate temperature optimization, and for different phases it is likely that different optimum temperatures would be required.

Intuitively it is also anticipated that the relative strength of specific intermolecular interactions will vary with temperature in a manner that will depend on individual properties of the solvent and that a solvent will possess different capacities for these interactions at different temperatures so that a single measure of solvent selectivity at one temperature cannot be used to predict the contribution of intermolecular forces to retention at other temperatures. Where different solvents are involved, the capacities for individual intermolecular interactions are unlikely to change in a proportionate manner with temperature. Thus some indication of changes in the solvation properties of a stationary phase as a continuous function of temperature is needed.

To shed some light on both of the above issues we have designed a study to define the general effect of temperature on the retention mechanism and the solvation process for a group of ten liquid stationary phases representing a wide range of solvent properties and a varied group of solutes representing an equally diverse range of solute size and polarity. To make the study realistic we have attempted to cover the widest possible temperature range over which individual solutes could be studied while still exhibiting acceptable chromatographic behavior. Experimentally it was determined that a 60°C temperature range was the maximum that could be explored if the extrapolation method was used to determine gas–liquid partition coefficients since a fairly wide range of phase loadings must be available to minimize the error in fitting the data to Eq. 1. The collection of experimental data was commenced using approximately 70 varied solutes from which about 46 gave acceptable retention properties on all stationary phases at all temperatures. These compounds are identified in Table 2. Two factors dictated the choice of temperature region employed. Solute–solvent intermolecular interactions should contribute more significantly to the retention process at lower temperatures and be more readily distinguished. Secondly, the model used to interpret the solution properties of the solutes uses squalane as a non-polar reference solvent and is constrained by the range of temperatures over which this solvent can be used. This is not a fundamental problem with the model and the change to another less volatile hydrocarbon solvent such as Apolane-87 would eliminate many of the deficiencies of squalane in future studies [4,43]. For the present we have continued to use squalane because of its connection to earlier studies so as to provide consistency in model evaluations and have accepted an upper temperature limit for its use of 120°C.

In this particular study it was necessary to make some compromises to create a complete data set with no missing entries for chemometric analysis. The most significant was that to calculate some solvent properties it was necessary to estimate partition coefficients for squalane at 141.2°C (Table 3). This was done by extrapolating experimental data from lower temperatures to the required temperature as explained in the experimental section. This data set should not be considered as reliable as the experimental data and we have only used it to illustrate general trends. Also, we used the solvation parameter model to calculate the gas–liquid partition coefficients for some solutes that had very long retention times on some phases at the lowest temperature extreme used for data acquisition. These values are less questionable and an estimate of the uncertainty in the data can be made as indicated in the experimental section. The number of solutes requiring this treatment are few in number and are collected in Table 4.

The effect of temperature on the retention mechanism can be deduced from the difference

in the specific retention volume calculated experimentally and the specific retention volume obtained from the gas–liquid partition coefficient. For any solute retained totally by gas–liquid partitioning the two values should agree within experimental error; where the two values differ the difference represents the contribution from interfacial adsorption. As well as temperature the relative contribution of absorption and interfacial adsorption will depend on the surface area to volume ratio of the stationary liquid phase, which can be demonstrated qualitatively by observing differences in the contributions to the retention mechanism as a function of the phase loading. All measurements made in this report are for a single batch of support and thus the surface area is fixed but unknown. For supports with different surface areas the contribution of interfacial adsorption to the retention mechanism is expected to vary directly with the surface areas of the support and coated liquid and the accessible liquid surface area to depend on the phase loading, since the support structure is comprised of a heterogeneous array of pores with different volumes. These pores are filled with liquid to different extents and at no time is the liquid surface area likely to be identical to the support surface area. Also the liquid surface area is expected to decline in a non-linear manner with the phase loading being largest at low phase loadings and then falling to an asymptotic value as high phase loadings are reached. Even if the fine details of the above assumptions are not known exactly there is ample evidence to support them, although accurate determinations of liquid surface areas in gas–liquid chromatography are few because of the technical problems in making such measurements [6,9,10,44].

The general trend observed for mixed retention mechanisms at a constant temperature is illustrated in Fig. 1 for the variation of the specific retention volume as a function of phase loading for dodecane at 121.2 and 81.2°C. The contribution of gas–liquid partitioning to the specific retention volume is constant while the experimental, and by difference the contribution from interfacial adsorption, falls significantly with increasing phase loadings in the range 8 to

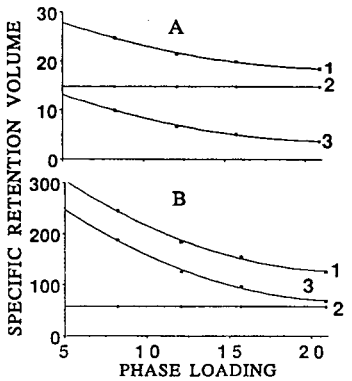

Fig. 1. Variation of the specific retention volume of dodecane as a function of phase loading for poly(diethylene glycol succinate) on Chromosorb W AW at 121.2°C (A) and 81.2°C (B). The experimental specific retention volume is designated as 1, the contribution to the experimental specific retention volume from gas–liquid partitioning as 2, and the contribution from interfacial adsorption to the experimental specific retention volume as 3.

22% (w/w). High phase loadings diminish the contribution from interfacial adsorption because the surface area of the liquid phase is diminished with respect to the increase in the volume of the bulk liquid. The contribution of interfacial adsorption will never fall to zero, however, when it is an intrinsic element of the retention mechanism, since the surface area will never fall to effectively zero with the mechanical constraints set by the available phase loadings for typical columns. Different phases may wet the support surface differently, and therefore, it cannot be assumed that at a constant phase loading the liquid surface area is constant. At a high phase loading the variation in surface area may not be great but it does mean that any further comparison of the interfacial adsorption properties of different phases, even at similar phase loadings, have to be viewed as qualitative. Also striking from Fig. 1 is the influence of temperature on the retention mechanism. For dodecane at 81.2°C on DEGS interfacial adsorption is the dominant retention mechanism, with a strong dependence on the phase loading, while at 121.2°C gas–liquid partitioning is the dominant retention mechanism accompanied by a significant contribution from interfacial adsorption.

Temperature and phase loading simultaneously affect the relative contribution of the individual retention mechanisms when solutes are retained by a mixed retention mechanism. Since we can predict the absorption component of the retention mechanism more reliably than the adsorption component it is important to note that higher temperatures and higher phase loadings favor the gas-liquid partition mechanism over the contribution from interfacial adsorption.

The effect of temperature on the retention mechanism for two phases with a fixed phase loading is shown in Fig. 2. In both cases interfacial adsorption is significant at the lowest temperatures but as the temperature increases its contribution to the retention mechanism decreases until eventually it becomes essentially zero. This is a general phenomena observed for all compounds in the data set which are retained by a mixed retention mechanism at some temperature. There always seems to be a higher temperature at which they are retained virtually exclusively by gas-liquid partitioning.

For members of a homologous series, such as

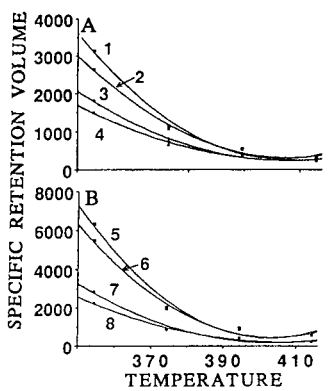

Fig. 2. Relation between temperature and the specific retention volume for four compounds at a fixed phase loading. In (A) results are shown for benzonitrile experimental (1), the contribution of gas–liquid partitioning to the retention of benzonitrile (2), benzaldehyde experimental (3) and the contribution of gas–liquid partitioning to the retention of benzaldehyde (4) on TCEP (11.94%, w/w). In (B) the results are shown for benzodioxane experimental (5), the contribution of gas–liquid partitioning to the retention of benzodioxane (6), octan-1-ol experimental (7) and the contribution of gas–liquid partitioning to the retention of octan-1-ol (8) on CW-20M (13.21%, w/w). Temperature in K.

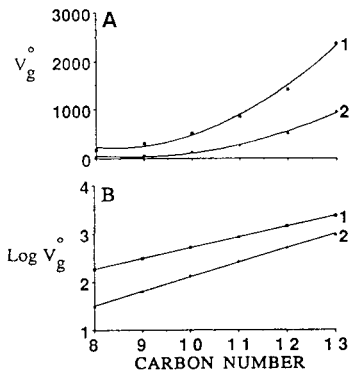

Fig. 3. Relation between chain length and the retention mechanism for members of a homologous series: the retention of fatty acid methyl esters at 81.2°C on TCEP 8.01% (w/w). In (A) the data are plotted in numerical format and (B) as the logarithm of the specific retention volume. The contribution of gas–liquid partitioning to retention is designated as 1 and interfacial adsorption as 2.

the fatty acid methyl esters illustrated in Fig. 3, the numerical contribution of the adsorption component to retention when a mixed retention mechanism occurs, increases with increasing carbon number. When plotted in logarithmic form two lines with different slopes are obtained for the adsorption and partition contribution to the retention mechanism indicating that at a constant temperature and phase loading increasing the chain length causes a proportional incremental increases in the adsorption contribution to the retention mechanism. This also explains why plots of the logarithm of the experimental specific retention volume as a function of the carbon number for a homologous series remain linear even when retention occurs by a mixed retention mechanism.

The above three illustrations serve to demonstrate the effect of temperature on the retention mechanism when an individual solute is retained by a mixed retention mechanism. It is not as easy to create a general sense of the importance of interfacial adsorption as a retention mechanism since the conditions of retention are a highly individualized matter. In Table 5 we have summarized the relative contribution of interfacial adsorption to the retention of 12 varied compounds on 10 phases under different experimen-

Table 5
Contribution of interfacial adsorption (%) to the retention of some typical solutes on 10 stationary phases at two temperatures

Compound	Stationary phase									
	SQ	OV-105	OV-17	OV-225	QF-1	CW-20M	THPED	QPTS	TCEP	DEGS
	Phase loading (%)									
	15.5	16.0	16.1	15.4	16.0	20.7	16.5	15.9	16.0	15.7
Temperature 81.2°C										
Tridecane	7.0	2.9	2.3	1.9	2.3	23.0	2.6	3.2	47.9	66.3
Oct-2-yne	7.8	3.5	2.1	7.0	2.9	11.9	5.0	6.0	8.3	32.3
Methyl octanoate	8.1	3.7	2.0	4.6	2.6	10.9	3.1	4.9	10.2	26.5
Heptan-2-one	8.6	3.3	1.4	6.7	2.8	7.2	5.8	5.3	3.9	9.5
Heptan-1-ol	15.5	4.5	2.3	6.0	5.5	8.9	0.7	2.1	5.2	14.7
Ethylbenzene	8.1	3.9	2.2	11.1	3.6	6.6	4.7	3.9	12.0	15.2
Acetophenone	8.1	5.6	2.1	13.7	4.0	6.1	2.3	5.1	14.9	33.1
Benzonitrile	7.8	5.6	2.1	12.2	3.9	7.2	14.7	5.4	16.0	37.1
Nitrobenzene	7.5	5.9	2.0	12.8	4.1	–	6.3	–	18.4	43.4
N-Methylaniline	11.4	6.0	2.1	27.3	5.4	–	4.4	–	19.2	38.8
N,N-Dimethylaniline	8.0	5.6	2.1	14.1	4.1	5.0	13.5	5.5	17.2	34.6
Dioxane	9.2	4.4	3.5	9.1	1.7	4.9	14.4	5.9	0.2	6.6
Temperature 121.2°C										
Tridecane	1.5	5.4	0.6	6.3	1.7	4.5	3.7	4.5	21.7	26.9
Oct-2-yne	2.1	4.2	0.6	0.6	6.0	5.9	4.3	3.5	7.1	11.2
Methyl octanoate	0.9	6.0	0.4	6.0	1.9	3.7	3.3	2.4	1.9	7.3
Heptan-2-one	1.0	5.4	0.8	3.9	2.3	1.8	4.3	2.9	3.3	7.0
Heptan-1-ol	2.6	4.1	0.6	10.8	2.3	1.9	0.5	3.0	2.0	6.6
Ethylbenzene	2.8	5.1	0.8	4.2	3.2	4.7	2.4	1.6	12.5	11.4
Acetophenone	2.3	5.2	0.8	2.3	1.9	4.0	2.3	2.6	1.2	7.5
Benzonitrile	2.6	5.7	0.6	3.0	1.7	2.9	15.5	2.7	1.2	5.3
Nitrobenzene	2.8	5.4	0.2	1.4	1.8	3.5	6.4	2.7	2.0	2.8
N-Methylaniline	3.1	5.5	0.6	2.1	1.9	2.7	4.4	1.6	0.6	8.4
N,N-Dimethylaniline	2.5	5.4	0.5	5.5	1.9	2.1	8.2	2.8	2.8	12.5
Dioxane	1.2	4.1	0.9	3.2	4.7	2.3	10.0	3.7	0.6	11.8

tal conditions. The relative contribution of interfacial adsorption being calculated as indicated by Eq. 6. The typical uncertainty in V_g^0(part) is about 3% R.S.D. [24]. V_g^0(exp) is obtained from a single phase loading and probably has a greater uncertainty than V_g^0(part). The cumulative uncertainty in the relative contribution of interfacial adsorption is about 4 to 5%. Thus, entries in Table 5 for the interfacial adsorption that are less than 5% are unlikely to be significant. In this context it can be seen that gas–liquid partition is the dominant retention mechanism for all solutes on all phases except for the hydrocarbon *n*-tridecane on TCEP and DEGS. At 81.2°C interfacial adsorption makes a significant contribution to the retention of several solutes on SQ, OV-225 (aromatic compounds), CW-20M (aliphatic compounds), THPED (benzonitrile and dioxane), and most solutes on TCEP and DEGS. At 121.2°C interfacial adsorption for the same compounds on the same columns is less significant, in general, but still contributes to the retention of benzonitrile and dioxane on THPED, tridecane, oct-2-yne and ethylbenzene on TCEP, and most solutes on DEGS. These results show that a partition model could be used selectively to predict the retention properties of certain solutes on a group of phases with acceptable accuracy.

The most likely failure would be the prediction of the retention properties of compounds of low polarity on polar phases, particularly at low temperatures.

To complement the data in Table 5 we have prepared a rough summary in Table 6 of our results obtained from a number of experiments reported here the elsewhere [4,41] as an aid to predicting those experimental conditions where interfacial adsorption is most likely to be a significant retention mechanism.

We now wish to discuss the influence of temperature on the solvation mechanism for the gas–liquid partition component of the retention mechanism using Eq. 3 as our model. Eq. 3 allows deconvolution of the solvation mechanism into two terms characterized as the cavity–dispersion contribution to solvation, representing the formation of a cavity in the solvent of sufficient size to hold the solute and the formation of dispersion interactions between the solute and solvent when the solute is placed into the cavity, and the sum of the polar interactions that result from solute–solvent interactions in excess of those characterized as dispersion when the solute is placed in the cavity. The general trends in the above processes can be illustrated by typical plots of the free energy terms contributing to the solvation process as a function of temperature. These are similar for all solutes and solvents studied in this work so we will choose two examples for the extremes of the polarity range as representative cases: the solvation of a weakly polar (*n*-butylbenzene) and a polar solute (1-nitrohexane) by a moderately polar (OV-17) and a polar stationary phase (TCEP). It is the general case that increasing temperature results in a less favorable solution free energy for all solutes and, therefore, a decrease in retention. For *n*-butylbenzene and 1-nitrohexane on OV-17 the cavity-dispersion term is the dominant contribution to the total solution free energy (Fig. 4). The polar interactions term makes a smaller contribution to the total solution free energy which, as would be predicted, is numerically larger for 1-nitrohexane than for *n*-butylbenzene. For *n*-butylbenzene and 1-nitrohexane on TCEP the cavity–dispersion contribution and the contribution from polar interactions to the total solution free energy are now of comparable magnitude due to an increase in the contribution of the polar interactions term and a decrease in the contribution from the cavity–dispersion term compared to the previous data for OV-17 (Fig.

Table 6
Summary of factors that affect the relative contribution of interfacial adsorption to the retention mechanism

1 At intermediate column temperatures, around 100°C, gas–liquid partitioning is the dominant retention mechanism for most compounds on all stationary phases.
2 When the retention mechanism is characterized as a mixed retention process interfacial adsorption increases in importance at lower temperatures.
3 Interfacial adsorption makes a greater contribution to the retention mechanism at lower phase loadings due to a combination of a larger accessible liquid surface area and a smaller bulk liquid volume.
4 When interfacial adsorption makes a significant contribution to the retention mechanism its contribution at constant temperature will never reach zero at any phase loading since mechanical constaints dictate the largest phase loading which can be used. For packed columns a significant residual liquid surface area remains at the highest practical phase loadings possible.
5 For non-polar phases interfacial adsorption can generally be related to support properties, and at intermediate column temperatutres it can usually be eliminated on adequately deactivated supports. For polar compounds at low temperatures a small contribution from adsorption at the gas–liquid interface may be observed.
6 Non-polar solutes such as hydrocarbons exhibit the greatest potential for interfacial adsorption on polar stationary phases. Simple aromatic compounds are far less influenced by the polarity of the stationary phase than are saturated hydrocarbons with a similar carbon number.
7 Interfacial adsorption is usually most significant for all compounds on highly cohesive stationary phases which includes TCEP, DEGS, THPED, OV-275, poly(ethylene glycol adipate), and the liquid organic salts tetra-*n*-butylammonium N,N-(bis-2-hydroxyethyl)-2-aminoethanesulfonate, 3-tris(hydroxymethyl)methylamino-2-hydroxy-1-propanesulfonate and 2-(2-acetamido)aminoethanesulfonate.

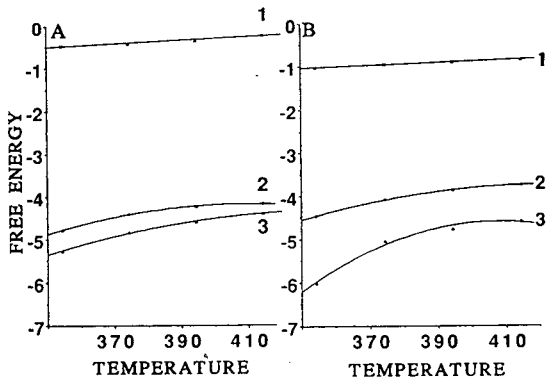

Fig. 4. Plot of the contributions from the polar interactions term (1) and the cavity–dispersion term (2) to the total solution free energy (3) for *n*-butylbenzene (A) and 1-nitrohexane (B) on OV-17 as a function of temperature (in K).

5). Within the constraints of the model the formation of dispersion interactions associated with the transfer of the solute from the gas phase (where ideal behavior is assumed) to solution must exceed the free energy required to form a cavity in the solvent of the same size as the solute since the cavity–dispersion term is always favorable for transfer. The cavity contribution is reflected in the magnitude of the cavity–dispersion term which is always less favorable for polar cohesive solvents, such as TCEP, DEGS and QPTS than for weak solvents, such as OV-105 and OV-17.

In general, the cavity–dispersion term shows the largest numerical change as a function of temperature, makes a less favourable contribution to solvation at higher temperature, and tends to show a smaller numerical variation between the experimental data points at higher temperatures (at least for the temperature range over which the data was collected). By comparison the contribution from the polar interactions term is less affected by temperature over the same temperature range exhibiting, usually, a small shallow decline (contribution to the solvation process becoming less favorable) at higher temperatures, although in a few cases the opposite behavior was observed.

For members of a homologous series the total solution free energy and the contribution to the total solution free energy from the cavity–dispersion term increase incrementally with carbon number while the free energy contribution attributable to the polar interactions term is nearly constant by comparison and not strongly influenced by temperature over the temperature range studied. This is illustrated for the alkan-2-ones (Fig. 6) and the *n*-alcohols (Fig. 7), at 81.2 and 121.2°C on the stationary phase of intermediate polarity CW-20M. The increasingly favorable contribution to the total solution free energy with increasing carbon number for the two series of homologues is due almost entirely to an increasingly favorable contribution from

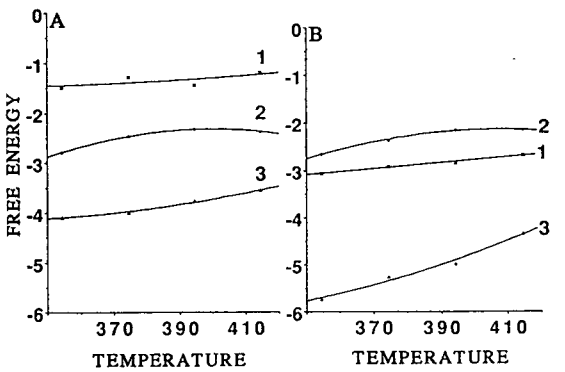

Fig. 5. Plot of the contributions from the polar interactions term (1) and the cavity–dispersion term (2) to the total solution free energy (3) for *n*-butylbenzene (A) and 1-nitrohexane (B) on TCEP as a function of temperature (in K).

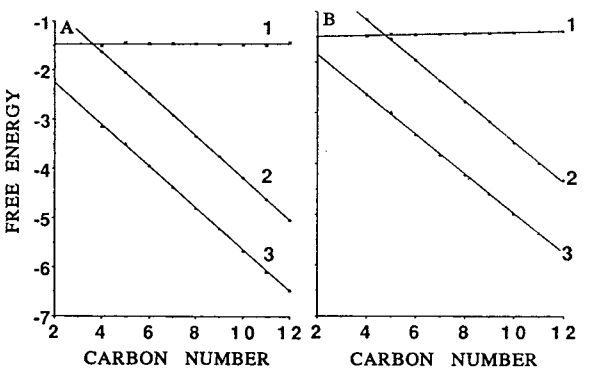

Fig. 6. Plot of the contributions from the polar interactions term (1) and the cavity–dispersion term (2) to the total solution free energy (3) for a homologous series of alkan-2-ones on CW-20M at 81.2°C (A) and 121.2°C (B).

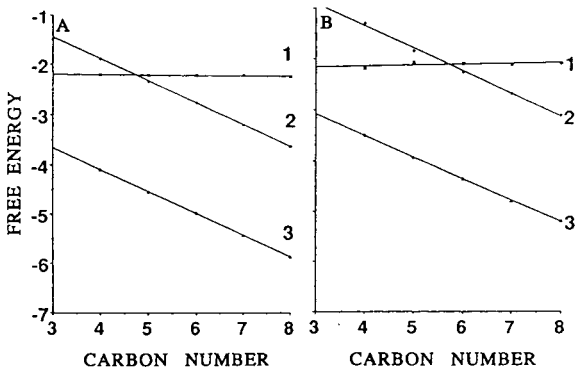

Fig. 7. Plot of the contributions from the polar interactions term (1) and the cavity–dispersion term (2) to the total solution free energy (3) for a homologous series of *n*-alcohols on CW-20M at 81.2°C (A) and 121.2°C (B).

the cavity–dispersion term. In turn this indicates that even for the most polar stationary phases studied here the contribution from dispersion interactions accompanying each incremental increase in the molecular volume of the homologs exceeds the free energy required to expand the cavity in the solvent by the same amount. The polar interactions contribution to the free energy of solution depends only on the identity of the polar functional group in the molecule and is sensibly independent of molecular size as demonstrated by the experimental data.

To provide further insight into the factors contributing to the solvation process principal component analysis was performed on the contributions to the solvation process previously characterized as the cavity–dispersion term and the polar interactions term. The cavity–dispersion term is characterized by a single component with greater than 99.7% of the total variance at all temperatures accounted for by this factor (Table 7). The contribution to the solvation process of the free energy required to open a cavity in the solvent and the subsequent contribution to the solvation process from solute-solvent dispersion interactions must be correlated. Logic dictates that the parameter connecting the two terms must be a size-related parameter such as the solute volume or a volume-dependent term such as the solvent-accessible surface area. A plot of the first principal component (PC-1) for all phases as a function of temperature is shown in Fig. 8. The general trend is for PC-1 to be numerically smaller at higher temperatures and to vary less at the highest temperatures used

Table 7
Summary of principal component analysis of the cavity–dispersion contribution to the solvation process

Temperature (°C)	Principal component number	Variance (%)	Number of phases
61.2	1	99.986	3
	2	0.014	
81.2	1	99.896	9
	2	0.089	
	3	0.015	
101.2	1	99.833	9
	2	0.153	
	3	0.014	
121.2	1	99.833	9
	2	0.147	
	3	0.020	
141.3	1	99.758	6
	2	0.213	
	3	0.029	

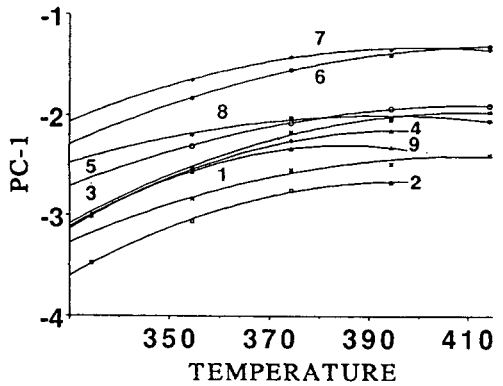

Fig. 8. Plot of the first principal component (PC-1) from the multivariate analysis of the contribution of the cavity–dispersion term to solvation fro nine stationary phases as a function of temperature. Identification: 1 = OV-17; 2 = OV-105; 3 = OV-225; 4 = QF-1; 5 = CW-20M; 6 = DEGS; 7 = TCEP; 8 = QPTS; 9 = THPED. Temperature in K.

to collect the data compared to the lower temperatures. At all temperatures PC-1 is numerically larger for the weakly polar phases such as OV-105 and OV-17 (with a more favorable contribution to the solvation process) than for the strongly polar phases such as TCEP and DEGS.

Principal component analysis of the contribution previously characterized as the polar interactions term reveals that three factors are important in describing the contributions of this term to the solvation process. The first component (PC-1) is dominant accounting for 95 to 99% of the total variance; the second component (PC-2) for about 1 to 5% of the total variance: and the third component (PC-3) for about 0.1 to 0.7% of the total variance over the temperature range used to acquire the experimental data (Table 8). Based on the following considerations we believe that PC-1 can be assigned to the capacity of a phase to enter into dipolar interactions characterized as orientation and induction. Whereas all phases have some capacity for these interactions, albeit small in some cases, other polar interactions such as hydrogen bonding are more specific and, therefore unlikely to be uni-

Table 8
Summary of principal component analysis of the polar interaction contribution to the solvation process

Temperature (°C)	Principal component number	Variance (%)	Number of phase
61.2	1	95.004	3
	2	4.788	
	3	0.212	
	4		
81.2	1	98.059	9
	2	1.133	
	3	0.703	
	4	0.063	
101.2	1	98.154	9
	2	1.113	
	3	0.625	
	4	0.068	
121.2	1	98.112	9
	2	1.085	
	3	0.700	
	4	0.043	
141.2	1	98.946	6
	2	0.806	
	3	0.170	
	4	0.052	

versal, as are the properties identified in PC-1. A summary of the loadings for each compound in the data set (the complementary solute property to the stationary phase property obtained by multivariate analysis) is given in Table 9. Qualitatively, those compounds expected to have significant dipole interactions have the most significant weighting and those compounds with little capacity for dipole interactions are found at the base of the table. A plot of the loadings against the dipole moment for the solutes (excluding those solutes which are self-associating, *e.g.* *n*-alcohols) shows good qualitative agreement in terms of trends even if extensive scatter exists around the best straight line (Fig. 9). This is not unexpected since the dipole moment values used for the plot are rough averages of several values from different solvents. Also, the bulk dipole moments may not accurately express the influence of the local dipole moment in determining solute–solvent interactions. Further, it could be argued that the dipole moment is not a free energy-related term and is not clearly

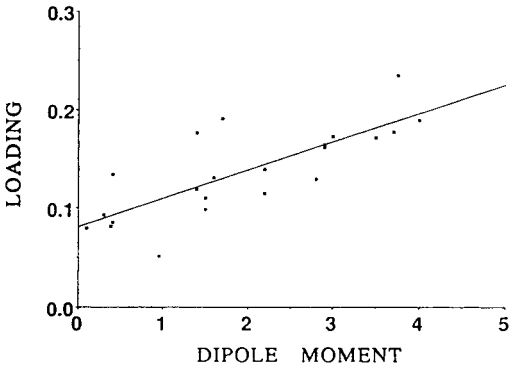

Fig. 9. Plot of the loadings for PC-1 at 101.2°C obtained by multivariate analysis of the contribution of the polar interactions term to solvation as a function of the solute dipole moment.

Table 9
Summary of loadings for principal component 1 based on the polar interaction contribution of the solvation process at 101.2°C

Compound	Loading	Compound	Loading
N,N-Dimethylacetamide	0.236	Methyl octanoate	0.132
Aniline	0.227	Hexan-2-one	0.132
N-Methylaniline	0.191	N,N-Dimethylaniline	0.131
Benzonitrile	0.190	Methyl heptanoate	0.131
Octan-1-ol	0.188	Butan-2-one	0.130
Hexan-1-ol	0.184	Pentan-2-one	0.130
Heptan-1-ol	0.184	Methyl hexanoate	0.130
Pentan-1-ol	0.182	Nonanal	0.124
Butan-1-ol	0.181	2,4,6-Trimethylpyridine	0.121
Nitrobenzene	0.178	Iodobenzene	0.120
Nitrohexane	0.176	Methylphenyl ether	0.120
1,1,2,2-Tetrachloroethane	0.176	*o*-Dichlorobenzene	0.115
Nitropropane	0.173	Bromobenzene	0.110
Nitropentane	0.172	Chlorobenzene	0.098
Acetophenone	0.165	Toluene	0.093
Benzaldehyde	0.162	*n*-Butylbenzene	0.085
Nitrocyclohexane	0.158	Ethylbenzene	0.081
2-Methylpentan-2-ol	0.151	Benzene	0.079
Pyridine	0.139	Dodec-1-yne	0.076
Dodecane-2-one	0.139	Oct-2-yne	0.051
Nonan-2-one	0.135		
Undecan-2-one	0.134		
Dioxane	0.134		
Octan-2-one	0.133		
Dodecan-2-one	0.133		
Heptan-2-one	0.133		

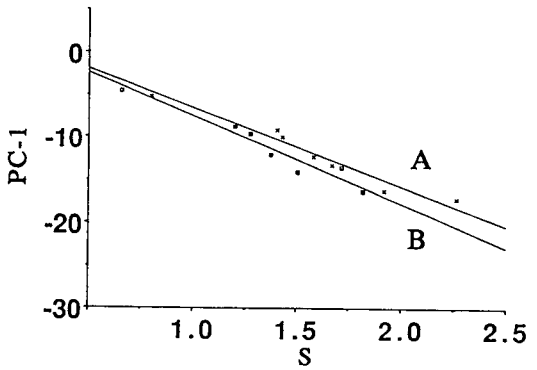

Fig. 10. Plot of PC-1 at 81.2°C (A) and 121.2°C (B) against the *s* parameter of Abraham and co-workers characteristic of solvent dipolarity/polarizability.

compatible with the properties of PC-1. A more significant correlation is found between PC-1 and the *s* coefficient of Abraham and co-workers defined in Eq. 2 (Fig. 10). The *s* coefficient is a measure of a solvent's capacity for dipole–dipole and dipole–induced dipole interactions and is established by an independent scale of solute properties. With the exception of the fluorocarbon phase QF-1, there is good agreement between the two properties at all temperatures with correlation coefficients (r^2) > 0.98.

The loading factors for the second principal component (PC-2) are summarized in Table 10. The large negative values in the table are associated with solutes capable of interacting as hydrogen-bond acids and the large positive values as solutes that can interact as hydrogen-bond bases. A large number of compounds in the center of the table have very small loading values indicting that PC-2 is a selective parameter that is not possessed to a significant extent by all compounds. It sees reasonable to identify PC-2 with the capacity of a stationary phase to form a hydrogen bond by acting as a hydrogen-bond

Table 10
Summary of loading for principal component 2 based on the polar interaction contribution to the solvation process at 101.2°C

Compound	Loading	Compound	Loading
Aniline	−0.249	Benzonitrile	0.022
Butan-1-ol	−0.222	Nitrocyclohexane	0.055
Pentan-1-ol	−0.217	Dioxane	0.070
N-Methylaniline	−0.214	Nitropropane	0.125
Hexan-1-ol	−0.211	Nitropentane	0.141
Heptan-1-ol	−0.208	Butan-2-one	0.142
Octan-1-ol	−0.199	Nonanal	0.143
Iodobenzene	−0.199	Pentan-2-one	0.157
1,1,2,2-Tetrachloroethane	−0.178	Nitrohexane	0.157
Bromobenzene	−0.127	Hexan-2-one	0.169
o-Dichlorobenzene	−0.127	Heptan-2-one	0.169
2-Methyl-2-pentanol	−0.118	Methyl hexanoate	0.178
Chlorobenzene	−0.101	Octan-2-one	0.183
Ethylbenzene	−0.077	Decan-2-one	0.184
Benzene	−0.049	Methyl heptanoate	0.184
Methylphenyl ether	−0.047	Nonan-2-one	0.187
Toluene	−0.046	Undecan-2-one	0.191
N,N-Dimethylaniline	−0.044	Methyl octanoate	0.196
Nitrobenzene	−0.031	N,N-Dimethylacetamide	0.200
Dode-1-yne	−0.029	Dodecan-2-one	0.217
Benzaldehyde	−0.028		
n-Butylbenzene	−0.023		
Acetophenone	−0.014		
2,4,6-Trimethylpyridine	−0.010		
Oct-2-yne	−0.009		
Pyridine	−0.005		

acid or hydrogen-bond base. In making this determination the position of the halobenzene compounds as moderate hydrogen-bond acids would seem to be slightly displaced based on general expectations.

The loading factors for the third principal component (PC-3) are summarized in Table 11. The large negative values are associated with the aliphatic alcohols and the large positive values with the aromatic components. PC-3 is perhaps characteristic of the capacity of a phase to form charge-transfer complexes involving π-electrons, a property that distinguishes the aromatic compounds from the aliphatic compounds in the data set. The large negative weighting of the alcohols suggests that mixed in with this mechanism is residual capacity of the alcohols to form hydrogen-bond complexes since the other aliphatic compounds have much smaller loading values than those for the alcohols. Thus to get an accurate picture of the hydrogen-bond base properties of the stationary phases it is necessary to consider properties of PC-2 and PC-3 together. A factor which may contribute to the ambiguous identification of the hydrogen-bonding capacity of the stationary phases is that none of the phases studied here are strong hydrogen-bond acids, and indeed, there are no common stationary phases in current use that have been identified as strong hydrogen-bond acids [4,26,29,34,39,40]. These features are born out by inspecting the loadings plot for PC-2 against PC-3 (Fig. 11). The solutes in the data set are separate into three major groups. Group 1 contains all the aliphatic alcohols (non-aromatic, hydrogen-bond acids). Group 2 contains the alkan-2-ones, fatty acid methyl esters, nitroalkanes, N,N-dimethylacetamide and nonanal (non-aromatic, hydrogen-bond bases). Group 3 is more diffuse than the other two groups and

Table 11
Summary of loading for principal component 3 based on the polar interaction contribution to the solvation process at 101.2°C

Compound	Loading	Compound	Loading
Octan-1-ol	−0.277	Nitrocyclohexane	0.031
Hexan-1-ol	−0.270	N-Methylaniline	0.059
Butan-1-ol	−0.269	Benzonitrile	0.062
Pentan-1-ol	−0.257	Dioxane	0.097
Heptan-1-ol	−0.254	Nitrobenzene	0.107
2-Methyl-2-pentanol	−0.192	Pyridine	0.121
N,N-Dimethylacetamide	−0.077	Oct-2-yne	0.137
Nitrohexane	−0.065	Toluene	0.160
Undecan-2-one	−0.058	Acetophenone	0.165
Dodecan-2-one	−0.058	Benzaldehyde	0.165
Nonan-2-one	−0.053	Ethylbenzene	0.168
Nitropentane	−0.050	Chlorobenzene	0.170
Decan-2-one	−0.048	2,4,6-Trimethylpyridine	0.170
Octan-2-one	−0.042	Benzene	0.174
Heptan-2-one	−0.034	Methylphenyl ether	0.184
Hexan-2-one	−0.032	*n*-Butylbenzene	0.196
Nitropropane	−0.030	Bromobenzene	0.211
Pentan-2-one	−0.021	*o*-Dichlorobenzene	0.216
Nonanal	−0.017	N,N-Dimethylaniline	0.257
1,1,2,2-Tetrachloroethane	−0.016	Iodobenzene	0.303
Dodec-1-yne	−0.015		
Methyl octanoate	−0.014		
Aniline	−0.010		
Butan-2-one	−0.005		
Methyl heptanoate	−0.004		
Methyl hexanoate	0.001		

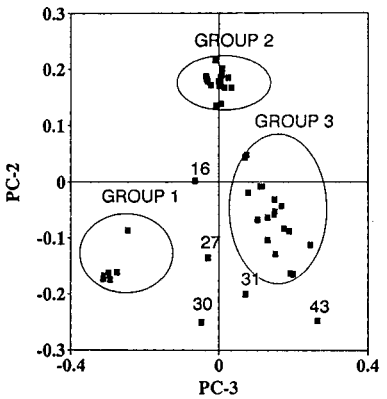

Fig. 11. Plot of the loadings for PC-2 against PC-3 extracted from the polar interactions term at 81.2°C. The compounds not assigned to a group are: 16 = dodec-1-yne; 27 = 1,1,2,2-tetrachloroethane; 30 = aniline; 31 = N-methylaniline; 43 = iodobenzene.

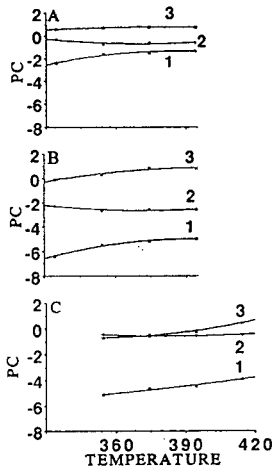

Fig. 12. Plot of the first three principal components extracted from the polar interactions term against temperature for the weakly polar phases OV-105 (A), QF-1 (B) and OV-17 (C). Temperature in K.

contains the aromatic compounds and oct-2-yne (compounds with a capacity for charge transfer interactions due to the presence of π-electrons). The weak hydrogen-bond acids dodec-1-yne, 1,1,2,2-tetrachloroethane, aniline and N-methylaniline are not assigned to any of the main groups reflecting their unusual mix of properties.

The trends in the principal components extracted from the contribution of the polar interactions term to the solvation process as a function of temperature provide some insight into how temperature influences the individual polar interactions identified in the above discussion. For the three phases, OV-105, OV-17 and QF-1, which on a relative basis have weak polar interactions, all three principal components are important to adequately define their properties (Fig. 12). OV-105, with the weakest capacity for polar interactions of the three phases, shows a sharp transition in properties in the low-temperature region. The magnitude of PC-1 is reduced sharply at first but then the decrease becomes shallower at higher temperatures. It posses a weak capacity for hydrogen-bonding and other complexation interactions which at the higher temperatures are not strongly temperature dependent. OV-17 has a modest capacity for orientation interactions (PC-1) which shows significant temperature dependence, being less influential at higher temperatures. Its capacity for hydrogen-bonding and complexation interactions (PC-2 and PC-3) are modest by comparison and decline with increasing temperature. QF-1 shows a unique blend of properties, a modest capacity for orientation interactions which declines with increasing temperature, significant capacity for hydrogen-bonding interactions (PC-2) which increases slightly with temperature, and a small contribution from PC-3 with weak temperature dependence.

The influence of temperature on the principal components extracted from the polar interactions term for the three moderately polar phases, OV-225, CW-20M and THPED is illustrated in Fig. 13. The properties of OV-225 and CW-20M are dominated by PC-1 which is only weakly temperature dependent. The capacity of both phases for hydrogen-bonding is weak (PC-2) and not strongly temperature dependent. Both phases have a weak capacity for complexation interactions (PC-3) but this is significantly more important for CW-20M than for OV-225. THPED shows different behavior; its properties are dominated by orientation interactions (PC-1) which shows a weak temperature dependence. Its capacity for hydrogen-bonding (PC-2) is significant at 61.2°C only. It retains a significant

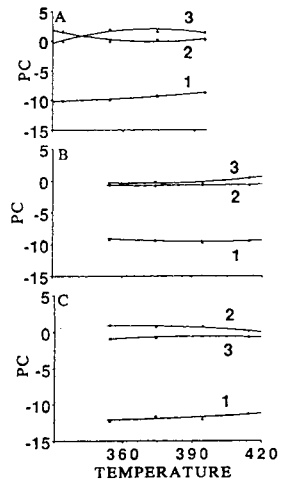

Fig. 13. Plot of the first three principal components extracted from the polar interactions term against temperature for the moderately polar phases THPED (A), OV-225 (B) and CW-20M (C). Temperature in K.

capacity for complexation interactions (PC-3) (which might be dominated by its hydrogen-bond basicity) at higher temperatures.

The influence of temperature on the principal components extracted from the polar interactions term for the three very polar phases, DEGS, TCEP and QPTS is illustrated in Fig. 14.

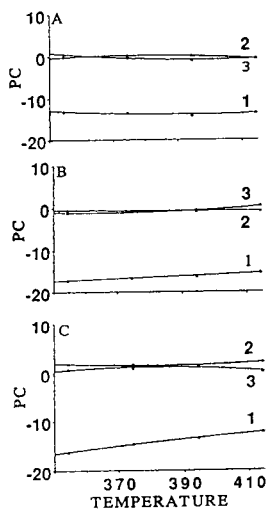

Fig. 14. Plot of the first three principal components extracted from the polar interactions term against temperature for the very polar phases DEGS (A), TCEP (B) and QPTS (C). Temperature in K.

In the case of DEGS its properties are dominated by its capacity for orientation interactions (PC-1) with only small contributions from PC-2 and PC-3. PC-1 for DEGS shows a slight temperature dependence with a slight increase in its magnitude at higher temperatures. The polar interactions of TCEP are again dominated by PC-1, which unlike DEGS shows a significant temperature dependence, declining in magnitude as the temperature is increased. PC-2 and PC-3 are small by comparison to PC-1 but are more significant than for DEGS. TCEP has a weak capacity for hydrogen-bonding and complexation interactions that is weakly temperature dependent. QPTS has a unique blend of properties compared to the other phases. Its general polar interactions are dominated by orientation interactions (PC-1) which are strongly temperature dependent, exhibiting the largest numerical change in value as a function of temperature. Hydrogen-bonding interactions (PC-2) are also significant for this phase and are only weakly temperature dependent.

The above studies provide some insights into the mechanisms by which compounds are retained in gas chromatography and their temperature variation. Gas–liquid partitioning is the major retention mechanism for most compounds. Mixed retention mechanisms are of importance when the stationary phase is unable to mask support activity and when there is a significant difference in the polarity between the solute and the stationary phase. Interfacial adsorption at the gas–liquid interface depends on both the stationary phase loading and the column temperature. The general influence of temperature is for higher temperatures to diminish the contribution to retention from interfacial adsorption. A cavity model of solvation behavior was used successfully to probe the influence of temperature on the intermolecular interactions responsible for solution. The contribution of the cavity–dispersion term to the free energy of solution showed significant temperature dependence and was always more favorable for solvation at lower temperatures. Even for the most polar phases this term remained favorable for solute transfer from the gas phase emphasizing

the importance of dispersion interactions in the solution behavior of even the most polar stationary phases. The polar interactions term is much more important in the solution behavior of polar compounds in polar stationary phases where it approaches or exceeds in magnitude the contribution to the total free energy of solution from the cavity–dispersion term. In the general case it is only weakly temperature dependent in the temperature range investigated. By principal component analysis it was shown that three contributing factors are required to analyze the properties of the polar interactions term as a function of temperature. The major component (PC-1) was identified with the capacity of the stationary phase for orientation and induction interactions and, with the exception of QPTS, was only weakly temperature dependent. The second and third principal components were tentatively identified with the capacity of the stationary phase to form hydrogen bond and π-electron complexation interactions. These interactions were most important in characterizing the properties of QF-1 and QPTS and were moderately temperature dependent being less effective at higher temperatures in influencing the solvation behavior of compounds with the necessary complementary properties for the interactions specified.

4. References

[1] C.F. Poole and S.K. Poole, *Chromatography Today*, Elsevier, Amsterdam, 1991.
[2] G. Guiochon and C.L. Guillemin, *Quantitative Gas Chromatography for Laboratory Analysis and On-Line Process Control*, Elsevier, Amsterdam, 1988.
[3] J.R. Conder and C.L. Young, *Physicochemical Measurement by Gas Chromatography*, Wiley, New York, 1979.
[4] C.F. Poole, T.O. Kollie and S.K. Poole, *Chromatographia*, 34 (1992) 281.
[5] M.H. Abraham, P.L. Grellier, I. Hamerton, R.A. McGill, D.V. Prior and G.S. Whiting, *Faraday Discuss. Chem. Soc.*, 85 (1988) 107.
[6] C.F. Poole and S.K. Poole, *Chem. Rev.*, 89 (1989) 377.
[7] B.R. Kersten and C.F. Poole, *J. Chromatogr.*, 399 (1987) 1.
[8] J.A. Jonsson, *Chromatographic Theory and Basic Principles*, Marcel Dekker, New York, 1987.
[9] V.G. Berezkin, *Gas–Liquid–Solid Chromatography*, Marcel Dekker, New York, 1991.
[10] R.L. Martin, *Anal. Chem.*, 33 (1961) 347.
[11] J.R. Condor, D.C. Locke and J.H. Purnell, *J. Phys. Chem.*, 73 (1969) 700.
[12] D.F. Cadogan, J.R. Condor and J.H. Purnell, *J. Phys. Chem.*, 73 (1969) 708.
[13] F. Riedo and E. sz. Kováts, *J. Chromatogr.*, 186 (1979) 47 and 63.
[14] H.-L. Liao and D.E. Martire, *Anal. Chem.*, 44 (1972) 498.
[15] R.N. Nikolov, *J. Chromatogr.*, 241 (1982) 237.
[16] B.L. Karger and H.S. Liao, *Chromatographia*, 7 (1974) 288.
[17] E.L. Arancibia, R.C. Castells and A.M. Nardillo, *J. Chromatogr.*, 398 (1987) 21.
[18] R.C. Castells, A.M. Nardillo, E.L. Arancibia and M.R. Delfino, *J. Chromatogr.*, 259 (1983) 413.
[19] B.R. Kersten, C.F. Poole and K.G. Furton, *J. Chromatogr.*, 411 (1987) 43.
[20] B.R. Kersten and C.F. Poole, *J. Chromatogr.*, 452 (1988) 191.
[21] R.M. Pomaville and C.F. Poole, *J. Chromatogr.*, 468 (1989) 261.
[22] S.K. Poole, K.G. Furton and C.F. Poole, *J. Chromatogr. Sci.*, 26 (1988) 67.
[23] Y. Zhang, A.J. Dallas and P.W. Carr, *J. Chromatogr.*, 638 (1993) 43.
[24] S.K. Poole and C.F. Poole, *J. Chromatogr.*, 500 (1990) 329.
[25] K. Naito, Y. Watanabe and S. Takei, *J. Chromatogr.*, 604 (1992) 225.
[26] M.H. Abraham, J. Andonian-Haftvan, I. Hamerton, C.F. Poole and T.O. Kollie, *J. Chromatogr.*, 646 (1993) 351.
[27] H. Rotzsche, *Stationary Phases in Gas Chromatography*, Elsevier, Amsterdam, 1991.
[28] M.H. Abraham, G.S. Whiting, R.M. Doherty and W.J. Shuely, *J. Chem. Soc., Perkin Trans. 2*, (1990) 1451.
[29] M.H. Abraham, G.S. Withing, R.M. Doherty and W.J. Shuely, *J. Chromatogr.*, 518 (1990) 329.
[30] M.H. Abraham, G.S. Whiting, R.M. Doherty and W.J. Shuely, *J. Chromatogr.*, 587 (1991) 213, 229.
[31] M.H. Abraham and G.S. Whiting, *J. Chromatogr.*, 594 (1992) 229.
[32] J. Li, A.J. Dallas and P.W. Carr, *J. Chromatogr.*, 517 (1990) 103.
[33] J. Li, Y. Zhang, A.J. Dallas and P.W. Carr, *J. Chromatogr.*, 550 (1991) 101.
[34] J. Li, Y. Zhang and P.W. Carr, *Anal. Chem.*, 64 (1992) 210.
[35] T.O. Kollie and C.F. Poole, *J. Chromatogr.*, 550 (1991) 213.
[36] T.O. Kollie and C.F. Poole, *J. Chromatogr.*, 556 (1991) 457.
[37] T.O. Kollie and C.F. Poole, *Chromatographia*, 33 (1992) 551.

[38] M.H. Abraham, *Chem. Soc. Rev.*, 22 (1993) 73.
[39] C.F. Poole and T.O. Kollie, *Anal. Chim. Acta*, 282 (1993) 1.
[40] T.O. Kollie, C.F. Poole, M.H. Abraham and G.S. Whiting, *Anal. Chim. Acta*, 259 (1992) 1.
[41] B.R. Kersten, S.K. Poole and C.F. Poole, *J. Chromatogr.*, 468 (1989) 235.
[42] K.G. Furton and C.F. Poole, *J. Chromatogr.*, 399 (1987) 47.
[43] C.F. Poole, R.M. Pomaville and T.A. Dean, *Anal. Chim. Acta*, 225 (1989) 193.
[44] D.E. Martire, R.L. Pecsok and J.H. Purnell, *Faraday Soc. Trans.*, 61 (1965) 2496.

ELSEVIER

Journal of Chromatography A, 664 (1994) 253–261

JOURNAL OF CHROMATOGRAPHY A

Isotopic ratio of molecular patterns via gas chromatography–mass spectrometry with selected-ion monitoring as a chemometric tool

S. Musil*[,a], J. Leško[b]

[a]Drug Research Institute, Horná 36, 90001 Modra, Slovak Republic
[b]CHTF Slovak Technical University, Radlinského 9, 81237 Bratislava, Slovak Republic

(First received April 27th, 1993; revised manuscript received December 13th, 1993)

Abstract

Information on isotopic ratios for molecular fragment ions obtained via a chromatographic process is helpful for determining the elemental formulae of the components of an eluted mixture. It can be used in chemometric detectors to determine chlorine, bromine or sulphur. If the isotopic ratios are obtained from the whole mass spectra, the precision is not of much use for this purpose. More precise isotopic ratios were obtained with acquisition data in the selected-ion monitoring mode and use as statistics in a chemometric approach. The isotopic ratios vary with the chromatographic peak and they depend on the GC–MS acquisition conditions. These disadvantages may be removed by setting optimum acquisition parameters. The technique was verified on polychlorinated biphenyls.

1. Introduction

Compounds with biological activity, such as toxic compounds and drugs, are conveniently studied by combined gas chromatography–mass spectrometry (GC–MS). Low-resolution mass spectrometry for the analysis of organic compounds has been used for the determination of elemental compositions from the isotopic distributions of molecular ions [1–7].

Because isotopic ratios from the measurement of the whole mass spectra were used, the precision was not very useful for determining the number of C, H, N and O atoms in a molecule. Better results were obtained for chlorinated compounds [8–11], because the isotopic occurrences of heavier isotopic ions are higher than those of isotopic ions of compounds containing only C, H, N and O atoms. The precise measurement of isotopic ratios can be used for determining the numbers of chlorine atoms in measured ions. Worse results are obtained with compounds containing sulphur atoms, but in many instances it is possible to determine the number of atoms of sulphur in a molecule from the isotopic distribution [7].

There are a growing number of systems [9–11] using GC–MS analysis for determining the number of atoms of chlorine, bromine and sulphur in components of a complex mixture. They involve selective chromatographic detectors based on the computer analysis of GC–MS data. The first step is the GC–MS analysis of a complex mixture, which does not require selective detection, but it

* Corresponding author.

0021-9673/94/$07.00
SSDI 0021-9673(93)E1297-D

is necessary to use high-performance gas chromatography. The second step involves the selection of compounds containing chlorine, bromine or sulphur by the application of chemometric software to multivariate mass spectrometric data in the chromatographic process. The best results have been obtained for chlorinated compounds. LaBrosse and Anderegg [10] described four types of errors in chlorine-selective detection. Sulphur-selective detectors are not so successful [12], because contributions of sulphur to the $(M+2)^+$ ion interfere with the contributions of hydrogen, carbon, oxygen and nitrogen.

The purpose of this paper is to demonstrate how the observed isotopic intensities for the molecular and fragment ions are changed via chromatographic peaks. We believe that GC–MS with selected-ion monitoring (SIM) is the method of choice for improving the accuracy and precision of isotopic ratios and is better than acquiring data for the whole mass spectra (scan mode). The isotopic ratio observations were applied to the analysis of compounds that give molecular patterns, with high relative intensities [polychlorinated biphenyls (PCBs)]. Strategies for obtaining better accuracy of intensities and removing the experimental errors are discussed. Studies of some of the experimental factors affecting the measurement of relative intensities are reported.

2. Experimental

GC–MS analyses were made on Hewlett-Packard 5977B and 5988A GC–MS systems. A fused-silica column (30 m × 0.25 mm I.D., 0.25 μm) coated with DB-5 was used throughout all experiments. Splitless injection (250°C) was employed. The GC oven temperature programme was 2 min at 50°C increased at 20°C/min to 164°C and then at 4°C/min to 280°C. The carrier gas was helium at a linear velocity of 30 cm/s. The quadrupole mass spectrometer was operated in the electron impact (EI) mode. The ionizing voltage was 70 eV. Acquisition was done in the SIM mode. The selected ions were M^+, $(M+2)^+$, $(M+4)^+$, etc.

Delor 104 (a mixture of PCBs) was purchased from Slovak Metrological Institute (Bratislava, Slovak Republic). The individual PCB congeners were synthesized at the Drug Research Institute (Modra, Slovak Republic).

3. Results and discussion

The computer program RATIO for computing isotopic ratios in chromatographic processes was written in macroprogramming language on a PASCAL MS Chemstation, software version 3.1.1. It computes the ratio of isotopic ions to the ion with the highest intensity via chromatographic peaks.

The principle of the SIM process on quadrupole analysers (HP 5977B and HP 5988A) is illustrated in Fig. 1. Instead of scanning the whole mass spectra and recording information on all relative intensities, the quadrupole mass filter can be programmed to select a few specific m/z values for measurement. The "dwell" time is the amount of time spent monitoring a specific m/z value during SIM. The SIM scan cycle time is the time required to complete one SIM scan and begin another. Fig. 1 shows that the SIM scan

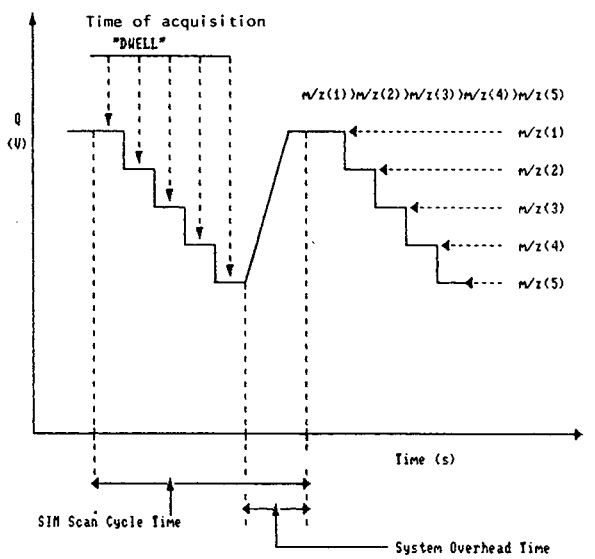

Fig. 1. Selected-ion monitoring process.

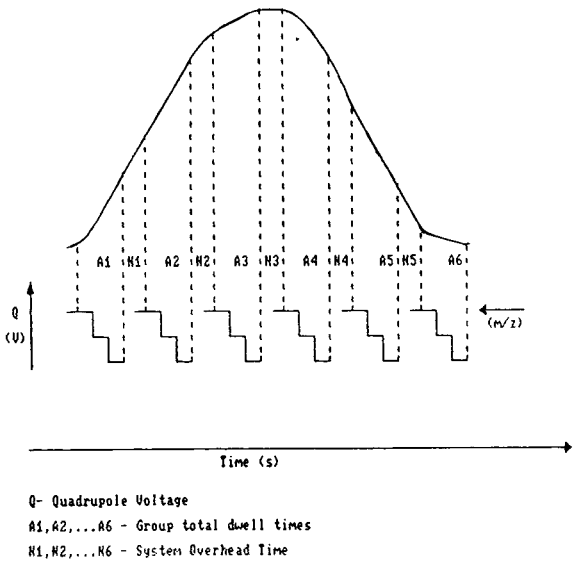

Fig. 2. Monitoring three ions as the GC peak elutes.

cycle time is numerically equal to the sum of the individual m/z dwell times plus the system overhead time. The system overhead time is the time between setting the system from the lowest to the highest m/z value. Fig. 2 shows the monitoring of three ions, which were monitored as the chromatographic peak eluted. In this example, the dwell time is equal to the system overhead time. When the quadrupole mass filter is tuned to transmit each of the selected m/z values, digitized information is accumulated for the duration of the user-specified dwell time. After completing the dwell time period, the accumulated count total is divided by dwell time and stored. The SIM scan cycle, *i.e.*, the dwell time followed by the system overhead time, is repeated until the user-specified run time is completed or the run is terminated by the user.

The principles of acquisition help us to understand the variability of the relative intensities of isotopic satellites during a chromatographic peak. The intensities of the individual ions in one SIM scan cycle time are not acquired in the same time, but their acquisition time is shifted by a few ms (dwell) (Fig. 2). The time of the first-acquired ion with the highest m/z belongs to the next acquired ions in one cycle in the control computer. The result is that the measured relative intensities are not the same as the theoretical relative intensities measured at the time of the highest m/z.

Isotopic ratios of the $(M+2)^+$ ion of a PCB with one atom of chlorine in a molecule in the SIM mode were measured. Graphical plots of isotopic ratio with various dwell times are shown in Fig. 3. The ratio y_{M+2}/y_M of the relative

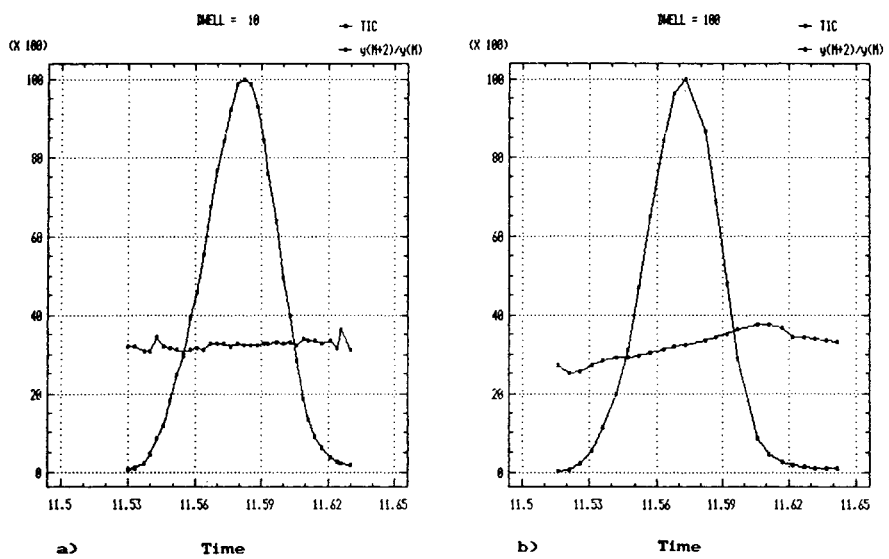

Fig. 3. Isotopic ratio via chromatographic peak. Time spent: (a) 10 and (b) 100 ms.

intensity of an ion with a lower m/z (y_M) to that of an ion with a higher m/z (y_{M+2}) is increased via the chromatographic peak. This increase depends on the time spent on the monitoring ion. A longer time spent causes a larger increase in the isotopic ratio of the ion with higher m/z via the chromatographic peak (Fig. 3). This effect can be explained as follows. The isotopic ratios y_{M+2}/y_M on the increasing slope of the chromatographic peak are lower than the theoretical isotopic ratio, because y_M is acquired later and their intensities are higher than if they had been acquired in the same time as y_{M+2}. The differences between the measured and theoretical ratio y_{M+2}/y_M is minimal at the top of the chromatographic peak because the measured y_M is almost equal to the theoretical value, although it is measured later than y_{M+2}. The y_{M+2}/y_M ratio on the decreasing slope of the peak is higher than the theoretical value because y_M is lower than if measured in the same time as y_{M+2}.

Another and possibly better example of intensity errors is presented in Fig. 4. The mass chromatograms of ions M^+ and $(M+2)^+$ are normalized on the maximum of their peak height. The mass chromatogram of the ion with lower m/z (y_M) is shifted to the left from the mass chromatogram of the ion with higher m/z (y_{M+2}) by the time spent on one ion (Dwell time value). If the relative intensities of both ions were measured in the same time, the normalized mass chromatogram would be ideally overlapping. These two negative influences can be removed by the measurement of intensities with the lowest time spent on selected ions (10 ms). The isotopic ratios fluctuate around the mean value and average values can be statistically computed.

There is no problem in calculating the theoretical ratios of isotope intensities of the molecular ion from the distribution of naturally occurring isotopic elements. It is possible to compare the theoretical and experimental relative intensities of the isotopic satellite of the molecular ion via the chromatographic process. The program for calculating the theoretical ratio of isotopic ions was written in BASIC on an HP 9000 Model 310 computer. The algorithm is the same as in the program used by Kavanagh [1].

We observed average relative intensities of individual congeners of PCBs (congeners 3, 8, 28, 52, 101, 138, 180, 203, 209) with 1, 2, 3, 4, 5, 6, 7, 8 and 10 atoms of chlorine in the molecule and they were compared with the theoretical intensities.

The data were averaged from 7 to 13 measurements of relative intensities of isotopic ions of congeners of PCBs. It was observed that the measurements of the average values of relative intensities of isotopic ions were not equal to the theoretical relative intensities. The errors between the theoretical and measured relative intensities were caused by the time shift in measuring the abundances of ions. A linear correction of the differences between theoretical and experimental relative intensities was suggested.

The relative errors D_0, D_1, $D_2, \ldots, D_i, \ldots, D_n$ between theoretical x_0, x_1,

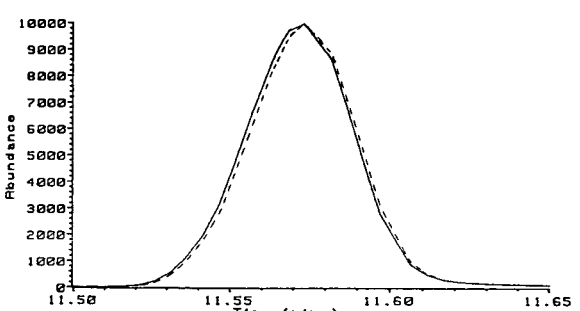

Fig. 4. Shift of mass chromatograms. Solid line: ion 188 u; dotted line: ion 190 u.

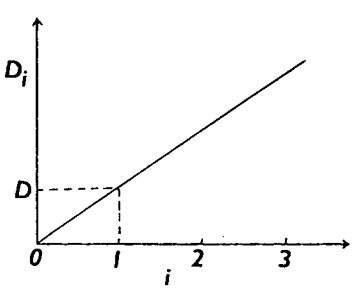

Fig. 5. Linear correlation of experimental error on the order of the measured ion.

$x_2, \ldots, x_i, \ldots, x_n$ ($x_0 = 100$) and experimental intensities $y_0, y_1, y_2, \ldots, y_i, \ldots, y_n$ ($y_0 = 100$), where i is the order of measured ion to the most intense ions ($i = 0$) of the molecular pattern, which can be negative if the molecule contains atoms of chlorine and (or) bromine, may be expressed as

$$D_0 = \frac{y_0 - x_0}{y_0} = 0 \quad (1)$$

$$D_1 = \frac{y_1 - x_1}{y_1} = D \quad (2)$$

$$D_2 = \frac{y_2 - x_2}{y_2} = 2D \quad (3)$$

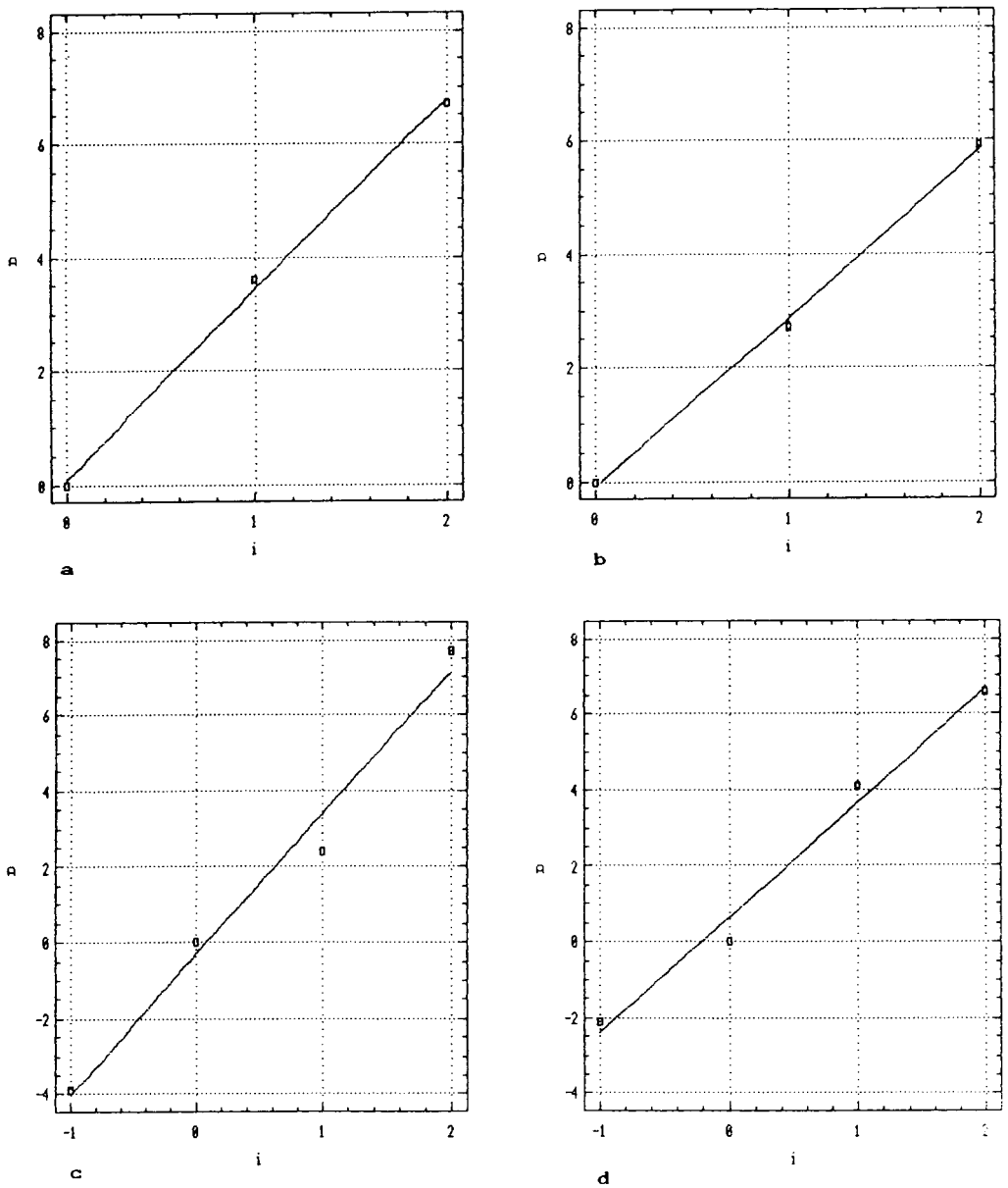

Fig. 6. Linear function errors D_i on ions i for PCBs with (a) 2, (b) 3, (c) 4 and (d) 5 atoms of chlorine.

$$\vdots$$

$$D_i = \frac{y_i - x_i}{y_i} = iD \quad (4)$$

$$\vdots$$

$$D_n = \frac{y_n - x_n}{y_n} = nD \quad (5)$$

and

$$D = D_0 - D_1 = D_1 - D_2 = D_i - D_{i-1} = D_n - D_{n-1} \quad (6)$$

where D is a correction factor. This value may be used for the characterization of the relative

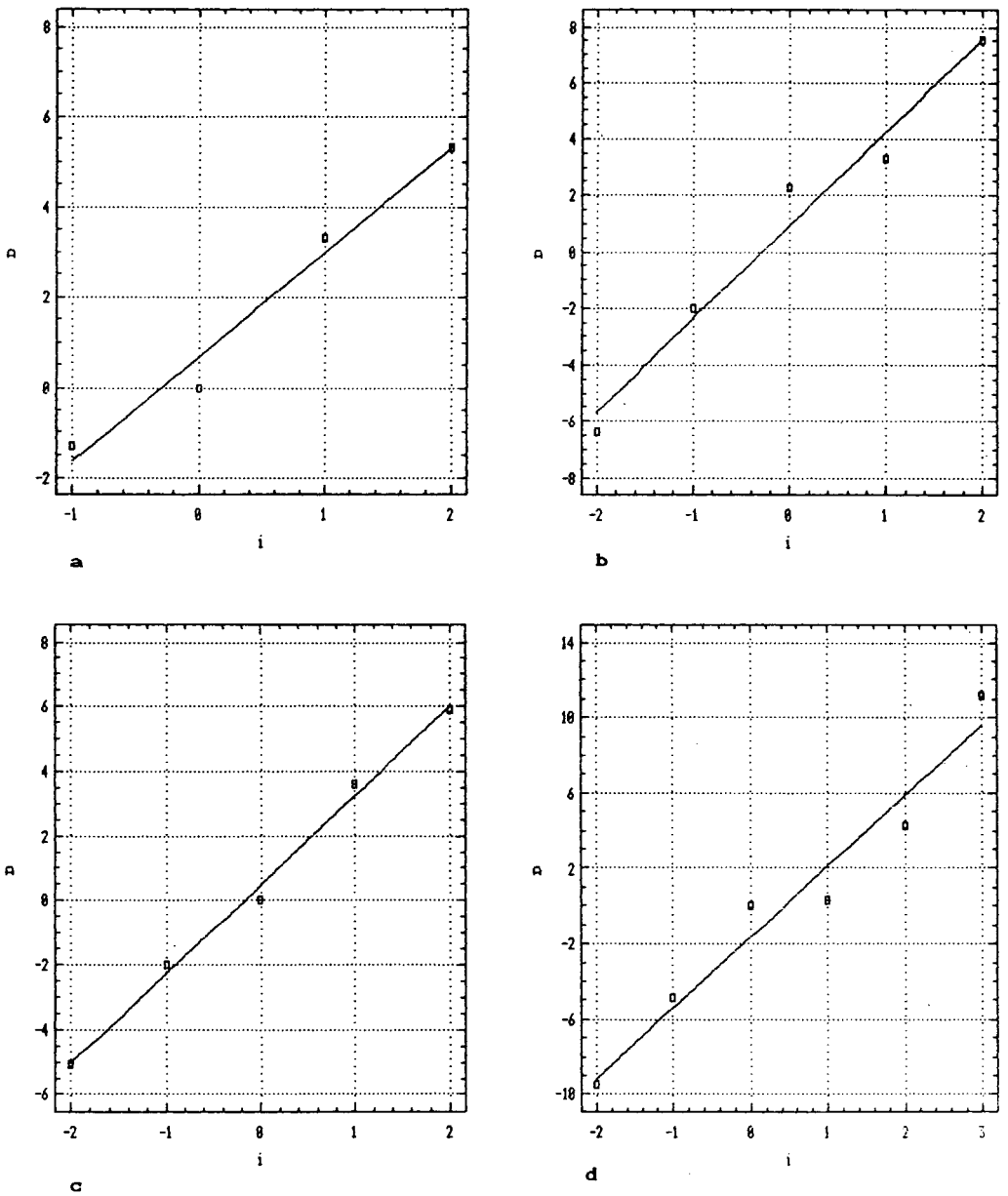

Fig. 7. Linear function errors D_i on ions i for PCBs with (a) 6, (b) 7, (c) 8 and (d) 10 atoms of chlorine.

error between experimental and theoretical intensities for two neighbouring ions.

In general, the error between theoretical and experimental intensities of isotopic pattern can be approximated by linear regression (Fig. 5):

$$D_i = a + Di \quad (7)$$

where a and D are coefficients of linear regression. If $a = 0$, then the experimental relative intensities must be corrected by the value of Di.

Table 1
Values of y_i, x_i, S.D., R.S.D., n, D_i, D and r for PCBs

N_0	M	y_i	x_i	S.D.	R.S.D.	n	D_i	D	r
1	188	10000	10000				0		
	190	3206	3323	68	2.1	10	+3.7	3.7	1
2	222	10000	10000				0		
	224	6336	6562	269	4.2		+3.6		
	226	1035	1104	52	5.0	10	+6.7	3.4	0.9991
3	256	10000	10000				0		
	258	9549	9802	289	3.0		+2.7		
	260	3051	3231	143	4.7	7	+5.9	3.0	0.9988
4	290	7981	7667	366	4.6		−3.9		
	292	10000	10000				0		
	294	4797	4912	121	2.6		+2.4		
	296	1006	1084	45	4.5	8	+7.7	3.7	0.9896
5	324	6247	6142	117	1.9		−2.1		
	326	10000	10000				0		
	328	6272	6530	113	1.8		+4.1		
	330	2010	2143	60	3.1	10	+6.6	3.0	0.9825
6	358	5191	5123	112	2.2		−1.3		
	360	10000	10000				0		
	362	7884	8148	390	4.9		+3.3		
	364	3374	3552	132	3.9	11	+5.3	2.3	0.9877
7	392	4695	4393	151	3.2		−6.4		
	394	9806	10000	230	2.4		−2.0		
	396	10000	9767				+2.3		
	398	5141	5310	111	2.2		+3.3		
	400	1617	1738	72	4.4	11	+7.5	3.3	0.9848
8	426	3553	3377	95	2.7		−5.1		
	428	8959	8782	178	2.0		−2.0		
	430	10000	10000				0		
	432	6288	6515	227	2.3		+3.6		
	434	2510	2659	149	3.1	13	+5.9	2.8	0.9970
10	494	2326	2105	123	5.3		−9.5		
	496	7193	6838	199	2.8		−4.9		
	498	10000	10000				0		
	500	8646	8673	242	2.8		+0.3		
	502	4737	4942	132	2.8		+4.3		
	504	1739	1934	64	3.7	12	+11.2	3.8	0.9779

N_0 = number of chlorine atoms in a molecule; M = nominal mass of ion; y_i = experimental relative intensities; x_i = theoretical relative intensities; S.D. = standard deviation; R.S.D. = relative standard deviation (%); n = SIM scan cycles; D_i = relative error of y_i as percentage of the base peak of the molecular pattern; D = correction factor; r = correlation coefficient of linear function for PCBs.

This theoretical procedure was verified by comparing measured and computed relative intensities. The plot of the linear function errors D_i on ions i for individual PCB congeners with two to ten atoms of chlorine are in Figs. 6 and 7. Table 1 gives measured (y_i) and theoretical relative intensities (x_i), standard deviations (S.D.) and relative standard deviations (R.S.D.) in percentages from n SIM scan cycles, values (D_i) in percentages of the base peak of the molecular pattern, correction factors (D) and correlation coefficients (r) of the linear function for PCBs with N_0 atoms of chlorine in a molecule and m/z equal to M. The correction factor D was computed from each PCB congener. The highest and the lowest values of D were statistically tested and the difference between these two values was not statistically significant. The average value of the correction factor was 3.2% and was applicable with both the HP 5977B and HP 5988A instruments.

The best way of computing the correction factor was from one GC–SIM-MS experiment of PCB congeners. PCB congeners were separated and the molecular ions with their isotopic satellites were acquired. Fig. 8 shows the chromatogram obtained with PCB congeners (Delor 104). Although the chromatographic peaks of some congeners were not resolved, this did not affect the results. The average value of the correction factor D was computed from all the congeners (Fig. 8). The correction factors and correlation coefficients of the linear regression (r) for PCB congeners with N_0 atoms of chlorine in the molecule are given in Table 2. The average correction factor D of 3.0% is similar to the average correction factor computed for individual PCBs and the difference is not statistically significant.

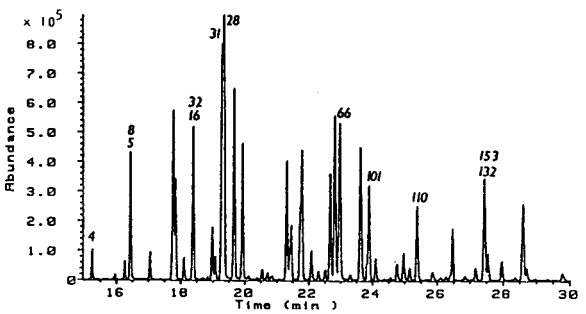

Fig. 8. Chromatogram of PCB mixture (Delor 104).

Table 2
Values of D and r for PCB congeners

N_0	Congeners	M	D	r
2	4	222	2.6	0.9806
2	5 + 8	222	2.9	1.0000
3	16 + 32	256	2.9	0.9414
3	28 + 31	256	2.5	0.8940
4	66	290	3.6	0.9326
5	110	324	3.2	0.9926
5	101	324	2.9	0.9998
6	132+ 153	358	3.3	0.9441

N_0 = number of chlorine atoms in a molecule; D = correction factor; r = correlation coefficient of linear function.

4. Conclusions

A knowledge of experimental errors in the relative intensities of ions helps in the determination of the relative intensities with sufficient accuracy for the determination of the elemental composition of ions. The measurement of relative intensities in the SIM mode give better results than those obtained in the scan mode. Greater sensitivity, accuracy and precision of measured intensities are the advantages of the proposed method.

5. References

[1] P.E. Kavanagh, *Org. Mass Spectrom.*, 15 (1980) 334.
[2] A. Tenhosaari, *Org. Mass Spectrom.*, 23 (1988) 236.
[3] C.S. Hsu, *Anal. Chem.*, 56 (1981) 1361.
[4] J.E. Evans and N.B. Jurinski, *Anal. Chem.*, 47 (1975) 961.
[5] Y.N. Sukharev, N.S. Molgachova, Y.S. Nekrasov and E.E. Tepfer, *Org. Mass Spectrom.*, 26 (1991) 770.
[6] K. Blom, *Anal. Chem.*, 60 (1988) 966.
[7] S. Musil and J. Lesko, *Chem. Listy*, 87 (1993) 310.
[8] I.K. Mun, R. Venkataraghavan and F.W. McLafferty, *Anal. Chem.*, 49 (1977) 1724.

[9] J.L. LaBrosse and R.J. Anderegg, *J. Chromatogr.*, 314 (1984) 83.
[10] J.L. LaBrosse and R.J. Anderegg, *J. Chromatogr.*, 314 (1984) 93.
[11] S. Jonsen and K. Kolset, *J. Chromatogr.*, 438 (1988) 233.
[12] S. Musil, *Dissertation*, CHTF Slovak Technical University, Bratislava, 1993.

ELSEVIER

Journal of Chromatography A, 664 (1994) 263–270

JOURNAL OF CHROMATOGRAPHY A

Thin-layer chromatography under tropical conditions: impact of high temperatures and high humidities on screening systems for analytical toxicology

R.A. de Zeeuw[a,*], J.P. Franke[a], M. van Halem[a], S. Schaapman[a], E. Logawa[b], C.J.P. Siregar[b]

[a] *Department of Analytical Chemistry and Toxicology, University Centre for Pharmacy, 9713 AW Groningen, Netherlands*
[b] *National Quality Control Laboratory for Drugs and Food, Jalan Percetakan 23, Jakarta, Indonesia*

(First received October 5th, 1993; revised manuscript received December 21st, 1993)

Abstract

The impact of high temperatures (33–38°C) and high relative humidities (80–100%) on the applicability of TLC systems for drug identification was studied during a six month climatologic cycle in Jakarta, Indonesia. In general, the R_F values as observed on the plates were substantially affected in comparison to values obtained at moderate climates: most substances gave higher R_F values under the tropical conditions, although exceptions may occur as well. The deviations tended to increase with increasing humidities and could amount easily to 20–30 R_F units. On the other hand, some TLC systems were more affected than others. Tropical conditions also had a negative effect on the reproducibility of the R_F values. However, when an R_F correction procedure was applied, using reference mixtures of standard drugs on each plate, accuracies as well as reproducibilities of the resulting R_F^c values were drastically improved and data thus corrected were found to be compatible with existing TLC data bases developed under moderate climatic conditions. These results are in line with earlier studies carried out in a relatively dry tropical climate. In the latter the observed R_F values tended to be lower than the ones published in the literature, but the R_F correction procedure was able to correct for this phenomenon.

1. Introduction

Because of its simplicity, speed and low costs, thin-layer chromatography (TLC) appears to be a suitable and versatile technique for qualitative and (semi)quantitative analyses in situations where financial constraints exist, such as in developing countries. The majority of these countries are in tropical areas, characterized by high temperatures (usually above 25°C) and humidities that may range from rather low (< 30% relative humidity) to very high (above 90% relative humidity). Yet, virtually all of the commonly used TLC procedures have been or are being developed in the Western world under moderate climatic conditions. This brings the paradoxical situation that, although it is known that TLC —as an open technique— can be affected by factors such as temperature and humidity [1], little or no information exists as to how these procedures behave under tropical conditions: do they still provide adequate separation efficiencies and are the resulting R_F values

* Corresponding author.

0021-9673/94/$07.00
SSDI 0021-9673(93)E0083-7

comparable to those listed as reference values, yet obtained in moderate climates?

In a previous paper [2] we described the influence of high temperatures (up to 39°C) and prevailing relative humidities (RH) of 20 to 70% (dry to moderately humid) as they occur in a semi-desert climate in Burkina Faso, West Africa. In general, the R_F values observed on the plates were found to be substantially affected as compared with values obtained at temperate climates. Most substances showed lower R_F values with lower humidities. The largest deviations were seen at the lowest humidities and were occasionally in the order of 30 R_F units.

We now report on a comparable study, done under hot and humid conditions (temperatures between 33 and 38°C and RHs between 80 and 100%), encountered during a 6-month climatological cycle in Jakarta, Indonesia, under routine laboratory conditions in non-climatized rooms. As we were primarily interested in TLC systems for drug screening in analytical toxicology, we examined a number of established screening systems with regard to the reproducibility and accuracy of the R_F values as observed on the plate and after applying a R_F correction procedure [3,4]. Accuracy was assessed by comparing the R_F values and corrected R_F values (R_F^c) under tropical conditions with the R_F data bases generated under moderate climatic conditions [3,4]. The present "on site" investigational setup was preferred over generating tropical conditions in climatized rooms, since the latter are too constant and do not accommodate for changes during the day (tropical rainstorms), draught, open doors and windows, etc.

2. Experimental

2.1. Selection of test drugs

Two groups were selected from the WHO list of essential drugs, in order to reflect their toxicological relevance. Also, care was taken to include various relevant pharmacological and chemical classes of drugs:

Acidic and Neutral Drugs (A/N drugs)

Aminophenazone	Paracetamol
Benzocaine	Pentobarbital
Caffeine	Phenacetine
Chlordiazepoxide	Phenobarbital
Diazepam	Phensuximide
Dichlorophen	Phenylbutazone
Diflunisal	Phenytoin
Gluthetimide	Piroxicam
Guaifenesine	Prazepam
Ibomal	Salicylamide
Ibuprofen	Salicylic acid
Indometacin	Secobarbital
Lorazepam	Temazepam
Meprobamate	Theophylline
Methyprylone	Tolbutamide
Naproxen	Triazolam
Oxazepam	

Basic and Neutral Drugs (B/N drugs)

Amitriptyline	Oxycodone
Amphetamine	Papaverine
Atropine	Pentazocine
Codeine	Pethidine
Desipramine	Pheniramine
Diphenhydramine	Procainamide
Dipyridamole	Procaine
Emetine	Promethazine
Ephedrine	Propranolol
Haloperidol	Pseudoephedrine
Hydrocodone	Quinine
Hydoxizine	Timolol
Lidocaine	Trazodone
Methamphetamine	Trifluperidol
Morphine	Trimipramine
Orphenadrine	

The above subdivision is based on the fact that specimens in analytical toxicology are usually extracted first at an acidic pH to isolate A/N drugs, then followed by extraction under alkaline conditions to isolate B/N drugs.

The test substances were of pharmacopoeial quality, with the basic substances usually present as their salt. Solutions were made in ethyl acetate in concentrations of 2 mg/ml. One or 2 μl was spotted, either by means of a Nanomat II automatic applicator (Camag, Muttenz, Switzerland, or by hand with glass capillaries. Solvents were of analytical grade (Merck, Darmstadt, Germany).

2.2. TLC systems

According to the recommendations of TIAFT/DFG [3,4], systems 1–4A were used to chromatograph A/N drugs and systems 4B–10 for B/N drugs. These systems are described in Table 1, together with the reference mixtures to be used with each system, the error windows and the respective discrimination powers [5] and identification powers [6] for the systems.The systems were run on Silica gel 60 F254 with fluorescence indicator, 20 × 10 cm (Merck), for systems 7–10 impregnated with KOH [3,4]. Paper-lined, saturated tanks (Camag) were used (presaturation time 30 min), except for systems 5 and 6 which were run in unsaturated tanks. Samples were spotted 2 cm from the bottom of the plate and at least 2 cm from the side edges. The running distance was 7 cm over the starting points [7]. The error window for a given system equals three times the interlaboratory standard deviation for that system.

Detection was done under UV light of 254 nm and by means of location reactions [8]. For each drug, R_F values were determined in 10 independent runs, spread over a period of 6 months (January through June).

2.3. R_F correction procedure

On each plate mixtures of four reference substances were spotted as described in Table 1, and the R_F values observed were compared with their corresponding values in a general data base, determined under moderate climatic conditions [4]. This allowed the construction of a six point correction graph, including the starting point (0,0) and the solvent front (100,100). The observed R_F values for the test drugs on the same plate were then corrected by means of the graph or by calculation [4]. Fig. 1 depicts typical correction graphs for systems 1, 5 and 9, respectively.

Mixtures of the four reference substances in ethyl acetate contained approximately 2 mg/ml of each substance and were stored in the refrigerator. One or two μl was spotted.

2.4. Climatic conditions

The temperature and relative humidity of each experiment was recorded when the plate was put in the tank for development. Temperatures varied from 26 to 38°C and RHs from 80 to 100%. The majority of the experiments was carried out between 33 and 38°C and 85 to 95% RH.

2.5. Evaluations

Reproducibility was assessed as follows. For each substance in a given system the individual standard deviations around the mean (S.D.) were calculated. Then, these S.D. values were averaged over all substances investigated in that system to give $\overline{\text{S.D.}}$. This was done for uncorrected R_F values as well as for corrected ones. The number of observations per substance was at least 10.

Accuracy was also assessed per system before and after correction of the R_F values. First, for each substance, the mean deviation (M.D.) between the observed R_F value and the one available in the literature was calculated:

$$\text{M.D.} = \frac{\sum(R_{F,\text{observed}} - R_{F,\text{literature}})}{n}$$

in which n represents the number of observations (at least 10) per substance. Then, these M.D.s were averaged over all substances investigated in that system to give the averaged mean deviation from the literature R_F values:

$$\overline{\text{M.D.}} = \frac{\sum M.D.}{m}$$

in which m represents the number of substances investigated. In addition, the mean *absolute* deviation (M.A.D.) from the literature was calculated in a similar way:

$$\text{M.A.D.} = \frac{\sum|R_{F,\text{observed}} - R_{F,\text{literature}}|}{n}$$

and for the averaged mean deviation from the literature:

$$\overline{\text{M.A.D.}} = \frac{\sum \text{M.A.D.}}{m}$$

Table 1
Details on the TLC systems

	Solvent [a]	Adsorbent compound	Reference [b]	hR_F^c	Error window [c]	DP [d]	IP [e]
1	Chloroform–acetone (80:20)	Silica	Paracetamol	15	7	0.83	14
			Clonazepam	35			
			Secobarbital	55			
			Methylphenobarbital	70			
2	Ethyl acetate	Silica	Sulfathiazole	20	8	0.88	10
			Phenacetin	38			
			Salicylamide	55			
			Secobarbital	68			
3	Chloroform–methanol (90:10)	Silica	Hydrochlorothiazide	11	8	0.78	17
			Sulfafurazole	33			
			Phenacetin	52			
			Prazepam	72			
4a	Ethyl acetate–methanol–conc. ammonia (85 + 10 + 5)	Silica	Sulfadimidine	13	11	0.76	19
			Hydrochlorothiazide	34			
			Temazepam	63			
			Prazepam	81			
4b	Ethyl acetate–methanol–conc. ammonia (85:10:5)	Silica	Morphine	20	10	0.71	21
			Codeine	35			
			Hydroxyzine	53			
			Trimipramine	80			
5	Methanol	Silica	Codeine	20	8	0.83	17
			Trimipramine	36			
			Hydroxyzine	56			
			Diazepam	82			
6	Methanol–*n*-butanol (60:40); 0.1 mol/l NaBr	Silica	Codeine	22	9	0.78	19
			Diphenhydramine	48			
			Quinine	65			
			Diazepam	85			
7	Methanol–conc. ammonia (100:1.5)	Silica impregnated with 0.1 mol/l KOH and dried	Atropine	18	9	0.77	18
			Codeine	33			
			Chlorprothixene	56			
			Diazepam	75			
8	Cyclohexane–toluene–diethylamine (75:15:10)	Silica impregnated with 0.1 mol/l KOH and dried	Codeine	6	8	0.75	19
			Desipramine	20			
			Prazepam	36			
			Trimipramine	62			
9	Chloroform–methanol (90:10)	Silica impregnated with 0.1 mol/l KOH and dried	Desipramine	11	11	0.76	18
			Physotigmine	36			
			Trimipramine	54			
			Lidocaine	71			
10	Acetone	Silica impregnated with 0.1 mol/l KOH and dried	Amitriptyline	15	9	0.74	20
			Procaine	30			
			Papaverine	47			
			Cinnarizine	65			

[a] Eluent composition: volume:volume; saturated systems are used except for systems 5 and 6 which are used with unsaturated solvent tanks. System 4 is split: 4a for acidic and neutral substances and 4b for basic and neutral substances.
[b] Solutions of the four reference compounds at a concentration of approximately 2 mg/ml of each substance.
[c] The error window for each system is based on multiplying by three the interlaboratory standard deviation of measurement of hR_F values.
[d] DP = Discriminating power calculated using the error window in the fifth column.
[e] IP = Identification power calculated using the error window in the fifth column and expressed as mean list length.

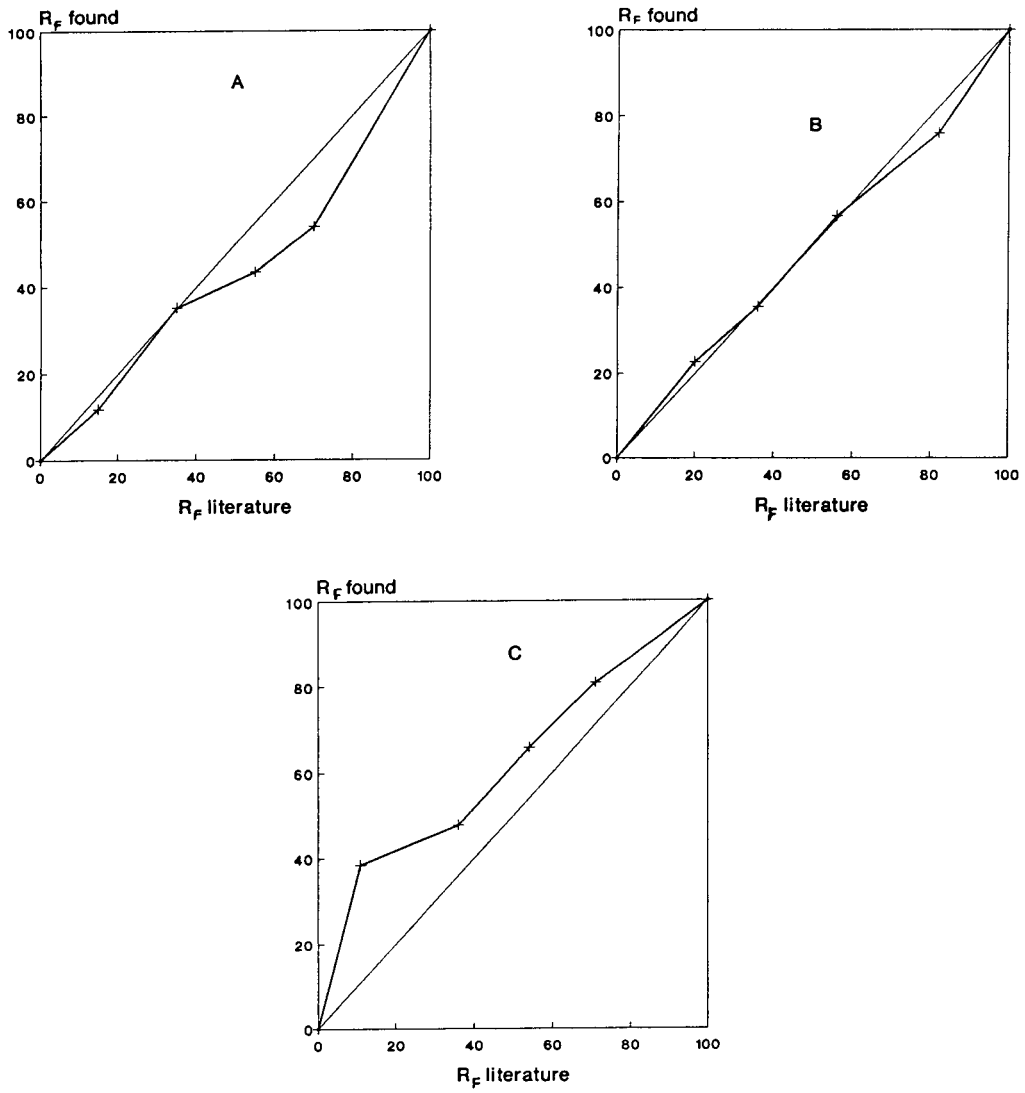

Fig. 1. Typical R_F correction graphs for individual TLC systems. Temperatures 33–38°C, relative humidities >90%. (A) System 1, reference substances ($R_{F,\text{literature}}$ in brackets): paracetamol (15), clonazepam (35), secobarbital (55), methylphenobarbital (70). (B) System 5, reference substances: codeine (20), trimipramine (36) hydroxyzine (56), diazepam (82). (C) System 9, reference substances: desipramine (11), physostigmine (36), trimipramine (54), lidocaine (71).

$\overline{\text{M.A.D.}}$ is the parameter of choice to assess accuracy because it considers deviations from the literature irrespective of sign. With $\overline{\text{M.D.}}$, deviations will level out if some substances run higher and with others running lower than their literature values. As a result, $\overline{\text{M.D.}}$ may be close to zero, even though the deviations can be substantial.

3. Results and discussion

In general, all systems could be used under the tropical conditions encountered, *i.e.* there was reasonable separation and the separation sequences were the same as under temperate conditions. However, at very high humidities (RH close to 100%) the silica on the plates

appeared to adsorb so much water vapor that the separation power was lost, with the spots running near to or with the solvent front. Such results were not further evaluated.

An other important observation was made when it was tried to avoid the rather unpleasant odor of the diethylamine in system 8 by carrying out the developments with that system in the fume hood. The air currents in the hood caused such a cooling of the walls of the tanks that solvent vapors condensed on the inside walls, thus causing highly irregular solvent flows and substance movements on the plate. Similar observations were made when some control experiments were done at temperatures around 25°C in an air conditioned room: the air currents were again so strong that solvent vapors condensed on the inside walls of the tanks, ruining the standard separation patterns.

Spotting was affected under very high humidities in that the organic spotting solution had to be applied rather slowly and preferably intermittently, to keep the spots small enough. The latter was occasionally a problem in the automatic spotting procedure with the Nanomat because it did not allow intermittent spotting. Therefore, spotting was done by hand when RHs exceeded 95%.

Our earlier observation [2], that at higher temperatures (>32°C) the ammonia lost gas bubbles when the bottle was opened, was also noted in the present study. Since this may lead to unacceptably high losses of ammonia when using bottles of 1 l that are opened frequently, ammonia was stored in bottles of 100 ml.

When the *observed, uncorrected* R_F values were considered, it became clear that the tropical conditions, and the high humidities in particular, could cause drastic changes as compared to the R_F data in the literature [4]. Conceivably, when exposed to the high ambient humidity, the silica on the plate will adsorb a substantial amount of surface water, which will make the stationary phase more polar and reduce the chances for solute interaction [9]. As a result, one may expect higher R_F values with increasing RHs, with the deviations becoming larger when the developing solvent becomes less polar. Indeed, the largest deviations were seen with the rather non-polar system 9. This is demonstrated in the correction graph for this system in Fig. 1 and in the M.D. values in Table 2: the uncorrected R_F values show a mean deviation of 27 R_F units. Yet, systems that employ more polar solvents are much less affected when high amounts of water vapour are being adsorbed. This is reflected for example by systems 5 and 7, in which the impact of extra water against the large amounts of methanol is relatively small (See Fig. 1B and Table 2). However, exceptions to the above general rule apparently exist, as demonstrated by system 1. In the latter, most substances were found to give lower R_F values with increasing humidities. This can be seen in Fig. 1A and in an M.D. for uncorrected R_F values of -5.1 in Table 2. The reasons for this behavior of system 1 remains as yet unknown.

Table 2 summarizes the impact of the tropical conditions on the uncorrected R_F values (the U-columns) with regard to precision (S.D.) and accuracy (M.D. and M.A.D.). It can be seen that some systems were more affected than others. Moreover, it should be noted that Table 2 shows the averages for the sets of about 30 substances each, obtained in 10 independent experiments. For individual drugs, deviations from the literature of some 30 R_F units were not unusual. This may be seen in Fig. 1C for desipramine: listed with an R_F value of 11 in the literature, an actual R_F of 40 was found in the experiment on the plate. Thus, the above observations clearly show that uncorrected R_F values obtained under hot and humid conditions cannot be compared with reference data collected under moderate climatic conditions.

However, *the use of the* R_F *correction procedure* drastically improved the applicability of all the systems under tropical conditions. This is reflected in a significant reduction in S.D. (better precision), but even more so by substantial reductions in the C-columns of M.D. and M.A.D. (better accuracy). Yet, despite the correction procedure, systems 1, 3, 7, 9 and 10 remain less suitable for work under hot and humid conditions because their M.A.D. values are still larger than 5. The other systems, nos. 2

Table 2
Reproducibilities and accuracies of uncorrected (U) and corrected (C) R_F values. Temperatures 33–38°C; relative humidities 80–100%

TLC system	$\overline{\text{S.D.}}$		$\overline{\text{M.D.}}$		$\overline{\text{M.A.D.}}$	
	U	C	U	C	U	C
1	1.6	1.6	−5.1	0.8	7.6	5.6
2	1.9	1.9	2.9	1.2	4.7	3.1
3	1.6	1.2	1.4	−0.4	5.9	5.2
4A	2.4	2.2	3.4	−1.1	5.2	2.9
4B	2.7	2.3	3.0	−0.8	5.4	2.9
5	2.2	1.6	−1.8	0.6	4.4	2.6
6	4.0	2.0	1.6	1.3	4.5	3.5
7	3.2	2.2	−1.6	2.2	6.0	5.0
8	2.8	1.3	5.9	0.3	6.9	2.8
9	3.8	3.4	27.2	13.6	27.2	15.2
10	4.1	2.5	7.6	3.6	12.6	7.3
Average	2.7	2.0	5.6	2.4	8.2	5.1

$\overline{\text{S.D.}}$ = averaged standard deviation of the mean per system.
$\overline{\text{M.D.}}$ = averaged mean deviation from the literature: $R_{F,\text{found}} - R_{F,\text{literature}}$ per system.
$\overline{\text{M.A.D.}}$ = averaged mean absolute deviation from the literature: $|R_{F,\text{found}} - R_{F,\text{literature}}|$ per system.

and 4A for A/N drugs and nos. 4B, 5, 6 and 8 for B/N drugs, behave well and can be recommended for screening in analytical toxicology under hot and humid conditions. Their M.A.D. values are between 2.6 and 3.5, which means that corrected R_F values obtained with these systems can be checked against the existing TLC data bases developed in moderate climates [4]. Virtually all data will then fall within the Error Windows as listed in Table 1. As for system 8, it was noted that high humidities ($>90\%$) had an especially pronounced effect on the second substance in the reference mixture, desipramine. Listed with an R_F value of 20, it showed R_F values up to 35 at high humidities, which is very close to that of the third reference, prazepam, whose listed R_F of 36 was far less affected. We are presently considering whether desipramine in the reference mixture can be replaced by noscapine with a listed R_F value of 21 [4].

When these findings are compared with those obtained in a semi-desert climate [2], it can be noted that the same systems also did well under hot and dry conditions. Other systems that did well under hot and dry conditions, such as nos. 3 and 7, were less satisfactory under humid conditions.

Thus, R_F corrections using reference mixtures on the same plate appear to be essential for TLC work under tropical conditions, especially to correct for the impact of very dry or of very humid conditions. The idea behind the correction is that the influence of the humidity is being reflected in the behavior of the substances in the reference mixture and that this influence is being corrected for in the behavior of the unknown substance by means of the correction graph that is being made for each plate. Corrected R_F^c values obtained in this way are then compatible with existing TLC data bases generated in temperate climates.

4. Acknowledgements

We thank E. Merck, Darmstadt, Germany, and Camag, Muttenz, Switzerland, for donating chemicals and chromatographic materials. M.

van Halem and S. Schaapman gratefully acknowledge travel and subsistence support from the University of Groningen for their stay in Jakarta.

5. References

[1] F. Geiss, *Fundamentals of Thin Layer Chromatography (Planar Chromatography)*, Hüthig, Heidelberg-Basel-New York, 1987.

[2] R.A. de Zeeuw, J.P. Franke, E. Dik, W. ten Dolle and B.L. Kam, *J. Forensic Sci.*, 37 (1992) 984–990.

[3] A.C. Moffat, J.P. Franke, A.H. Stead, R. Gill, B.S. Finkle, M.R. Möller, R.K. Müller, F. Wunsch and R.A. de Zeeuw, *TIAFT/DFG Thin Layer Chromatographic Rf-Values of Toxicologically Relevant Substances on Standardized Systems*, VCH, Weinheim, New York, 1987.

[4] R.A. de Zeeuw, J.P. Franke, F. Degel, G. Machbert, H. Schütz and J. Wijsbeek, *TIAFT/DFG Thin Layer Chromatographic Rf-Values of Toxicologically Relevant Substances on Standardized Systems*, 2nd ed., VCH, Weinheim, New York, 1992.

[5] A.C. Moffat, K.W. Smalldon and C. Brown, *J. Chromatogr.*, 90 (1974) 1–7.

[6] P. Schepers, J.P. Franke and R.A. de Zeeuw, *J. Anal. Toxicol.*, 7 (1983) 272–278.

[7] J.P. Franke, P. Schepers, J. Bosman and R.A. de Zeeuw, *J. Anal. Toxicol.*, 6 (1982) 131–134.

[8] *Toxi-Lab Drug Compendium*, Toxi-Lab, Irvine, CA, USA, 1989.

[9] R.A. de Zeeuw, in L. Meites (Editor), *Critical Reviews in Analytical Chemistry*, The Chemical Rubber Co., Cleveland, OH, 1970.

ELSEVIER

Journal of Chromatography A, 664 (1994) 271–275

JOURNAL OF CHROMATOGRAPHY A

Isolation of hydrophobic lipoproteins in organic solvents by pressure-assisted capillary electrophoresis for subsequent mass spectrometric characterization ☆

Wolfgang Weinmann[a], Claudia Maier[a], Kerstin Baumeister[a], Michael Przybylski*,[a], Carol E. Parker[b], Kenneth B. Tomer[b]

[a] *Fakultät für Chemie, Universität Konstanz, Postfach 5560 M731, 78434 Konstanz, Germany*

[b] *Laboratory of Molecular Biophysics, National Institute of Environmental Health Sciences, Research Triangle Park, NC, USA*

(First received January 26th, 1993; revised manuscript received December 17th, 1993)

Abstract

Two capillary electrophoretic (CE) separation techniques with either simultaneous solvent flow induced by hydrostatic pressure or CE followed by low pressurization with helium were developed for the analysis of extremely hydrophobic proteins, such as the lung surfactant protein SP-C. For both related procedures, buffer solutions containing up to 70% of 2-propanol were used for the capillary electrophoretic separation. This high concentration of organic co-solvent, needed to solubilize the protein, dramatically reduces the electroosmotic flow (EOF) in aminopropyltrimethoxysilane-treated fused-silica capillaries. Because the EOF was insufficient to elute the separated analytes from the capillary, two "pressure-assisted" CE techniques were developed. An additional flow to elute the separated analytes was produced either by raising the inlet of the capillary or by helium pressure. Using the pressurization procedure a baseline separation of the SP-C protein and its dimeric complex was obtained in a 55-minute electrophoretic run, followed by pressure elution of the analyte to the detector. The present combination of pressurization and capillary electrophoresis does not require any detergents or involatile buffer additives, which are usually needed to solubilize extremely hydrophobic lipoproteins. It is therefore applicable to on-line coupling with electrospray mass spectrometry for the direct structural characterization of hydrophobic proteins.

1. Introduction

Separation by capillary electrophoresis (CE) combined with desorption–ionization mass spectrometry such as ^{252}Cf plasma desorption (PD-MS) or electrospray mass spectrometry (ES-MS) has been developed as an efficient method for the characterization of primary structure and molecular homogeneity of proteins [1–4].

Highly hydrophobic proteins and many lipoproteins are poorly soluble or insoluble in aqueous buffers without the use of detergents or organic solvents. Combining CE with PD-MS or ES-MS, however, requires the use of volatile

* Corresponding author.

☆ Presented at the *5th International Symposium on High Performance Capillary Electrophoresis, Orlando, FL, January 25–28, 1993.* The majority of the papers presented at this symposium were published in *J. Chromatogr. A*, Vol. 652 (1993).

0021-9673/94/$07.00
SSDI 0021-9673(93)E0069-7

buffers containing minimal amounts of inorganic salts or detergents. To avoid the use of detergents in CE–MS, buffers containing, *e.g.*, 20% of 2-propanol or 25% of acetonitrile in 10 m*M* acetic acid have been employed for the separation and identification of water-insoluble lipopeptides, both by the "off-line" combination of CE and PD-MS and by "on-line" CE–ES-MS [5].

Even higher concentrations of organic solvents, *e.g.*, 50–70% of 2-propanol, are required for solubilizing extremely hydrophobic proteins such as the lung surfactant protein SP-C [6]. Also, for the separation and mass spectral analysis of hydrophobic proteins, acidic conditions are desirable because of the instability of these compounds in basic buffers; further, the separation of peptides as negative ions, followed by analysis by positive-ion ES-MS, can lead to reduced mass spectrometric sensitivity. The use of untreated fused-silica capillaries with acidic mobile phases, however, leads to significant peak broadening for strongly hydrophobic proteins due to adsorption on the capillary wall. Capillary treatment with aminopropyltrimethoxysilane (APS) produces a positively charged capillary wall, repelling positively charged proteins and leading to reduced wall adsorption [2,7]. In CE with APS-treated capillaries, where reversed polarity is used, there are two competing driving forces: (i) the movement of the positively charged analyte upstream towards the cathode and (ii) downstream movement resulting from the electroosmotic flow (EOF). With aqueous acidic buffers the EOF predominates, whereas with organic modifiers the EOF is strongly decreased, as demonstrated for peptides using buffers containing up to 25% of acetonitrile [5]. Owing to its high viscosity, 2-propanol has an even greater effect on decreasing the EOF [5,8]. At a concentration of 50% of 2-propanol highly hydrophobic proteins migrate very slowly and the analysis times become very long, resulting in severe peak broadening and reduced mass flow to the detector.

Two procedures applying the same principle, called "pressure-assisted capillary electrophoresis", are described here which avoid these problems and significantly shorten the analysis times of extremely hydrophobic proteins even in high concentrations of organic solvents.

2. Experimental

2.1. Capillary electrophoresis

A 75 μm I.D. fused-silica capillary (Polymicro Technologies, Phoenix, AZ, USA) derivatized with APS (Aldrich, Milwaukee, WI, USA) [7] was cut to a length of 71 cm. A small area of the polyimide coating was burned off to form a window for UV detection by an SSI-500 UV detector (Applied Science Labs., State College, PA, USA). The CE conditions were as follows: APS capillary, 71 cm × 75 μm I.D. (UV detection at 44 cm); hydrostatic procedure, buffer, 50% propanol in 10 m*M* acetic acid *ca.* 5 nl of protein solution (2.6 ng of SP-C) were loaded by a 7-s hydrostatic injection; separation voltage, −20 kV (282 V/cm). The hydrostatic solvent flow was obtained by a 20-cm height difference between the cathode and anode ends of the capillary.

For the determination of the hydrostatic flow-rate, a solution of 2% acetone and 50% 2-propanol in 10 m*M* acetic acid was loaded and the elution of acetone was monitored by measuring the UV absorbance at 279 nm. The hydrostatic flow-rate was 1 cm/min (20-cm height differential), which is *ca.* 44 nl/min for a 75 μm I.D. capillary. The pressurized procedure was carried out with buffer, 10 m*M* acetic acid–70% 2-propanol. A protein solution of 0.5 μg/μl in 70% 2-propanol in 10 m*M* acetic acid was loaded by pressure injected for 1 s from a pressurized injection vessel (1 bar) [9]. The sample was pushed on to the capillary for 3 min.

The inlet end of the capillary was then removed from the injection system and placed in a buffer solution maintained at 20 cm above the anode end, and a voltage of −25 kV (350 V/cm) was applied for 55 min. After disconnecting the high voltage, the capillary inlet was placed in the buffer solution in the injection system, which was then pressurized to 0.5 bar for elution of the

separated proteins. Using 70% instead of 50% of 2-propanol reduced the hydrostatic flow-rate by an order of magnitude to *ca.* 4 nl/min (20-cm height differential, no voltage).

2.2. Lung surfactant protein SP-C

Human-identical, biscysteinylpalmitoylated lung surfactant SP-C protein was obtained by chemical palmitoylation of recombinant SP-C, expressed in *Escherichia coli* [10,11]. The structure and homogeneity of the protein were established by PD-MS and ES-MS [6,12]. The lyophilized protein was dissolved in 50% 2-propanol in 10 m*M* acetic acid to give a solution of 0.5 μg/μl prior to CE separation. Approximately 5 nl of sample solution (2.6 ng of protein) were loaded in a 7-s hydrostatic injection with a height difference of 20 cm.

2.3. Electrospray mass spectrometry

The ES mass spectrum was obtained on a Vestec-A201 single-quadrupole electrospray mass spectrometer (Vestec, Houston, TX, USA) by direct injection of 20 μl of protein solution (0.1 μg/μl of protein in 50% 2-propanol + 50% acetic acid).

3. Results

The analysis of the homogeneous human identical recombinant SP-C protein by ES-MS (Fig. 1) shows a triply protonated molecule (*m/z* 1343) as the base peak and also a quadruply protonated molecule (*m/z* 1007) (M_r 4025) together with the $[M + 5H]^{5+}$ ion of an SP-C "leucine-zipper" analogue dimer complex (*m/z* 1612) [12]. As SP-C is a highly surface-active compound of therapeutic importance, the specific dimerization has recently attracted major interest and is thought to be biologically significant. The separation and characterization of such supramolecular structures requires the development of a capillary electrophoresis procedure which can eventually be combined with mass spectrometry.

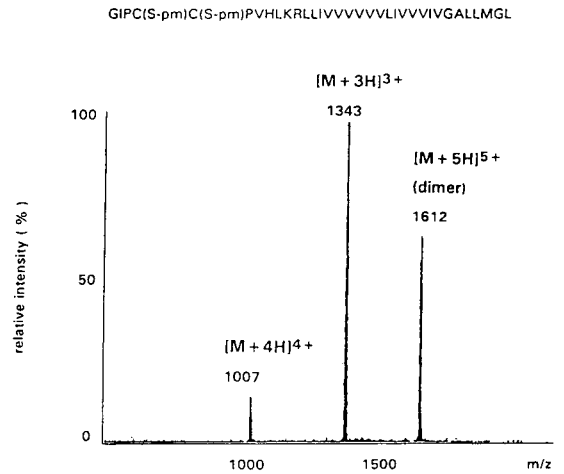

Fig. 1. ES mass spectrum of recombinant palmitoylated SP-C showing the triply and quadruply protonated molecular ions of the SP-C monomer (M_r 4025) and the $[M + 5H]^{5+}$ ion of the dimeric SP-C complex (M_r 8048).

The separation of the SP-C protein was achieved by applying two different procedures. In the first procedure, the protein (0.5 μg/μl in 50% 2-propanol–10 m*M* acetic acid) was loaded hydrostatically and the sample pushed *ca.* 22 cm on to the capillary by applying a low pressure (the total time to the detector was determined in this way to be *ca.* 65 s). The capillary (cathodic end) was then disconnected from the pressure system and placed in the CE buffer reservoir, which was raised 20 cm above the anode buffer reservoir. This mode produced a hydrostatic flow of 44 nl/min. As a result of the combination of hydrostatic pressure and electrophoretic mobility, two major components could be separated in less than 30 min (Fig. 2A).

In the second pressure-assisted procedure, with 70% 2-propanol buffer, the hydrostatic flow-rate was dramatically decreased as determined in a separate experiment. After 55 min of hydrostatic pressure-assisted CE the analyte was still on the capillary. The high voltage was then switched off and the analyte was eluted from the capillary at low pressure (*ca.* 0.5 bar). This mode resulted in a nearly baseline separation of the two SP-C components, as shown in Fig. 2B. As SP-C has been established to have a homogeneous chemical structure [11,12], the electro-

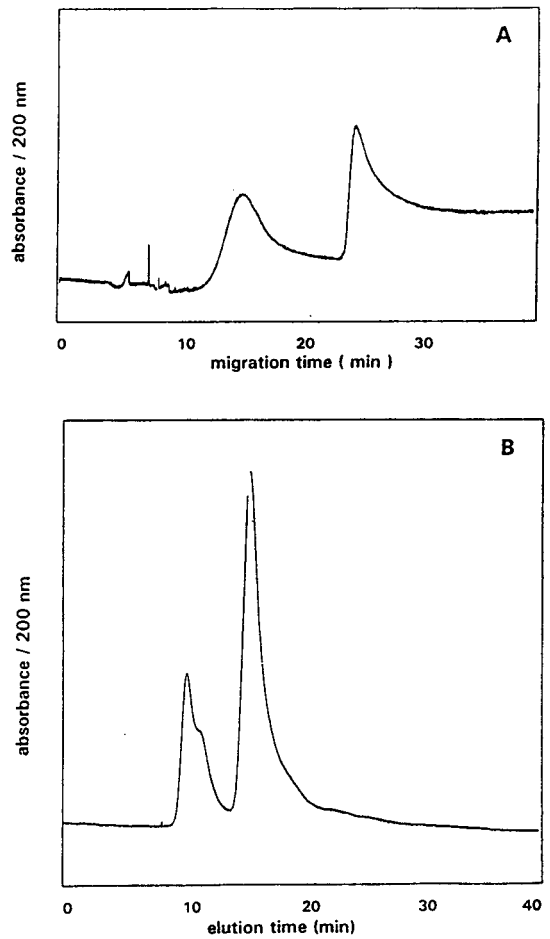

Fig. 2. (A) Capillary electropherogram of recombinant palmitoylated SP-C obtained by applying −20 kV and simultaneous hydrostatic pressure with a 50% 2-propanol buffer. (B) Capillary electropherogram of recombinant palmitoylated SP-C obtained by applying −25 kV for 55 min for CE separation and subsequent pressure elution of the analyte to the detector with 70% 2-propanol.

pherograms in Fig. 2 probably represent the separation of monomeric SP-C and its dimeric complex; confirmation of the latter by CE–ES-MS of the separated peaks is in progress.

4. Discussion

The "pressure-assisted" CE method allows the application of CE to highly hydrophobic analytes in buffers with high organic solvent concentrations without the use of any detergent by first forcing the analyte into the capillary, followed by (i) slow elution by hydrostatic pressure during CE separation at high voltage, or (ii) CE separation and subsequent elution from the capillary by pressurization. It will thus permit the on-line combination with MS at a controllable flow-rate. Without the pressure elution, the mass flow would be too low for subsequent MS analyses. The use of a shorter capillary might decrease the peak broadening caused by the parabolic pressure-induced flow profile and increase the separation efficiency, but the minimum length with our CE–ES-MS system is limited to 70 cm. Although a baseline separation is desirable, it is not required for CE–ES-MS, because discrete m/z values are registered even for overlapping compounds (a significant advantage over absorbance measurements). No effort has been made so far to determine the reproducibility of migration times, because the main goal was to develop a method of the CE separation of lipoproteins. Although the pressurization induces a hydrodynamic flow profile leading to peak broadening, it is necessary to shorten analysis times and increase the mass flow for coupling with mass spectrometry. The effects on separation efficiencies will be the subject of further investigations, as also will be the on-line coupling of the procedure with ES-MS.

5. Acknowledgements

This work was supported by the Deutsche Forschungsgemeinschaft, Bonn. We thank the German Academic Exchange Service (DAAD, Bonn, Germany) for providing a fellowship to one of us (W.W.).

6. References

[1] W. Weinmann, K. Baumeister, I. Kaufmann and M. Przybylski, *J. Chromatogr.*, 628 (1993) 111.
[2] M.A. Moseley, L.J. Deterding, K.B. Tomer and J.W. Jorgenson, *Anal. Chem.*, 63 (1991) 109.

[3] R.D. Smith, J.A. Loo, R.R. Ogorzalek Loo, M. Busman and H.R. Udseth, *Mass Spectrom. Rev.*, 10 (1991) 358.
[4] E.D. Lee, W. Muck, J.D. Henion and T.R. Covey, *J. Chromatogr.*, 458 (1988) 313.
[5] K. Baumeister, W. Weinmann, C. Maier and M. Przybylski, *Electrophoresis*, in press.
[6] A. Schäfer, P.F. Nielsen, T. Voss, E. Hannappel, C. Maier, J. Maassen, E. Sturm, K. Klemm, K.P. Schäfer and M. Przybylski, in A. Giralt and D. Andreu (Editors), *Peptides 1990*, Escom Science Publishers, Amsterdam, 1991, p. 350.
[7] M.A. Moseley, J.W. Jorgenson, J. Shabanowitz, D.F. Hunt and K.B. Tomer, *J. Am. Soc. Mass Spectrom.*, 3 (1992) 289.
[8] C. Schwer and E. Kenndler, *Anal. Chem.*, 63 (1991) 1801.
[9] R.T. Caprioli and K.B. Tomer, in R.M. Caprioli (Editor), *Continuous Flow Fast Atom Bombardment Mass Spectrometry*, Wiley, New York, 1990, p. 93.
[10] T. Voss, K.P. Schäfer, P.F. Nielsen, A. Schäfer, C. Maier, E. Hannappel, J. Maassen, B. Landis, K. Klemm and M. Przybylski, *Biochim. Biophys. Acta*, 1138 (1992) 261.
[11] C. Maier, K. Hägele, K. Baumeister, R. Nave, K.P. Schäfer, U. Krüger, K. Melchers and M. Przybylski, *Proceedings 13th Am. Pept. Symposium*, 1993, in press.
[12] C. Maier, K. Baumeister, K. Hägele, E. Bauer, E. Hannappel, R. Nave, E. Sturm, U. Krüger, K.P. Schäfer and M. Przybylski, in C.H. Schneider and A.N. Eberle (editors), *Peptides 1992*, Escom Science Publishers, Amsterdam, 1993, p. 915.

ELSEVIER

Journal of Chromatography A, 664 (1994) 276–279

JOURNAL OF CHROMATOGRAPHY A

Short Communication

Direct resolution of naproxen on a non-covalently molecularly imprinted chiral stationary phase☆

Maria Kempe, Klaus Mosbach*

Pure and Applied Biochemistry, University of Lund, P.O. Box 124, S-221 00 Lund, Sweden

(First received October 18th, 1993; revised manuscript received December 7th, 1993)

Abstract

A synthetic polymer selective for (*S*)-naproxen was prepared by molecular imprinting. 4-Vinylpyridine and ethylene glycol dimethacrylate were copolymerised in the presence of the template, (*S*)-naproxen. The template was extracted from the polymer, leaving specific recognition sites, complementary to the template. The polymer was utilized as a stationary phase in HPLC. Racemic naproxen was efficiently resolved on the polymer. Furthermore, the polymer was able to separate naproxen from the structurally related ibuprofen and ketoprofen.

1. Introduction

Naproxen (6-methoxy-α-methyl-2-naphtyleneacetic acid) (**1**, Fig. 1) is a 2-arylpropionic acid non-steroidal anti-inflammatory drug (2-APA-NSAID). Drugs of this class, the majority of which possess a chiral centre, are generally administered as their racemates, with the exception of naproxen, which is administered as its *S* enantiomer. This has stimulated extensive interest in the resolution of racemic 2-APA-NSAIDs, especially in the areas of quality control analysis [1] and pharmacokinetic studies [2]. This is reflected by the number of chromatographic studies that has been published, including direct resolution on chiral stationary phases (CSPs) [1,3–7], derivatization with chiral/non-chiral reagents followed by resolution on non-chiral/chiral stationary phases [1,8–12] and direct resolution on non-chiral stationary phases using chiral mobile phase additives [13]. The acidic nature of NSAIDs precludes the use of most of the commercially available HPLC CSPs for direct resolution [3].

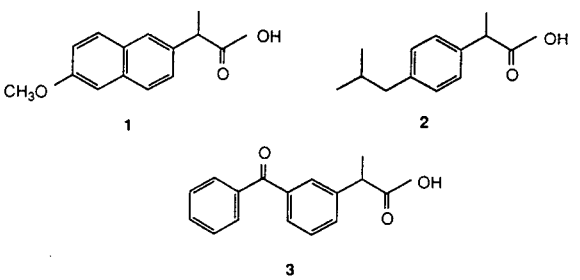

Fig. 1. Structures of the studied compounds, (**1**) naproxen, (**2**) ibuprofen and (**3**) ketoprofen.

This communication describes, to the best of our knowledge, the first report of the preparation of a CSP tailor-made for the enantioseparation of naproxen. The CSP is prepared using non-covalent molecular imprinting, sometimes referred to as template polymerisation, which is

* Corresponding author.

☆ Publication delayed at authors' request.

0021-9673/94/$07.00
SSDI 0021-9673(93)E0014-L

a technique for preparing recognition sites of predetermined specificity in synthetic polymers. This technique entails the prearrangement of functional monomers with the molecule of interest, the template (synonymous definition used is print molecule). After copolymerisation of functional monomers and cross-linker, the template is removed from the polymer by extraction, resulting in a polymer with specific recognition sites, complementary to the template in the positioning of the functional groups and in the shape. Due to the cognitive properties of the polymer, it is able to selectively rebind the template species [14–16]. Molecular imprinting has previously been applied in optical resolutions of amino acid derivatives [17–24] and β-blockers [25].

2. Experimental

2.1. Chemicals

(*R*)-Naproxen was a gift from Syntex Nordica (Södertälje, Sweden). (*S*)-Naproxen, ibuprofen and ketoprofen were from Sigma (St. Louis, MO, USA). 4-Vinylpyridine, ethylene glycol dimethacrylate and 2,2′-azobis(2-methylpropionitrile) were purchased from Merck–Schuchardt (Germany). All organic solvents were of analytical or HPLC grades.

2.2. Equipment

The bulk polymers were ground in a Retsch end runner mill Model RM O (Haan, Germany). A 25-μm Retsch sieve was used for particle sizing. The HPLC analyses were performed using a Kontron HPLC system comprising a pump 420, a gradient former 425 and a variable-wavelength detector 432. The column was packed using an air-driven fluid pump from Haskel Engineering (Burbank, CA, USA).

2.3. Preparation of the polymer

A 0.46-g amount of (*S*)-naproxen (2 mmol), 1.26 g 4-vinylpyridine (12 mmol), 11.89 g ethylene glycol dimethacrylate (60 mmol) and 0.115 g 2,2′-azobis(2-methylpropionitrile) (0.7 mmol) were dissolved in tetrahydrofuran (THF) (18 ml). The mixture was sonicated and deoxygenated with a stream of nitrogen, then irradiated with UV light (366 nm) at 4°C for 48 h. The bulk polymer was ground in a mechanical mortar and wet-sieved by hand with water and ethanol through a 25-μm sieve. The particles which passed the sieve were collected, dried on a sintered glass funnel and allowed to sediment (5 × 20 min) in acetonitrile (300 ml). The particles that did not sediment were discharged.

2.4. High-performance liquid chromatography

The sieved and sedimented polymer particles were packed at 300 bar into a stainless-steel HPLC column (200 × 4.6 mm) using acetonitrile as solvent. After packing, the column was eluted with THF–acetic acid (7:3, v/v) at 1 ml/min until a stable baseline was achieved. The eluent used for the separation studies was THF–heptane–acetic acid (250:250:1, v/v/v). The flow-rate was 0.1 ml/min, the elution was monitored at 260 nm and the separation was performed at ambient temperature.

The separation factor (α) was determined using the relationship $\alpha = k'_S/k'_R$, where k'_S is the capacity factor of the *S* enantiomer and k'_R is the capacity factor of the *R* enantiomer. The capacity factors were determined according to $k'_S = (t_S - t_0)/t_0$, where t_S is the retention time of the *S* enantiomer and t_0 is the retention time of the void, which was determined by injection of toluene. The resolution factor was determined according to Meyer [26].

3. Results and discussion

The aim of this study was to use molecular imprinting for the preparation of a synthetic polymer selective for naproxen. The clinically useful (*S*)-naproxen was used as template molecule. 4-Vinylpyridine was chosen as the functional monomer, on the basis that it has previously been shown to be efficient in the prepara-

Table 1
Resolution of naproxen on the molecularly imprinted polymer

Loaded amount of (*R*,*S*)-naproxen (μg)	k'_R	k'_S	α	R_s
2	2.17	3.58	1.65	0.83
20	1.74	2.20	1.26	0.69

tion of molecularly imprinted polymers selective for N-protected amino acids [22]. It is assumed that 4-vinylpyridine interacts with the carboxy group in naproxen by ionic interactions. (*R*,*S*)-Naproxen was well resolved on this CSP, as can be seen in Table 1 and Fig. 2. The flow-rate was 0.1 ml/min. Higher flow-rates resulted in less resolved peaks. A separation factor of 1.65 and a resolution factor of 0.83 were obtained when 2 μg of the racemate was loaded on the column (Fig. 2). When the loaded amount was increased to 20 μg, the separation factor was 1.26 and the resolution factor was 0.69. These values compare well with those previously reported for direct resolution of naproxen on conventional CSPs ($\alpha = 1.71$ [1], 1.32 [3] and 1.31 [7]).

The imprinting procedure gives rise to specific recognition sites in the polymer. It was of interest to investigate if this CSP, designed specifically for naproxen, was able to resolve other 2-APA-NSAIDs. The methyl and the carboxy groups attached to the chiral carbon are common to all 2-APA-NSAIDs, though the aryl-substituents vary. According to Dalgliesh [27], a "three-point" interaction is necessary for stereochemical specificity. Therefore, it is required that not only the carboxy group attached to the chiral carbon interacts with the imprinted polymer, as discussed above, but also the methyl and aryl substituents. The role of the aryl substituent in the recognition mechanism was elucidated by investigation of whether the polymer was able to resolve related 2-APA-NSAIDs. It was shown that neither the racemate of ibuprofen (**2**, Fig. 1) nor ketoprofen (**3**) were resolved on this CSP. Accordingly, the shape, size and nature of the aryl substituent is important for the recognition under the conditions chosen.

We were also interested to see if this molecularly imprinted stationary phase was able to separate a mixture made up of the optical antipodes of ibuprofen, ketoprofen and naproxen. As can be seen in Fig. 3, (*R*,*S*)-ibuprofen and (*R*,*S*)-ketoprofen were both eluted as single peaks, whereas (*R*)- and (*S*)-naproxen were clearly resolved. The polymer may therefore be used as a stationary phase also for separation of various 2-APA-NSAIDs.

We believe that this tailor-made polymer,

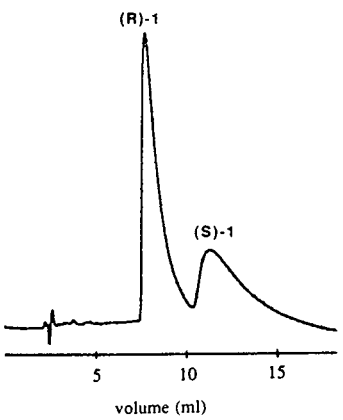

Fig. 2. Chromatographic resolution of 2 μg (*R*,*S*)-naproxen on the naproxen-imprinted polymer.

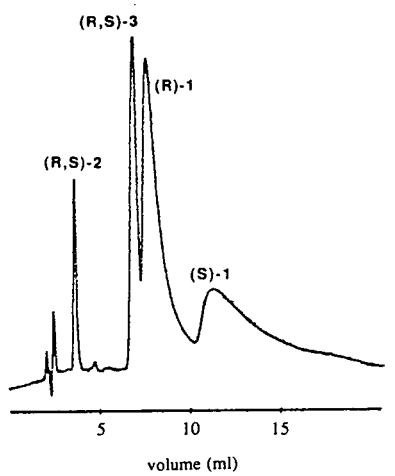

Fig. 3. Separation of a mixture of ibuprofen (2 μg), ketoprofen (0.2 μg) and naproxen (2 μg) on the naproxen-imprinted polymer. Only naproxen was resolved into its enantiomers ($\alpha = 1.70$).

specific for the determination of naproxen, represents, due to its excellent chemical and physical stability, a valuable alternative to existing CSPs utilizing biomolecules, such as bovine serum albumin, α_1-acid glycoprotein or ovomucoid. In this context, it should be mentioned that the polymer investigated here was used over 80 times without any decrease in performance. We are currently investigating the preparation of molecularly imprinted polymers selective for other NSAIDs.

4. Acknowledgement

The authors express their gratitude to Dr. Ian A. Nicholls for linguistic advice.

5. References

[1] J.R. Kern, *J. Chromatogr.*, 543 (1991) 355.
[2] W.J. Wechter, D.G. Loughhead, R.J. Reischer, G.J. Van Giessen and D.G. Kaiser, *Biochem. Biophys. Res. Commun.*, 61 (1974) 833.
[3] T.A.G. Noctor, G. Felix and I.W. Wainer, *Chromatographia*, 31 (1991) 55.
[4] T. Miwa, T. Miyakawa, M. Kayano and Y. Miyake, *J. Chromatogr.*, 408 (1987) 316.
[5] J. Hermansson and M. Eriksson, *J. Liq. Chromatogr.*, 9 (1986) 621.
[6] Y. Okamoto, R. Aburatani, Y. Kaida, K. Hatada, N. Inotsume and M. Nakano, *Chirality*, 1 (1989) 239.
[7] S. Allenmark and S. Andersson, *Chirality*, 1 (1992) 24.
[8] I.W. Wainer and T.D. Doyle, *J. Chromatogr.*, 284 (1984) 117.
[9] D.A. Nicoll-Griffith, *J. Chromatogr.*, 402 (1987) 179.
[10] D.A. Nicoll-Griffith, T. Inaba, B.K. Tang and W. Kalow, *J. Chromatogr.*, 428 (1988) 103.
[11] D.M. McDaniel and B.G. Snider, *J. Chromatogr.*, 404 (1987) 123.
[12] R. Dernoncour and R. Azerad, *J. Chromatogr.*, 410 (1987) 355.
[13] C. Pettersson and K. No, *J. Chromatogr.*, 282 (1983) 671.
[14] R. Arshady and K. Mosbach, *Makromol. Chem.*, 182 (1981) 687.
[15] B. Ekberg and K. Mosbach, *Tibtech.*, 7 (1989) 92.
[16] G. Wulff, *Am. Chem. Soc. Symp. Ser.*, 308 (1986) 186.
[17] L. Andersson, B. Sellergren and K. Mosbach, *Tetrahedron Lett.*, 25 (1984) 5211.
[18] B. Sellergren, M. Lepistö and K. Mosbach, *J. Am. Chem. Soc.*, 110 (1988) 5853.
[19] D.J. O'Shannessy, B. Ekberg and K. Mosbach, *Anal. Biochem.*, (1989) 144.
[20] L.I. Andersson and K. Mosbach, *J. Chromatogr.*, 516 (1990) 313.
[21] M. Kempe and K. Mosbach, *Anal. Lett.*, 24 (1991) 1137.
[22] M. Kempe, L. Fischer and K. Mosbach, *J. Mol. Recogn.*, 6 (1993) 25.
[23] M. Kempe and K. Mosbach, in preparation.
[24] O. Ramström, L.I. Andersson and K. Mosbach, in press.
[25] L. Fischer, R. Müller, B. Ekberg and K. Mosbach, *J. Am. Chem. Soc.*, 113 (1991) 9358.
[26] V.R. Meyer, *Chromatographia*, 24 (1987) 639.
[27] C.E. Dalgliesh, *J. Chem. Soc.*, 137 (1952) 3940.

ELSEVIER

Journal of Chromatography A, 664 (1994) 280–283

JOURNAL OF CHROMATOGRAPHY A

Short Communication

Purification of glutamine synthetase by adenosine-affinity chromatography

Mark Dowton*[,a], Ivan R. Kennedy[b]

[a]Department of Crop Protection, Waite Campus, Adelaide University, Glen Osmond 5064, Australia
[b]Department of Agricultural Chemistry, Sydney University, Sydney 2006, Australia

(First received September 22nd, 1993; revised manuscript received December 24th, 1993)

Abstract

The ability to purify insect flight muscle glutamine synthetase using various adenosine ligands was assessed. The enzyme bound most strongly to the ADP analogue (5′-ADP-agarose), followed by the NADPH analogue (2′,5′-ADP-Sepharose 4B), and least strongly to the cyclic AMP analogue (3′,5′-ADP-agarose). In all cases, binding was strongest in the presence of Mn^{2+} when compared to Mg^{2+}. These results suggest that the binding of glutamine synthetase to adenosine-affinity media is related to the participation of Mn · ADP in the γ-glutamyl transferase reaction that is catalyzed by glutamine synthetase.

1. Introduction

Glutamine synthetase has been purified from both procaryotic and eucaryotic sources using various types of affinity chromatography. For example, ADP-agarose has been used to purify glutamine synthetase from photosynthetic bacteria [1], while the related "Blue" chromatography media (*e.g.* Affigel Blue) have been used to purify glutamine synthetases from a variety of sources (*e.g.* ref. 2). In addition, 2′,5′-ADP-Sepharose 4B has been used to purify glutamine synthetase from procaryotes [3], plants [4] and insects [5]. However, this latter affinity ligand resembles NADP more than ADP, particularly with respect to the position of the phosphate moieties. This is reflected in the more general use of this affinity ligand in the purification of NADPH-dependent enzymes (*e.g.* refs. 6 and 7). In the present report, we characterize the ability of glutamine synthetase to be purified by three different adenosine-affinity ligands: 5′-ADP-agarose (an ADP analogue), 2′,5′-ADP-Sepharose 4B (an NADP analogue) and 3′,5′-ADP-agarose (a cyclic AMP analogue). We report conditions for the successful purification of insect glutamine synthetase using each of these three different affinity ligands.

2. Experimental

2.1. Insects

Parasarcophaga crassipalpis larvae were reared on liver; adults were fed sugar and water. Four days after emerging, adults were given a liver meal to allow development of sexual ma-

* Corresponding author.

0021-9673/94/$07.00
SSDI 0021-9673(93)E0081-5

turity and to provide a medium in which to lay eggs. All insects used in the present study were adults and were at least four days old.

2.2. Chemicals

EDTA and Triton X-100 were from BDH. β-Mercaptoethanol was from Calbiochem. 2′,5′-ADP-Sepharose 4B, 3′,5′-ADP-agarose, 5′-ADP-agarose, DEAE-Sepharose CL-6B and Sephadex G-15 were from Pharmacia. ADP, glutamine, γ-glutamyl hydroxamate, glutathione and imidazole were from Sigma.

2.3. Partial purification of insect glutamine synthetase

Glutamine synthetase was extracted from *P. crassipalpis* flight muscle, and purified by precipitation with 40–55% ammonium sulphate and ion-exchange chromatography on DEAE-Sepharose CL-6B, as previously described [5]. Glutamine synthetase was measured by the γ-glutamyl transferase assay (1 unit = 1 μmol γ-glutamyl hydroxamate produced per min), as outlined in ref. 5.

2.4. Affinity chromatography of glutamine synthetase

Active fractions from the DEAE ion-exchange chromatography fractionation were pooled and aliquots (0.2 transferase units) dialysed against 35 volumes of 10 m*M* imidazole · HCl buffer containing 10 m*M* β-mercaptoethanol prior to chromatography. Glutamine synthetase was then applied to pre-equilibrated columns of 2′,5′-ADP-Sepharose 4B, 5′-ADP-agarose or 3′,5′-ADP-agarose. Unbound protein was removed by washing the columns with five bed volumes of 10 m*M* imidazole · HCl buffer containing 10 m*M* β-mercaptoethanol, and bound protein eluted with 5 m*M* ADP in 10 m*M* imidazole · HCl buffer containing 10 m*M* β-mercaptoethanol.

3. Results

3.1. Affinity chromatography of glutamine synthetase

A typical purification of glutamine synthetase with each of the affinity media is shown in Fig. 1. Partially purified glutamine synthetase was equilibrated in 10 m*M* imidazole · HCl buffer (pH 6.3) containing 2.5 m*M* $MnCl_2$ and 10 m*M* β-mercaptoethanol. The enzyme was then applied to the various affinity columns, the column washed with five bed volumes of buffer and bound enzyme eluted with 5 m*M* ADP in buffer. Recoveries of glutamine synthetase were consistently high (70–100%), suggesting that the enzyme did not bind irreversibly to any of the affinity media.

The binding of glutamine synthetase to each of the affinity media was subsequently characterized. Aliquots of partially purified glutamine synthetase were equilibrated in 10 m*M* imidazole · HCl buffers of various pH containing either 2.5 m*M* $MnCl_2$ or 5 m*M* $MgCl_2$, and

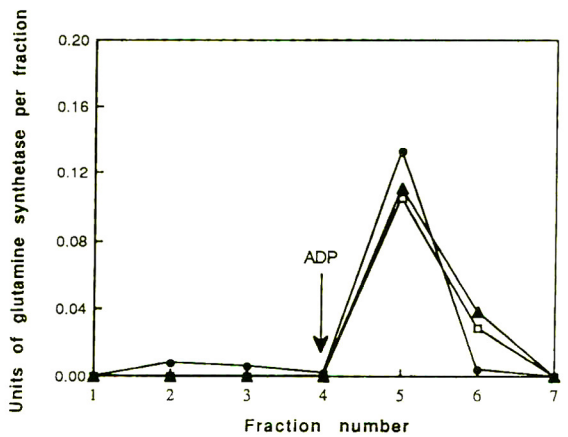

Fig. 1. The binding of insect glutamine synthetase to adenosine-affinity ligands. Partially purified glutamine synthetase (0.2 transferase units) was pre-equilibrated in 10 m*M* imidazole · HCl buffer (pH 6.3) containing 2.5 m*M* $MnCl_2$ and 10 m*M* β-mercaptoethanol. The enzyme was then applied to (□) 5′-ADP-agarose, (▲) 2′,5′-ADP-Sepharose 4B, and (●) 3′,5′-ADP-agarose, and bound enzyme eluted with 5 m*M* ADP in 10 m*M* imidazole · HCl buffer (arrow).

chromatographed. In the presence of Mn^{2+}, variation in pH over the range 6.3–8.3 had little effect on the binding of glutamine synthetase to either 5′-ADP-agarose or 2′,5′-ADP-Sepharose 4B (Fig. 2). By contrast, glutamine synthetase bound much less strongly to 3′,5′-ADP-agarose as the pH increased (Fig. 2). The latter trend was observed with all three forms of affinity media when the chromatography was performed in the presence of Mg^{2+} (Fig. 3).

The effect of the form of the divalent cation present during chromatography is evident when Fig. 2 is compared with Fig. 3. At pH 6.3, no effect of the form of the divalent cation was observed when the chromatography was carried out with 5′-ADP-agarose or 2′,5′-ADP-Sepharose 4B. However, in the case of 3′,5′-ADP-agarose, binding was much stronger in the presence of Mn^{2+} than it was with Mg^{2+}. At both pH 7.3 and 8.3, binding was stronger in the presence of Mn^{2+} to all three forms of affinity media. The effect of the form of the ADP-affinity media used can also be seen in Figs. 2 and 3. Throughout the range of conditions examined, glutamine synthetase bound most strongly to 5′-ADP-agarose, followed by 2′,5′-ADP-Sepharose 4B, and only weakly to 3′,5′-ADP-agarose.

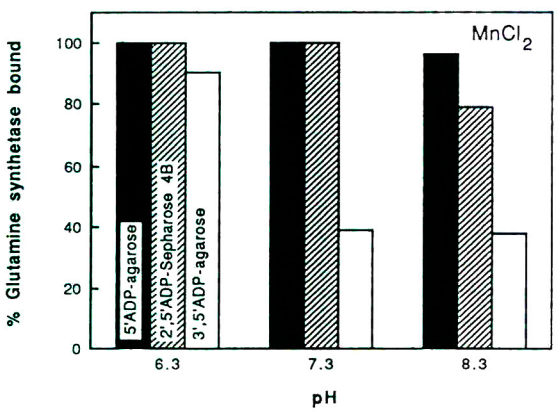

Fig. 2. The effect of pH on the binding of insect glutamine synthetase to adenosine-affinity ligands in the presence of Mn^{2+}. Partially purified glutamine synthetase was pre-equilibrated in 10 m*M* imidazole · HCl buffers of various pH containing 10 m*M* β-mercaptoethanol and 2.5 m*M* $MnCl_2$, and chromatographed. "% Glutamine synthetase bound" was calculated as the amount of glutamine synthetase that eluted from the column upon application of 5 m*M* ADP, expressed as a percentage of the amount of glutamine synthetase recovered during chromatography.

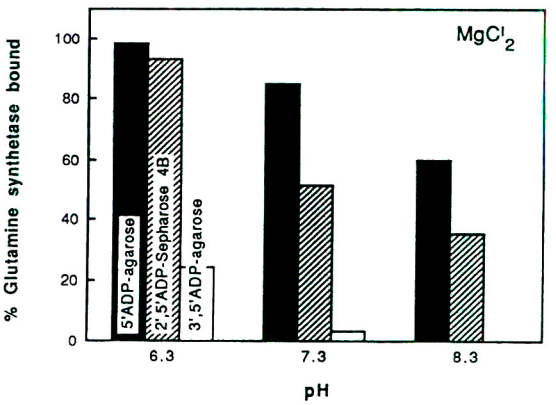

Fig. 3. The effect of pH on the binding of insect glutamine synthetase to adenosine-affinity ligands in the presence of Mg^{2+}. Partially purified glutamine synthetase was pre-equilibrated in 10 m*M* imidazole · HCl buffers of various pH containing 10 m*M* β-mercaptoethanol and 5 m*M* $MgCl_2$, and chromatographed. Calculation of % glutamine synthetase bound is outlined in the legend to Fig. 2.

4. Discussion

The three different forms of affinity media used in the present study have been used for the affinity purification of a number of enzymes. 2′,5′-ADP-Sepharose 4B has been used predominantly to purify NADP-dependent enzymes (*e.g.* refs. 6 and 7) because of the similarity of 2′,5′-ADP to NADP; the position of the monophosphate groups on the adenosine moiety are identical in these two molecules. Similarly, 3′,5′-ADP-agarose has been used to purify cAMP-dependent enzymes because of the similarity of these two molecules [8]; both have phosphate groups on the 3′ and 5′ carbon of the adenosine ring. In the present study, we found that glutamine synthetase bound most consistently to 5′-ADP-agarose; the position of a diphosphate group in this affinity ligand is identical to that found in ADP.

Our results are consistent with the hypothesis

that the binding of glutamine synthetase to adenosine-affinity media is related to the participation of Mn · ADP in the γ-glutamyl transferase reaction catalyzed by glutamine synthetase [9]. The γ-glutamyl transferase reaction shows a preference for Mn^{2+} over Mg^{2+} (*e.g* ref. 10), and has maximal activity at slightly acid pH (*e.g.* ref. 11). Similarly, the binding of insect glutamine synthetase to adenosine-affinity media also showed a preference for Mn^{2+} over Mg^{2+}, and highest binding at slightly acid pH. Furthermore, glutamine synthetase bound most consistently to the adenosine-ligand that most closely resembles ADP. These results suggest that insect glutamine synthetase has a Mn · ADP binding site similar to the one described on each sub-unit of bovine brain glutamine synthetase [12].

5. References

[1] A. Soliman, S. Nordlund, B.C. Johansson and H. Baltscheffsky, *Acta Chem. Scand., Ser. B*, 35 (1981) 63.
[2] J.E. Lepo, G. Stacey, O. Wyss and F.R. Tabita, *Biochim. Biophys. Acta*, 568 (1979) 428.
[3] F.J. Florencio and J.M. Vega, *Z. Naturforsch., C: Biosci.*, 38 (1983) 531.
[4] R.K. Iyer, R. Tuli and J. Thomas, *Arch. Biochem. Biophys.*, 209 (1981) 628.
[5] M. Dowton and I.R. Kennedy, *Insect Biochem.*, 15 (1985) 763.
[6] A. De Flora, A. Morelli, U. Benatti and F. Guiliano, *Arch. Biochem. Biophys.*, 169 (1975) 362.
[7] Y. Yasukochi and B.S.S. Masters, *J. Biol. Chem.*, 251 (1976) 5337.
[8] D. Sakac and C.A. Lingwood, *Biochem. J.*, 261 (1989) 423.
[9] B.M. Shapiro and E.R. Stadtman, *Methods Enzymol.*, 17 (1970) 910.
[10] W.B. Rowe, R.A. Ronzio, V.P. Wellner and A. Meister, *Methods Enzymol.*, 17 (1970) 900.
[11] J. Chen and I.R. Kennedy, *Phytochemistry*, 24 (1985) 2167.
[12] M.R. Maurizi, H.B. Pinkofsky and A. Ginsburg, *Biochemistry*, 26 (1987) 5023.

ELSEVIER

Journal of Chromatography A, 664 (1994) 284–288

JOURNAL OF CHROMATOGRAPHY A

Short Communication

Determination of salinomycin by high-performance liquid chromatography using a precolumn derivatization technique

Arun Kumar Mathur

Quality Control Department, Depco United Laboratory, 2433 MK1, Tingkat Perusahaan Enam, 13600 Prai, Malaysia

(First received September 23rd, 1993; revised manuscript received December 20th, 1993)

Abstract

An improved method for the determination of salinomycin by high-performance liquid chromatography using precolumn derivatization is described. Salinomycin was derivatized with 2,4-dinitrophenylhydrazine in acidic medium and separated on an ODS column using methanol–1.5% aqueous acetic acid (94:6, v/v) as a mobile phase.

1. Introduction

Salinomycin, a polyether antibiotic, is obtained from a stain of *Streptomyces albus* (ATCC 21838). It has a unique tricyclic spiroketal ring system and a unsaturated six-membered ring in the molecule (Fig. 1).

The UV absorption spectrum of salinomycin in methanol shows very poor absorption at 285 nm (ε 108) and in methanolic sodium hydroxide at 285 nm (ε 218), corresponding to a carbonyl group, making it difficult to determine it by a direct spectrophotometric method. However, a non-specific colour development method based on the reaction of salinomycin with vanillin in presence of sulphuric acid to give a pink colour has been reported [1].

Salinomycin has also been determined by microbiological methods using *Bacillus subtilis* in a diffusion method [2] and *Streptococcus faecalis* in a turbidimetric method [3], but these methods are non-specific, less sensitive and time consuming.

As the use of salinomycin is constantly increasing in veterinary formulations, a suitable and conventional chromatographic method is re-

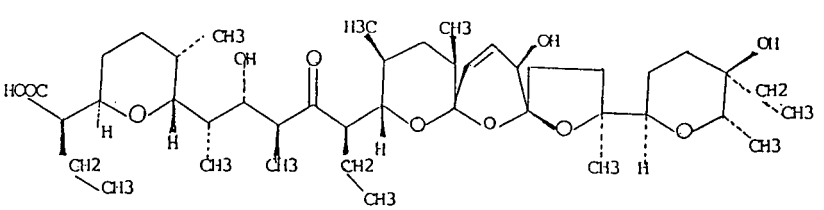

Fig. 1. Structure of salinomycin.

0021-9673/94/$07.00
SSDI 0021-9673(93)E0067-5

quired for its precise determination in feed samples. A method based on postcolumn derivatization has been reported [4] but requires extra components such as a pump, postcolumn reactor and heating coil, which is not practicable in conventional chromatography.

The proposed method is based on the precolumn derivatization of salinomycin with 2,4-dinitrophenylhydrazine (DNP) to form a highly UV-active hydrazone derivative. Derivatization was achieved by the method proposed by Siggia [5] and the product was chromatographed directly without work-up.

It is also known that some carbonyl-containing drugs give isomeric 2,4-dinitrophenylhydrazones which are separable by TLC [6] and can also be separated on HPLC using high-resolution columns. The present HPLC method was developed after thoroughly studying the reaction kinetics and other factors affecting the stability of the coloured complex.

2. Experimental

2.1. Chemicals and solvents

Most reagents were of analytical-reagent grade form Merck. Methanol was of HPLC grade form BDH. HPLC-grade water was obtained from an Elgastat UHQ system. Salinomycin sodium reference standard (98%) was obtained from Hoechst. Samples of salinomycin were feed-grade commercial samples containing 6% and 12% of salinomycin.

2.2. Instrumentation

The HPLC system consisted of Gilson Model 302 and 305 pumps, a Gilson Model 116 UV detector operated at 380 nm, a dynamic mixer and a manometric module, all controlled by computer using Gilson 712 software. Samples were injected through a Rheodyne Model 7161 injector fitted with a 20-μl fixed loop. The column used for the separation was Inertsil ODS-2 (150 × 4.6 mm I.D.; 5 μm) from G.L. Sciences. The eluent was methanol–1.5% aqueous acetic acid (94:6, v/v) at a flow-rate of 1.0 ml/min.

2.3. Standard preparation

A solution of about 300 μg/ml of salinomycin was prepared by dissolving about 31 mg of salinomycin sodium reference standard in 100 ml of absolute ethanol. This solution was stable when refrigerated at 4°C and could be used for 2 months.

2.4. Sample preparation

All feed samples were pulverized in a grinder to obtain a homogeneous powder and a suitable amount was mixed with ethanol ultrasonically for 5 min. The solution and filtered through a 0.45-μm filter and derivatized.

2.5. Derivatization reagent

A 60-mg amount of 2,4-dinitrophenylhydrazine was dissolved in 100 ml of methanol.

2.6. Linearity

Different aliquots (1, 2, 3, 4 and 5 ml) from the standard solution were taken in 10-ml volumetric flasks and diluted to 5 ml with ethanol. A 1-ml volume of the reagent was added followed by 1 drop of concentrated hydrochloric acid. All the flasks were kept at 50°C for about 3 min, cooled to room temperature, diluted to 10 ml with absolute ethanol and injected in duplicate. All the concentrations were found to be in the linear range with the linear regression line $y = -0.2240 + 0.04909x$ [where y is area counts and x is the concentration (ppm)] and a correlation coefficient (r) of 0.9996.

3. Results and discussion

3.1. Derivatization mechanism and kinetics

The ideal derivative is one that is formed rapidly under mild conditions, preferable at

lower temperatures with good sensitivity and without significant side-product formation.

With carbonyl-containing drugs, most derivatization reactions proceed with the initial attack of a nucleophilic reagent followed by dehydration of the intermediate adduct. In the presence of acid, the dehydration step becomes fast and the nucleophilic attack controls the reaction rate. The carbonyl carbon bears a partial positive charge, and addition of the nucleophile to the carbonyl group resembles protonation of the nucleophile. Therefore, basicity can be a good measure of nucleophilicity. A reagent with a negative charge is invariably a powerful nucleophile and among neutral compounds, the reactivity decreases in the order N > O > S nu-

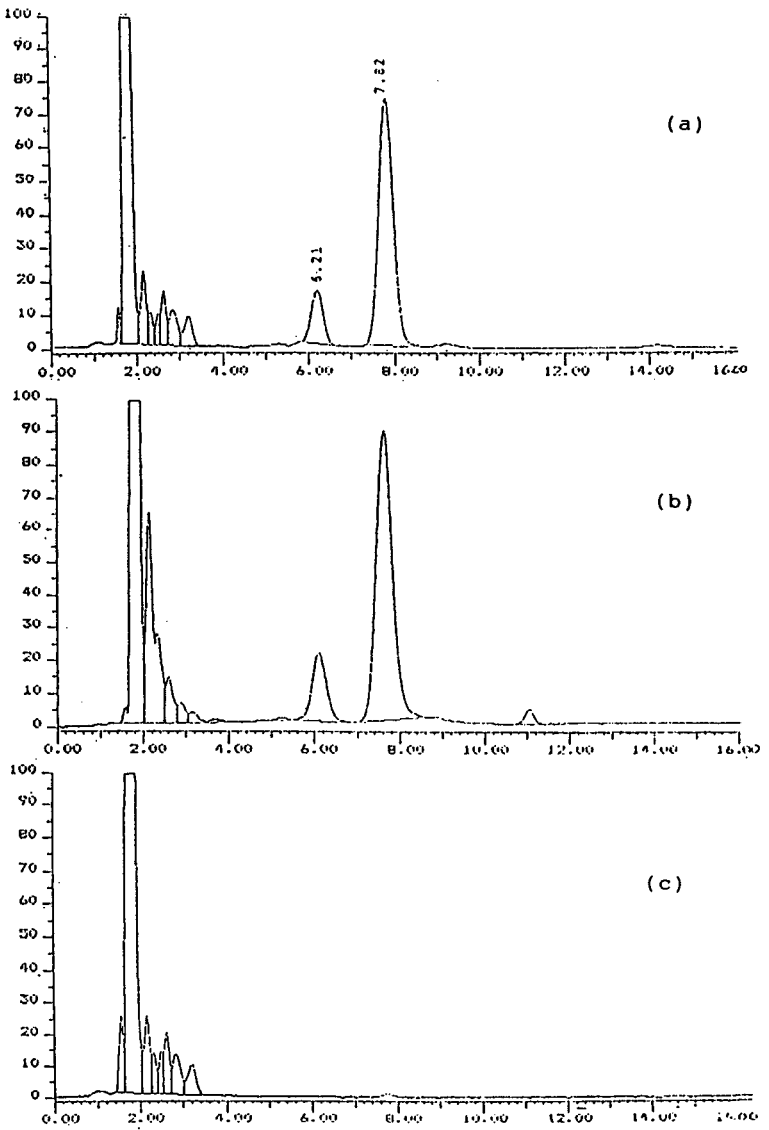

Fig. 2. Typical chromatograms after derivatization. (a) Salinomycin reference standard with unknown peak at 6.2 min and salinomycin at 7.8 min; (b) feed sample containing 12% of salinomycin; (c) blank run with all reagents but without salinomycin. Time scale in min. *y*-Axes are in $mV \cdot 10^{-1}$.

cleophiles. For this reason, hydrazines are most suited for the derivatization of carbonyl compounds.

To study the kinetics of the reaction, the reagent was allowed to react with salinomycin at 50°C for different intervals of time varying from 1 to 10 min and chromatographed. The area counts obtained with 1- and 10-min reacted solution were almost the same, indicating a spontaneous rection. However, in absence of hydrochloric acid the reaction proceeds very slowly.

3.2. Chromatography

Using the conditions mentioned under Experimental, the peak of salinomycin was well resolved and eluted at about 7.8 min along with an additional unknown peak at 6.2 min, even with the standard (Fig. 2a). A blank reaction mixture without salinomycin was also injected to make sure that the unknown peak was not from any other source (Fig. 2b).

To check the precision of the chromatographic conditions, the same derivatized solution was injected ten times and the relative standard deviation (R.S.D.) was 0.6%.

3.3. Method validation

To check the stability of the derivatized solution at ambient temperature, the same reaction mixture was chromatographed every 30 min for 4 h, and no degradation was observed. Moreover, a sample injected 24 h after derivatization showed only 1% degradation.

The sensitivity of the method is fairly high. At 380 nm, the limit of quantification was about 25–50 ng of salinomycin. For experimental purposes all the measurements were made at 380 nm as this was the maximum value that could be selected on the instrument used, but the derivatized complex showed maximum absorbance at about 419 nm with an increased sensitivity of about 11-fold (Fig. 3). Therefore, selecting 419 nm as the wavelength, a 2.5–5.0-ng amount of salinomycin can easily be detected under these conditions.

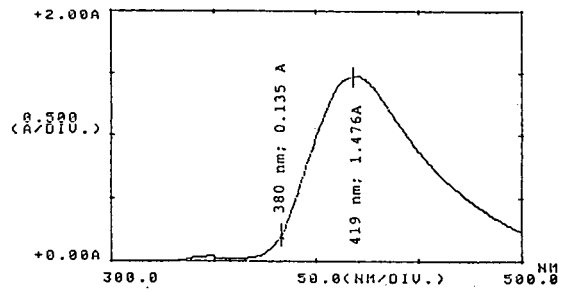

Fig. 3. UV absorption spectra of derivatized salinomycin against blank showing the difference in, absorbance values at 380 and 419 nm (path length = 1 cm; $c = 90$ μg/ml).

For evaluation of the method, different commercial samples containing 6% and 12% of salinomycin were tested (Table 1). The samples were analysed using the external standard method. The repeatability of these samples was well within limits with R.S.D. = 0.20–2.7%.

4. Conclusions

The simplicity of derivatization and the strong absorption of these derivatives indicate that 2,4-dinitrophenyhydrazine should be broadly applicable as a derivatization agent in the HPLC of carbonyl-containing drugs. The method is suitable for testing salinomycin in all kind of samples even at low concentrations and free from other UV-active interferences.

Table 1
Determination of salinomycin in commercial feed samples

Sample	Salinomycin content (%, w/w)		R.S.D. (%)
	Claimed	Found	
1[a]	6	6.15	0.46 ($n = 2$)
2[a]	12	11.55	2.7 ($n = 3$)
3[a]	12	12.11	1.8 ($n = 3$)
4[a]	12	11.98	0.20 ($n = 3$)
5[b]	6	6.21	1.27 ($n = 4$)
6[b]	6	6.06	2.3 ($n = 3$)
7[b]	6	5.71	2.2 ($n = 3$)

[a] Hoechst.
[b] Kaken Pharmaceutical.

5. Acknowledgements

The author is grateful to Mr. Teoh Lam Eng for providing all the facilities and to Ms. Teoh Lay Hoon and Ms. Zaiton Abu Baidah for their assistance in the method development.

6. References

[1] T. Golab, S.J. Barton and R.T. Scroggs, *J. Assoc. Off. Anal. Chem.*, 56 (1973) 171–173.

[2] R.M. Kline, R.P. Stricker, J.D. Coffman and H. Bikin, *J. Assoc. Off. Anal. Chem.*, 53 (1970) 49–53.

[3] F.M. Kavanagh and M. Willis, *J. Assoc. Off. Anal. Chem.*, 55 (1972) 114–118.

[4] M. Sokolic and M. Pokorny, *J. Pharm Biomed. Anal.*, V 9 (1991) 1047–1053.

[5] S. Siggia, *Organic Analysis via Functional Groups*, Wiley, New York, 1963, pp. 85–87.

[6] R.H. King, L.T. Grady and J.T. Reamer, *J. Pharm, Sci.*, 63 (1974) 1591.

ELSEVIER

Journal of Chromatography A, 664 (1994) 289–294

JOURNAL OF CHROMATOGRAPHY A

Short Communication

Determination of aldicarb, aldicarb sulfoxide and aldicarb sulfone in tobacco using high-performance liquid chromatography with dual post-column reaction and fluorescence detection

S.S. Yang*, I. Smetena

Research Center, Philip Morris USA, P.O. Box 26583, Richmond, VA 23261, USA

(First received November 15th, 1993; revised manuscript received January 24th, 1994)

Abstract

A screening method for the determination of aldicarb (AS) and its sulfoxide (ASX) and sulfone (ASN) metabolites in tobacco at low ppm levels is described. Tobacco samples are extracted using methanol with the aid of sonication at ambient conditions. The extract is filtered and then injected into a high-performance liquid chromatograph equipped with a dual post-column reaction system and a fluorescence detector. Chromatographic separation is performed on a C_{18} column with a mixture of methanol–acetonitrile–water containing 0.1% of triethanolamine as the mobile phase. Triethanolamine is added to improve peak shape of AS residues and to reduce the undesired interaction between residual silanols and interferences, mainly amino acids and other amines. The average recoveries for AS residues spiked in tobacco are higher than 95% for AS, 91% for ASN and 85% for ASX at levels of 0.5–10 ppm (w/w). The detection limit is 0.5 ppm for each of the target compounds.

1. Introduction

Aldicarb (AS) is an N-methylcarbamate pesticide for the control of insects, mites and nematodes in the farming of fruits, vegetables, tobacco and other agriculture products. After its application, AS gradually turns into the metabolites, aldicarb sulfoxide (ASX) and aldicarb sulfone (ASN), and can be further degraded to oxime and nitrile forms. The wide use of AS has led to increasing demand for monitoring of its residues in both crops and the environment (*i.e.*, farm soil and ground water) [1–11]. Both gas chromatographic (GC) and high-performance liquid chromatographic (HPLC) methods have been used to measure AS and its degradation products. Because of their thermal instability, GC analysis usually requires conversion of AS residues to nitriles by pyrolysis on the GC injection port at a temperature above 300°C [12–15] or conversion to sulfone by precolumn oxidation. This latter method provides no information for the individual quantities of AS, ASX and ASN. Because of these problems with the GC methods, most of the reported analyses have been based on HPLC with dual post-column reaction and fluorescence detection (Fig. 1) [1–3,7–9,11,16–18]. In the first reactor, aldicarb

* Corresponding author.

0021-9673/94/$07.00
SSDI 0021-9673(94)00077-M

residues in the HPLC eluate are hydrolyzed with aqueous NaOH solution at an elevated temperature to yield methylamine, which is subsequently derivatized in the second reactor with *o*-phthaladehyde (OPA) prior to fluorescence detection.

To determine AS residues at sub-ppm or ppb levels, the GC or HPLC procedures usually involved an extensive sample cleanup procedure using liquid–liquid or solid-phase extraction. These cleanup procedures are necessary, especially for crop samples in which severe matrix interferences exist. During the prolonged cleanup steps, sample loss leading to low recovery is a common problem. Recoveries for polar compounds such as ASX usually range from 20 to 50% [3,5,16]. However, it should be noted that the low recoveries of these polar compounds, normally seen in the methylene chloride extraction of water or high water-content samples, is for a large part due to the unfavorable partitioning [16]. For water samples containing little organic matter, these extraction and cleanup steps are eliminated and direct large volume injection (up to 500 μL) is employed [7,8]. Although providing satisfactory recovery, this approach is restricted by the loss of column efficiency, shorter column life and impracticality when dealing with complex samples.

In this study, a screening method using HPLC with post-column reaction and fluorescence detection for the determination of AS, ASX and ASN in tobacco at low ppm levels was developed. Tobacco samples were extracted using methanol with the aid of sonication. No sample cleanup other than filtration was involved. Chromatographic separation was performed on a C_{18} column. Triethanolamine (TEOA) was added to the mobile phase to mask the residual silanols on the surface of HPLC packing (*e.g.*, chemically modified silica particles). The use of TEOA as the mobile phase modifier improved peak shape of AS residues and, more importantly, reduced the undesired interaction between residual silanols and interferences, mainly amino acids and other amines. Most of these amines were eluted from the HPLC column immediately after the solvent peak, thus eliminating their interference with peaks for aldicarb residues. The elution order of AS and its metabolites, ASX and ASN, on C_{18} columns with different carbon loading and surface bonding chemistry was also studied.

2. Experimental

2.1. Chemicals

Methanol and acetonitrile were HPLC grade from Baxter (McGaw Park, IL, USA). Distilled and deionized water was obtained from a Milli-Q system. AS, ASX and ASN were manufactured by Riedel-de Haen (Germany). OPA and N,N-dimethyl-2-mercaptoethylamine hydrochloride (tradename Thiofluor) were purchased from Pickering Lab. (Mountain View, CA, USA). Other chemicals were purchased from various sources.

Sodium hydroxide solution (0.1 *M*) was prepared by dissolving 4 g of NaOH in 1 l of water. Tetraborate buffer (pH 9.1, 50 m*M*) was prepared by dissolving sodium tetraborate decahydrate in water. Both tetraborate buffer and NaOH solution were thoroughly degassed by sparging with helium. OPA solution was prepared by dissolving 100 mg of OPA in 10 ml of methanol, then added to a premixed solution of 2 g Thiofluor in 1 l of tetraborate buffer.

2.2. Preparation of standard solution

Stock solutions of AS, ASX and ASN were prepared by dissolving approximately 10 mg of each compound (weighed to 0.1 mg) into 250 ml of methanol (nominally 40 μg/ml). Working standards were prepared by pipetting 0.5, 1.0, 3.0 and 10 ml of the stock solution separately into four 100-ml volumetric flasks (nominally 0.2, 0.4, 1.2 and 4 μg/ml of each compound) and diluting to volume with methanol.

2.3. Sample preparation

A portion of ground tobacco (1.0 g) was placed in a 30-ml glass vial with a PTFE-lined cap. After adding 6 ml of methanol, the vial was

capped, placed in an ultrasonic bath, and sonicated for 30 min. A 1-ml aliquot of the extract was filtered through a Gelman filter (0.45 μm) into an 1.5-ml autosampler vial and capped for HPLC analysis.

2.4. Instrument and procedure

A Hewlett-Packard Model 1090L HPLC system equipped with an autosampler, a Model 1046A programmable fluorescence detector and a Hewlett-Packard 9000 LC workstation was used. A dual post-column reaction system (Pickering Lab) was connected to the HPLC system. The post-column reaction unit consisted of two reagent pumps (flow-rate fixed at 0.3 ml/min), an HPLC column thermostat controlled at 42°C and two reaction coils. The first rection coil was heated to 100°C for NaOH hydrolysis and the second one was kept at ambient temperature for OPA derivatization.

The analytical column selected for routine analysis a was a Hewlettt-Packard Hypersil C_{18} column (200 mm × 4.6 mm I.D.). The other columns tested in this study included a Waters Novapak C_{18} column (150 mm × 3.9 mm I.D., 4 μm packing), a Phenomenex Ultracarb C_{18} column (150 mm × 4.6 mm I.D.) and two Pickering C_{18} columns for carbamate analysis 150 mm × 4.6 mm I.D. and 250 mm × 4.6 mm I.D.). For each test, HPLC column was placed in the thermostat of the post-column reaction unit and maintained at 42°C.

The mobile phase consisted of two solutions: solvent A was 0.1% of TEOA in a mixture of acetonitrile–methanol (20:80, v/v); solvent B was 0.1% of TEOA in water. The initial composition of 10% solvent A was maintained for a 4-min hold period, after which a 7-min gradient program to 30% of solvent A was begun. Mobile phase composition was then changed over a 5-min period to 90% solvent A, and finally, 90% solvent A was held for 10 min to provide column cleanup before returning to the initial conditions. The flow-rate was 1 ml/min. The HPLC run was stopped at 30 min. Both the NaOH solution and the OPA solution in the post-column reaction unit were constantly pumped at a flow-rate of 0.3 ml/min during the whole sequential cycle. The injection volume of tobacco extract was 10 μl. Excitation and emission wavelengths of the fluorescence detector were set at 330 and 465 nm, respectively. Calculation was based on the external standard procedure.

3. Results and discussion

Shown in Fig. 1 are the representative chromatograms from an AS-free, mixed tobacco

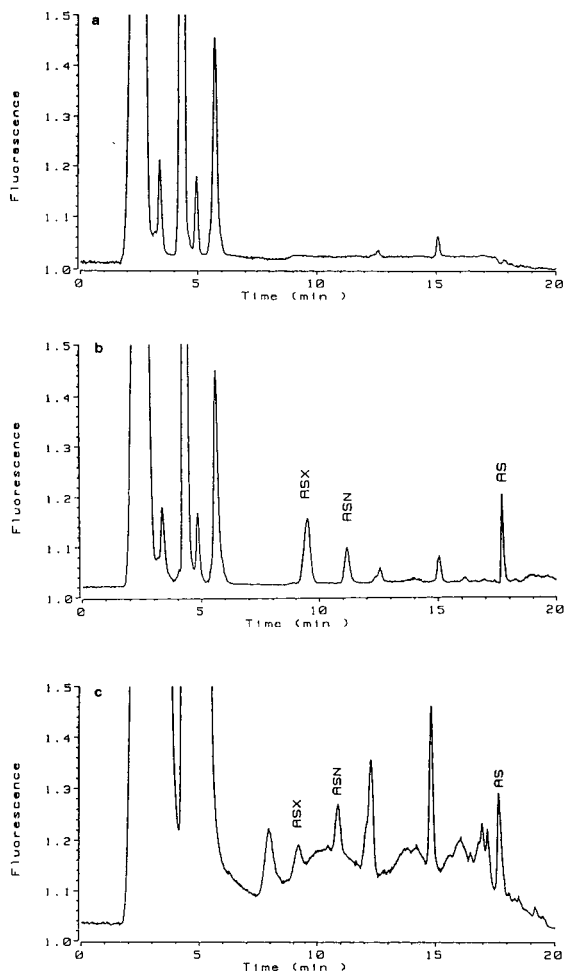

Fig. 1. Representative chromatograms for tobacco sample spiked with aldicarb residues (the sum of ASX, ASN and AS) at (a) 0 ppm, (b) 15 ppm and (c) 3 ppm levels. Details and chromatographic conditions are described in the text.

sample (burley–bright–oriental, 1:1:1) and tobacco samples spiked with aldicarb residues at levels of 15 and 3 ppm (the sum of AS, ASN and ASX). Tobacco samples were extracted by methanol with sonication and, after filtration, an aliquot of 10 μl was injected into the HPLC system. Chromatographic separation was performed on a Hypersil C_{18} column. The mobile phase was a mixture of acetonitrile–methanol (20:80, v/v) and water under a gradient elution mode. TEOA was added to the mobile phase at 0.1% level as the modifier. Relative standard deviation (2σ) for peak area of the target compounds in 10 replicate injections was 7%.

Satisfactory recoveries were obtained using methanol as the extraction solvent. For the spiking levels of 0.5–10 ppm of each target compound, the average recoveries were 98% for AS, 91% for ASN and 85% for ASX (Table 1). Other organic solvents, such as methylene chloride, were also tested for extraction efficiency. Methylene chloride has been frequently used to extract AS residues and other carbamates from water samples [7–9,11,16]. However, the extraction efficiency for polar compounds, such as ASX, were low and improvement can only be made by time-consuming multiple extractions [16]. The poor recovery was explained as a result of unfavorable partitioning of ASX into the organic layer due to its polarity [16]. For tobacco samples, methylene chloride demonstrated the advantage of extracting less polar interferences but, as in the cases of water samples, it failed to provide sufficient extraction of aldicarb residues, particularly ASX.

In the published reports for the determination of aldicarb residues [1–11,17], chromatographic separations were performed on columns of various types such as C_{18}, C_8, cyano, phenyl and silica. Although reasonable separation was accomplished in each case, C_{18} columns were the most commonly used. In this study, silica-based C_{18} columns evaluated included Hypersil C_{18} (1), NovaPak C_{18} (2), Phenomenex Ultracarb C_{18} (3) and two Pickering C_{18} columns of different lengths (150 mm, 4; 250 mm, 5). The first three columns gave the elution order of ASX-ASN-AS, which is consistent with most of the reported reversed-phase separations for aldicarb residues [1–11,17]. Under the same chromato-

Table 1
Recoveries of aldicarb residues spiked in tobacco samples

Compound	Concentration (ppm)		Recovery (%)
	Added[a]	Found[b] (S.D.)	
Aldicarb	0.50	0.48 (0.06)	95
	2.0	1.98 (0.11)	99
	5.0	4.95 (0.26)	99
	10.0	9.80 (0.32)	98
Average			98
Aldicarb sulfone	0.5	0.44 (0.08)	88
	2.0	1.86 (0.20)	93
	5.0	4.55 (0.41)	91
	10.0	9.20 (0.88)	92
Average			91
Aldicarb sulfoxide	0.5	0.41 (0.08)	82
	2.0	1.72 (0.22)	86
	5.0	4.41 (0.50)	88
	10.0	8.60 (0.98)	86
Average			85

[a] Individual amount of aldicarb, aldicarb sulfone and aldicarb sulfoxide spiked in tobacco.
[b] Average value of five replicate analyses.

graphic conditions, the last two columns gave a different elution order, ASN-ASX-AS. Although detailed information for the manufacturing of each column is not available, it can be speculated that columns 4 and 5 are significantly different from the others in several aspects, including the nature of silica support and the chemical modification of the silica surface (*e.g.*, carbon loading, bonding chemistry, endcapping etc.) [19,20].

Without the addition of OPA reagent, chromatograms (not shown) obtained from a tobacco extract gave a clean baseline, indicating that most of the peaks detected under the given conditions were OPA derivatives, presumably from amino acids and other amines. Since tobacco abounds in amino acids [21], under the experimental conditions used in the current study, these compounds may be the major peaks on the chromatograms. This assumption was further confirmed by injecting a mixture of 18 amino acids commonly found in tobacco and obtaining a chromatographic pattern similar to that of a tobacco extract.

In this study, the mobile phase was a mixture of acetonitrile–methanol (20:80, v/v) and water containing 0.1% TEOA as the modifier. Initially, when methanol and water were used as the mobile phase without any modifier, the elution of the major peaks, *e.g.*, amino acids, shifted and became faster as the column aged. Peak shifting made the separation of target peaks from matrix a difficult job. A possible explanation for the peak shifting is that the amino acids strongly interact with residual silanols on the silica surface of HPLC packing. Eventually, when the residual silanols are "shielded" and hydrophobic interaction with the immobilized C_{18} ligands dominated the solute retention, these polar amino acids are quickly eluted from the column. By adding TEOA as the mobile phase modifier, the residual silanols can be masked and peak shifting, as described above, can be eliminated. As shown in Fig. 1a, most of these amines are eluted immediately following the solvent peak, leaving a big window in the chromatogram for the latter eluted aldicarb residues.

Triethylamine (TEA) also was tested as a modifier at 0.1% level for the same purpose. Theoretically TEA, a tertiary amine, should be retained strongly by silanols on the silica surface and, if eluted, should not react with OPA and become detectable by fluorescence. However, adding 0.1% TEA in the aqueous part of the mobile phase gave a drifting baseline with a broad peak on the second half of the chromatogram. It was possible that TEA molecules retained in the column initially were eluted when the gradient mobile phase became rich in organic solvent. These eluted TEA might be decomposed and could then be derivatized by OPA.

In the post-column reactions, 0.1 *M* NaOH solution and 0.05 *M* of tetraborate buffer were used. The concentrations of these two solutions are higher than the average of reported values, *e.g.*, 0.05 to 0.2 *M* for NaOH solution and 0.01 to 0.05 *M* for tetraborate buffer [1–3,7–9,11,16]. However, the factory preset flow-rate, 0.3 ml/minute, is lower than the 0.5 ml/min rate used in the other reported procedures. Excitation and emission wavelengths for the fluorescence detection were set at 330 and 465 nm, respectively. Excitation at 230 nm using a deuterium lamp was reported to increase the sensitivity by three-fold [3,7]; however, no significant improvement was observed from the fluorescence detector equipped with a xenon lamp used in this study.

4. Conclusions

A quick screening method for the determination of AS, ASX and ASN in tobacco at low ppm levels is described. An HPLC system equipped with a dual post-column reaction system and a fluorescence detector is used for the analysis. Sample preparation consists of a single extraction with methanol. Chromatographic separation is performed on a Hypersil C_{18} column. Mobile phase composition is optimized so that major interferences (amino acids and other amines) are eluted as early peaks and are well separated from the peaks of target compounds. With modification, this procedure could be extended to the determination of the other carbamates in tobacco.

5. References

[1] K.C. Ting, P.K. Kho, A.S. Musselman, G.A. Root and G.R. Tichelear, *Bull. Environ. Contam. Toxicol.*, 33 (1984) 538.
[2] C.E. Goewie and E.A. Hogendoorn, *J. Chromatogr.*, 404 (1987) 352.
[3] D. Chaput, *J. Assoc. Off. Anal. Chem.*, 71 (1988) 542.
[4] C.J. Miles and H.A. Moye, *Chromatographia*, 23 (1987) 109.
[5] A. DeKok and M. Hiemstra, *J. Assoc. Off. Anal. Chem. Int.*, 75 (1992) 1063.
[6] A. Guhlmann, J. Hollweg, F. Seehofer, *Beitr. Tabakforsch. Int.*, 12 (1983) 87.
[7] C.J. Miles and J.J. Delfino, *J. Chromatogr.*, 299 (1984) 275.
[8] K.M. Hill, R.H. Hollowell and L.A. Dal Cortivo, *Anal. Chem.*, 56, (1984) 2465.
[9] D. Chaput, *J. Assoc. Off. Anal. Chem.*, 69 (1986) 985.
[10] L.Y. Lin and W.T. Cooper, *J. Chromatogr.*, 390 (1987) 285.
[11] S. Lesage, *LC · GC*, 7 (1989) 268.
[12] L. Muszkat and N. Aharouson, *J. Chromatogr. Sci.*, 21 (1983) 411.
[13] M.L. Trehy, R.A. Yost and J.J. McCreary, *Anal. Chem.*, 56 (1984) 1281.
[14] M.L. Trehy, R.A. Yost and J.G. Dorsey, *Anal. Chem.*, 58 (1986) 14.
[15] M. Galoux, J.C. Van Damme, A. Bernes and J. Potvin, *J. Chromatogr.*, 177 (1979) 245.
[16] A. de Kok, M. Hiemstra and U.A.Th. Brinkman, *J. Chromatogr.*, 623 (1992) 265.
[17] S. Chiron and D. Barcelo, *J. Chromatogr.*, 645 (1993) 125.
[18] M.V. Pickering, *LC · GC*, 6 (1988) 994.
[19] S.S. Yang and R.K. Gilpin, *J. Chromatogr.*, 439 (1988) 414.
[20] R.K. Gilpin, S.S. Yang and G. Werner, *J. Chromatogr. Sci.*, 26 (1988) 388.
[21] S.S. Yang and I. Smetena, *Chromatographia*, 37 (1993) 593.

ELSEVIER

Journal of Chromatography A, 664 (1994) 295–300

JOURNAL OF CHROMATOGRAPHY A

Short Communication

Evaluation of a "Chirasil-Val" capillary for the gas chromatography of volatile oil constituents, including sesquiterpenes in patchouli oil

T.J. Betts

School of Pharmacy, Curtin University of Technology, P.O. Box U1987, Perth, Western Australia 6000, Australia

(First received November 22nd, 1993; revised manuscript received January 3rd, 1994)

Abstract

The methyl-polysiloxane phase "Chirasil-Val" containing about 6% branched aliphatic side chains with L-valine in diamide linkage, has had its response assessed to various volatile oil constituents. Changes in relative retention times with temperature increase were distinctively large for camphor and fenchone. There was a greater spread of retention indices for seven solutes than on fully methyl polysiloxane, although less difference for another three solutes. Isothermally at 130°C, Chirasil-Val gave better resolution of the sesquiterpene hydrocarbon mix in patchouli oil than methyl polysiloxane, and could then be temperature programmed to evaluate patchoulol, etc. Carbowax 20M is a poor phase for patchouli analysis.

1. Introduction

This author has previously used some chirally selective cyclodextrin phases to identify constituents from volatile oils [1–3] and analyse oils of sweet fennel, mace [4] and dill [3]. It was now of interest to try for this a different chirally selective phase —a modified polysiloxane with branched aliphatic diamide sidechains, "Chirasil-Val". This was invented by Frank *et al.* in 1977 [5] for amino acid esters, and named and used a year later [6] for some sympathomimetic drugs and metabolites including ephedrine, penicillamine and L-DOPA. The phase has high thermal stability, unlike the modified cyclodextrins which are subject to thermal shock. It is depicted in Fig. 1, where the diamide-linked L-valine is attached to about every eighth silicon atom of

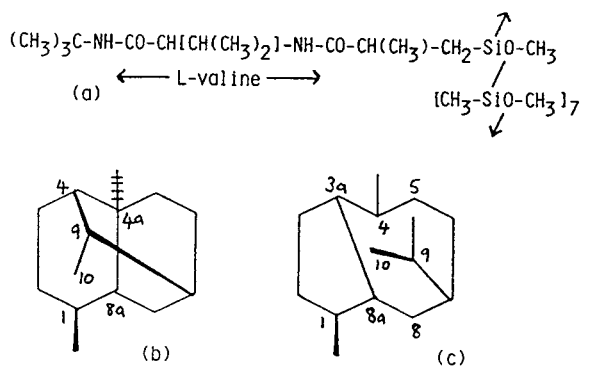

Fig. 1. (a) Chirasil-Val stationary phase [6]. (b) Patchoulol is saturated with 4-OH and 9-CH_3 groups. Seychellene is a 9–10 monoene with a 4-CH_3-group. (c) α-Bulnesene is a 3*a*–4,9–10 diene. α-Guaiene is a 3*a*–8*a*,9–10 diene. α-Gurjunene is a tricyclic (8–9)1–8*a* monoene. α-Patchoulene is a tricyclic (3*a*–9)4–5 monoene. β-Patchoulene is a tricyclic (4–9)3*a*–8*a* monoene.

0021-9673/94/$07.00
SSDI 0021-9673(94)00029-9

Table 1
Retention indices and relative retention times (linalol = 1.0) of various solutes on Chirasil-Val and other phases at given temperatures (°C)

Solute		Retention indices (*vs. n*-alkanes)								Relative retention times						
		Chirasil-Val							MPS[a]	Chirasil-Val						Chiraldex-A-DA [3]
		110°C — inc[b] →		170° ← inc —		140°C ← inc —				110°C — inc →		170° ← inc —		140°C — inc →		140°C
Caryophyllene	BH[c]			1523	29	1494	66		1428				3.59	0.03	3.56	0.05	3.61
Anethole	AE			1430	18	1412	95	142	1270	201			2.31	−0.05	2.36	1.36	*3.72*[d]
Cuminal	AC			1425	26	1399	172		1227				2.28	0.09	2.19	1.03	3.22
Borneol	BL			1395	14	1381	217		*1164*				1.97	−0.02	1.99	0.39	2.38
α-Terpineol	ML			1380	5	1375	190		1185				1.86	−0.08	1.94	0.24	2.18
Isoborneol	BL			1370	19	1351	194		*1157*				1.76	0.03	1.73		
4-Terpineol	ML	1328	18	1346	7	1339	164	126	*1175*	49	1.65	−0.05	1.60	−0.01	1.61	0.22	1.83
Estragole	AE	1291	38	1329	16	1313	130		1183		1.35	0.12	1.47	0.05	1.42	0.62	*2.04*
Camphor	BC	1271	64	*1335*	35	1300	164		1136		1.17	0.32	*1.49*	0.16	1.33	−0.07	1.26
Citronellal	NC	*1238*	28	1266	11	1255	118		1137		*0.98*	0.13	1.11	0.05	1.06	0.08	1.14
Linalol	NL	1246	−10	1236	−7	1243	151		1092		1.00		1.00		1.00		1.00
Fenchone	BC	1196	40	1236	17	1219	139		1080		0.74	0.26	1.00	0.11	0.89	−0.10	0.79
γ-Terpinene	MH	1110	17	1127	7	1120	63		1057		0.45	0.16	0.61	0.07	0.54	−0.01[e]	0.44[e]
Cineole	BE	1096							1027		0.41					0.03	0.44
p-Cymene	AH	1088							1020		0.39					−0.01	0.38
Limonene	MH	1078							*1030*		0.36					0.03	0.39

[a] Fully methyl polysiloxane phase, *e.g.* OV-101 [13]. No temperature given.
[b] Difference in values for a solute between adjacent columns, with increase (inc) direction shown by arrow. Note columns are not in order of temperature sequence.
[c] Information about the chemical nature of the solutes. A = Aromatic; B = bicyclic; C = ketone/aldehyde; E = ether; H = hydrocarbon; L = alcohol; M = monocyclic; N = acyclic.
[d] Numerical values out of descending sequence are italicized.
[e] These, and values below them in these columns at 110°C.

the otherwise methyl polysiloxane (about 6% of the side chains).

The important perfumery fixative patchouli oil is distilled from the leaves of *Pogostemon cablin* Benth. Its main constituents are sesquiterpene hydrocarbons and alcohols, the latter being mostly the tricyclic patchoulol [7] which forms about one-third of the oil. Another one-quarter or more is formed by two bicyclic hydrocarbons α-guaiene and α-bulnesene (synonym δ-guaiene) [8]. See Fig. 1 for formulae. Significant minor hydrocarbons include the tricyclic β-patchoulene, α-gurjunene [8] and seychellene [9]. α-Gurjunene is possibly a sign the patchouli oil has been adulterated with gurjun balsam [9], although other gurjunenes should then be found.

In the first gas chromatographic study of patchouli oil in 1962, Bates and Slagel [10] used a packed column of Carbowax 20M at 193°C and found (in retention time sequence) approximately 2% β-patchoulene, 21% α-guaiene, 21% α-bulnesene and 35% patchoulol. In 1967, Tsubaki *et al.* [8] used a similar polar phase capillary at 150°C for the hydrocarbons (!) only, obtaining β-patchoulene (12.8 min.) α-gurjunene (14.1 min), β-elemene (15.0 min), α-guaiene (16.0 min.), mixed caryophyllene (16.5 min.), mixed α-patchoulene, etc. (19.8 min.) and α-bulnesene (23.4 min.). α-Guaiene and α-bulnesene were the main constituents. In 1970, Henderson *et al.* [11] used a polar free fatty acid phase capillary to obtain the same sequence, but without any gurjunene or elemene directly from *Pogostemon* plant tissue. Since this, the gas chromatography of patchouli oil has been reviewed [12]. In the present work, a Chirasil-Val capillary was used for patchouli oil, after checking its performance with a number of volatile oil constituents used before [1–4]. Under the operating conditions used here, resolution of any enantiomers (if present) was unlikely.

2. Experimental

2.1. Apparatus

A Hewlett-Packard 5790A gas chromatograph was used, fitted with a capillary control unit, and a splitter injection port (split ratio 90:1 or more) and flame ionisation detector, both set at 215°C.

The Chirasil-Val capillary was purchased from Alltech (Deerfield, IL, USA) and was 25 m × 0.25 mm I.D. with film thickness given as 0.16 μm. Helium was the mobile phase, used at about 1 ml min^{-1}, and as "makeup" gas to the detector.

GC–MS apparatus used as an adjunct has been recorded previously [1].

2.2. Materials and methods

Solutes from various commercial sources were used [3]. The patchouli oil (Rivendell, Bunbury, Western Australia) was very dark brown, and 0.1 μl was injected from a microsyringe. Patchouli was run isothermally at 130°C for 8 min to elute the sesquiterpene hydrocarbons, then programmed up at 5°C min^{-1} to 190°C. Patchoulol emerged at 168°C. Single oil constituents were studied at 110°, 140° and 170°C. Trace residues from an "emptied" syringe were sufficient for the solutes. Holdup times of the solutes, obtained by extrapolating to methane the times for *n*-heptane and *n*-hexane on semi-logarithmic graph paper, were deducted from observed retention times.

3. Results and discussion

Results for various solutes compared with some literature values are given in Table 1 and some depicted in Fig. 2. Retention indices on Chirasil-Val usually increase with a rise in temperature, linalol being the exception. This gives a solute sequence "switch" with citronellal at about 120°C. It appears that fenchone-linalol also "crossover" at 170°C due to the declining values of the latter. Another "switch" occurs with camphor–estragole at about 160°C, due to the exceptionally rapid increase in camphor values (by +64 retention index units; other solutes only increase +17 to +40) going from 110°C to 170°C (see Table 1).

Camphor is a bicyclic ketone, and fenchone, which is another molecule of this type, increases by +40. However, a similar increase is shown by

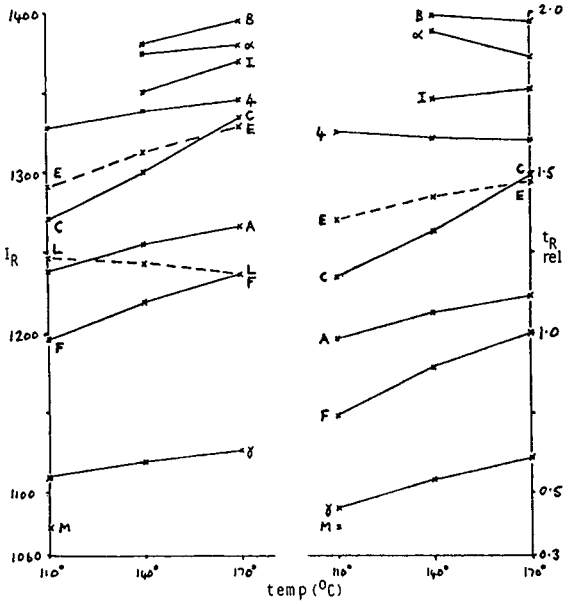

Fig. 2. Plots of retention indices (left) (I_R) and relative retention times (linalol = 1.00, right) ($t_{R,rel}$) for some solutes on Chirasil-Val phase. A = Citronellal; B = borneol; C = camphor; E = estragole; F = fenchone; I = isoborneol; L = linalol; M = limonene; α = α-terpineol; γ = γ-terpinene; 4 = 4-terpineol.

the aromatic estragole and other diverse solutes over 140°C to 170°C. But if relative retention times against linalol are examined, camphor and fenchone again exhibit considerable increase (+0.32 and +0.26 respectively) compared to a +0.14 average for the dissimilar estragole, citronellal and γ-terpinene from 110 to 170°C. 4-Terpineol gives a slight decrease; as do α-terpineol, borneol and anethole going from only 140 to 170°C.

Retention indices on fully methyl polysiloxane (MPS) are all lower [13] than those on Chirasil-Val at 140°C (Table 1), even for the hydrocarbon solutes (by about −65). Bicyclics borneol and isoborneol show the greatest increases going to Chirasil-Val at 140°C of +217 and +194 respectively, with other increases being +118 (citronellal) or more. The Chirasil-Val modified methyl polysiloxane exhibits a greater spread of indices for seven solutes (126, see Table 1) which are "condensed" over only 49 retention index units on the fully methyl polymer (citronellal to borneol). In contrast, the solutes cuminal–anethole–caryophyllene are expanded on MPS, with bigger gaps between their retention indices, than on Chirasil-Val (totals of 201 *vs.* 95, respectively). Comparing solute elution sequences on the two phases, borneol, isoborneol and 4-terpineol are "out of order", being eluted later from Chirasil-Val. Limonene, however, elutes earlier from this phase.

Relative retention times on Chirasil-Val were compared with other phases capable of enantiomer resolution from which they had been obtained previously —modified α-cyclodextrin capillaries [3]. "Chiraldex-A-TA" (trifluoracetyl, dipentyl) gave the closest resemblance, with half of fourteen solutes closely similar, particularly the bicyclics. However, this phase gave less satisfactory patchouli oil chromatograms than "Chiraldex A-DA", which showed five similar results. Chirasil-Val had considerably less affinity than A-DA (dipentyl, monohydroxy) for anethole, cuminal and estragole. Thus there is similar "selection" for terpenoids, but less retention of aromatics by Chirasil-Val. With these characteristics it was possible that this phase would be valuable for sesquiterpene oils.

It is difficult to see why bicyclic ketones should be "favoured" by Chirasil-Val with its branched aliphatic (six methyl groups) di-amides (see Fig. 1a). Perhaps their rigid "box-like" molecules fit well, unlike flat aromatics, between these special side chains which are only present on every eighth silicon atom of the polymer backbone? The polarity of Chirasil-Val is low, though higher than fully methyl polysiloxane (0.46 at 140°C compared to 0.27 respectively by "*c* ratio" [14]) both rising slightly with temperature increase. The *c* ratio (0.75[retention times of cuminal/caryophyllene]) of Chiraldex-A-DA at 140°C is higher still, 0.67, although it is the least polar of the three α-cyclodextrin modifications studied [3].

A "test" mixture of three commercially available, fairly pure, sesquiterpene hydrocarbons was used to evaluate Chirasil-Val as a phase for the analysis of volatile oils containing such substances. At 155 and 140°C, longifolene and caryophyllene emerged close together, but at

130°C they gave uncorrected retention times of 5.07 and 5.30 min, respectively, with humulene appearing at 6.10 min. The mix present in patchouli oil resolved quite well when programmed up after 8 min at 130°C (Fig. 3).

Peak identities for patchouli were assigned from a GC–MS run on a low polarity (MPS) DB-1 capillary. For the temperature programmed study of patchouli oil, Chirasil-Val gave better resolution of the complex mixture of sesquiterpenes than MPS although with the same retention sequence. The last main peak, patchoulol, was resolved from another constituent (Fig. 3) and shown to form only about 28.5% of the oil, and not "35%" (as on MPS). The earlier hydrocarbon peak of seychellene was well resolved from α-guaiene and reliably found to form about 7% of the oil. The very early β-patchoulene peak was seen to consist of two components, and only formed less than 2% of the oil. A 20M capillary also gave inferior resolution —high patchoulol and obviously impure peaks for α-bulnesene and α-guaiene (each about "18%") approaching early values found on this phase [10]. Chiraldex-A-DA also gave unsatisfactory values for α-bulnesene and α-guaiene.

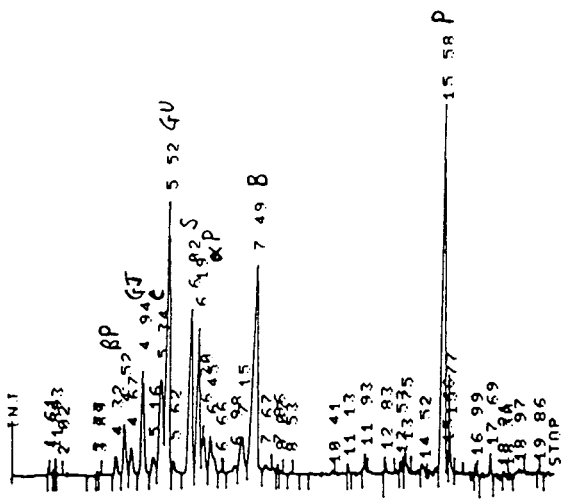

Fig. 3. Chromatogram of patchouli oil on Chirasil-Val capillary with chartspeed doubled between 4 and 8 min. Peak retention times printed in min. Peaks named from GC–MS runs on DB-1 and DB-23 with percentage identification *quality* from the computer library shown, together with the largest MS ions (m/z, in brackets). αP = α-Patchoulene *91* (93, 107, 135); βP = β-patchoulene *97* (161, 189, 119); B = α-bulnesene *99* (93, 107, 108); C = caryophyllene *99* (69, 93, 133); GJ = α-gurjunene *99* (204, 161, 189); GU = α-guaiene *99* (105, 147, 93). P = patchoulol peak at 168°C *97* (83, 98, 138, 222); S = seychellene —not in Wiley library (122 distinctive [8], 204). The area percentages of the identified peaks, in elution sequence, were β-patchoulene 1.7, α-gurjunene 3.9, caryophyllene 4.7, α-guainene 10.4, seychellene 6.9, α-patchoulene 6.4, α-bulnesene 12.0 and patchoulol 28.5.

It is logical that β-patchoulene elutes earlier from gas chromatographic phases than most other tricyclic mono-unsaturated sesquiterpene hydrocarbons. Its double bond is sterically hindered between two rings, and is tetra-substituted (Fig. 1c), allowing faster elution. In contrast, the exocyclic double-bond in seychellene is not hindered, with two hydrogen atoms at the outer end, and shows relatively long retention. Of the two dienes, α-guaiene has a sterically hindered double bond, and so elutes earlier than α-bulnesene.

4. Acknowledgements

The patchouli oil GC–MS runs were made by Mr. G.E. Chidlow and Mr. B. MacKinnon on DB-1 and DB-23 respectively. The observations on it using Chiraldex-A DA were made by Ms. S.C. Wong and Mr. D. Biancuzzo.

5. References

[1] T.J. Betts, *J. Chromatogr.*, 606 (1992) 281.
[2] T.J. Betts, *J. Chromatogr.*, 639 (1993) 366.
[3] T.J. Betts, *J. Chromatogr.*, 653 (1993) 167.
[4] T.J. Betts, *J. Chromatogr.*, 626 (1992) 294.
[5] H. Frank, G.J. Nicholson and E. Bayer, *J. Chromatogr. Sci.*, 15 (1977) 174.
[6] H. Frank, G.J. Nicholson and E. Bayer, *J. Chromatogr.*, 146 (1978) 197.
[7] G. Buchi, R.E. Erickson and N. Wakabayashi, *J. Am. Chem. Soc.*, 83 (1961) 927.
[8] N. Tsubaki, K. Nishimura and Y. Hirose, *Bull. Chem. Soc. Japan*, 40 (1967) 597.
[9] G. Wolff and G. Ourisson, *Tetrahedron*, 25 (1969) 4903.

[10] R.B. Bates and R.C. Slagel, *Chem. Ind.*, (1962) 1715.
[11] W. Henderson, J.W. Hart, P. How and J. Judge, *Phytochemistry*, 9 (1970) 1219.
[12] B.M. Lawrence, *Perf. Flav.*, 6 (1981) 73.
[13] W. Jennings and T. Shibamoto, *Qualitative Analysis of Flavour and Fragrance Volatiles*. Academic Press, London, 1980.
[14] T.J. Betts, *J. Chromatogr.*, 628 (1993) 138.

ELSEVIER

Journal of Chromatography A, 664 (1994) 301–305

JOURNAL OF CHROMATOGRAPHY A

Short Communication

Capillary zone electrophoresis of humic acids

A. Rigol, J.F. López-Sánchez, G. Rauret*

Departament de Química Analítica, Universitat de Barcelona, Av. Diagonal 647, E-08028 Barcelona, Spain

(First received July 16th, 1993; revised manuscript received December 20th, 1993)

Abstract

Capillary zone electrophoresis (CZE) was used for the separation of humic acids. The influence of the buffer solution on the separation of a commercial humic acid was studied. The use of an 8 mmol l^{-1} HCl–59.8 mmol l^{-1} L-alanine buffer (pH 3.17) leads to the separation of humic acids into two fractions. The composition and pH of this buffer and some instrumental parameters such as voltage, injection volume and wavelength of detection were optimized and the quality parameters of the method were determined. Two further commercial humic acids were assayed. The one that showed the highest peak signal was used as a reference for the rough quantification of the others.

1. Introduction

The high structural complexity and the wide range of molecular masses of humic acids have led to the application of different approaches to obtain more information about them. Many techniques and methods have been used for this purpose, most of which are based on the fractionation and characterization of these substances.

Size-exclusion chromatography is the most widely used technique for humic acid studies. There are many papers describing the use of this technique followed by IR [1,2], UV [2,3,4], fluorescence [2] and electrochemical detection [4], pulse polarography [5] and electrophoretic techniques using polyacrylamide gel with densitometry [6], staining [1] or UV detection [7]. Other chromatographic techniques used in these studies are HPLC with fluorescence [8] or UV detection [9], gas chromatography with microwave emission [10] or nitrogen-selective detection [11] and sorption chromatography followed by ^{13}C NMR spectrometry [12].

Because of the ionic nature of the humic acids, it is possible to study them using electrophoretic techniques. Most of these techniques use polyacrylamide gel as a stabilizing medium. Studies have been reported using zone electrophoresis followed by densitometry, IR or pyrolysis–GC–MS [13], paper electrophoresis followed by densitometry [14,15], isoelectric focusing followed by GC [16], staining or densitometry [17] and isotacophoresis followed by densitometry [18]. To our knowledge, only one study of humic acids by a capillary technique, capillary isotachophoresis, has been published [7]. However, there are very few suitable methods for the determi-

* Corresponding author.

0021-9673/94/$07.00
SSDI 0021-9673(93)E0063-Z

Table 1
Elemental analysis, A_{465}/A_{665} absorbance ratio and absorptivity for three commercial humic aids

Source	C (%)	H (%)	N (%)	A_{465}/A_{665}	Absorptivity
Fluka	45.91	3.73	0.56	4.3080	0.0229
Aldrich	42.17	3.90	0.53	4.7945	0.0196
Janssen	39.17	4.02	0.55	3.6091	0.0193

nation of humic acids. Of the studies of humic acids mentioned above, only one [8] proposes a method for determining them directly from the information obtained in the separation process. In other studies, the carbon percentage is used as a parameter to quantify humic acids.

These substances play an important role in environmental chemistry, mainly forming chelates with metal ions. Moreover, in soils with a high content of organic matter such as peaty soils of Chernobyl, the content of radionuclides was higher than expected [19]. To study the role of organic matter in radionuclide retention it is necessary to develop methods able to determine the different organic matter fractions.

For this purpose, the possibility of establishing a method for the determination of the humic acid content in soils has been studied. CZE was chosen as a technique with high separation efficiency and resolution, which has been applied in biochemistry for the study of substances with high molecular mass (proteins [20,21], nucleic acids [22] and amino acids [23,24]).

2. Experimental

2.1. Apparatus

A Model 270A capillary zone electrophoresis system from Applied Biosystems was used with a 72 cm × 50 μm I.D. fused-silica capillary filled with the respective buffer. High voltages, from 10 to 30 kV, were applied in both polarities (cathodic injection/anodic detection or *vice versa*). This instrument is equipped with a UV detector with a deuterium lamp working from 190 to 700 nm. The electropherograms were recorded using a Hitachi Model D-2500 integrator.

2.2. Reagents

Washing solutions

Solutions of 0.1 mol l^{-1} NaOH or 0.1 mol l^{-1} HCl were prepared using analytical-reagent grade reagents from Carlo Erba and Merk, respectively.

Buffer solutions

Twelve buffers were used at different concentrations: 2-(N-morpholino)ethanesulphonic acid (MES)–NaOH, HCl–tris(hydroxymethyl) aminomethane (Tris), citric acid–citrate, HCl–imidazole, HCl–glycylglycine, HCl–glycine, HCl–L-alanine, HCl–L-leucine, HCl–L-serine, HCl–L-lysine, HCl–β-alanine and L-aspartic acid. All were of analytical-reagent grade from Merck, except for MES which was from Sigma. For the preparation of buffer solutions, Culligan Ultrapure GS doubly deionized water of 18.3 MΩ cm resistivity was used.

Buffers were prepared by mixing a measured mass of the compound with a volume of 0.1 mol l^{-1} HCl or NaOH solution in various proportions to obtain the appropiate pH and concentration. The solutions were filtered through a 0.22-μm nylon filter (Scharlau).

2.3. Samples

Commercial humic acids from Fluka, Aldrich and Janssen were used. Some of their characteristics, such as elemental composition, ratio of absorbances at 465 and 665 nm (A_{465}/A_{665}) and absorptivity (expressed in terms of absorbance at 400 nm per mg C l^{-1} in a 1-cm cell [25]) are given in Table 1. Solutions were prepared by dissolving the humic acid in 10^{-3} mol l^{-1} NaOH.

2.4. Capillary electrophoresis procedure

The capillary was washed with 0.1 mol l^{-1} HCl for 2 min, then the buffer solution (59.8 mmol l^{-1} in L-alanine and 8 mmol l^{-1} in HCl at pH 3.17) was applied for 5 min to condition the capillary. In both steps the solution was introduced into the capillary by means of the vacuum. The sample was injected for 12 s (48.6 nl) by the vacuum technique, and separation was achieved using a voltage of 15 kV with anodic injection and cathodic detection. Each sample was injected in triplicate. Detection was carried out at 215 nm by means of an optical window for UV detection 50 cm from the injection site. The column temperature was set at 40°C.

3. Results and discussion

3.1. Buffer selection

The reagents used to study the effect of the buffer composition on the separation were chosen according to the literature [7,26] and taking into account the presence of different functional groups.

Some buffer solutions showed an electropherogram with overlaping bands (MES–NaOH, critic acid–citrate and HCl–imidazole) or with low sensitivity (HCl–Tris). Of the amino acids assayed, only those with a pK between 2.2 and 2.4, containing only one carboxylic acid group and one amino group in the α-position (L-alanine, L-glycine, L-leucine and L-serine) gave good results when the buffer was prepared at pH $\approx$ 3. The electropherograms obtained with these buffers were similar and included four fractions, referred to as A, B, C and D according to their migration time. HCl–L-alanine buffer was chosen for the determination studies as it gave the narrowest peaks. Fig. 1 shows the electropherogram obtained with a commercial humic acid from Fluka.

Only fractions A and D were attributable to humic acids, because the peaks corresponding to fractions B and C were independent of the humic acid content and they sometimes appeared when a blank was injected.

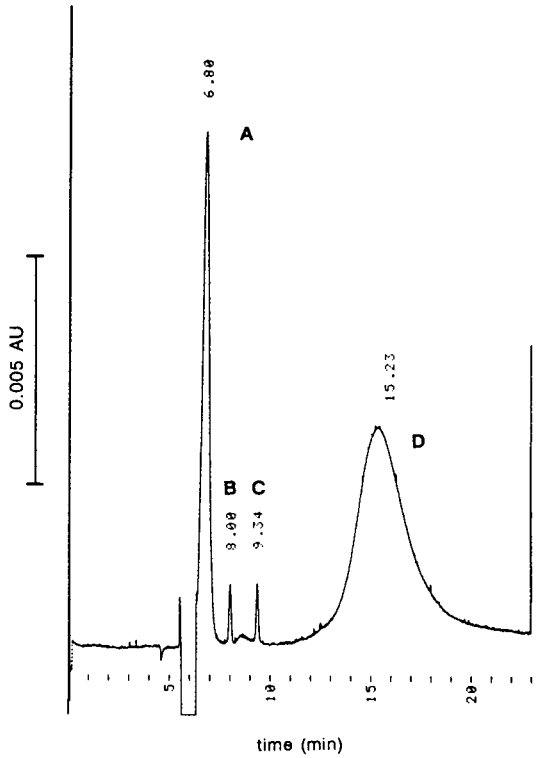

Fig. 1. Electropherogram of a sample of 100 μg ml^{-1} humic acid from Fluka. Conditions: buffer, 8 mmol l^{-1} HCl–59.8 mmol l^{-1} L-alanine (pH 3.17); temperature 40°C; applied voltage, 15 kV; anodic injection and cathodic detection; injection volume, 48.6 nl; detection at 215 nm; attenuation, 2^4 mV.

To optimize the HCl–L-alanine buffer solution, nine solutions were prepared with different pH values (between 2.7 and 3.2) and concentrations (5.4–11.6 mmol l^{-1} for HCl and 14.4–88.8 mmol l^{-1} for L-alanine). Considering the criteria of efficiency, resolution and reproducibility (R.S.D. $\leq$ 2%), the buffer chosen was 8 mmol l^{-1} in HCl and 59.8 mmol l^{-1} in L-alanine and had a pH of 3.17.

3.2. Quality parameters

Linearity, limit of quantification and precision were determined using the described procedure. Linear relationships were obtained for peak area

(or peak height) *versus* humic acid concentration (from 5 to 100 μg ml^{-1}) with correlation coefficients better than 0.99. In relation to fraction A, higher sensitivity was obtained when the peak height was used. For fraction D both peak height and peak area gave similar sensitivities. On the other hand, the slopes obtained on different days had good reproducibility (R.S.D. $<4\%$ for peak height and R.S.D. $<8\%$ for peak area). Concentrations below 5 and 20 μg ml^{-1} were not suitable for determining the contents of fractions A and D, respectively.

The precision for the measurements of fractions A and D was calculated by injecting different solutions with 20 and 80 μg ml^{-1} of humic acid for fraction A and 80 μg ml^{-1} for fraction D. The recovery of humic acid was measured in quadruplicate over 20 days. The R.S.D. was better for peak-area measurements (2–4%) than for peak-height measurements (6–7%).

Because of the difficulty in obtaining a certified reference material, the validation of the method was carried out by calculating the recovery for the Fluka humic acid in a simple matrix such as bottled drinking water. The values obtained were satisfactory for fraction A (96.44%) but lower for fraction D (86.02%), perhaps owing to matrix effects. However, humic acids are normally extracted with an alkaline medium and they are precipitated at acidic pH. The humic acid obtained in this way can be dissolved in 10^{-3} mol l^{-1} NaOH, diminishing these matrix effects.

3.3. Capillary electrophoresis of other commercial humic acids

Commercially available humic acids from Aldrich and Janssen were used. The electropherograms obtained for these samples were similar to those from Fluka, as shown in Fig. 1. The recoveries obtained for the Aldrich sample were 92.43% for fraction A and 80.79% for fraction D, whereas those obtained for the Janssen sample were 75.67% and 79.24%, respectively.

The contents of fractions A and D were determined using Fluka humic acid as a reference. The content of the fractions observed for Aldrich humic acid was higher than that obtained for Janssen humic acid. This may be related to the different characteristics or origins of the humic acid samples. On the other hand, the humic acid from Fluka showed the highest signal and it was selected for use as reference for further determinations of humic acid contents.

4. Conclusions

CZE is a useful technique for studying humic acids, because two fractions can be separated, different commercial humic acids show similar electropherograms and there is a linear relationship between the signal obtained and concentration, which allows a rough determination of these substances.

5. References

[1] N. Mora, M. Castagnola and D. Rossetti, *J. Chromatogr.*, 209 (1981) 421.
[2] N. Plechanov, *Org. Geochem.*, 5 (1983) 143.
[3] J.P. Morizur, B. Monegier, L. Silly and P.L. Desbene, *C.R. Acad. Sci., Ser. II*, 229 (18) (1984) 1269.
[4] C. Chiavari, V. Concialini, M.T. Lippolis and F. Scarponi, *J. Chromatogr.*, 281 (1983) 319.
[5] M.T. Lippolis, V. Concialini and G. Chiavari, *Talanta*, 31 (1984) 107.
[6] N.R. Curvetto and G.A. Orioli, *Plant Soil*, 66 (1982) 205.
[7] P. Kopáček, D. Kaniansky and J. Hejzlar, *J. Chromatogr.*, 545 (1991) 461.
[8] M. Susic and K.G. Boto, *J. Chromatogr.*, 482 (1989) 175.
[9] L. Serve, L. Piovetti and N. Longuemard, *J. Chromatogr.*, 292 (1984) 458.
[10] B.D. Quimby, M.F. Delaney, P.C. Uden and R.M. Barnes, *Anal. Chem.*, 52 (1980) 259.
[11] E. Granada, J. Blasco, L. Comellas and M. Gassiot, *J. Anal. Appl. Pyrol.* 19 (1991) 193.
[12] L.R. Wershaw, D.J. Pinkney, E.C. Laguno and V. Vicente-Becket, *Anal. Chim. Acta*, 232 (1990) 31.
[13] M. Nobili, G. Bragato, J.M. Alcañiz, A. Puigbo and L. Comellas, *Soil Sci.*, 150 (1990) 763.
[14] R.C. Ghosh, R.M. Singhal and S.D. Sharma, *Indian For.*, 106 (1980) 205.
[15] R.M. Singhal and S. Soni, *Indian For.*, 116 (1990) 669.
[16] D. Zhang and S. Lu, *Sci. Total Environ.*, 62 (1987) 89.
[17] M. Govi, O. Francioso, C. Ciavatta and P. Sequi, *Soil Sci.*, 154 (1992) 8.

[18] G.A. Orioli and N.R. Curvetto, *Plant Soil*, 55 (1980) 353.
[19] A. Fraiture, *Introduction to the Radioecology of Forest Ecosystems and Survey of Radioactive Contamination in Food Products from Forests* (*Report on Radiation Protection*, No. 57), Commission of the European Communities, Luxembourg, 1992, p. 18.
[20] R.M. McCormick, *Anal. Chem.*, 60 (1988) 2322.
[21] H.H. Lauer and D. McManigill, *Trends. Anal. Chem.*, 5 (1986) 11.
[22] A.S. Cohen, S. Terabe, J.A. Smith and B.L. Karger, *Anal. Chem.*, 59 (1987) 1021.
[23] J.S. Green and J.W. Jorgenson, *J. Chromatogr.*, 352 (1986) 337.
[24] R.A. Wallingford and A.G. Ewing, *Anal. Chem.*, 59 (1987) 678.
[25] S. Alegret, J. Alió, J.M. Alcañiz and E. Casassas, *Agrochimica*, 33 (1988) 31.
[26] X. Huang, J.A. Luckey, J. Gordon and R.N. Zare, *Anal. Chem.*, 61 (1989) 766.

Author Index

PUBLICATION SCHEDULE FOR THE 1994 SUBSCRIPTION

Journal of Chromatography A and *Journal of Chromatography B: Biomedical Applications*

MONTH	O 1993	N 1993	D 1993	J	F	M	A	
Journal of Chromatography A	652/1 652/2 653/1	653/2 654/1 654/2 655/1	655/2 656/1 + 2 657/1 657/2	658/1 658/2 659/1 659/2	660/1 + 2 661/1 + 2 662/1 662/2	663/1 663/2 664/1	664/2 665/1 665/2 666/1 + 2 667/1	The publication schedule for further issues will be published later.
Bibliography Section						681/1		
Journal of Chromatography B: Biomedical Applications				652/1	652/2 653/1	653/2 654/1	654/2 655/1	

INFORMATION FOR AUTHORS

(Detailed *Instructions to Authors* were published in *J. Chromatogr. A*, Vol. 657, pp. 463–469. A free reprint can be obtained by application to the publisher, Elsevier Science B.V., P.O. Box 330, 1000 AH Amsterdam, Netherlands.)

Types of Contributions. The following types of papers are published: Regular research papers (full-length papers), Review articles, Short Communications and Discussions. Short Communications are usually descriptions of short investigations, or they can report minor technical improvements of previously published procedures; they reflect the same quality of research as full-length papers, but should preferably not exceed five printed pages. Discussions (one or two pages) should explain, amplify, correct or otherwise comment substantively upon an article recently published in the journal. For Review articles, see inside front cover under Submission of Papers.

Submission. Every paper must be accompanied by a letter from the senior author, stating that he/she is submitting the paper for publication in the *Journal of Chromatography A* or *B*.

Manuscripts. Manuscripts should be typed in **double spacing** on consecutively numbered pages of uniform size. The manuscript should be preceded by a sheet of manuscript paper carrying the title of the paper and the name and full postal address of the person to whom the proofs are to be sent. As a rule, papers should be divided into sections, headed by a caption (*e.g.*, Abstract, Introduction, Experimental, Results, Discussion, etc.). All illustrations, photographs, tables, etc., should be on separate sheets.

Abstract. All articles should have an abstract of 50–100 words which clearly and briefly indicates what is new, different and significant. No references should be given.

Introduction. Every paper must have a concise introduction mentioning what has been done before on the topic described, and stating clearly what is new in the paper now submitted.

Experimental conditions should preferably be given on a *separate* sheet, headed "Conditions". These conditions will, if appropriate, be printed in a block, directly following the heading "Experimental".

Illustrations. The figures should be submitted in a form suitable for reproduction, drawn in Indian ink on drawing or tracing paper. Each illustration should have a caption, all the *captions* being typed (with double spacing) together on a *separate sheet*. If structures are given in the text, the original drawings should be provided. Coloured illustrations are reproduced at the author's expense, the cost being determined by the number of pages and by the number of colours needed. The written permission of the author and publisher must be obtained for the use of any figure already published. Its source must be indicated in the legend.

References. References should be numbered in the order in which they are cited in the text, and listed in numerical sequence on a separate sheet at the end of the article. Please check a recent issue for the layout of the reference list. Abbreviations for the titles of journals should follow the system used by *Chemical Abstracts*. Articles not yet published should be given as "in press" (journal should be specified), "submitted for publication" (journal should be specified), "in preparation" or "personal communication".

Vols. 1–651 of the *Journal of Chromatography*; *Journal of Chromatography, Biomedical Applications* and *Journal of Chromatography, Symposium Volumes* should be cited as *J. Chromatogr.* From Vol. 652 on, *Journal of Chromatography A* (incl. Symposium Volumes) should be cited as *J. Chromatogr. A* and *Journal of Chromatography B: Biomedical Applications* as *J. Chromatogr. B.*

Dispatch. Before sending the manuscript to the Editor please check that the envelope contains four copies of the paper complete with references, captions and figures. One of the sets of figures must be the originals suitable for direct reproduction. Please also ensure that permission to publish has been obtained from your institute.

Proofs. One set of proofs will be sent to the author to be carefully checked for printer's errors. Corrections must be restricted to instances in which the proof is at variance with the manuscript.

Reprints. Fifty reprints will be supplied free of charge. Additional reprints can be ordered by the authors. An order form containing price quotations will be sent to the authors together with the proofs of their article.

HPLC'95: Innsbruck, Austria

19th International Symposium on Column Liquid Chromatography

May 28–June 2, 1995

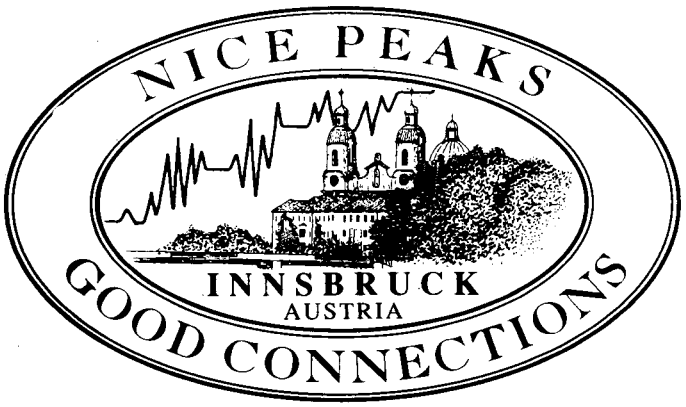

Chairman: **W. Lindner**
University of Graz
Austria

Honorary Chairman: **J.F.K. Huber**
University of Vienna
Austria

FORMAT: The HPLC'95 Symposium in Innsbruck follows the eighteen successful meetings held earlier in this series in Europe and the U.S.A. The format will be similar, covering a broad range of topical issues in Separation Science by oral and poster presentations, together with a series of Poster Discussion Sessions. An International Technical Exhibition on instrumentation, accessories and services will form an integral part of the scientific program.

TOPICS: The broad spectrum of Lecture and Poster Sessions will highlight recent advances in:

- Separation Methods, HPLC, SFC, HP-Affinity Chromatography, etc.
- Capillary Electrophoresis
- Hyphenated Techniques, Mass Spectrometry
- Separation of Stereoisomers and Chiral Recognition
- Separation Techniques in Biotechnology
- New Developments of Sorption Materials
- Preparative Techniques in Chromatography
- Sample Preparation and Derivatization
- Selective and Sensitive Detection Principles
- Clinical, Pharmaceutical, Environmental Applications and Implications
- Applications in Food Analysis
- Chemometrics in Separation Science, Validation and Regulatory Issues.

The central core of the Symposium will focus on the **Poster Sessions**, which will provide a unique forum for lively discussions on recent research and new developments and for the exchange of ideas together with an informal opportunity to meet colleagues from all over the world. To facilitate a wider discussion of current research and its implications Poster Presenters will be invited to make short oral presentations in discussion group format.

HPLC'95 POSTER AWARD: To acknowledge the major input of Poster Presentations to the continuing success of these Symposia, a number of "HPLC'95 Poster Awards" have been established in order to recognize outstanding contributions to Separation Sciences. The First Prize will be US$ 3000.- to enable the winner to attend the next meeting in the series, HPLC'96 in San Francisco. Scientific calculators will be presented as second and third prizes. This endowment has been make possible by courtesy of Hewlett-Packard and will continue for subsequent Symposia in the series.

SOCIAL EVENTS: The social program will include an Opening Mixer on Sunday evening at the Casino Innsbruck, a reception by the Mayor and County Chancellor, a concert by courtesy of Perkin Elmer, and a grand Farewell Party on Thursday evening.

ENQUIRIES: If you are interested in attending HPLC'95 and wish to be on our mailing list to receive the registration package, please contact:
HPLC'95 Secretariat, Tyrol Congress, Marktgraben 2, A-6020 Innsbruck, Austria
Tel.: +43-512-575600 Fax.: +43-512-575607

0021-9673(19940401)664:2;1-Z